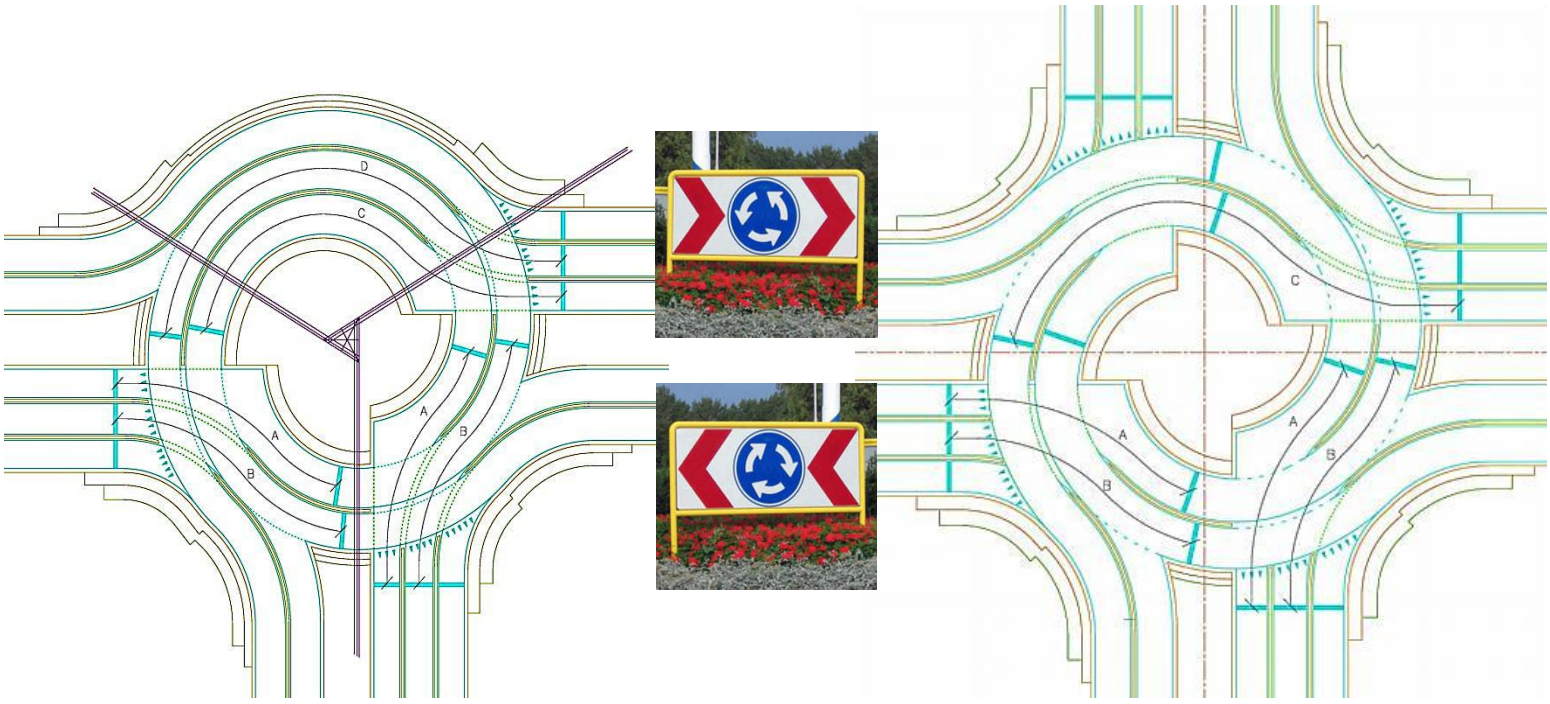
SIGNALIZED TURBO ROUNDABOUTS

A Study into the Applicability of Traffic Signals on Turbo Roundabouts



Rogier R.M. Hoek
July, 2013

TU Delft Delft University of Technology

SIGNALIZED TURBO ROUNDABOUTS

A Study into the Applicability of Traffic Signals on Turbo Roundabouts

Author	*Student ID*
R.M. Hoek BSc	**1353993**

Graduation committee

Chairman	
Prof. dr. ir. S.P. Hoogendoorn	**TU Delft, faculty of Civil Engineering and Geosciences**
Daily supervisor intern	
Dr.ir. W. Daamen	**TU Delft, faculty of Civil Engineering and Geosciences**
Graduation coordinator	
Ir. P.B.L. Wiggenraad	**TU Delft, faculty of Civil Engineering and Geosciences**
Advisor extern	
Dr.ir. L.G.H. Fortuijn	**Turbo Traffic Solutions**
Auditor	
Dr.ir. H.M. Jagtman	**TU Delft, faculty of Technology, Policy and Management**

Delft, University of Technology
Faculty of Civil Engineering and Geosciences
Section Transport and Planning

TU Delft

Preface

"Education is an admirable thing, but it is well to remember from time to time that nothing that is worth knowing can be taught."

Oscar Wilde

Taking a five-year study programme at the Delft University of Technology, and finally sharing this conclusion, is not much of a compliment to the university. Comfortably, I do not agree with Wilde; here is why.

In September 2007, I commenced with the Bachelor's course Civil Engineering and Geosciences, ignorant of the scientific fields of traffic and transport engineering. Six years later, I finalize the Master's curriculum of Transport and Planning; this report is the icing on the cake. The vast amount of knowledge on civil engineering in general, and traffic and transport engineering in particular, which I gained during the last six years, is the least argument for disagreeing with Wilde. The competence to cope with intellectual challenges and to catch a problem in a clear and definite description has proven to be of immense relevance. The utility of fundamental research is at least as valuable, so is the fruitful offspring of a critical attitude. DUT offers its students the opportunity to develop these competences and many more.

This document reports the graduation project, that is the completion of the Master's curriculum. The subject of the project is turbo roundabouts. The turbo roundabout was invented by Bertus Fortuijn in 1996, I am honoured to have been supervised by him during the graduation. The turbo roundabout appeared to offer major advantages with regard to traffic safety and capacity, in comparison with conventional intersection solutions. However, the quest for capacity (to be described in the introduction to this thesis) still continues, and incited the central question of the project:

What is the applicability range of traffic signals on turbo roundabouts?

Bertus Fortuijn offered me the challenges and tools for completing the project. Especially during the early months of the graduation these challenges were big. I had trouble to keep up with Fortuijn; with his 40-year experience as a traffic engineer he made thinking leaps that were too big for a graduating student to comprehend. Thanks to his time investments I was able to gain the knowledge on his invention, that was required for this project. I admire Fortuijn for his devotion, his seemingly inexhaustible source of energy, knowledge and experience, his past and present effort for the scientific field of traffic engineering (which is amazing regarding his pensionable age) and our faith we have in common.

Furthermore, I would like to address acknowledgement to the graduation committee, chaired by Serge Hoogendoorn. Notably, Winnie Daamen has daily supervised the project. She has a great enthusiasm for the process of fundamental research, urging my own enthusiasm. By means of her critical notes and hints, I was able to streamline the process of the project and deal with the challenges efficiently.

Numerous persons outside the graduation committee have contributed to the project in various ways. Maria Salomons was able to answer my questions with regard to traffic control and provided me patiently with explanations on modelling by means of VRIGen. Moreover, a few dozens of people contributed to the project by sharing information on various subjects; I got in touch with them via the networks of my (former) professors and LinkedIn. Finally, many thanks to my parents for their mental and financial support, even when all of my nights and weekends were sacrificed to the thesis, often to their regret.

Rogier R.M. Hoek

Delft, July 2013

Table of contents

List of translations 12
List of abbreviations 13

Summary 14
Samenvatting 16

1. Introduction 19
   1.1. Introduction to roundabouts 19
   1.2. The quest for a larger capacity 23
   1.3. Problem statement 24
   1.4. Aim of the research project 24
   1.5. Problem approach 24
   1.6. Research questions 25
   1.7. Structure of the report 26

2. Literature review: possibilities for signalizing turbo roundabouts 29
   2.1. Rotor and star roundabout: design and capacity 29
   2.2. Roundabout metering signal 30
   2.3. Control structures 31
      2.3.1. Leg-by-leg control 31
      2.3.2. Two-phase control 32
      2.3.3. Leg-by-leg control vs. two-phase control 33
      2.3.4. Signalized turbo roundabout: leg-by-leg control 33
      2.3.5. Turbo circle: two-phase control 35
   2.4. Models for evaluating the capacity 35
      2.4.1. MSRV 35
      2.4.2. Black box approach 36
      2.4.3. Simulation models 37
   2.5. Summary and conclusions 37

3. Experimental design 39
   3.1. Delineation of the project 39
      3.1.1. Inside or outside the urban area? 39
      3.1.2. Choice for turbo roundabout types 40
      3.1.3. Signalized turbo roundabout and the two-phase control 40
      3.1.4. Demand patterns 42

3.2. Capacity models 44
3.2.1. MSRV 44
3.2.2. Black box approach: analytical approach 44
3.2.3. VISSIM 45
3.3. Evaluation method 55
3.4. Validation, calibration 56
3.5. Summary and conclusions 56

4. Capacity modelling 57
4.1. MSRV 57
4.2. Analytical approach 58
4.2.1. Step 1: green phase overlap 58
4.2.2. Step 2: control structures 59
4.2.3. Step 3: saturation flow 60
4.2.4. Capacity of the signalized rotor roundabout 61
4.3. VISSIM 64
4.3.1. VRIGen: leg-by-leg control and two-phase control 65
4.3.2. VISSIM: rotor roundabout, inscribed radius 12 m 66
4.3.3. VISSIM: rotor roundabout, inscribed radius 20 m 69
4.3.4. VISSIM: star roundabout, inscribed radius 12 m 70
4.3.5. VISSIM: star roundabout, inscribed radius 20 m 71
4.3.6. VISSIM: partial turbo circle, inscribed radius 12 m 72
4.3.7. VISSIM: partial turbo circle, inscribed radius 20 m 73
4.3.8. VISSIM: four-leg turbo circle, inscribed radius 12 m 74
4.3.9. VISSIM: four-leg turbo circle, inscribed radius 20 m 75
4.3.10. VISSIM: four-leg turbo circle, inscribed radius 30 m 76
4.3.11. VISSIM: three-leg turbo circle, inscribed radius 12 m 77
4.3.12. VISSIM: three -leg turbo circle, inscribed radius 20 m 78
4.3.13. VISSIM: three -leg turbo circle, inscribed radius 30 m 79
4.4. Summary and conclusions 80
4.4.1. Un-signalized rotor and star roundabouts: results of the MSRV 80
4.4.2. Un-signalized rotor and star roundabout: results of the analytical approach 80
4.4.3. Signalized intersections: results of VISSIM 80

5. Other performance indicators 83
5.1. Space requirements 83
5.2. Robustness 83
5.3. Traffic safety 84

5.3.1. Comparison of the conventional intersection and the roundabout 84
5.3.2. Consequences of traffic signals on the roundabout 85
5.4. Environmental considerations 86
5.5. Summary and conclusions 86

6. Conclusions 87
6.1. Findings from the application of the models 87
6.2. Conclusions 90
6.2.1. Conclusions with respect to the application of the models: results 90
6.2.2. Conclusions with respect to the models 92
6.2.3. Conclusions with respect to control structures 92
6.3. Implications 93
6.3.1. Implications for scientific research 93
6.3.2. Implications for professional traffic engineering 93
6.4. Future research 94
6.4.1. Fundamentals of the models 94
6.4.2. (Intermediate) results of the models 94
6.4.3. Consequences to traffic safety 95
6.4.4. LED illumination 95
6.4.5. Topics outside the scope of this study 96

7. Reflection 97

References 99

Appendix A: Discussion of the terminology 109
Appendix B: Demand patterns 111
Appendix C: Saturation flow, field measurements 115
Appendix D: Geometrical designs 121
Appendix E: Clearance time calculation 149
Appendix F: Simplified acceleration model 153
Appendix G: Green phase overlap calcution 157
Appendix H: Control structures for the turbo roundabout 161
Appendix J: Cycle time optimization 165
Appendix K: VRIGen model development 175
Appendix L: VISSIM model development 195
Appendix M: LED illumination 225

List of translations

English	Dutch
apron	rammelstrook (aan middeneiland)
broken line	onderbroken streep
centre island	middeneiland
circulatory roadway lanes	rotondestroken
clearance time	ontruimingstijd
conflict area	conflictvlak
continuous line	doorgetrokken streep
curve widening	bochtverbreding
cut-off conflict	snijconflict
cycle time	cyclustijd
double-lane roundabout	tweestrooksrotonde
driving curve	doorrijcurve
exemption	ontheffing
extension detector	voormelddetector
fixed-time control	starre regeling
hard shoulder	draagkrachtige berm
home zone	woonerf
interception signals (traffic stream 62 through 72)	opvanglichten (verkeersstromen 62 t/m 72)
jerk	ruk (afgeleide van de acceleratie naar de tijd)
landscape buffer	rammelstrook (aan oksels van de takken)
lane	rijstrook
leg-by-leg control	tak-voor-tak regeling
lost time	verliestijd (in een verkeersregeling)
main signals (traffic streams 01 through 12)	hoofdlichten (verkeersstromen 1 t/m 12)
mountable	overrijdbaar
multilane roundabout	meerstrooksrotonde
non-mountable	niet-overrijdbaar
normative	maatgevend
pseudo-conflict	schijnconflict
queuing length	opstellengte
queuing space	opstelruimte
rate of saturation (RS)	verzadigingsgraad (VG)
request detector	aanmelddetector
roadway	rijbaan
rotary	'oude' of 'traditionele' verkeersplein
roughness	stroefheid
roundabout metering signal	rotondedoseerinstallatie (RDI)
saturation flow (also: queue discharge rate)	afrijcapaciteit

separation taper	scheidingband (tussen twee rotondestroken)
single-lane roundabout	enkelstrooksrotonde
spatial coverage	ruimtegebruik
splitter island	middenberm
swept path	bestreken baan
system of equations	stelsel van vergelijkingen
traffic signals (not: traffic control)	verkeersregelingsinstallatie (VRI)
urban area	bebouwde kom
vehicle-actuated control	verkeersafhankelijke regeling
weaving conflict	weefconflict

List of abbreviations

Abbreviation	Full
a.o.	among others
c.q.	*casu quo* (in which case)
ca.	*circa* (about, environ)
e.g.	*exempli gratia* (for example)
etc.	*et cetera* (and so on)
i.c.	*in casu* (in this case)
i.e.	*id est* (that is)
pcu/h	person-car units per hour
resp.	respectively
vs.	versus
w.r.t.	with respect to

Summary

Since the 1980s, the modern single-lane roundabout has been applied in the Dutch road network. The roundabout offered major safety benefits compared to the conventional signalized intersection, however, it also required more space. Influenced by society's growing mobility, the capacity requirements to intersections increased. This quest for capacity gave rise to the concentric multi-lane roundabout: a roundabout with two or more circulatory lanes and one or more lanes on the entrance and exit legs. The concentric multi-lane roundabout offered a higher capacity, but compromised the safety benefits of the single-lane roundabout. As an answer to the safety problems on the multilane concentric roundabout, Fortuijn developed the turbo roundabout in 1996. The turbo roundabout offers the same safety level as the single-lane roundabout and a higher capacity.

Nowadays, the quest for a higher capacity continues unabated. This graduation project aims to contribute to the quest by investigating the combination of turbo roundabouts and traffic lights. The central question is whether traffic signals enhance the capacity of the turbo roundabout. The two largest turbo roundabout types have been investigated: the rotor roundabout (four-leg) and the star roundabout (three-leg). Three models (the MSRV, an analytical approach and VISSIM) have been applied to evaluate the capacity of the rotor and star roundabout (signalized and un-signalized). In addition, this project states proposals for future research into other performance indicators than the capacity; namely space requirement, delay time, robustness, traffic safety and environmental issues.

This research shows that the signalized turbo roundabout only allows for a leg-by-leg control. However, the lane configuration on the rotor and star roundabout can be adjusted such, that the turbo roundabout is suitable for the more efficient two-phase control, which is currently being applied to the turbo circle. The results are the partial turbo circle (adjusted rotor roundabout) and the three-leg turbo circle (adjusted star roundabout). The latter intersection types require more space than the rotor and star roundabouts. The capacity evaluation shows that the partial turbo circle has no applicability range, because the capacity for left-turning traffic streams is very limited. The three-leg turbo circle has potential, because it offers a higher capacity than the star roundabout.

The geometrical design of the signalized turbo roundabout allows for phase overlap within the leg-by-leg control. Thanks to the phase overlap, two subsequent legs can obtain green simultaneously for a period in the order of 1 to 8 seconds. Consequentially, the aggregated green time within one hour can be extended compared to the leg-by-leg control without any phase overlap, enhancing the capacity of the turbo roundabout.

The capacity of the signalized turbo roundabout has been evaluated analytically by means of the analytical approach, which was developed by Fortuijn simultaneously with the development of the turbo roundabout. The analytical approach calculates the capacity by multiplying the green time per hour with the saturation flow. The capacity of the signalized rotor roundabout ranges from 2800 pcu/h to 3700 pcu/h; the capacity of the signalized star roundabout ranges from 4400 pcu/h to 5200 pcu/h, depending on the demand pattern. Using the green phase overlap, the rotor roundabout may offer 5% to 6% more capacity; the star roundabout may offer 7% to 9% more capacity.

Moreover, the microscopic simulation tool VISSIM has been applied to evaluate the capacity of and delay time on the signalized turbo roundabout and the (partial and three-leg) turbo circle. The capacity results of the analytical approach and VISSIM do not differ much, except for the results for the star roundabout with an inscribed radius of 20 m. No explanation has been found.

In order to compare the capacities of the signalized and the un-signalized turbo roundabouts, the capacity of the un-signalized turbo roundabout has been evaluated by means of the *Meerstrooksrotondeverkenner* (Multilane roundabout explorer). The un-signalized rotor roundabout offers a capacity ranging from 2900

pcu/h to 4500 pcu/h. The signalized rotor roundabout offers a lower capacity; this intersection type is not recommendatory for application. The same conclusion holds for the partial turbo circle, however, the partial turbo circle offers a higher capacity in situations with low left-turning intensities (in the range of 20% of the straight-ahead intensities). The turbo circle offers a much higher capacity than the (un-)signalized rotor roundabout (ranging from 4700 pcu/h to 9300 pcu/h, depending on diameter and demand pattern), but requires more space.

With regard to the three-leg intersections: the capacity of the signalized star roundabout (ranging from 4400 pcu/h to 5200 pcu/h) is larger than the capacity of the un-signalized star roundabout (ranging from 3700 to 5100 pcu/h). However, the signalized star roundabout induces longer delay times (nearly twice as long), and probably less traffic safety and higher environmental burdens. The three-leg turbo circle offers an even higher capacity than the signalized star roundabout (ranging from 5400 pcu/h to 7100 pcu/h), but requires more space.

From this study, it can be recommended to pay further attention to the signalized star roundabout and the smaller three-leg turbo roundabouts (both in scientific research as well as in practical engineering), because the signalized star roundabout has a larger capacity than the un-signalized star roundabout. The signalized rotor roundabout and the partial turbo circle are not recommendatory for further research, because the un-signalized rotor roundabout offers a higher capacity.

Samenvatting

Sinds de jaren ‘80 van de vorige eeuw is de enkelstrooksrotonde toegepast in het Nederlandse wegennetwerk. Ten opzichte van het conventionele geregelde kruispunt biedt de rotonde veiligheidsvoordelen, maar de rotonde vereist ook meer ruimte. Door de groeiende vraag naar mobiliteit werden steeds hogere capaciteitseisen aan kruispunten gesteld. Daarom werd de concentrische meerstrooksrotonde toegepast: een rotonde met twee of meer rondgaande stroken en een of meer stroken op de toe- en afvoerbanen. De concentrische meerstrooksrotonde bood een hogere capaciteit, maar kon de veiligheidsvoordelen niet bieden die de enkelstrooksrotonde wel te bieden had. In antwoord op de veiligheidsproblematiek van de concentrische meerstrooksrotonde, ontwikkelde Fortuijn de turborotonde in 1996. De turborotonde biedt niet alleen de veiligheidsvoordelen van de enkelstrooksrotonde, maar ook een hogere capaciteit.

Tegenwoordig duurt de zoektocht naar meer capaciteit onverminderd voort. Dit afstudeerproject draagt bij aan de zoektocht door de combinatie van turborotondes en verkeerslichten te onderzoeken. De centrale vraag is of verkeerslichten de capaciteit van de turborotonde vergroten. De twee grootste turborotondes zijn in dit onderzoek betrokken: de rotorrotonde (viertaks) en de sterrotonde (drietaks). Drie modellen (de MSRV, een analytisch model en VISSIM) zijn toegepast om de capaciteit van de rotor- en sterrotonde (geregeld en ongeregeld) te berekenen. Bovendien presenteert dit project toekomstige onderzoeksvoorstellen met betrekking tot andere prestatie-indicatoren dan de capaciteit; namelijk het ruimtegebruik, vertragingstijden, robuustheid, verkeersveiligheid en milieubelasting.

Deze studie toont aan dat alleen de tak-voor-tak regeling toepasbaar is op de geregelde turborotonde. De strookconfiguraties van de rotor- en sterrotonde kunnen echter zodanig worden aangepast, dat de turborotonde geschikt is voor de efficiëntere twee-fase regeling, die momenteel wordt toegepast op het turboplein. Het resultaat bestaat uit het partiële turboplein (aangepaste rotorrotonde) en het drietaks turboplein (aangepaste sterrotonde). De laatst genoemde kruispunten hebben een groter ruimtegebruik dan de rotor- en sterrotonde. De capaciteitsberekeningen tonen aan dat het partiële turboplein geen toepassingsgebied heeft, omdat de capaciteit voor de linksafslaande verkeersstromen zeer klein is. Het potentiele toepassingsgebied van het drietaks turboplein is groter, omdat het meer capaciteit biedt dan de sterrotonde, aan alle stromen.

Het geometrisch ontwerp van de geregelde turborotonde leent zich voor de toepassing van groenfase-overlap in de tak-voor-tak regeling. Dankzij de groenfase-overlap kunnen twee opeenvolgende takken gelijktijdig groen krijgen voor een periode van circa 1 tot 5 seconden, afhankelijk van de afstand tussen twee naburige takken. Daardoor kan de totale effectieve groentijd in een uur worden verlengd, waardoor de capaciteit van de turborotonde toeneemt.

De capaciteit van de geregelde turborotonde is analytisch berekend met behulp van een benadering, die gelijktijdig met de turborotonde is ontwikkeld door Fortuijn (2013). De analytische benadering berekent de capaciteit door de totale effectieve groentijd per uur te vermenigvuldigen met de afrijcapaciteit. De capaciteit van de geregelde rotorrotonde varieert van 2800 pae/h tot 3700 pae/h; de capaciteit van de geregelde sterrotonde varieert van 4400 pae/h tot 5200 pae/h (rekening houdend met groenfase-overlap). Met het benutten van groenfase-overlap kan de rotorrotonde 5% tot 6% meer capaciteit bieden; voor de sterrotonde is dit 7% tot 9%.

Bovendien is het microscopische simulatiemodel VISSIM toegepast om de capaciteit van en verliestijd op de geregelde turborotonde en het (partiële en drietaks) turboplein te berekenen. De resultaten van de analytische methode en VISSIM met betrekking tot de geregelde rotor- en sterrotonde verschillen niet veel, met uitzondering van de resultaten voor de sterrotonde met een binnenstraal van 20 m. Hiervoor is geen verklaring gevonden.

De capaciteit van de ongeregelde rotonde is berekend met behulp van de *Meerstrooksrotondeverkenner*, dit is gedaan om de capaciteiten van de geregelde en ongeregelde turborotondes te kunnen vergelijken. De ongeregelde rotorrotonde biedt een capaciteit tussen 2900 pae/h en 4500 pcu/h. De geregelde rotorrotonde biedt een lagere capaciteit; deze kruispuntoplossing wordt daarom niet aanbevolen voor implementatie. Deze conclusie geldt ook voor het partiële turboplein. Alleen in situaties waarin de linksafslaande intensiteiten klein zijn (tot ongeveer 20% van de rechtdoorgaande intensiteiten) biedt het partiële turboplein een hogere capaciteit. Het turboplein biedt een aanzienlijk hogere capaciteit dan de ongeregelde rotorrotonde (variërend van 4700 pae/h tot 9300 pae/h, afhankelijk van de diameter en het vraagpatroon), maar vereist meer ruimte.

De capaciteit van de geregelde sterrotonde (variërend van 4400 pae/h tot 5200 pae/h) is groter dan de capaciteit van de ongeregelde sterrotonde (variërend van 3700 pae/h tot 5100 pae/h). Echter, de geregelde sterrotonde brengt langere verliestijden met zich mee (bijna twee keer zo lang), en waarschijnlijk een verslechterde verkeersveiligheid en een grotere milieubelasting. Het drietaks turboplein biedt een nog hogere capaciteit dan de geregelde sterrotonde (variërend van 3700 pae/h tot 5100 pae/h), maar vereist ook meer ruimte.

Uit dit onderzoek volgt de aanbeveling om de geregelde sterrotonde en de geregelde drietaks knierotonde verder te onderzoeken en te implementeren in de praktijk, omdat de geregelde sterrotonde een hogere capaciteit biedt dan de ongeregelde sterrotonde. De geregelde rotorrotonde en het partiele turboplein worden niet aanbevolen voor verder onderzoek of implementatie, want de ongeregelde rotorrotonde biedt een hogere capaciteit.

1. Introduction

The subject of the graduation project described in this document is: roundabouts. In particular, the project aims to indicate the usefulness of traffic signals on roundabouts, with respect to capacity. This introduction will address the concept of roundabouts, and their hierarchical relationship with other intersection solutions. Then, the initiative of traffic lights on the roundabout will be introduced, from which the problem statement follows. From the problem statement, the main goal of this research project will be formulated, followed by the problem approach. The research questions aim to structure all research that needs to be done, in order to accomplish the main goal. Finally, a structure for the remainder of this report will be introduced, logically following from the research questions.

1.1. Introduction to roundabouts

Figure 1-1 shows the single-lane roundabout. It consists of a circulatory roadway containing one lane, around a non-mountable middle island. The entrance and exit legs contain one lane as well; they join the circulatory roadway perpendicularly in The Netherlands. In some other countries, it is more common to construct roundabouts with radially joining legs.

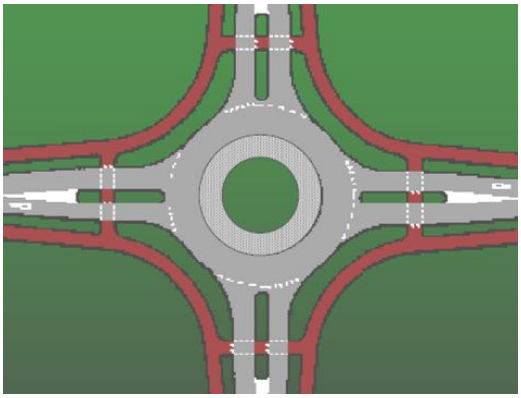


Figure 1-1 The single-lane roundabout

Dutch roundabout design guidelines consider a traffic circle to be a roundabout if and only if it has the following characteristics:

- Priority to circular traffic by traffic rule;
- Perpendicular joining entrance and exit legs.

In other countries, the second characteristic is being argued. For instance, the American engineers commonly construct circular intersections with tangentially joining legs, which they call roundabout.

The following two characteristics may be added. They have not been stated yet in any official document, but all roundabouts in The Netherlands apply to these characteristics.

- Due to the absence of weaving sections, the diameter of a roundabout is comparably small. Fortuijn (2013) mentions this in reaction to *Report 672* (TRB, 2010);
- Entrance traffic has to give priority to traffic on no more than two circulatory lanes. According to Dutch guidelines (SWOV, 2006), a traffic circle on which entrance traffic has to give priority to more lanes, traffic signals are required to maintain road safety on an acceptable level.

The most original and basic form of the roundabout is the single-lane roundabout (see Figure 1-1). In the 1960s, when it was introduced (SWOV, 2012), it was an innovative concept with large societal benefits. The single-lane roundabout offers a capacity of 2000 through 2500 pcu/h (Fortuijn, 2011), similar to the

conventional non-circular intersection (see Figure 1-3), which was the most applied intersection solution till then. Furthermore, the roundabout offers significant safety benefits.

This introduction aims to indicate why and how the roundabout has been implemented in history. Figure 1-2 shows a classification of circular intersections. The purpose of this classification is to show the hierarchical role of roundabouts in the road system: the roundabout is just one of a large set of intersection solutions. Of course, numerous different intersection types are possible. The following sections will focus on the intersection types in Figure 1-2. At the end of the section, Table 1-1 gives an overview of the most important characteristics of the intersection types in the classification.

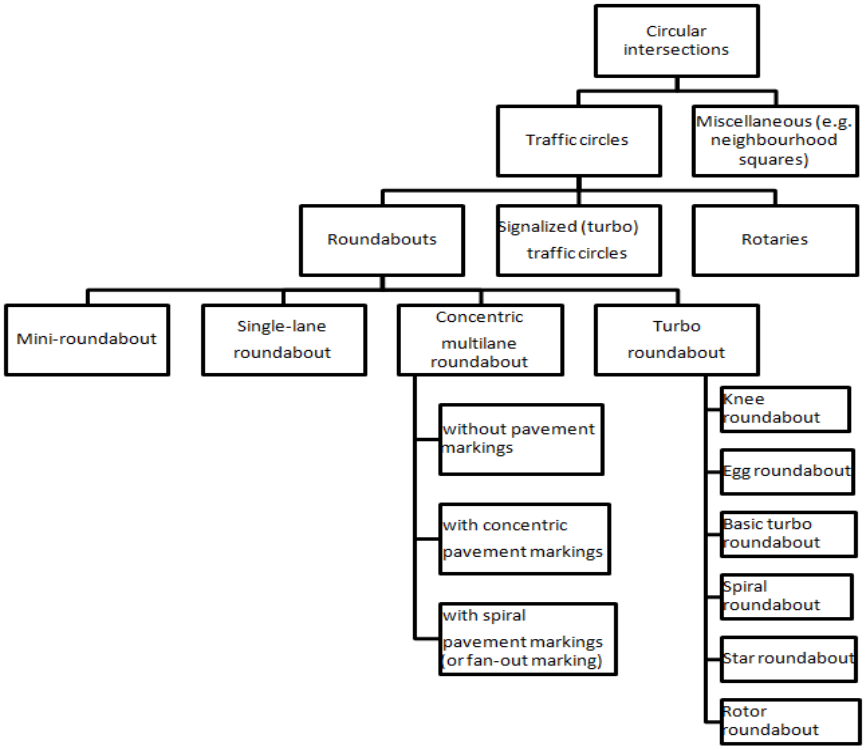


Figure 1-2 Classification of traffic intersections (based on Fortuijn, 2013 and TRB, 2010)

Non-circular intersection

Figure 1-2 only depicts the classification of circular intersections. Of course, the category non-circular intersection also offers solutions to traffic problems. Figure 1-3 shows the conventional, non-circular intersection. Before the dawn of the roundabout in the 1960s, this was the most applied intersection type in urban areas.

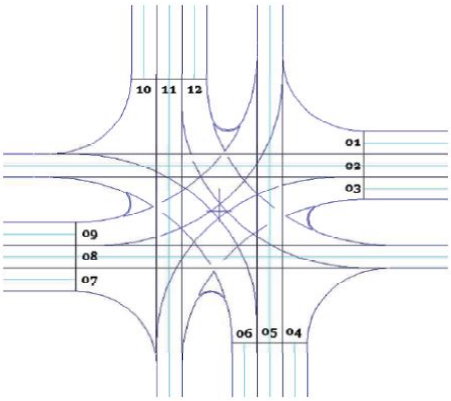


Figure 1-3 Schematization of the conventional non-circular intersection

Traffic circle

The traffic circle does not have the same definition in all countries. In The Netherlands, the definition by the CROW (1998, p.76) is generally accepted: the traffic circle is a single-level intersection where traffic flows in a circular movement, indicated by means of a particular traffic sign (RVV 1990, sign D1: a blue, round sign with white circulatory arrows). Additively, the traffic flows circularly in the same direction, around a central island which can be mountable or not. Fortuijn (2013) uses 'traffic cirle' as a collection name for roundabouts, turbo circles and rotaries (see Figure 1-2).

Rotary

A rotary is a traffic circle with a large diameter to allow traffic to weave on the road stretches between two legs. Figure 1-4 presents an example of a rotary (TRB, 2010, p.1:5).

Until the 1960s, it was common in the USA and in The Netherlands to build traffic circles as a part of the national highway network. On the traffic circle, traffic had to weave in order to enter or leave the traffic circle. Moreover, traffic from the right-hand side (from the entry legs) had priority. In order to enable traffic to merge, and to prevent the traffic circle from being blocked by large intensities, the traffic circle must have a large diameter and tangential joining entry and exit legs. In fact, American traffic engineers use 'traffic circle' and 'rotary' for the same un-signalized intersection type. This introduction uses the definitions applied by Dutch traffic engineers (a.o. Fortuijn, 2013): the traffic circle is the collection name for roundabouts, turbo circles and rotaries.



Figure 1-4 Rotary near Fort Worth, Texas (currently a non-circular signalized intersection)

Single-lane roundabout

Figure 1-1 depicts the single-lane roundabout. In general, the roundabout distinguishes itself from the traffic circle in the absence of weaving sections. Therefore, the legs can join perpendicularly to the roundabout. Because of the absence of weaving sections (and to a less extent the perpendicular joining legs), the roundabout can be constructed with a smaller diameter. Because of its small diameter, traffic cannot queue on the roundabout, and therefore the right-hand rule cannot be applied on the roundabout: circulatory traffic must have priority.

Concentric multi-lane roundabout

The multi-lane roundabout (see Figure 1-5) was implemented for intersections on which the traffic demand was so high, that the single-lane roundabout did not offer enough capacity. If a straight road stretch does not offer enough capacity, one the solutions is to add a lane. The traffic engineers who invented the multi-lane roundabout followed the same rationale: the extra lane would offer higher capacity. When the double-lane roundabout was implemented, the traffic engineers found out that this thought was not entirely true: the left lane appeared to enhance the capacity, but with less than a factor two. This was caused by the poor usage of the left lane: drivers tend to use the right lane by preference.

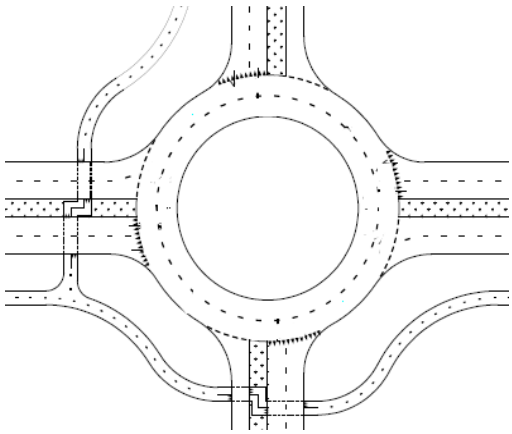


Figure 1-5 A double-lane roundabout

A major drawback of the concentric multi-lane roundabout is the lack of traffic safety. By introducing a second circulatory lane, a lot of cut-off and weaving conflicts are introduced on the circulatory lanes in near the connections with the exit legs.

Turbo roundabout

Fortuijn (2013) invented the turbo roundabout as an answer to the safety problems on the double-lane roundabout. On the turbo roundabout, many conflict points are removed by configuring the circulatory lanes such, that lane changes on the roundabout are not necessary (and prohibited; RVV, 1990). The turbo roundabout has six fundamental forms: the knee roundabout, the egg roundabout, the basic turbo roundabout, the spiral roundabout, the star roundabout and the rotor roundabout. Figure 1-6 depicts the basic turbo roundabout in order to illustrate the concept; a roundabout is a turbo roundabout if it complies to all of these ten characteristics. For the geometrical design of the other forms, the reader is referred to Fortuijn (2013).

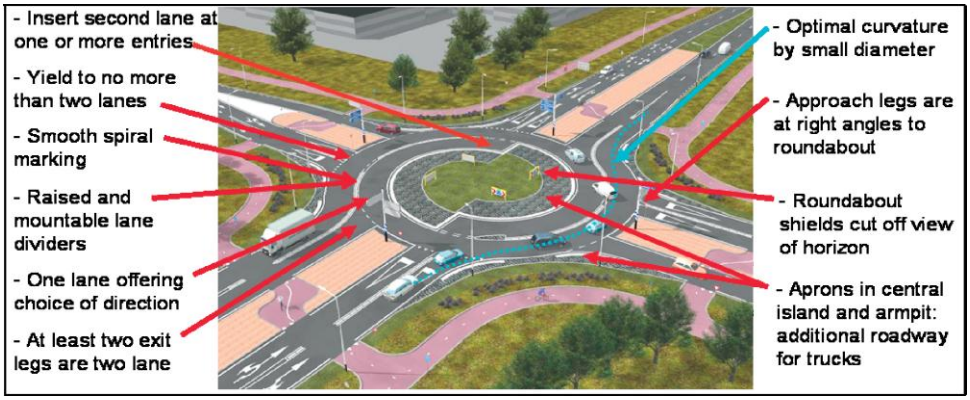


Figure 1-6 Characteristics of the turbo roundabout (subtracted from Fortuijn, 2013, p.47)

Turbo circle

Together with the turbo roundabout, Fortuijn (2013) also invented the turbo circle, shown in Figure 1-7. Essentially, the turbo circle is based on the same principles as the turbo roundabout. However, the turbo circle is equipped with traffic signals.

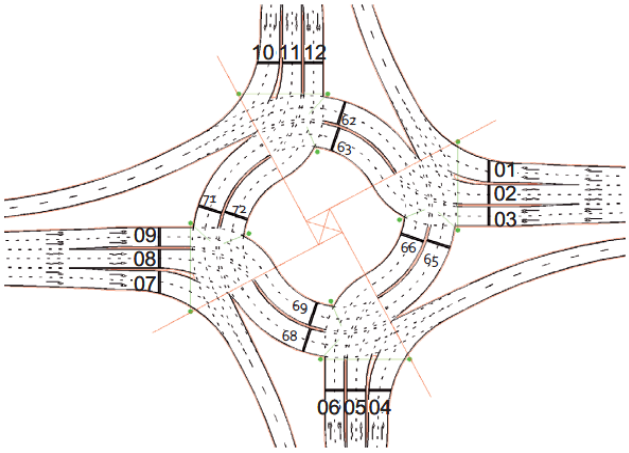


Figure 1-7 Turbo circle (Fortuijn, 2013, p.142)

Table 1-1 Characteristics of the intersection types

	Traffic flow based on	Legs join	Traffic safety
Single-lane roundabout	priority to circulating traffic	perpendicularly	+
Conventional intersection	right-hand rule	perpendicularly	0
Rotary	weaving sections	tangentially	-
Concentric multi-lane roundabout	priority to circulating traffic	perpendicularly	-
Turbo roundabout	priority to circulating traffic	perpendicularly	+
Turbo circle	pre-emption by traffic signals	perpendicularly and tangetially	+

1.2. The quest for a larger capacity

The former section already addressed a major point of concern with respect to intersections: the capacity. For capacity considerations, the single-lane roundabout was extended to the double-lane roundabout. This quest for capacity is initiated by the fact that governmental institutions have the task to provide travellers with good infrastructure, in order to enhance the accessibility of infrastructural networks. The demand for mobility has grown during the past decades, and it will presumably keep on growing, inciting the quest for intersections with larger capacities.

This research project aims to contribute to this quest by examining the capacity of the turbo roundabout. Following the historical development described in the previous section (conventional signalized intersection -> single-lane roundabout -> double-lane roundabout -> turbo roundabout), the question arises how this development can be continued. A next step might consist of (one of, or a combination of) the following options:

- Adapting the lane configuration of the turbo roundabout;
- Adapting the road environment on the intersection;
- Inventing entirely new philosophies, such as the shared space philosophy;
- Mixing two ingredients of existing intersection solutions: traffic lights and the turbo roundabout.

These options are the result of a brainstorm session, a lot of other options might be possible. This research project focuses on the latter option.

1.3. Problem statement

This project elaborates on the argument made in the previous section: to equip the turbo roundabout with traffic signals and investigate whether the capacity of the turbo roundabout increases. If traffic signals do considerably enhance the capacity, there may be a need for signalizing turbo roundabouts. In that case, the question arises in which cases and under which circumstances the traffic signals may be favourable, taking into account a selection of other performance criteria besides the capacity (see section 1.5). In order to indicate the influence of traffic signals on turbo roundabouts, non-signalized and signalized turbo roundabouts will be compared by means of models.

1.4. Aim of the research project

The aim of this project follows from the problem statement: the aim is to determine whether traffic signals are beneficial to the turbo roundabout. The central performance indicator is capacity: the main aim is to determine whether signalized turbo roundabouts [1] offer a higher capacity than un-signalized turbo roundabouts. If traffic signals indeed enhance the capacity, then the question arises whether traffic signals are in general beneficial to turbo roundabouts. Consequentially, other performance indicators than the capacity need to be invoked in the project. This report mainly pays attention to the capacity question; the performance of (signalized) turbo roundabouts with respect to the other indicators will roughly be estimated. Hypotheses for further research will be mentioned.

In general, this research project aims to explore the applicability range of traffic signals on turbo roundabouts; to explore the circumstances under which traffic signals are beneficial to turbo roundabouts.

1.5. Problem approach

The question arises how the aim of the project can be accomplished. In other words: how can the capacity of the signalized turbo roundabout can be estimated? Basically, there are two ways to calculate the capacity of traffic circles: to build them in the actual traffic system and measure the capacity (field experiments), or to calculate the capacity by means of models. The first way yields reliable results (if the field measurements are performed correctly), but it is very expensive and the chance of creating traffic blunders is large. Other disadvantages are: collecting and analyzing measurements may take (very) long; multiple locations are needed for obtaining reliable data; the possibilities of adapting the intersection (flexibility) are limited; and dangerous situations might occur if the concept appears not to work. Therefore, traffic engineers commonly build models and assess those models, before deciding to actually implement a proposed solution. These models vary from general rules of thumb to advanced micro-simulation models. Models are also subject to some disadvantages. For instance, models are always a simplification of reality; the model developer cannot take into account any aspect he is ignorant of. The model developer is always challenged to invoke as many aspects into the model, so as to obtain results as reliable as possible. This project invokes models instead of field experiments.

Now the question remains how to evaluate the performance of the signalized turbo roundabout by means of models. Basically, there are two kinds of models by which the capacity of the signalized turbo roundabout can be calculated: analytical models and simulation models. This project includes both kinds of models. The analytical models to be applied are the *Meerstrooksrotondeverkenner* (MSRV) for the un-signalized turbo roundabout, and the black box approach for the signalized turbo roundabout. The simulation models to be applied is VISSIM [2].

[1] *From here on, the terminology signalized turbo roundabout will be used to indicate a turbo roundabout with traffic signals. Appendix A elaborates on a discussion with respect to this terminology.*

[2] *The choice for the selected models will be motivated in chapter 3.*

Performance indicators

The 'performance of intersections' cannot be assessed as such; performance indicators are necessary to compare the intersection types. Logically, the first and foremost indicator is capacity. The foremost reason for signalizing the turbo roundabout is to increase the capacity. If the capacity does not increase, then installing traffic signals does not make any sense. Another performance indicator is delay time. Chapter 2 (Literature review) will indicate that the metering signal reduces delay times on the turbo roundabout by 50%. In that sense, it would be interesting to draw conclusions on the influence of a full signalization on the delay times of the turbo roundabout. Also, space requirement is an important performance criterion, because it influences the construction costs of the intersection (the amount of land to acquire). For instance, although the turbo circle offers a higher capacity than the un-signalized turbo roundabout (Fortuijn, 2013), the turbo circle requires a lot more space. In general, the larger the intersection, the higher the capacity. Moreover, robustness is an important performance criterion, because it indicates the performance of an intersection if the prevailing traffic demand pattern differs from the pattern for which the intersection was designed. In synthesis studies, the performance indicators traffic safety and environmental considerations are important, especially with regard to the environmental impact assessment [3]. Although this project is not a synthesis study, invoking these indicators by formulating generic hypotheses and proposals for future research may add practical value to this research.

1.6. Research questions

From the problem statement, the research questions can be drawn. Their function is to structure the research and to state the focus of the project. From section 1.4, the following question arises:

Under what conditions does it make sense to apply traffic signals on turbo roundabouts?

In order to answer this question, un-signalized and signalized turbo roundabouts will be assessed based on the set of performance indicators. The first indicator is the capacity of the intersection. The first sub question will therefore be answered in chapter 2 (Literature review):

1. *Which models are suitable to calculate the capacity of the (un-)signalized turbo roundabout?*

As already mentioned, three models will be applied. Chapter 3 addresses why and how these models can be implemented to the (signalized) turbo roundabouts.

2. *How can the capacity of the (un-)signalized turbo roundabout be calculated by means of the MSRV?*
3. *How can the capacity of the (un-)signalized turbo roundabout be calculated by means of the black box approach?*
4. *How can the capacity of the (un-)signalized turbo roundabout be calculated by means of VISSIM?*

With respect to the other indicators [4]:

5. *What is the delay time on the (un-)signalized turbo roundabout?*
6. *What is the space requirement of the (un-)signalized turbo roundabout?*
7. *How can the robustness of the (un-)signalized turbo roundabout be assessed and is the signalized turbo roundabout more robust than the un-signalized turbo roundabout?*
8. *How can traffic safety be assessed and is the signalized turbo roundabout safer than the un-signalized turbo roundabout?*

[3] *In Dutch: milieueffectrapportage (m.e.r.)*

[4] *The reader should keep in mind that the main focus of the project is the capacity of the (un-)signalized turbo roundabout; therefore the other criteria will not be paid as much attention to as the capacity criterion.*

9. *How can the environmental burden caused by an intersection be assessed, and does the signalized turbo roundabout cause a smaller environmental burden than the un-signalized turbo roundabout?*

1.7. Structure of the report

This project starts with an overview of all knowledge that has already been gathered on the subject, in order to prevent from including issues that have already been studied, thereby performing 'double work'. Therefore, chapter 2 will be devoted to a literature review. In that chapter, the fundamentals of the MSRV, the black box method and VISSIM will be explained and the possibilities of traffic signals and control types on the turbo roundabout will be discovered.

The third chapter (Experimental design) will delineate the project, in order to determine the scope. Furthermore, the third chapter explains how the capacity of the (signalized) turbo roundabout can be evaluated by means of the MSRV, the black box approach and VISSIM. The choice to apply these models will be motivated. The application of the models to the (un-)signalized turbo roundabout will be explained as well, but the calculations are carried out in the following chapters.

The fourth chapter elaborates on the calculations of the capacity modelling by means of the MSRV, the black box approach and VISSIM.

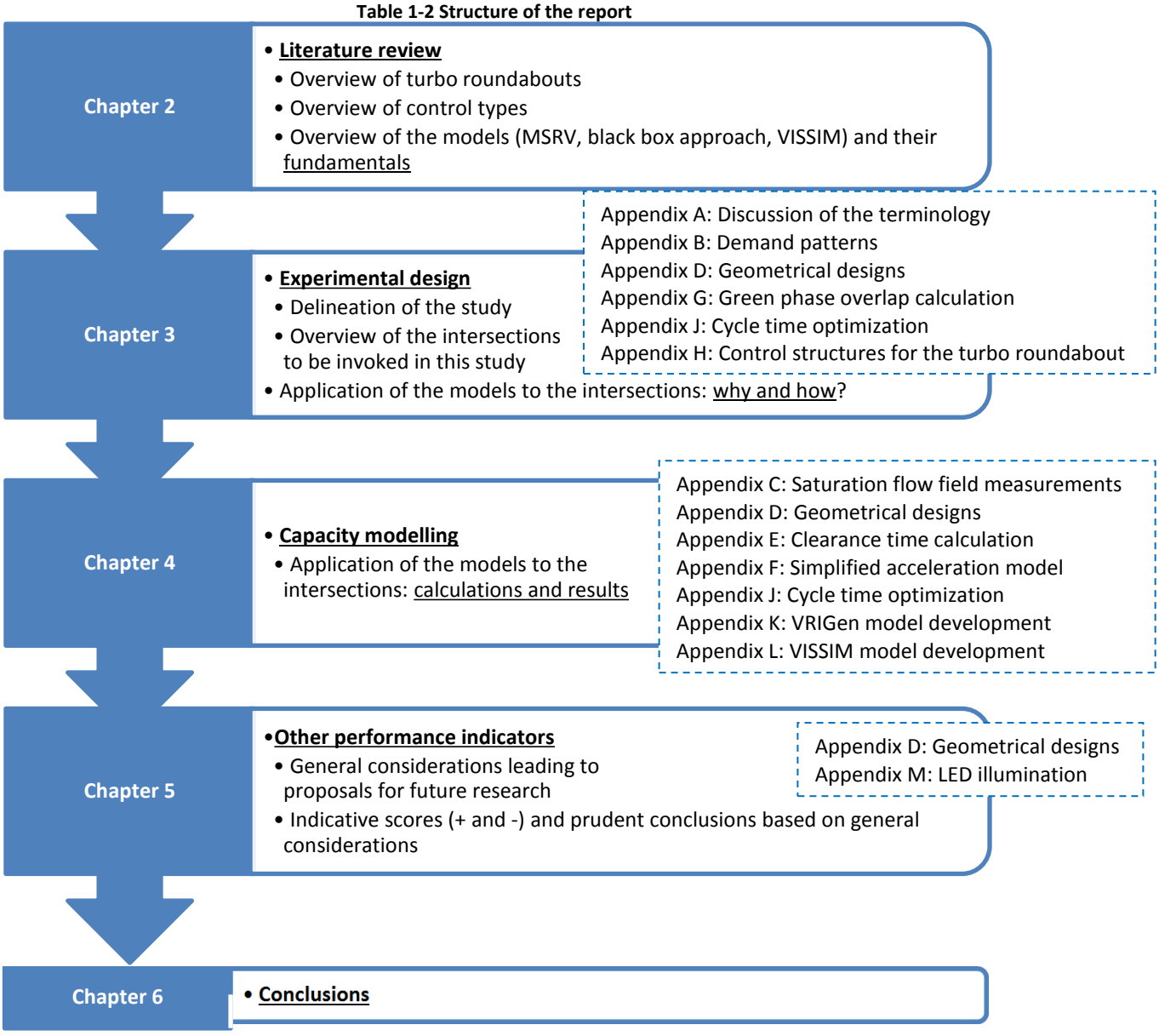
The fifth chapter (Other performance indicators) pays attention to the other performance indicators. As indicated in the previous sections, the focus of this chapter will be dedicated to the capacity. Chapter 5 will present general considerations, mainly based on literature and rationality. Finally, a set of hypotheses will be formulated based on the considerations; these are proposals for future research.

The balance will be made in chapter 6 (Conclusions). The results of the calculations in chapter 4 and the scores on the performance indicators in chapter 5 will be summarized and compared in an overview. From these findings, the conclusions will be drawn and the implications for scientific studies and practical implementation will be outlined. Finally, chapter 6 will present an overview of proposals for future research.

Chapter 7 presents a reflection on the process of the graduation project.

Table 1-2 presents an schematic overview of the report.

Table 1-2 Structure of the report



2. Literature review: possibilities for signalizing turbo roundabouts

This chapter presents a literature review: all knowledge already developed with respect to the topic of this project, will be addressed. First, the attention will be aimed at turbo roundabout types. In the second section, recent study on the metering signal will be addressed. The third section addresses two control structures: the leg-by-leg control and the two-phase control, and their applicability to the signalized turbo roundabout. The fourth section presents the fundamentals of the models to be applied in this study: the MSRV, the black box approach and VISSIM. The chapter finalizes with a summary and conclusions.

2.1. Rotor and star roundabout: design and capacity

Fortuijn (2009) introduced the roundabout, he distinguished six elementary types: the knee roundabout, star roundabout (Figure 2-1), the egg roundabout, the basic turbo roundabout, the spiral roundabout and the rotor roundabout (Figure 2-2).

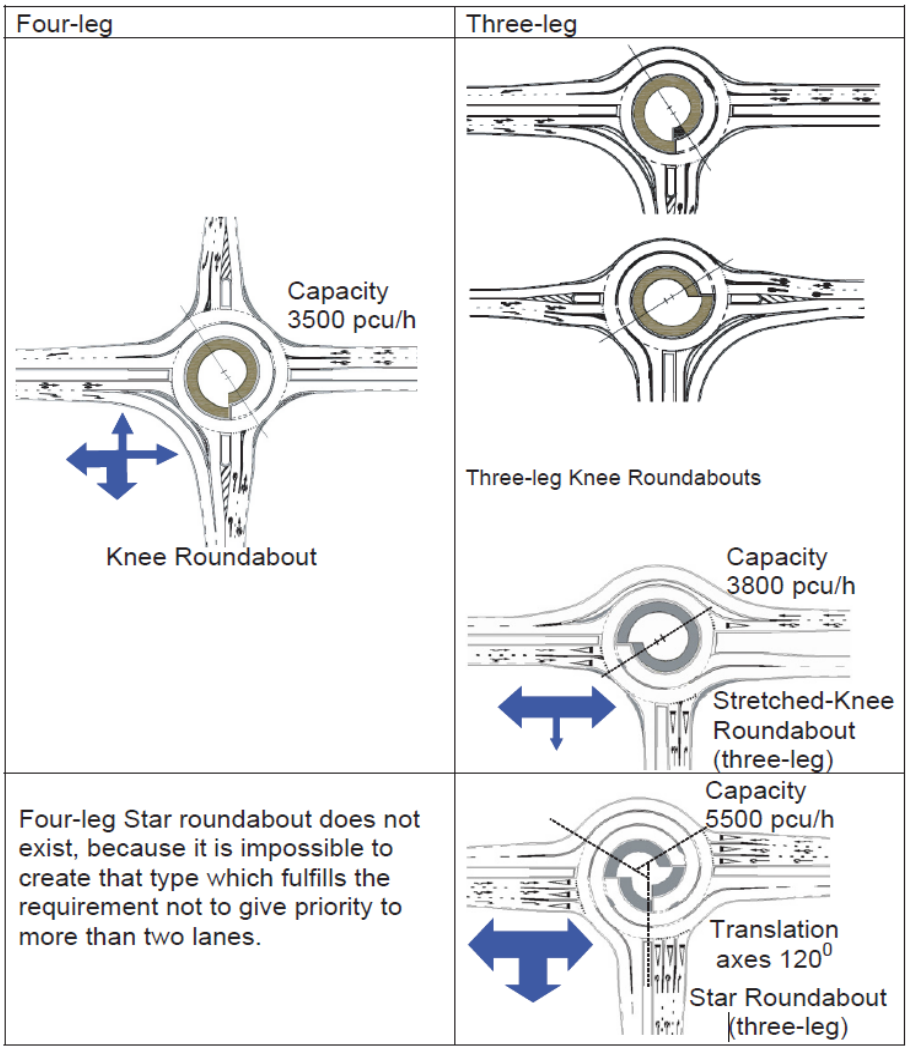


Figure 2-1 The designs, main directions [5] and capacity of the turbo roundabout types (subtracted from Fortuijn, 2009, p.18)

[5] *The main directions are the directions in which the intersection offers the highest capacity.*

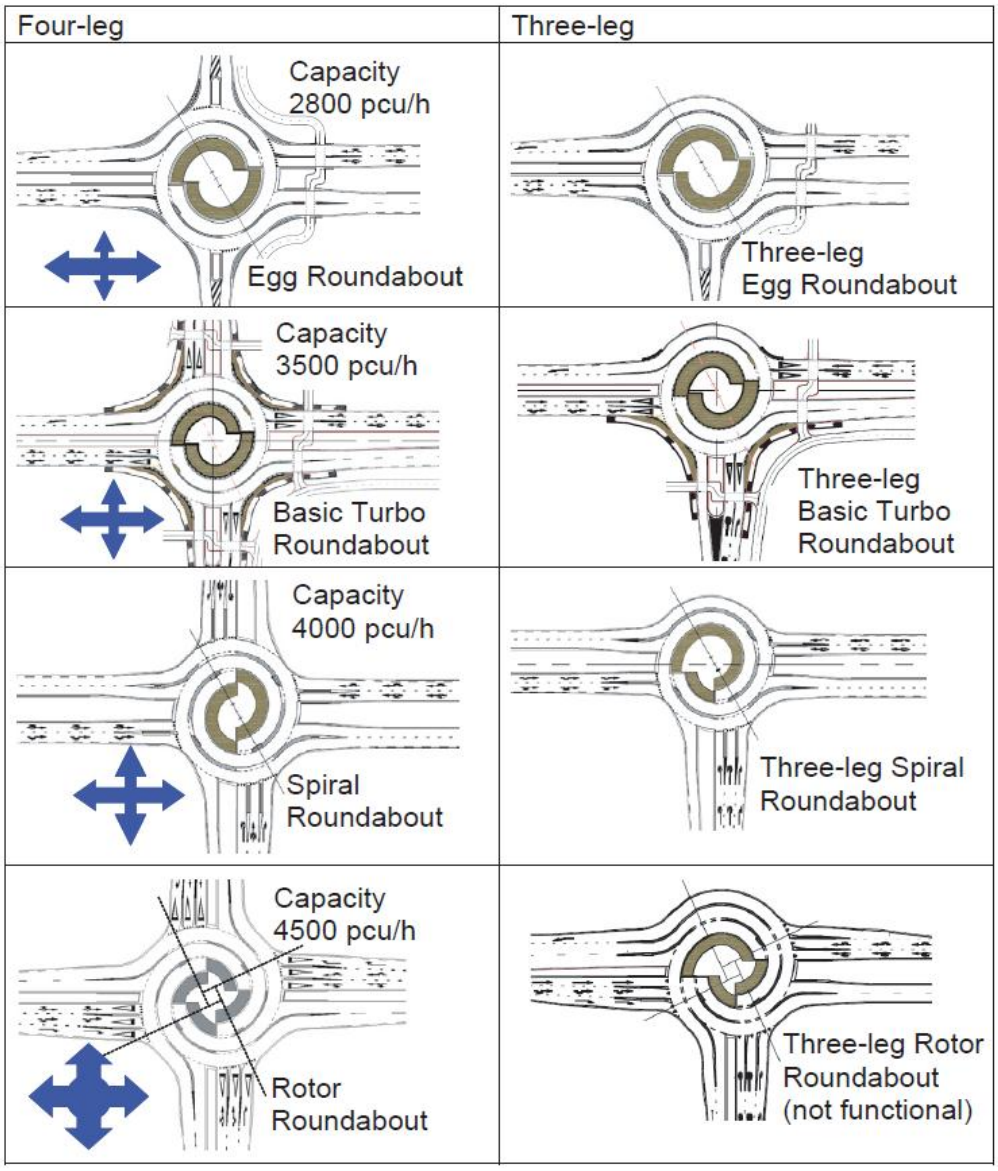


Figure 2-2 The designs, main directions and capacity of the turbo roundabout types (subtracted from Fortuijn, 2009, p.18)

The notion that the turbo roundabout types contain main directions, implies that the capacity depends on the prevailing demand pattern. (Therefore, this project will apply a specific set of demand patterns, to be explained in chapter 3: Experimental design). The capacity values in Fortuijn (2009) are calculated based on a large variety of demand patterns.

2.2. Roundabout metering signal

Fortuijn (2013) describes the concept of the turbo roundabout and the turbo circle. The turbo roundabout is un-signalized by definition. However, Fortuijn (2013, chapter 5) proposed to equip the turbo roundabout with traffic signals. In general, he proposed two possibilities for signalizing the turbo roundabout: by means of a roundabout metering signal (one leg signalized) and a full signalization (all legs signalized). Granneman (2011) has investigated the roundabout metering signal, where only one leg is equipped with a traffic signal. One of his conclusions is that the metering signal may increase the capacity of the roundabout by ca. 10%. The total delay time may decrease by ca. 50%. The magnitude of these

beneficial influences depends on the prevailing demand pattern. In particular, the influence is large if one of the legs is highly saturated, compared to the other legs.

In this research project, the attention will be focussed on fully signalized turbo roundabouts. With the beneficial influence of the metering signal in mind, the question can be posed whether the benefit of traffic signals on all legs of the turbo roundabout is larger than the metering signal.

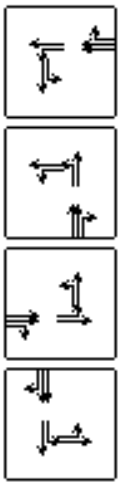
2.3. Control structures

This section explores the control types by which a fully signalized turbo roundabout can be managed. Fortuijn (2013) describes two control types: the leg-by-leg control and the two-phase control.

2.3.1. Leg-by-leg control

As its name implies, the leg-by-leg control serves every leg separately. Every leg obtains green in one distinct stage of the control. Consequentially, the leg-by-leg control consists of four stages for a four-leg intersection, such as the rotor roundabout. The leg-by-leg control consists of three stages for a three-leg intersection, such as the star roundabout.

Figure 2-3 illustrates the leg-by-leg control on the four-leg intersection. The signalized turbo roundabout contains main signals (01 through 12) on the entrance legs and interception signals [6] (62 through 72) on the circulatory roadways. Principally, the stages in the leg-by-leg control can obtain any (random) sequence. In order to maximize capacity, the leg-by-leg control should 'turn clockwise': firstly the eastern leg, then the southern leg, then the western leg and finally the northern leg [7]. The reason for this, is that in that case the green phase overlap can be used optimally.



Stage 1: Eastern leg
Streams 01, 02, 03,
62, 63, 71 and 72

Stage 2: Southern leg
Streams 04, 05, 06,
65, 66, 62 and 63

Stage 3: Western leg
Streams 07, 08, 09,
68, 69, 65 and 66

Stage 4: Northern leg
Streams 10, 11, 12,

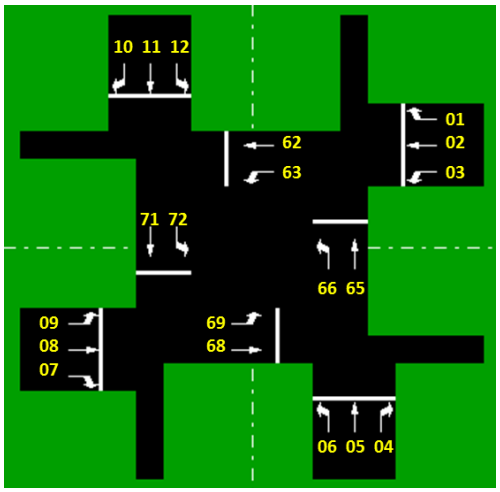


Figure 2-3 In the leg-by-leg control, every leg is served in one stage

Green phase overlap and the clockwise control

Imagine a clockwise leg-by-leg control program on the roundabout, starting on the eastern leg (leg E). After leg E has been served, the southern leg (leg S) will be served, then the western leg (leg W) and finally the northern leg (leg N). At the moment leg N has been served and leg E obtains green, the full

[6] *In Dutch: opvanglichten. These are traffic signals aside the circulatory roadways, in order to secure the conflict area between the circulatory roadways and the entrance leg.*

[7] *It is not important which direction is first, only the order.*

cycle has been covered; the duration of the cycle is called *cycle time* [8]. The traffic circulates counter-clockwise on the roundabout, so the green phase of leg S may already start when leg E still has green (or yellow) [9], because the traffic from leg S has to cover the length of the road stretch between legs S and E before it reaches the conflict area with leg E. The time interval in which both legs obtain green simultaneously, is called *green phase overlap*. In order to obtain green phase overlap, the first departing vehicle from leg S should take at least 3 seconds to arrive at the stop line of the interception signal (65 or 66), because:

- the yellow time of leg E lasts for 3 seconds;
- the green phase of interception signals 65 and 66 may start with or after the end of the yellow phase of leg E.

A roundabout with a counter-clockwise control program suffers from internal lost times, because the green phase of a leg can start after the yellow phase end of the former leg, plus the time it takes to cover the length of the road stretch between the legs. The time to cover the distance between the stop line of a leg and the nearest border of a conflict area, is called *clearance time* [10]. In conclusion: in case of a clockwise control program, the green phase of a leg can start at the end of the yellow phase of the former leg *minus* the clearance time, and in case of a counter-clockwise control program, the green phase of a leg can start at the end of the yellow phase of the former leg *plus* the clearance time. Therefore, a clockwise control program is always preferred.

Influence of the diameter

The green phase overlap depends on the diameter of the roundabout: as the diameter increases, the length of the road stretch between every pair of neighbouring entrance legs increases, and the green phase overlap increases. This yields the presumption that the larger the signalized turbo roundabout, the higher the capacity [11].

2.3.2. Two-phase control

The two-phase control serves all traffic streams in two stages [12]. Figure 2-4 illustrates the two-phase control. In one phase, two opposing legs obtain green, while the two left-turning streams queue up on the traffic circle. This is the reason why an intersection with a two-phase control should offer sufficient queuing space on the intersection itself; the two-phase control is not efficient in case of busy left-turning streams.

---

[8] *Theoretically, the longer the cycle time, the higher the capacity of the intersection (Muller, 2011), because the saturation flow increases as the green period increases and internal lost time per hour decreases. In Dutch practice, the cycle time is bound to 120 s. From that limit on, the capacity does not increase significantly and the waiting times grow so large, that the traffic control is not effective anymore and another intersection solution should be designed.*

[9] *The order of the phases is: green – yellow – red – green – … This order is used in The Netherlands and many other western countries. The end of the yellow phase is equal to the start of the red phase; the end of the red phase is equal to the start of the green phase; the end of the green phase is equal to the start of the yellow phase. This project assumes that the yellow phase duration is 3 seconds. This duration of the yellow time is derived from CROW (2006). The value will be applied during the entire research project.*

[10] *The concept of clearance time is more complex, but this explanation is provided in order to comprehend the choice for a clockwise traffic control. In the following section more information on the clearance time.*

[11] *This presumption will be shown to be false in chapter 4 (Capacity modeling).*

[12] *The terminology stages and phases are inconsistently used in literature. This is quite confusing, because the word phase is used for a stage in the traffic control, and for indicating the state of a traffic light (green phase, yellow phase, red phase). The two-phase control is called as it is, because it is the name given by its author. The name two-stage control would be more adequate.*

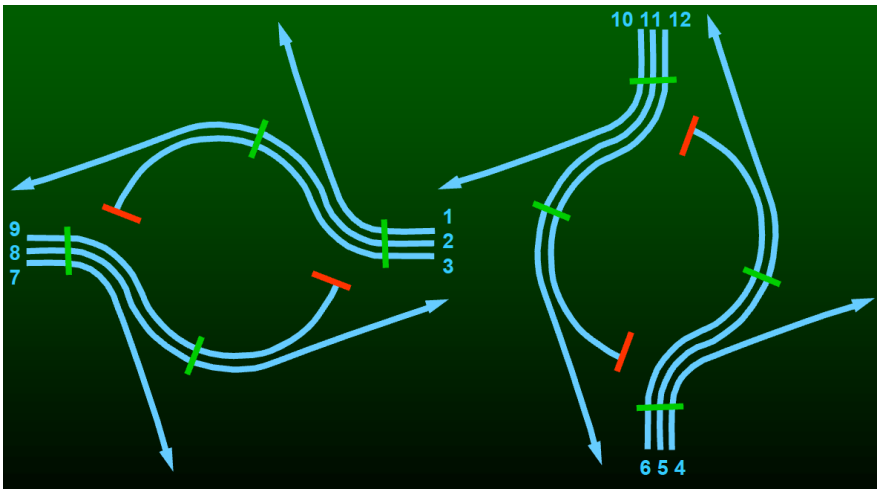


Figure 2-4 The two-phase diagram of the turbo circle (Fortuijn, 2011)

Basically, two phase transitions are possible, shown in Figure 2-5 (left). On the one hand: leg W obtains red while the green phase of leg E still continues (1a). Consequentially, stream 03 will flow unhindered by red phases of 63 or 71 for a certain time interval. Afterwards, leg S may obtain green ($1a^{I}$) or leg E obtains red in order have the queued vehicles in stream 65 to flow off ($1a^{II}$). On the other hand: leg E obtains red while the green phase of leg W still continues (1b). Then stream 09 will not have to queue up for a certain time interval. Afterwards, leg N may obtain green ($1b^{I}$) or leg W obtains red in order to have the queued vehicles in stream 71 to flow off ($1b^{II}$)

In this project, a specific set of demand patterns will be used to determine the capacity of the partial turbo circle (see appendix B: Demand patterns). In those demand patterns, stream 08 accounts for 80% of stream 02. Therefore, the phase transition via sub-phase 1a seems the most logical sequence. In phase 1, the left-turning vehicles in streams 03 and 09 will queue up on the circle. If streams 05 and 06 (and 11, 12) would obtain green immediately after 09 (and 03) obtained red (as in sub-phase $1a^{I}$), the vehicles on streams 05 and 06 (and 11, 12) would probably be blocked by the queued vehicles. In conclusion, the phase transition 1 – 1a – $1a^{II}$ – $1a^{III}$ – 2 seems the most logical sequence.

2.3.3. Leg-by-leg control vs. two-phase control

Bureau Goudappel Coffeng (1987) concluded that the two-phase control is more efficient than the leg-by-leg control, regarding the traffic flow. The reason for this is that in one stage, more streams are being served, and therefore less stages are necessary in one cycle. However, the leg-by-leg control might be preferred in situations with busy left-turning streams, because the two-phase control needs a lot of space to store the left-turning vehicles. If the available queuing space is insufficient, the traffic circle may be blocked by the left-turning vehicles.

2.3.4. Signalized turbo roundabout: leg-by-leg control

The characteristics of the turbo roundabout have been presented in the introduction (see Figure 1-6). One of the characteristics is the presence of at least one choice lane on the turbo roundabout. The choice lanes are illustrated by means of Figure 2-6, showing that the rotor roundabout contains four choice lanes (one on every exit leg). In the choice between a leg-by-leg control and a two-phase control, these choice lanes exclude the possibility of applying the two-phase control to the rotor roundabout. In a two-phase control the left-turning vehicles have to queue up. On a rotor roundabout, they would block the passage for the straight-ahead vehicles using the left entrance lane, and thereby cause spill-back. The spill-back effect might be so prominent, that the queuing vehicles cause a gridlock on the rotor roundabout. To prevent this, vehicles should not queue up on the rotor roundabout.

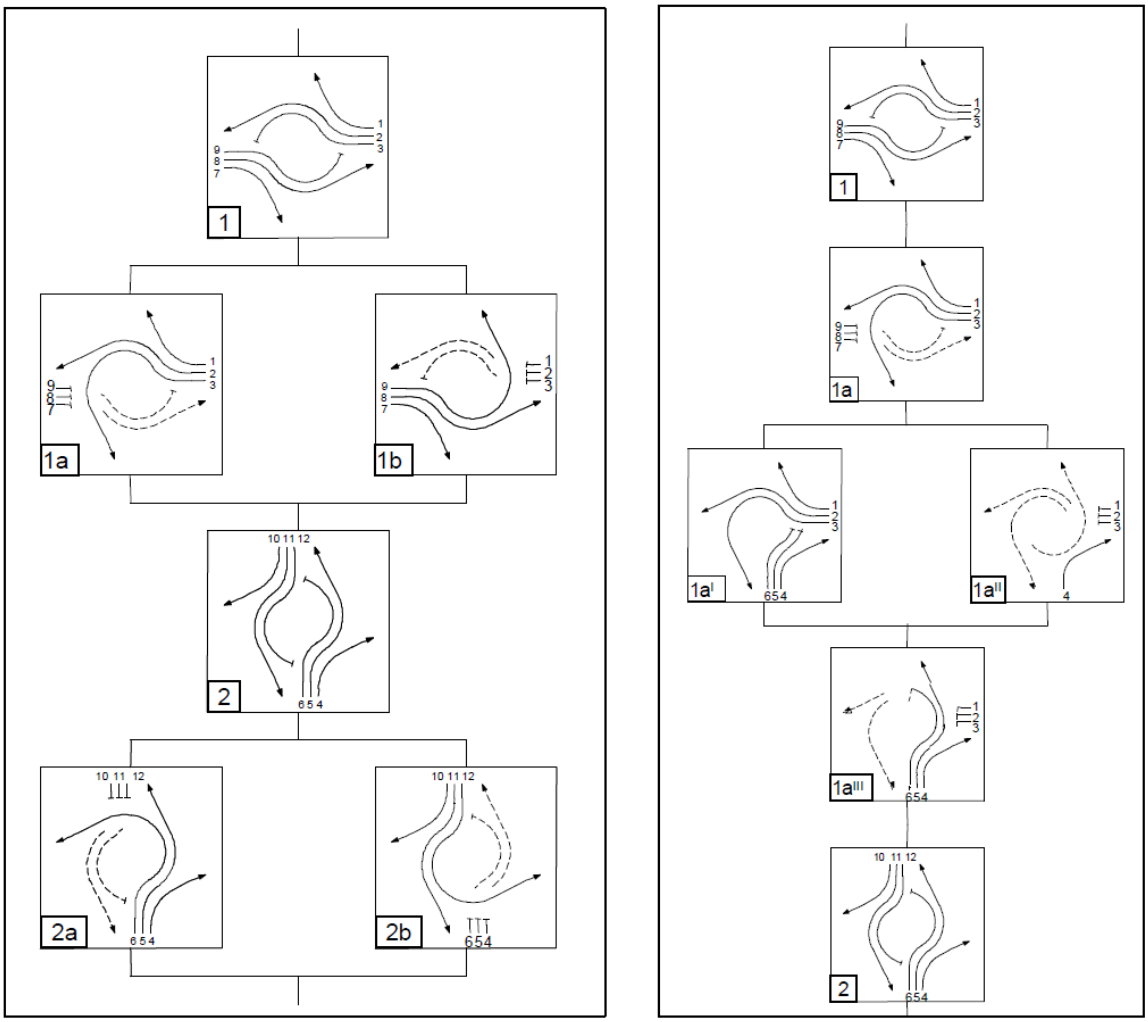


Figure 2-5 Two phase transitions are possible in the two-phase control (subtracted from Fortuijn, 2013, p.329)

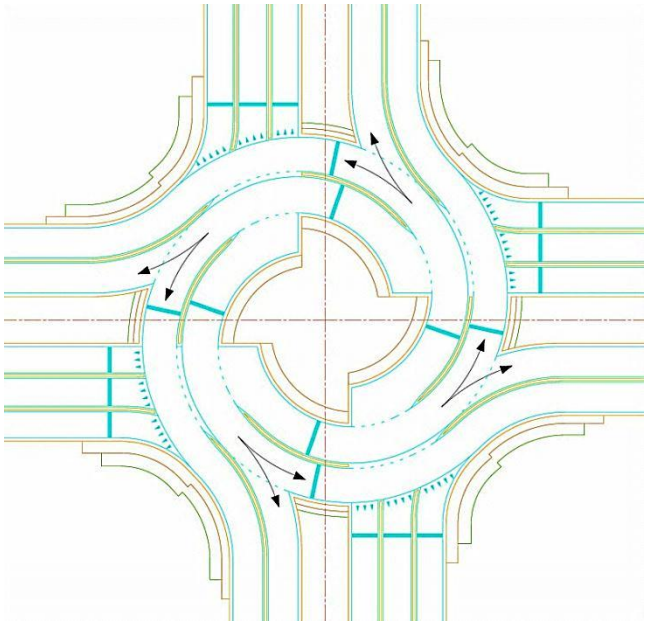


Figure 2-6 Geometrical design of the rotor roundabout, the arrows indicate the choice lanes

2.3.5. Turbo circle: two-phase control

The turbo circle (illustrated by Figure 2-7) offers the left-turning streams dedicated lanes, and therefore offers the possibility of queuing up on the circle itself, without causing a gridlock. The turbo circle is suitable for a two-phase control.

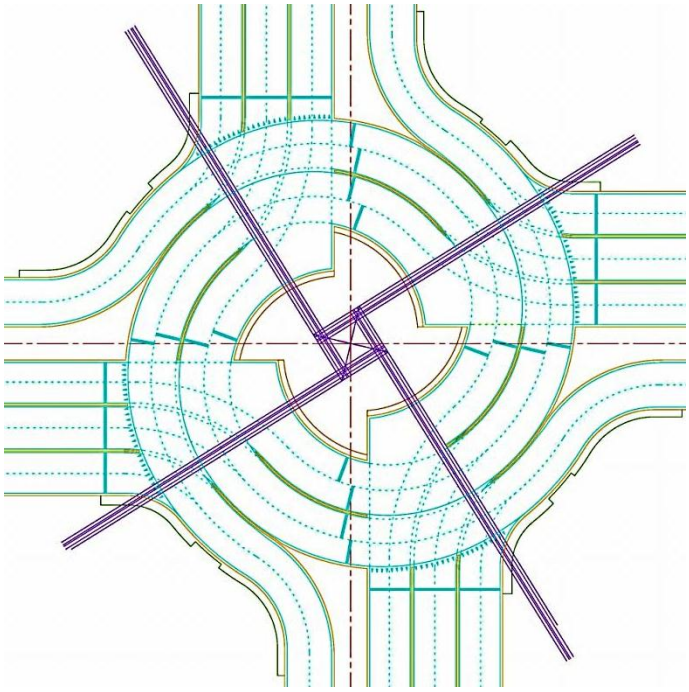


Figure 2-7 Geometrical design of the turbo circle

2.4. Models for evaluating the capacity

For the evaluation of the capacity of turbo roundabouts, multiple models can be used. This section will discuss the fundamentals of three models: the MSRV, the black box approach, and VISSIM.

2.4.1. MSRV

The MSRV (*Meerstrooksrotondeverkenner* – Multilane Roundabout Explorer) is an analytical tool, especially designed to estimate the capacity of the un-signalized turbo roundabout. The MSRV is a computer program, that appears as an Excel-spreadsheet (Figure 2-8). It has been founded at the TNO Institute for Spatial Organization (Arem, 1992), and has been developed and extended since then continuously. Nowadays, it is suitable to analyze traffic flow on single- and multilane roundabouts (in particular, the turbo roundabout). The model has been validated by means of various Dutch field measurements.

The Excel-spreadsheet contains a set of formulas derived from various analytical capacity studies. Arem presents an overview of these studies and the formulas. While developing the MSRV, a selection has been made based on the nature and magnitude of input data, past validation of the formulas, computation time and consistency with the MSRV.

Figure 2-8 shows the input for the spreadsheet: the prevailing traffic demand. Moreover, the output of the spreadsheet consists of the degree of saturation (column VG – *verzadigingsgraad*) and the average waiting time (Tgem – *gemiddelde wachttijd*).

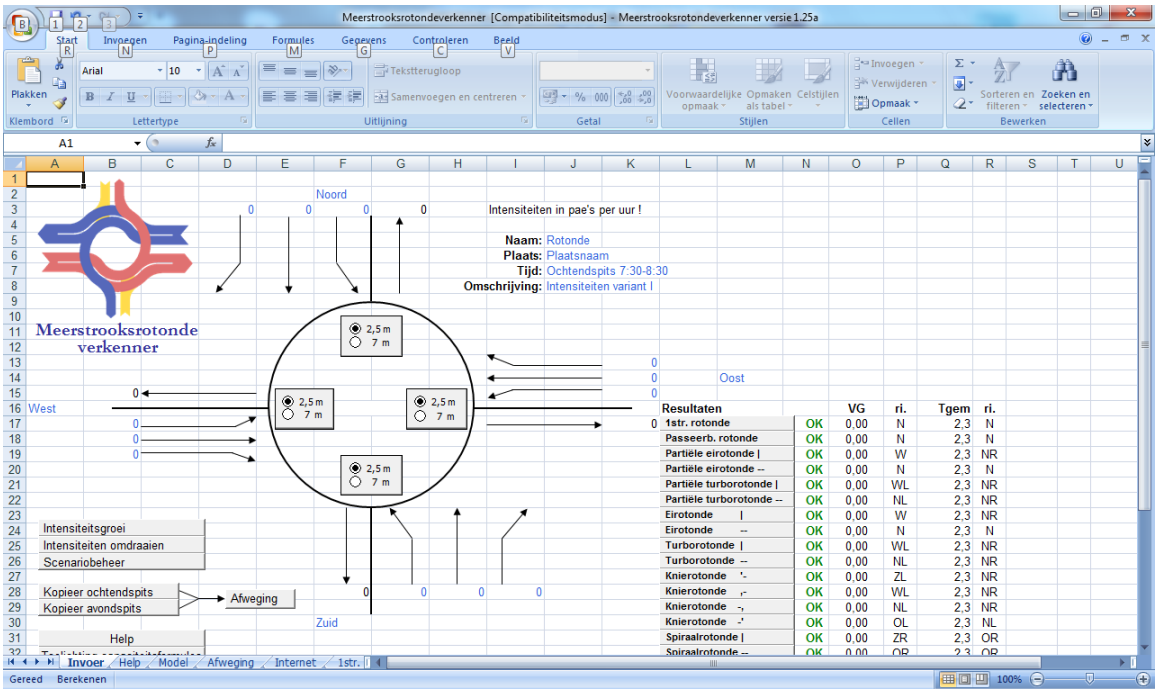


Figure 2-8 User interface of the MSRV

2.4.2. Black box approach

Fortuijn (2013, p.115) introduces a method by which the capacity of a signalized (turbo) roundabout can be estimated, called the *black box approach*. This model applies the general idea of the black box, depicted by Figure 2-9. Here, the black box contains a number of transfer characteristics, which use the input variables to compose the output.

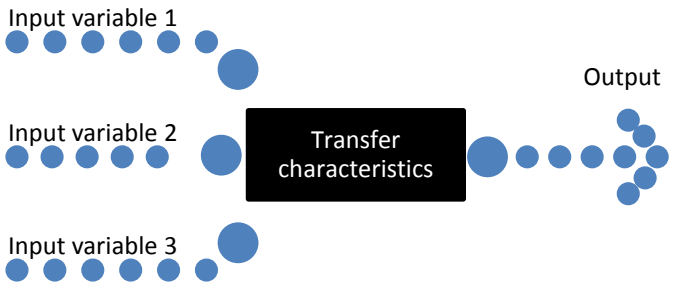


Figure 2-9 General overview of a black box, the number of input variables might be larger or smaller

In the *black box approach*, the capacity of the roundabout is considered equal to the amount of vehicles that can flow onto the roundabout from the entrance legs. The determinants of this inflow are the effective green time per leg, aggregated over one hour, and the hourly saturation flow per leg. The sum of the capacities of all legs is the roundabout capacity. In terms of the general idea of the black box: the input variables are the amount of legs, the green time of a leg and the saturation flow on the same leg. The roundabout is the black box; the traffic process on the roundabout is not being considered. Instead, the assumption is being made that traffic on the roundabout can flow freely; the internal lost times on the roundabout is zero. The output of the *black box approach* is the capacity of the roundabout.

The aggregated green time in one cycle is influenced by the phase overlap. Fortuijn applies the method to a single-lane roundabout and the basic turbo roundabout. In order to illustrate the *black box approach*, the method will be applied to the single-lane roundabout in the next paragraph.

On an average single-lane roundabout with a diameter of 20 to 25 m, the green phase overlap is 0 s (there is no overlap) [13], so the aggregated green time in one hour is 3600 s. The average saturation flow is 1700 to 1750 pcu/h; resulting in a capacity of 1700 to 1750 pcu/h. The capacity of a non-signalized single-lane roundabout is 2000 to 2500 pcu/h (CROW, 1998), so traffic signals on single-lane roundabouts are not beneficial.

2.4.3. Simulation models

There are multiple microscopic simulation tools for evaluating the traffic flow on a random infrastructural network. Examples are *VISSIM* (a tool of German origin and applied in many European countries), *Paramics* (frequently used in the UK and the USA) and *Aimsun* (a tool of Spanish origin). In all simulation models, the traffic flow is being evaluated mainly based on three input parameters: the infrastructural network (a set of links, nodes, traffic management systems, priority rules, etc.), the traffic demand (the OD-matrix, stating the amount of vehicles per unit of time travelling from each origin node to each destination node), and microscopic behavioural models (e.g. longitudinal and lateral models, the car-following model, behaviour near traffic signals, etc.). Microscopic simulation tools simulate traffic applying a random seed. The random seed is an integer, and it enables the user to take into account of stochasticity: coincidental factors, such as weather conditions and variability in driving behaviour.

A disadvantage of simulation models is the computation time. Depending on the magnitude of the network, the desired output and the amount of random seeds to be applied. Another disadvantage is that the pseudo-conflict [14] on the roundabout cannot be modeled properly in VISSIM. Van Beinum (2007) studied the possibility of modelling the pseudo-conflict in VISSIM, and concluded that an extensive calibration procedure is necessary to model the pseudo-conflict reliably. Unfortunately, calibration is not possible in this project.

Simulation models offer the possibility to measure a lot of performance indicators in the network, such as the actual traffic flow at any road section, travel and delay times on any road stretch, individual vehicle data (e.g. speed and acceleration) and the amount of lane changes on any road stretch.

VRIGen and TrafCOD

Chapter 3 (Experimental design) motivates why VISSIM will be used in this project. VISSIM applies VRIGen and TrafCOD to generate a traffic control for the signalized turbo roundabouts. VRIGen is based on an analytical model, it is developed for generating control programs for conventional non-circular signalized intersections. VISSIM applies TrafCOD to turn the fixed control, generated by VRIGen, into a vehicle-actuated control. Thereby, extension green can be assigned according to the prevailing arrival pattern.

2.5. Summary and conclusions

Fortuijn (2013) introduced the turbo roundabout; this intersection solution appears in six types with different geometrical designs, main directions and capacities. Simultaneously, Fortuijn proposed to ways of signalizing the turbo roundabout: the metering signal and the (fully) signalized roundabout. Granneman (2011) explored the benefits of the metering signal.

The signalized turbo roundabout is only suitable for the leg-by-leg control, this is due to the presence of choice lanes on the connection between the circulatory roadway every exit leg. The turbo circle is suitable for the more efficient two-phase control.

---

[13] *Calculated by means of the calculation method in CROW (1996).*

[14] *The pseudo-conflict is an event; it happens when a vehicle on an approach lane decelerates in order to yield to a vehicle on the circulatory roadway, while the latter vehicle leaves the circulatory roadway. This is not a physical conflict, but the driver on the approach lane perceives a conflict with another vehicle.*

Three model types are applicable to calculate the capacity of the (un-)signalized turbo roundabout: the MSRV, the *black box approach* and simulation models. The MSRV is a spreadsheet, in which the input consists of the prevailing demand pattern. The output consists of the saturation rate of and delay time on any turbo roundabout type. The *black box approach* is an analytical model developed by Fortuijn (2013). This model is developed simultaneously with the turbo roundabout; it is especially designed for calculating the capacity of the signalized turbo roundabout. VISSIM is a microscopic simulation model, in which any infrastructural network (such as the signalized turbo roundabout) can be modelled.

3. Experimental design

This chapter describes the experimental design; an explanation of how this study will be carried out. The first section will delineate the study; the scope will be described. In the second section, the three models will be addressed, by which the capacities of the signalized turbo roundabouts will be calculated. The previous chapter described their fundamentals, this chapter will elaborate on why and how the models will be applied to the signalized turbo roundabouts. The third section explains the evaluation method, describing how the scores on the performance indicators will be weighed. The fourth section motivates why validation of the results of the models is not possible. The chapter finalizes with a summary and conclusions.

3.1. Delineation of the project

This section describes the boundaries of the project: the choices about what is within the scope of the study and what is not. This delineation is necessary for two reasons. Firstly, the project is constrained to a time limitation [15]. Secondly, the comprehensibility of the study decreases as the magnitude increases. Together with the boundaries of the project, proposals for future research will be formulated.

The delineation comprises four aspects of the study. In the first section, the differences between turbo roundabouts inside and outside the urban area will be addressed, together with the arguments for invoking only turbo roundabouts outside the urban area in this study. The second section motivates why it is not sensible to invoke all six turbo roundabout types in this study; only the rotor and star roundabouts will be studied. The third section discovers the possibilities to adjust the rotor and star roundabouts such, that they are suitable for the two-phase control. The fourth section pays attention to the set of demand patterns to be invoked in this study.

3.1.1. Inside or outside the urban area?

When studying roundabouts, it is important to distinguish between roundabouts inside and outside the urban area, for two reasons:

- On roundabouts inside the urban area, slow traffic streams (cyclists and pedestrians) are often present. Therefore, it is common practice that these traffic streams are only being invoked in studies on roundabouts inside the urban area. In models of roundabouts outside the urban area, slow traffic streams are often excluded.
- In The Netherlands, roundabouts inside the urban area are not equipped with side marking, roundabouts outside the urban area are. This has consequences for the design of the turbo roundabout. In particular, the presence of lane marking has consequences for the circulatory lane width, and therefore on the diameter of the roundabout. The diameter influences the required space of the intersection, which is one of the assessment criteria in this project.

This project investigates roundabouts outside the urban area for the following reason. The research questions inquire for the influence of traffic signals on the capacity of turbo roundabouts. By installing traffic signals, the elementary traffic flow process on the roundabout is being altered: the pre-emption is no longer assigned to vehicles on the circulatory roadways, but to vehicles in the traffic streams obtaining green. This change in traffic flow influences the capacity, to be investigated. On the other hand, slow traffic streams also influence the capacity of the intersection, but in an entirely different way. This project is solely interested in the influence of traffic signals. Therefore, in order to reduce the influence of slow traffic streams, they will not be regarded.

[15] *Commonly, graduation projects in The Netherlands are performed within six months.*

Moreover, Dutch design guidelines discourage the single-level pedestrian and cycle crossings on turbo roundabouts (CROW, 2008), especially on the rotor and star roundabouts, because are the largest types containing three lanes per entrance leg. Crossing three entrance lanes at once is quite a heavy and unsafe task for the cyclist and pedestrian. This is another reason to exclude slow traffic streams from the models.

3.1.2. Choice for turbo roundabout types

In principle, every roundabout can be equipped with traffic signals, but under which conditions does it make sense?

Single-lane roundabouts

Traffic signals are not recommended to the single-lane roundabout, because they do not enhance the capacity, on the contrary. This is illustrated by the example in section 2.4.2 (Literature study into the *black box approach*).

Multilane roundabouts

Under certain conditions, it is recommended to apply traffic signals to roundabouts. One strict condition has already been stated in the introduction: on a roundabout on which the entering traffic has to give priority to circulatory traffic on more than two lanes, traffic signals are necessary out of safety considerations, regardless of the traffic demand.

Whereas the single-lane roundabout allows for one lane on the approach legs, multilane roundabouts allow for multiple lanes on the approaching lanes. According to the *black box approach*, a signalized double-lane roundabout should provide a capacity of 3400 to 3500 pcu/h; similar to the capacity of the basic turbo roundabout (Fortuijn, 2011, p.115). In conclusion, the utility of traffic signals on multilane roundabouts is likely to be higher than the utility of traffic signals on single-lane roundabouts. This notion gives rise to the assumption that the probability that traffic signals enhance the capacity of turbo roundabouts, increases as the amount of lanes on the entrance legs increases.

Turbo roundabouts

Effectively, the turbo roundabout types with the largest amount lanes per approach leg should be chosen first, to investigate the influence of traffic signals. The largest types are the rotor roundabout (four-leg) and the star roundabout (three-leg).

The rotor and star roundabouts will be invoked in the project at first hand. If traffic signals appear to enhance the capacity of these types, investigating the smaller types would be recommended. If the capacity of the largest types does not benefit from traffic signals, then the smaller types are probably not worth investigating.

3.1.3. Signalized turbo roundabout and two-phase control

The literature study drew two important conclusions with respect to signalized turbo roundabouts: the turbo roundabout is not suitable for the two-phase control, and the two-phase control is more efficient than the leg-by-leg control. Therefore, it would be interesting to investigate the possibilities for adjusting the rotor and star roundabouts such, that it is suitable for the two-phase control.

Geometrical adaptations

The two-phase control cannot be applied to the rotor roundabout because it contains choice lanes on the connection with every exit leg (see Figure 2-6). The straight-ahead streams should be prevented from being blocked by the left-turning streams. This goal can be pursued in two ways:

- Widening the splitter islands of the legs, thereby creating more space for the left-turning vehicles to queue on the roundabout;
- Removing the direction choice on the circulating lanes.

Both solution directions require major geometrical changes to the turbo roundabout. With respect to the first solution direction: the roundabout by definition has perpendicularly joining legs (according to Dutch guidelines). The purpose of perpendicular joining entrance legs is to sharpen the driving curve, so to create a comfort incentive for the road user to slow down, thereby enhancing traffic safety on the intersection (CROW, 1998). If the splitter islands are being widened in order to offer more queuing space, the driving curve is not as sharp anymore; the average velocity will increase, affecting traffic safety negatively. From appendix D (Geometrical designs) can be concluded that the entrance curve almost immediately transfers to the exit curve. That means, that as the exit curve shifts outward (increasing the width of the splitter island), the entrance and exit curves become one curve. This increases the space requirement of the rotor roundabout, even for a very small shift outward. Therefore, it is not sensible to design the rotor roundabout with wide splitter islands.

Furthermore, it is not robust, because any perturbation causing (temporarily) higher left-turning intensities would block the roundabout. The first solution direction will not be further investigated.

With respect to the second solution direction: the circulating lanes offering a route choice need to be removed. In that case, the connection of the legs to the circulatory roadways and the turboblock itself need to be changed. This design process will be elaborated on in appendix D. The result – the four-leg partial turbo circle (adjusted rotor roundabout) – is illustrated by Figure 3-1. Appendix A (Discussion of the terminology) addresses a motivation for the terminology *partial turbo circle*.

The adjustment can be made to the star roundabout as well; the result is a three-leg turbo circle with one lane per stream. This roundabout is suitable for a two-phase control in which left-turning traffic from the eastern leg queues up on the roundabout. The queuing space is quite limited, because only one lane is available for queuing. Therefore, the cycle time of the traffic control must probably be very short. The queuing space can be enlarged by increasing the diameter of the roundabout or by adding an extra lane. Both solution directions increase the required space of the intersection. Moreover, increasing the diameter will create space for an extra lane. Therefore, the remainder of this project invokes the three-leg turbo circle with two lanes for streams 03, 06 and 08, see Figure 3-2.

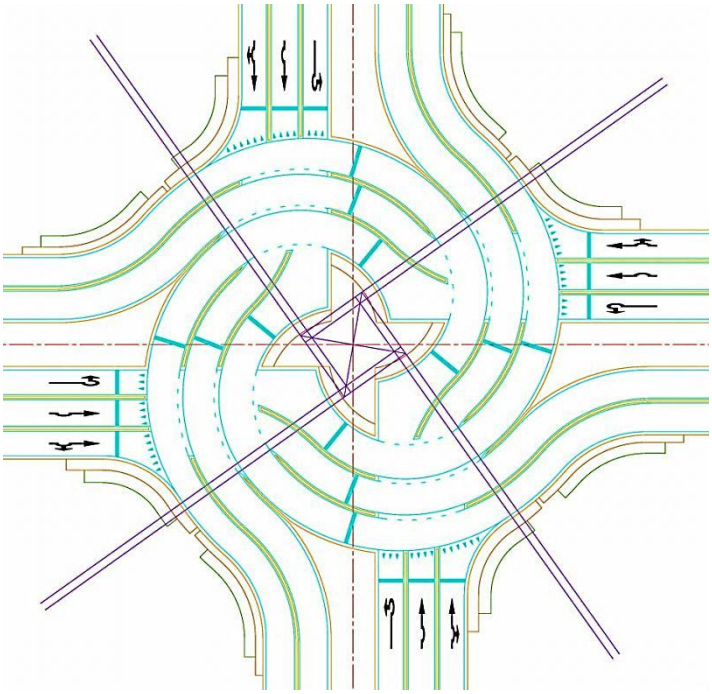


Figure 3-1 Geometrical design of the partial turbo circle

On the three-leg turbo circle, only vehicles in stream 03 (the left-turning stream on the eastern leg) have to queue up on the circle, where on the four-leg turbo circle, vehicles in all four left-turning streams have to queue up on the circle.

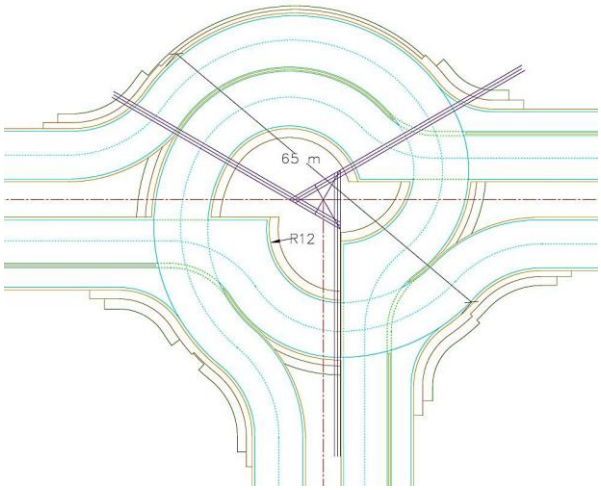


Figure 3-2 The three-leg turbo circle

Implications for the spatial requirement: diameter constraints

The statements that the two-phase control is more efficient than the leg-by-leg control, and that the turbo roundabout can be adjusted such, that it is suitable for the two-phase control, leaves the question whether the signalized turbo roundabout (with a leg-by-leg control) is still worth investigating. The answer to this question can be found by comparing the space requirements of the signalized turbo roundabout and the partial turbo circle. Appendix D (Geometrical designs) states the minimum value for the inscribed radius of the turbo roundabout and circle: 12 m. In that case, the outer diameter is 52 m. With an inscribed radius of 20 m, the outer diameter of the rotor roundabout is 64 m. The outer diameter of the partial turbo circle with an inscribed radius of 12 m amounts to 66 m. That means the rotor roundabout can be applied with an inscribed radius ranging from 12 m to 20 m, without competing with the partial turbo circle, because the space requirements differ. The same applies to the star roundabout: the star roundabouts with inscribed radii of 12 m and 20 m require less space than the three-leg turbo circle with an inscribed radius of 12 m. Therefore, this project will investigate the rotor and star roundabout with inscribed radii of 12 m and 20 m [16].

The same also applies to the partial turbo circle, with the turbo circle as upper boundary. With an inscribed radius of 20 m, the outer diameter of the partial turbo circle equals the outer diameter of the turbo circle with an inscribed radius of 12 m. Therefore, this project invokes the partial turbo circle with inscribed radii ranging from 12 m to 20 m.

The turbo circle will be invoked in this project with inscribed radii of 12 m, 20 m and 30 m. The turbo circle could be invoked with larger inscribed radii, because there is no 'upper boundary' to it. However, this choice has been made for delineating the project.

3.1.4. Demand patterns

From the introduction of the two-phase control in section 2.3, it can be concluded that the capacity of a turbo circle depends on the prevailing demand pattern (in particular, on the left-turning intensities).

[16] *This choice is made, because the partial turbo circle is equipped with the two-phase control, which is more efficient than the leg-by-leg control on the rotor roundabout. Therefore, the partial turbo circle will probably offer a higher capacity than the signalized rotor roundabout with the same outer diameter.*

Indeed, in the two-phase control, the left-turning vehicles have to queue up on the circle itself; therefore the combination of the left-turning intensities and the available queuing space is a constraint to the capacity.

This project will calculate the capacities based on a set of demand patterns, with different intensities for the left-turning traffic streams. Appendix B (Demand patterns) elaborates on the demand patterns to be applied. The resulting set consists of ten demand patterns: DP20, DP40, DP60 through DP200. All patterns contain a ratio for the primary streams (08/02) of 80% and the ratio secondary/primary streams (05/02 and 11/02) is 60%. The right-turning streams amount to 30% of the neighbouring straight-ahead stream. The demand patterns differ with respect to the left-turning intensity: in DP20, the left-turning streams amount to 20% of the neighbouring straight-ahead stream; in DP40, the left-turning streams amount to 40% of the neighbouring straight-ahead stream, etc. The demand patterns are illustrated by Figure 3-3 and Figure 3-4.

These demand patterns have been chosen because they differ solely with respect to the left-turning intensities. As noted in the previous paragraphs, the left-turning intensities determine the capacity difference between the signalized rotor roundabout and the turbo circle.

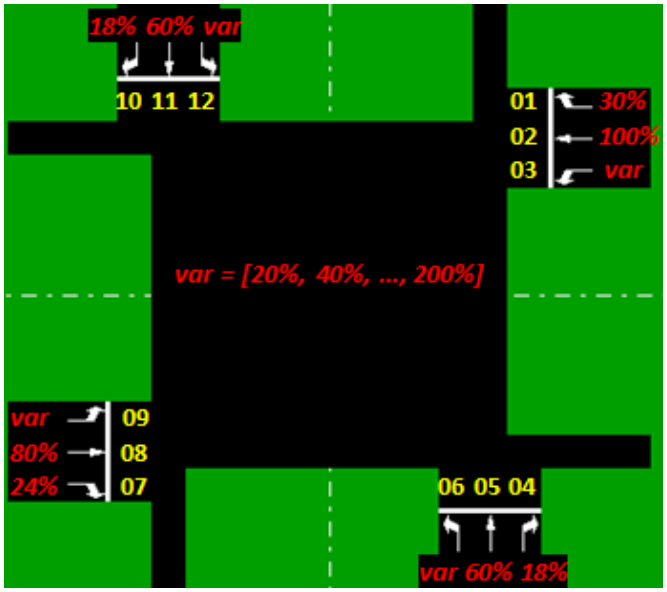


Figure 3-3 Illustration of the demand patterns for the four-leg intersections

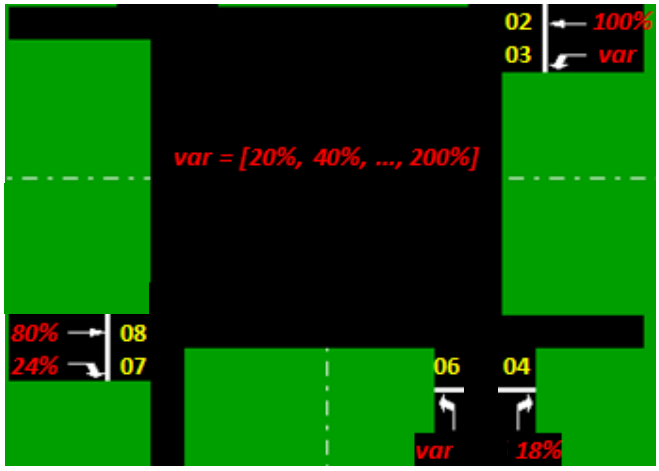


Figure 3-4 Illustration of the demand patterns for the three-leg intersections

3.2. Capacity models

Section 2.4 introduced three models by means of which the capacity of (un-)signalized turbo roundabouts can be calculated: the MSRV, the *black box approach* and VISSIM. This section will motivate why and how these models will be applied to the signalized rotor and star roundabouts. The next chapter shows the calculations in detail and presents the results.

3.2.1. MSRV

This model will be applied to the un-signalized rotor and star roundabouts for the following reasons:

- The model is especially designed for evaluating the traffic flow on turbo roundabouts;
- The model has been validated by means of various Dutch field measurements;
- The model offers the possibility to calculate two of the performance indicators chosen in this project: the capacity and waiting times.

The MSRV will be applied to the rotor and star as follows. The ten demand patterns chosen in this project (see appendix B) describe the ratios among the intensities in the traffic streams. The traffic demand in the MSRV will be configured according to these ratios, and the total demand will be increased gradually (traffic demand input is required in pcu/h). The capacity of the turbo roundabout can be found by means of the degree of saturation and the average delay time (two output parameters of the MSRV). The capacity of the turbo roundabout has been reached if:

- The saturation degree (traffic demand divided by traffic supply) is smaller than 80%;
- The average waiting time is smaller than 80 s/pcu.

3.2.2. Black box approach: analytical approach

The black box approach is developed parallel to the concept of the turbo roundabout, and explicitly presented as a model to calculate the capacity of the signalized turbo roundabout. This is the reason why this model will be applied in this project.

The model complies to the general idea of the black box, however, the terminology is not undisputed. Appendix A (Discussion of the terminology) addresses the discussion. The conclusion from the discussion in appendix A, is to apply the fundamentals of the *black box approach*, but calling it the *analytical approach*. The reason is that the fundamentals will be applied to the signalized rotor and star roundabout, extended to a high level of detail. The details are elaborated on such, that the terminology *black box approach* would be confusing.

Application to the signalized rotor and star roundabouts

The analytical approach will be applied to the signalized rotor and star roundabouts in several steps. In the first step, the optimal control structure will be constructed, based on the leg-by-leg control. Before constructing this control structure, the maximum possible green phase overlap has to be calculated. Appendix G (Green phase overlap calculation) shows the calculations, based on the geometrical designs of the rotor and star roundabouts, and a simplified acceleration model. Table 3-1 shows the result of this appendix.

Based on these values for the green phase overlap, the control structures will be constructed in the second step (the details and calculations are explained in appendix H: Control structures for the turbo roundabout). The control structure should be constructed such, that the capacity of the intersection is maximized (i.e. the aggregated phase overlap per cycle should be maximized). In this step, it appears that the capacity of the signalized rotor and star roundabouts depend on the duration of the cycle time.

Table 3-1 Maximum possible green phase overlap (SG = start green) [17]

	SG main signal - SG interception signal	Green phase overlap
Rotor roundabout, 12 m	3.8 s	0.8 s
Rotor roundabout, 20 m	4.3 s	1.3 s
Star roundabout, 12 m, E-S and S-W	3.9 s	0.9 s
Star roundabout, 12 m, W-E	5.0 s	2.0 s
Star roundabout, 20 m, E-S and S-W	4.4 s	1.4 s
Star roundabout, 20 m, W-E	7.1 s	4.1 s

The third step consists of the calculation of the saturation flow. In the control structure, the green phase duration for every leg has been determined. The effective green time can be calculated from the green phase duration. The effective green time is the time in which vehicles can be served at saturation flow, consisting of the green time minus the reaction time (drivers perceive and react on the signal turning green; 1 s [18]) plus the used yellow time (the part of the total yellow time in which vehicles are still served; 2 s [19]. The effective green time per leg can thus be calculated be means of the following formula:

$$t_{eff.green,leg} = t_{green,leg} - t_{reaction} + t_{yellow,used} = t_{green,leg} + 1$$

Equation 3-1

where:

$t_{eff.green,leg}$ = duration of the effective green time in one phase per leg [s]
$t_{yellow,used}$ = used yellow time [s]
$t_{reaction}$ = reaction time [s]

By means of the model in section J.6, the saturation flow can be calculated by means of the effective green time.

In the final step, the capacity of each leg will be calculated separately, by multiplying the effective green time per leg and the saturation flow per leg. The capacity of the signalized rotor roundabout can be calculated by summing the capacities of all legs.

3.2.3. VISSIM

VISSIM will be used in this project, in order to be able to compare the results of the analytical models with the results of a simulation model. This simulation model has been chosen from the other simulation models mentioned in section 2.4.3, although those simulation models do not differ fundamentally; the most important differences concern the user interface. The arguments for choosing VISSIM are:

- VISSIM is able to present the output necessary for the evaluation, and in such a way, that the output data can be analyzed and evaluated efficiently;
- The reliability of VISSIM is sufficient, because the model is in development continuously, based on state-of-the-art research in traffic engineering;
- VISSIM is widely being used in European countries, because the model is commonly appreciated for its quality and realistic presentation;

[17] *The rotor roundabout is symmetrical; therefore, the green phase overlaps within all phase transitions are equal. The star roundabout is not symmetrical; therefore, the green phase overlap within the phase transition from the stage in which leg W has green, to the stage in which leg E obtains green, differs from the green phase overlap within the two other phase transitions.*

[18] *Commonly accepted value for the reaction time, used by Dutch traffic control engineers.*

[19] *Derived from Salomons (2012).*

- The microscopic models applied by VISSIM (e.g. longitudinal and lateral models, car-following model, etc.) are easy to adjust by means of functions and distributions (this report discusses them intensively in section L.2).

VISSIM drawback: lane choice behaviour

VISSIM also has some drawbacks, one of which is the lane choice behaviour. Appendix L discusses the construction of the VISSIM-network of the signalized turbo roundabout. In that network, vehicles have a route choice [20]. For instance, for turning right on a rotor roundabout, the driver may choose between the right and middle approach lanes [21]. For going straight-ahead on a rotor roundabout, the driver may choose between the middle and left approach lanes. VISSIM adopts a highly inefficient lane choice behaviour, because VISSIM distributes vehicles evenly and randomly over the lanes. The route choice is determined at the moment the vehicle enters the network; it will not change while driving in the network. As a consequence, it might occur that all right-turning vehicles use the middle lane, leaving the right lane unused and unnecessarily overloading the middle lane. This is one of the drawbacks of VISSIM: approaching vehicles do not consider the actual queue length on each of the approach lanes, while in reality drivers do. This drawback can be relieved by closing edges [22] within the network.

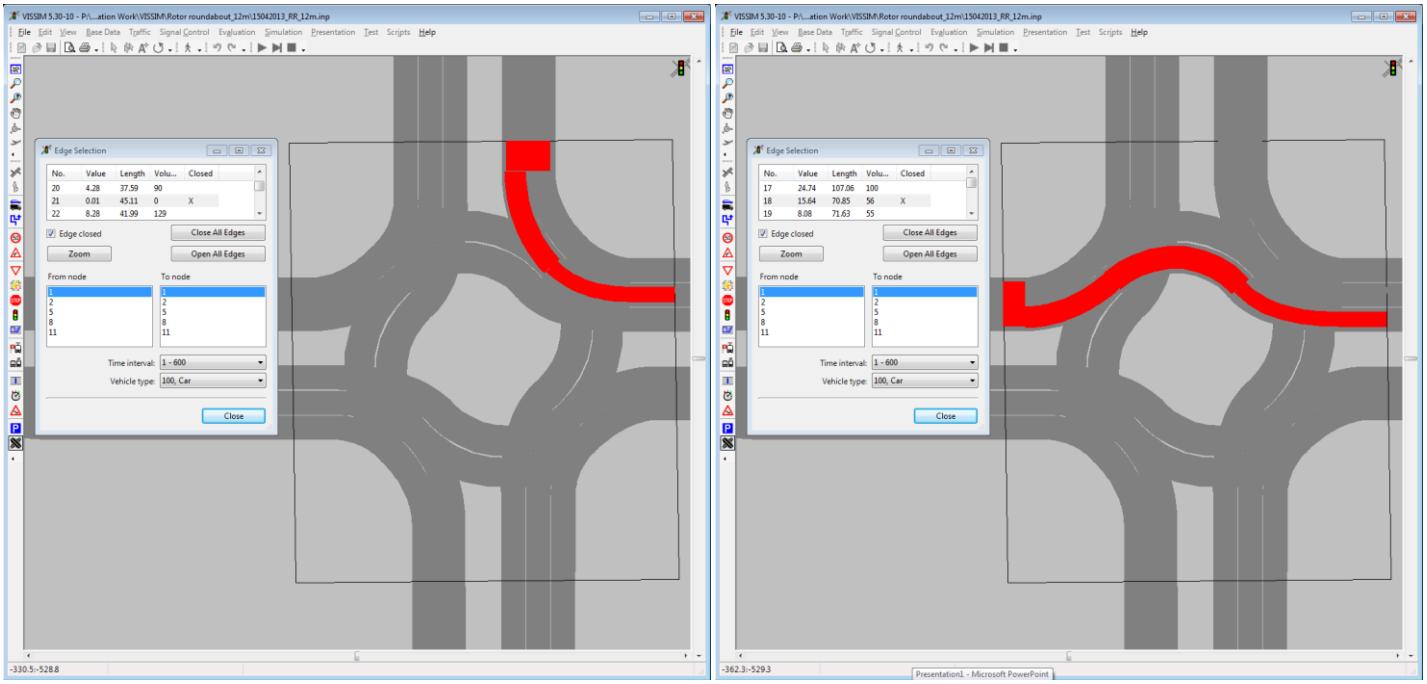


Figure 3-5 Edge closure. Left: the middle lane does not serve right-turning traffic. Right: the left lane does not serve straight-ahead traffic if the left turning stream is busier than the straight-ahead stream

With respect to the right approach lane; all right-turning vehicles should use this lane, so the edge closure should be such that the middle lane does not serve any right-turning traffic (see Figure 3-5 left). With respect to the left lane: all left-turning vehicles should use this lane, and it should also serve a share of the straight-ahead traffic if the straight-ahead streams are larger than the left-turning vehicles (this is the case for demand patterns DP20 through DP80, see appendix B: Demand patterns). So for demand patterns

[20] *A route in VISSIM consists of the set of links and connectors leading from the origin to the destination. A network contains route choice if multiple routes lead from a particular origin to a particular destination.*

[21] *The three lanes on the approach legs and the circulatory lanes, are modelled by means of separate links, in order to prevent vehicles from changing lanes.*

[22] *An edge is a series of links and connectors within a node or between two nodes.*

DP100 through DP200, the edge indicated by Figure 3-5 (right) needs to be closed. For demand patterns DP20 through DP80, this edge will not be closed. This introduces the risk of overloading the left lane with too large a share of straight-ahead traffic.

This leaves the following drawback. In the models for demand patterns DP20 through DP80, the latter edge (Figure 3-5 right) has not been closed; all straight-ahead vehicles are distributed randomly over the middle and left approach lane. All left-turning vehicles have to choose for the left lane, so situations in which the left lane is more occupied than the middle lane occur. As a consequence, the extension green time for a particular leg is longer than necessary because the left approach lane is occupied longer than necessary, influencing the capacity of the roundabout negatively.

This problem cannot be solved by closing the edge, because in that case the middle lane is more occupied than necessary; a share of the straight-ahead vehicles (all choosing the middle lane) can be served by the left-lane. Then, the extension green time of a particular leg is longer than necessary because the middle lane is occupied longer than necessary, influencing the capacity of the roundabout negatively.

In conclusion: the capacity estimates of the signalized turbo roundabouts, by means of the VISSIM models, for demand patterns DP20 through DP80, are probably conservative. Chapter 7 (Reflection) will pay further attention to a possible solution to this problem.

Step-wise increasing traffic demand

In order to estimate the capacity by means of simulation, the total traffic demand should increase in time. As the demand increases, the intersection becomes more and more saturated until it reaches capacity. In this project, the traffic demand increases stepwise, by 200 pcu/h every 15 minutes (see Figure 3-6).

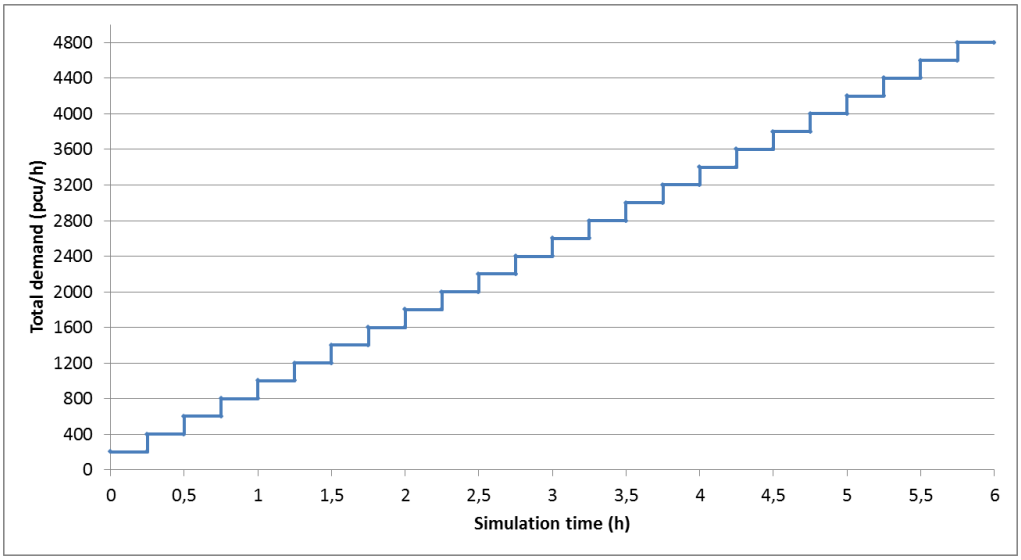


Figure 3-6 Input to VISSIM (dynamic assignment): every 15 minutes, the total demand increases by 200 pcu/h

Performance indicators to be measured

The saturation rate cannot be measured directly from simulations, nor from field observations. However, there are indicators for the saturation rate which can be measured directly. These are: the delay time and the queue length. VISSIM offers to measure these indicators for the saturation, by means of Travel Time Sections and Queue Length.

- Intermezzo: determining the capacity from the travel time and queue length -

Indicator for saturation: travel time

The Travel Time Sections register the travel time from entering the network to exiting the network, for every vehicle. The distance between the entrance and exit locations is set to 2000 meters. The speed limit in the entire network is set to 50 km/h by the settings in the Parking Lots (see appendix L: VISSIM model development) [23]. Effectively, vehicles should be able to cross the network in 144 seconds, if they exactly comply to the speed limit at all locations in the network, and if the intersection were not present in the network. In order to obtain the delay times induced by the intersection, the measured travel time should be subtracted by 144 seconds. Following this strategy results in a few negative delay times. These are measurements of fast drivers, who drove somewhat faster than the speed limit (the actual speed a vehicle is driving, is not exactly 50 km/h, but a value from the Speed Distribution) and who did not have to stop for a red light.

All travel time measurements can be plot in a diagram, then one obtains diagrams like the one shown in Figure 3-7. Every point represents a measurement. This diagram should be carefully interpreted with respect to the horizontal axis; it is a time axis. By means of Figure 3-6, the total demand at any time can be determined.

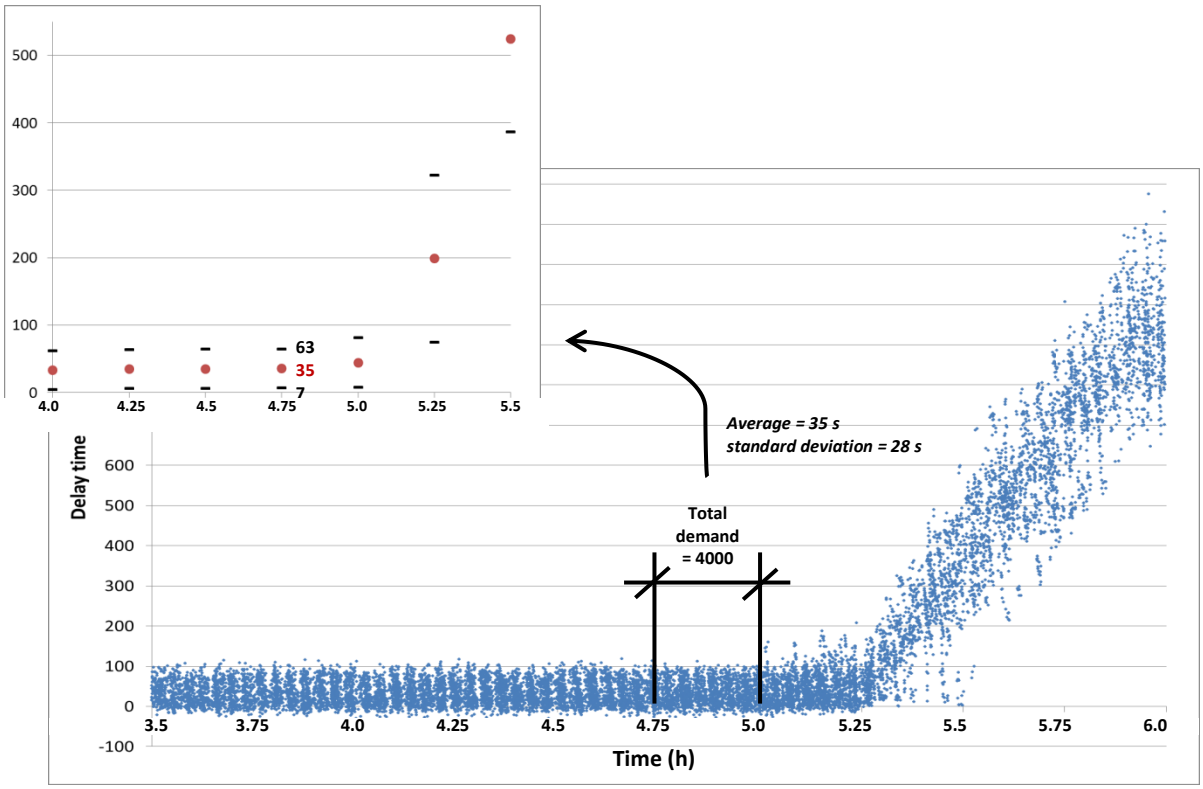


Figure 3-7 Diagrams of all travel times on the rotor roundabout with inscribed diameter 12 m, demand pattern 20, traffic stream 01, random seed 1

It takes quite a lot of computation time to produce this kind of tables; the magnitude can easily be reduced without reducing the quality of the data. Therefore, in the remainder of this evaluation, the data in a range of 15 min will be averaged. This range will be taken because the demand increases with steps of 200 pcu/h, every 15 min. Figure 3-7 shows how the data are averaged: within a range of 15 min (where

[23] *The Reduced Speed Areas do not represent a speed limit, but the necessity to reduced speed in order to cross a bend safely. Legally, drivers are allowed to cross a bend with 50 km/h.*

the total demand is constant) the average and standard deviation of all measurements are calculated and plot in a separate diagram. Moreover, the data of all random seeds will be averaged. In that case, one obtains a diagram like the following:

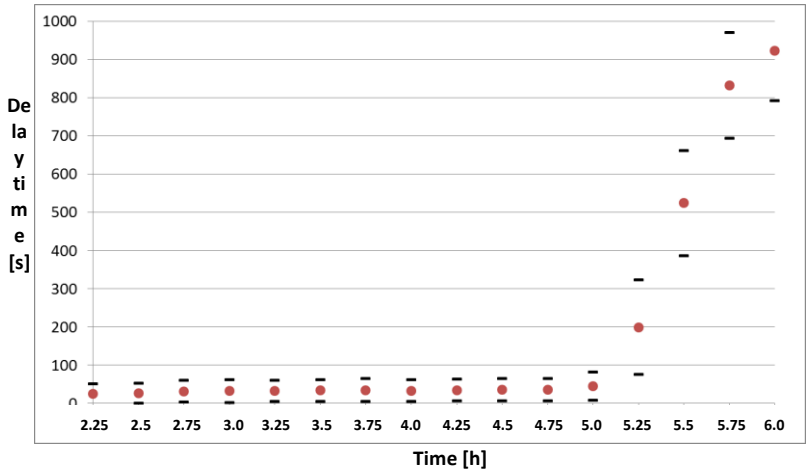


Figure 3-8 Average and standard deviation of all travel times on the rotor roundabout with inscribed diameter 12 m, demand pattern 20, traffic stream 01, averaged over all random seeds

Apparently, the delay times are highly variable, but the point of saturation is clearly visible (at t = 5.0 h; the total traffic demand at that time is 4200 pcu/h). In under-saturated conditions, the delay time caused by the intersection ranges from 0 to 100 seconds. In over-saturated conditions, the delay time vastly increases, up to 15 minutes and longer (over a road stretch 1000 m long). Also, the standard deviation of the measurements increases.

From this diagram, the conclusion can be drawn that from a total demand of ca. 4200 pcu/h on, the delay time of vehicles in stream 01 increases vastly (only for this specific demand pattern: DP20). The explanation is that the intersection becomes over-saturated. The queue of vehicles cannot be served entirely in one green phase anymore. The last vehicle(s) have to wait for the next green phase; they have to wait the duration of the cycle time (minus the duration of the green phase). Because the traffic demand keeps increasing, the delay time increases along with the queue. The value of 4200 pcu/h will be chosen as an indication for the capacity of stream 01.

Indicator for saturation: queue length

The second indicator for the saturation rate that can be evaluated by VISSIM is the queue length in front of a traffic signal. In the network, every stream (01 through 12) has been supplied with a Queue Counter, measuring the average queue every minute. Again, the measurements from the queue counters can be plot against the total traffic demand on the intersection. One obtains diagrams like Figure 3-9. Every point represents a measurement of the average queue length, measured every minute. Effectively, for one ‘step’ in total demand (200 pcu/h), there are 15 measurements, because one ‘step’ lasts for 15 minutes.

The measurements are averaged every 15 minutes, in order to obtain the diagram upper left in Figure 3-9.

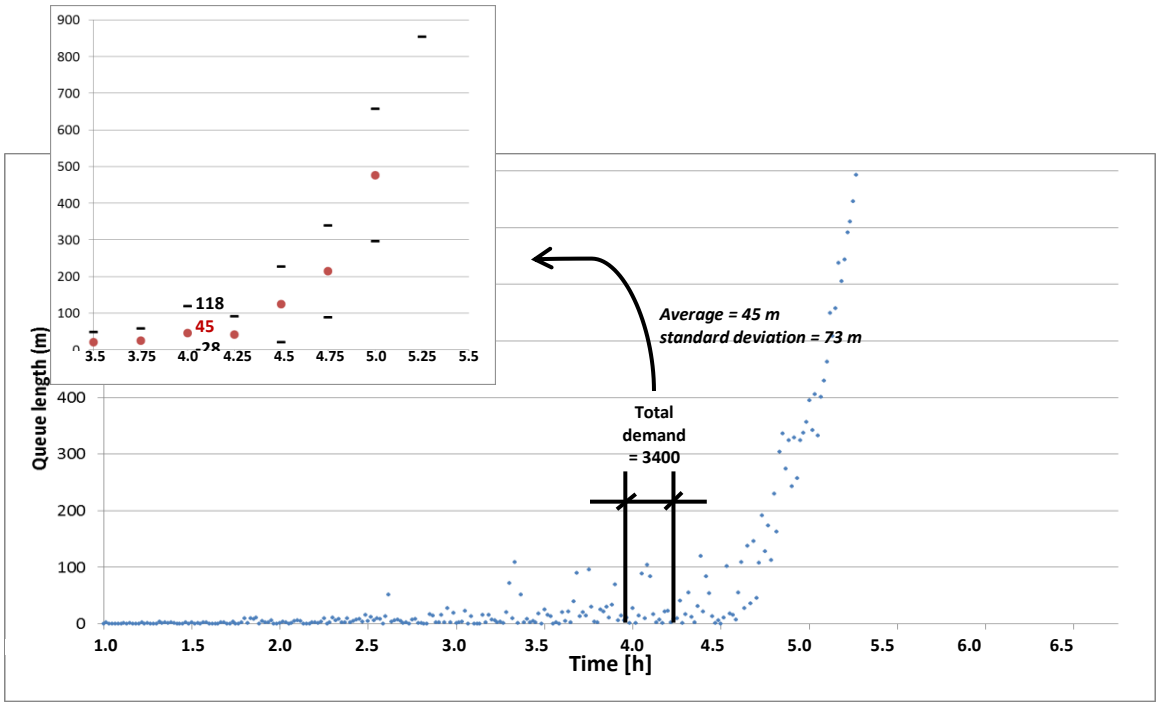


Figure 3-9 Diagram of the queue length on the rotor roundabout with inscribed diameter 12 m, demand pattern 20, traffic stream 01, random seed 1

Regardless of a few outliers [24], it appears from Figure 3-9 that from t = 4.25 h (total demand of ca. 3600 pcu/h), the queue increases quickly. This value is considerably lower than the indication for the capacity found in the previous section (4200 pcu/h, for random seed 1, and the average over all random seeds).

Cause for the differences: lane change behaviour in saturated conditions

From the diagrams in the former section can be concluded that the average delay time starts to increase once the average queue has reached a length of ca. 500 m, which is quite a queue. From visual observations of the simulations, it is concluded that a green phase (with maximum extension green) cannot serve such a queue.

This is a remarkable observation: the queue length starts to increase rapidly at t = 4.25 h (total traffic demand of 3600 pcu/h), where the delay time lags behind and starts to increase at t = 5.0 h (total traffic demand of 4200 pcu/h). This discrepancy (one would assume that the delay time increases along with the queue length) can be explained by means of Figure 3-10.

The total traffic demand increases in time. From a certain moment, vehicles are not able to change lanes on the leg anymore (which has a length of 1000 m). They already try to change lanes at the start of the leg, but if they cannot find a suitable gap, they drive through. These vehicles stop at the decision point, that is the point where the three connectors connect the three-lane leg with the single-lane links leading to the Signal Heads. If they have stood still for 60 s, they disappear from the network. This is an (unrealistic) default solution of VISSIM. The time value of 60 s can be adjusted manually, but this is not recommended (PTV Vision, 2011). From the moment this occurs, the simulation results are not reliable anymore, because the total demand passing the intersection is not equal to the generated demand anymore. In other words: the intersection is not 'exposed' to the total traffic demand anymore (Figure 3-9, horizontal axis), because the traffic on the right approach lane is absent. Therefore, from the point of

[24] *These outliers are probably caused by stochasticity: the number of arrivals was suddenly high at that moment.*

saturation on, the simulation results should not be regarded anymore. However, these measurements are not relevant, since only the point of saturation is relevant to this project.

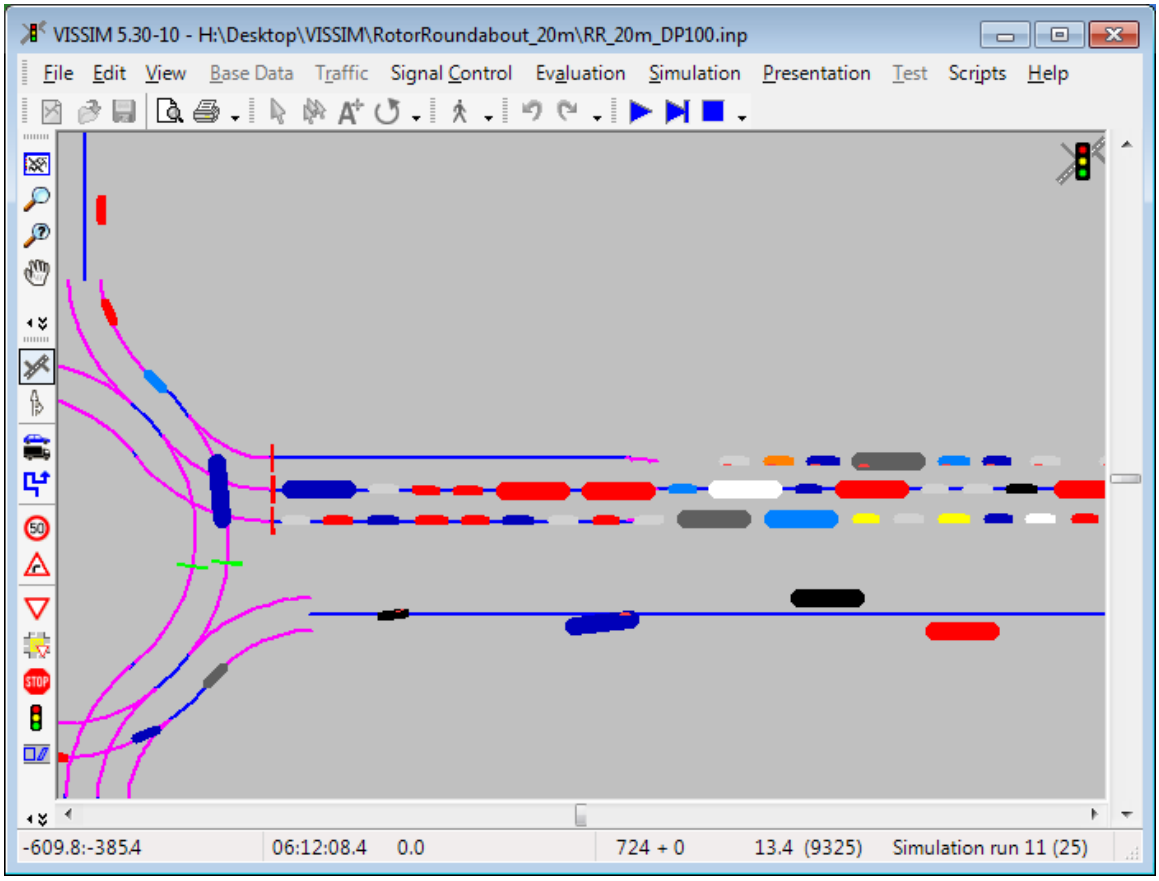


Figure 3-10 Vehicles stop in front of the decision point; they were not able to change lanes upstream

Due to the vehicles standing still in front of the connector leading to stream 01, the queue length increases unnecessarily (spill-back). However, during the first minutes of over-saturation, the standing vehicle does not have to incur extra delay time to the following vehicles, because these vehicles would have to wait in front of the traffic signal, which is ca. 50 m downstream. They only spend their waiting time 50 m upstream. This is an explanation for the notion that the queue length on stream 01 starts to increase earlier than the delay time. Later on during the over-saturation phase, multiple vehicles come to a stand-still, all standing still for 60 seconds; and the extra delay time for following vehicles increases.

This explanation is also supported by the diagram for stream 02 (see Figure 3-11). There, the queue length starts to increase at t = 4.25 h (total traffic demand of 3600 pcu/h), along with the delay time. Due to this queue on the middle lane, vehicles on the right lane are not able to change lanes anymore. They come to a standstill in front of the connector shortly after the queue on the middle lane started to increase (from t = 4.25 h on).

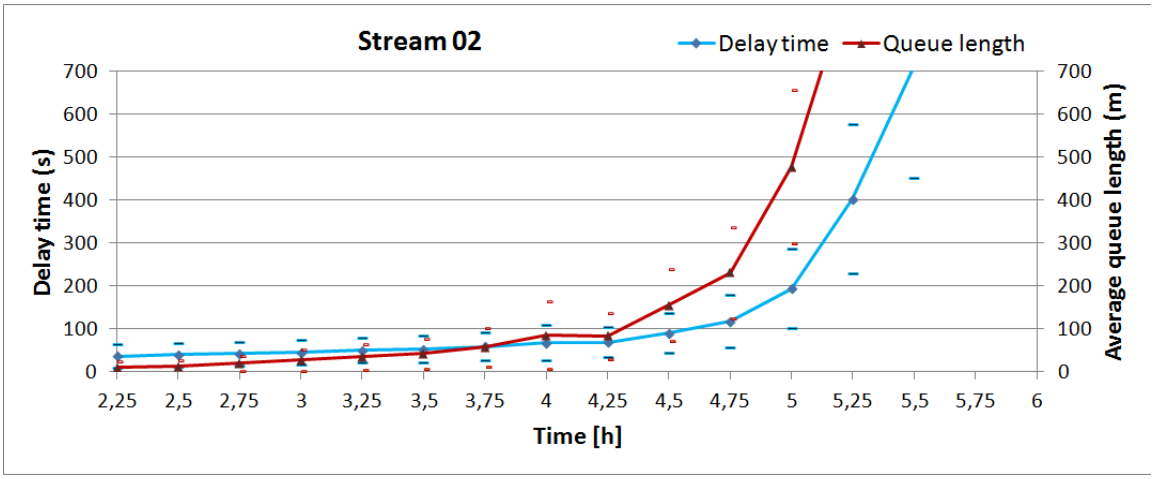


Figure 3-11 Diagram of the delay time and the queue length on the rotor roundabout with inscribed diameter 12 m, demand pattern 20, traffic stream 01, averaged over all random seeds

Determining the capacity

From the previous sections can be concluded, that stream 02 imposes a constraint on the capacity of the eastern leg. Likewise, every leg can be assigned a restrictive stream, to be observed from the delay time/queue length diagrams. The capacity can be determined in this way for every leg, on every intersection in this project.

Conclusively, the point where the delay time starts to increase, indicates the capacity of the intersection. Unfortunately, this point is not clearly observable for every stream because the line representing the delay time bends faintly, or the lines show multiple bends. Therefore, an extra criterion for observing the capacity will be added: the increment of the standard deviation. Oversaturation is characterized by highly variable delay times and queue lengths.

- End of intermezzo –

Intersections to be modelled in VISSIM

All intersections invoked in this project can be modelled by means of VISSIM. However, this project will not apply VISSIM to evaluate the performance of the un-signalized rotor and star roundabouts. The argument is that the pseudo-conflict cannot be modelled in VISSIM properly. Therefore, all signalized intersections invoked in this project will be modelled by VISSIM:

- the signalized rotor roundabout (with inscribed radii of 12 m and 20 m, see section 3.1.3);
- the signalized star roundabout (with inscribed radii of 12 m and 20 m);
- the partial turbo circle (with inscribed radii of 12 m and 20 m);
- the four-leg turbo circle (with inscribed radii of 12 m, 20 m and 30 m);
- the three-leg turbo circle (with inscribed radii of 12 m, 20 m and 30 m).

Amount of random seeds

VISSIM applies random seeds to take account of randomness. In order to obtain reliable results, a model needs to be evaluated based on a certain amount of random seeds. In principle, a large amount of random seeds yields very reliable results. However, the marginal utility of a random seed (its contribution to the reliability of the results) decreases as the amount of random seeds increases. Moreover, the computation time increases as the amount of random seeds increases.

In order to determine the amount of random seeds to be applied, the Z-test can be carried out. This empirical test is denoted by the following formula (Verhaeghe, 2007, p.55):

$$N \geq \frac{Z^2}{d^2}\sigma^2$$

Equation 3-2

where:
N = required amount of random seeds for one model;
Z = value from the normal distribution, representing the required reliability of the model results;
d = required accuracy of the model results;
σ = standard deviation of the population, representing the variation in de model results.

The required reliability is chosen to be 95%, this yields Z = 1.96 from the normal distribution. The capacity of the intersection types need to be estimated with an accuracy of 200 pcu/h. From a test run based on ten different random seeds appears that the standard deviation (of the population) amounts to 526 pcu/h. From Equation 3-2 follows that the simulation needs to be based on 25 random seeds, in order to obtain sufficient reliable results.

VRIGen

A signalized intersection requires a traffic control: a structure which describes green periods of all signals on the intersection. It describes which signals can have green simultaneously, which signals cannot have green simultaneously, and how long the green period for each signal should last. A traffic control should be optimized with respect to the traffic management goal pursued by the road authority (Muller *et al.*, 2011). This project applies the goals of maximizing the intersection capacity and minimizing the delay times.

The optimum traffic control (consisting of the sequence and the minimum and maximum (extension) green times) can manually be calculated by means of a standardized algorithm (Van Nes *et al.*, 2010, part 4, chapter 2). The geometrical design is an important input factor for determining the conflict matrix and the clearance times within. Another important input factor is the traffic demand for assigning the green times to the signal groups.

This study will not elaborate on the specific algorithm. Rather, it describes the model developed in VRIGen [25] : a software package by which the algorithm can automatically (by means of a computer) be executed. VRIGen will be applied in this project, because it enables the user to execute the algorithm faster and more accurate than executing the algorithm manually.

VISSIM applies VRIGen to generate a static control structure, and TrafCOD to generate a vehicle-actuated control, based on the static structure. The control structures used in this project will be generated by means of VRIGen; appendix K (VRIGen model development) will show how.

VRIGen and phase overlap

The leg-by-leg control should contain green phase overlap, which can be invoked in the third tab: couplings. Here, every pair of a main signal and the successive interception signal can be defined (see Figure 3-12). VRIGen allows to incorporate different moments of start green and end green, by means of *TYveh* (the time lag between start green of the interception signal and start green of the main signal). *TYveh* should obtain a negative values in order to incorporate the phase overlap.

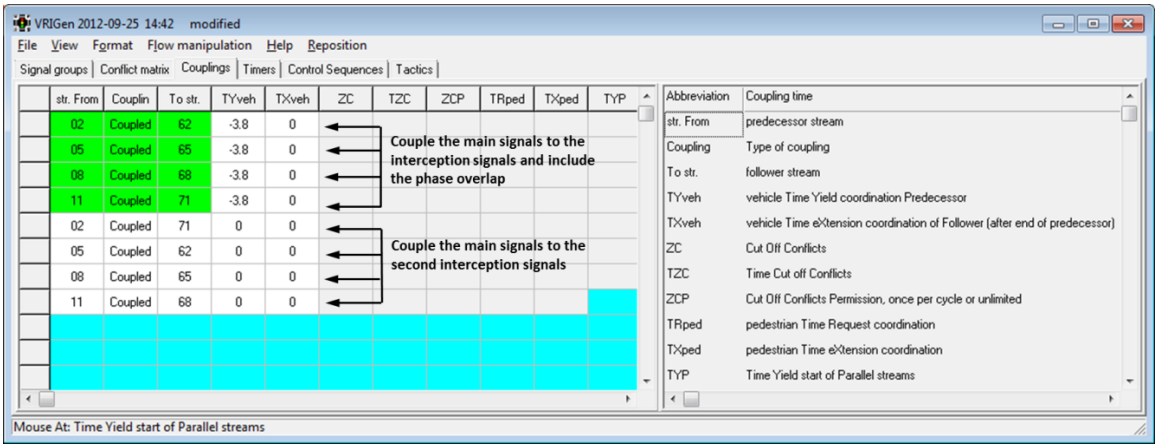


Figure 3-12 The tab *Couplings* in VRIGen

The need for using spare streams

Unfortunately, VRIGen produces a traffic control without the phase overlap. In fact, it treats negative values for *TYveh* as if they were equal to zero. Possibly, this is an erroneous default setting in VRIGen (source: A.M. Salomons, personal communication, June 2013) [26].

A solution to this problem is to invoke spare streams in the traffic control. The strategy for applying spare streams is explained in section K.3. All settings to be applied in the tabs in VRIGen are addressed in that section as well; the result is the desired leg-by-leg control with phase overlap, illustrated by Figure K-13.

TrafCOD

VISSIM applies a control structure that is generated by VRIGen. Furthermore, VISSIM applies TrafCOD to generate a semi-actuated traffic control, based on the control structure. The only input to TrafCOD is the

[25] *Abbreviation for VerkeersRegelInstallatieGENerator; traffic control generator*

[26] *Others claim that this default setting might be the result of the discussion among traffic control engineers, on the question whether phase overlap should be allowed on intersection in The Netherlands. In this discussion, opponents are concerned about the consequences for traffic safety. However, the explanation in the text (erroneous default setting) has been confirmed; the discussion is irrelevant to the problem in VRIGen and to the concept of green phase overlap in general.*

traffic control; the program itself consists of a set of guidelines. In this project, the program language in which TrafCOD is programmed will not be considered.

TrafCOD has a drawback: the user cannot check the decisions made by TrafCOD with respect to extension green. In section 4.3 (Capacity modelling: VISSIM) will appear that leg N on the rotor roundabout and leg S on the turbo circle with an inscribed radius of 12 m have an extraordinary high capacity, in comparison to the other legs. This is caused by the excessively long extension green times assigned by TrafCOD to these legs [27]. This is a 'blank edge' of the project: TrafCOD's choices with respect to extension green times cannot be traced.

3.3. Evaluation method

When the performance of all intersections has been assessed, the intersections can be compared based on the performance indicators. The aim is to capture all scores in a table, Table 3-2 presents the structure of the table.

Table 3-2 Evaluation method: the intersections will be compared by means of this table

Intersection type			Capacity			Delay	Robustness	Safety	Env.
	Inscribed radius	Space requirement	MSRV	VISSIM	AA				
Un-signalized rotor roundabout	12 m								
Un-signalized rotor roundabout	20 m								
Un-signalized star roundabout	12 m								
Un-signalized star roundabout	20 m								
Signalized rotor roundabout	12 m								
Signalized rotor roundabout	20 m								
Signalized star roundabout	12 m								
Signalized star roundabout	20 m								
Partial turbo circle	12 m								
Partial turbo circle	20 m								
Turbo circle	12 m								
Turbo circle	20 m								
Turbo circle	30 m								
Three-leg turbo circle	12 m								
Three-leg turbo circle	20 m								
Three-leg turbo circle	30 m								

In this study, the performance of the indicators will not be weighed by assigning weigh factors to the performance indicators; this is commonly done in variant studies (e.g. multi-criteria evalutation). However, this study does not invoke a practical case in which an optimum intersection solution has to be found. Instead, this study aims to consider the intersections, primarily based on their capacity. The other performance indicators will not be evaluated to the same extent as the capacity. Therefore, the intersection will be compared by primarily comparing the capacity values, and secondarily comparing the other indicators, rather than assigning weigh factors.

[27] *The extension green times are bound to the maximum extension green prescribed by the control structure from VRIGen. TrafCOD cannot assign extension green times that exceed the prescribed maximum value.*

3.4. Validation, calibration

The signalized rotor roundabout has not been constructed in The Netherlands yet. Therefore, the possibilities for validation of the model results are absent. For compensation, the parameters in the models will be extensively studied and the chosen values motivated. For instance, appendix F (Simplified acceleration model) presents a detailed discussion and a sensitivity analysis on the parameters chosen in the acceleration model, which is an important part of the black box approach. Also, section L.2 elaborates on the parameters of the microscopic models (Base Data) in the simulation tool VISSIM.

3.5. Summary and conclusions

This chapter indicated the scope of the study by means of four subjects. Firstly, this study will only invoke intersections inside the urban area. Secondly, this study will invoke the two largest turbo roundabout types: the rotor and star roundabouts. These turbo roundabouts can be adjusted such, that the two-phase control is applicable, resulting in the partial turbo circle (adjusted rotor roundabout; four-leg) and the three-leg turbo circle (adjusted star roundabout). This study will therefore also invoke the (partial and three-leg) turbo circles. Finally, the choice has been made to apply a set of ten demand patterns which only differ with respect to the left-turning intensities.

This project will consider turbo roundabouts with inscribed radii ranging from 12 m through 20 m. The minimum value of 12 m is based on safety considerations (speed on the roundabout). The rotor roundabout with an inscribed radius larger of 20 m is as large as the partial turbo circle with an inscribed inscribed radius of 12 m. The latter intersection type applies a more efficient control structure, therefore it is not sensible to investigate the rotor roundabout with an radius diameter larger than 20 m. The same holds for the star roundabout.

The MSRV will be used to analytically calculate the capacity of and delay times on the un-signalized turbo roundabout. The black box approach will be used to calculate the capacity of the signalized turbo roundabout. VISSIM will be used to calculate the capacity of and delay times on all signalized intersections in this model. VISSIM applies VRIGen en TrafCOD to generate a vehicle-actuated control. Table 3-3 presents an overview of the models to be applied in this project.

Table 3-3 Overview of intersection types and evaluation methods

	MSRV	BBA	VISSIM
	Analytical	Analytical	Simulation
Un-signalized rotor roundabout	✓		
Un-signalized star roundabout	✓		
Signalized rotor roundabout		✓	✓
Signalized star roundabout		✓	✓
Partial turbo circle			✓
Four-leg turbo circle			✓
Three-leg turbo circle			✓

Due to a lack of signalized turbo roundabouts already constructed in the physical network, the possibilities for validating the results from this project are limited.

4. Capacity modelling

This project applies three models to calculate the capacity of the (signalized) turbo roundabout and the (partial) turbo circle: the MSRV, an analytical approach and VISSIM. This chapter addresses the application of these models to the intersections invoked in this study, according to Table 3-2. One section will be dedicated to each model. The results of the models will be shown graphically.

Before applying the analytical approach and VISSIM to the signalized rotor and star roundabouts, the maximum possible green phase overlap has to be calculated, appendix G shows the calculations. Moreover, the leg-by-leg control structure should be calculated, in order to calculate the capacity of the signalized rotor and star roundabouts by means of the analytical approach; appendix H shows the calculations.

4.1. MSRV

Section 3.2.1 addressed the application of the MSRV to the un-signalized rotor and star roundabouts. Table 4-1 and Figure 4-1 show the results of the calculations: the capacity values of the turbo roundabout types for these demand patterns. They also show the waiting times on the roundabout, if the total traffic demand is exactly equal to the capacity.

Table 4-1 Overview of capacity values, waiting times and constraining legs

Demand	Rotor roundabout			Star roundabout		
pattern	Capacity	Delay	Leg	Capacity	Delay	Leg
DP20	4553 pcu/h	40.3 s	Leg E	5075	33.0 s	Leg W
DP40	4250 pcu/h	39.2 s	Leg E	4659	23.1 s	Leg W
DP60	4012 pcu/h	35.1 s	Leg E	4482	26.7 s	Leg W
DP80	3839 pcu/h	32.7 s	Leg E	4368	30.1 s	Leg W
DP100	3707 pcu/h	31.0 s	Leg E	4278	33.4 s	Leg W
DP120	3458 pcu/h	26.0 s	Leg E	4206	36.7 s	Leg W
DP140	3271 pcu/h	25.5 s	Leg E	4142	40.0 s	Leg W
DP160	3125 pcu/h	25.0 s	Leg E	4022	40.4 s	Leg W
DP180	3008 pcu/h	24.7 s	Leg E	3830	30.1 s	Leg E
DP200	2912 pcu/h	24.4 s	Leg E	3676	25.0 s	Leg E
Average	3614	29,3		4274	31,7	
St. dev.	552	5,4		406	6,3	

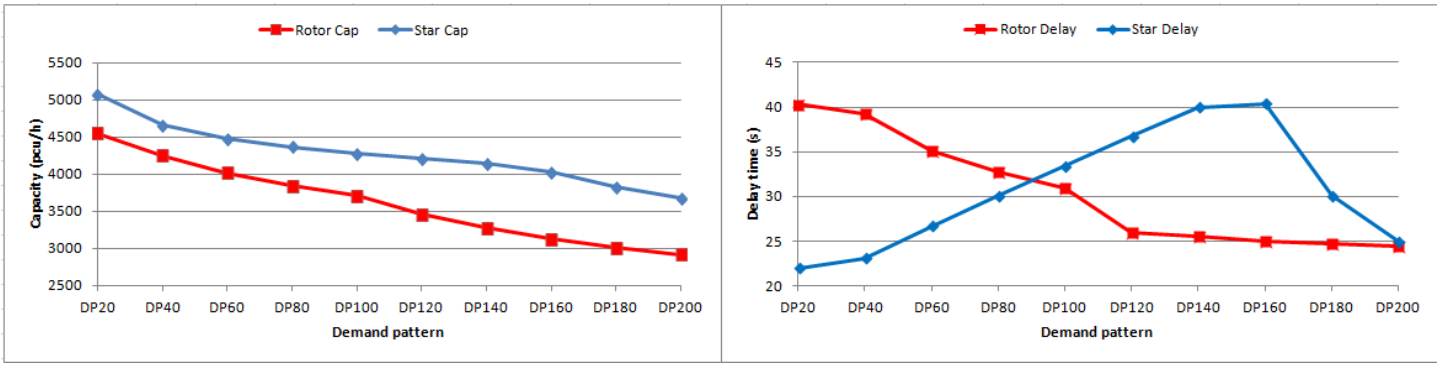


Figure 4-1 Capacity of and delay time on the un-signalized rotor and star roundabout

Remark with the diagram: the values are connected by straight lines. This is done for convenience: to enhance the readability of the diagrams. These lines do not indicate a (linear) increase between the points.

From Figure 4-1 it appears that:

- the capacity of the star roundabout (three-leg) is structurally higher than the capacity of the rotor roundabout (four-leg), in accordance with Fortuijn (2009). This can be explained by the fact that the rotor roundabout contains four legs; the star roundabout contains three legs. As a result, the star roundabout contains less (potential) conflict points and therefore has a higher capacity;
- the capacities of the rotor and star roundabouts decrease as the left-turning intensities increase. This can be explained by the fact that the left-turning streams conflict with the circulatory roadways and two entrance legs. In comparison: the straight-ahead streams conflict with the circulatory roadways and one entrance leg; the right-turning stream only conflicts with the entrance roadways. As the left-turning intensities increase, the amount of conflicts increases, decreasing the capacity;
- the delay time on the rotor roundabout decreases as the left-turning intensities increase. This can be explained by the fact that less total demand (in saturated conditions) yields a lower delay time;
- the delay time on the star roundabout increases as the capacity decreases (with increasing left-turning intensities), except for DP180 and DP200. Figure 4-1 shows this by the sudden decrease of the line representing the delay time on the star roundabout. The cause for this phenomenon can be found in Table 4-1: leg W constrains the capacity of the star roundabout, except for DP180 and DP200, where leg E constrains the capacity. For DP20 through DP160, the delay increases because vehicles on leg W (the constraining leg) have to wait for vehicles in stream 03 (this left-turning intensity increases). For DP180 and DP200, leg E suddenly constrains the capacity, just like the rotor roundabout (and the line representing delay starts to decrease, just like the rotor roundabout).

4.2. Analytical approach

This section addresses the calculations of the analytical approach to the signalized rotor and star roundabouts. These calculations comply to the stepwise application of the analytical approach, outlined in section 3.2.2.

4.2.1. Step 1: green phase overlap

The green phase overlap has been calculated in appendix G; Table 4-2 shows the result.

Table 4-2 Maximum possible green phase overlap (SG = start green)

	SG main signal - SG interception signal	Green phase overlap
Rotor roundabout, 12 m	3.8 s	0.8 s
Rotor roundabout, 20 m	4.3 s	1.3 s
Star roundabout, 12 m, E-S and S-W	3.9 s	0.9 s
Star roundabout, 12 m, W-E	5.0 s	2.0 s
Star roundabout, 20 m, E-S and S-W	4.4 s	1.4 s
Star roundabout, 20 m, W-E	7.1 s	4.1 s

4.2.2. Step 2: control structures

The signalized rotor and star roundabouts are suitable for the leg-by-leg control. Appendix H (Control structures for the turbo roundabout) explains how the optimum leg-by-leg control can be determined. The result of this appendix consists of the optimized control structures for the rotor roundabout (Figure 4-2 left) and the star roundabout (Figure 4-2 right).

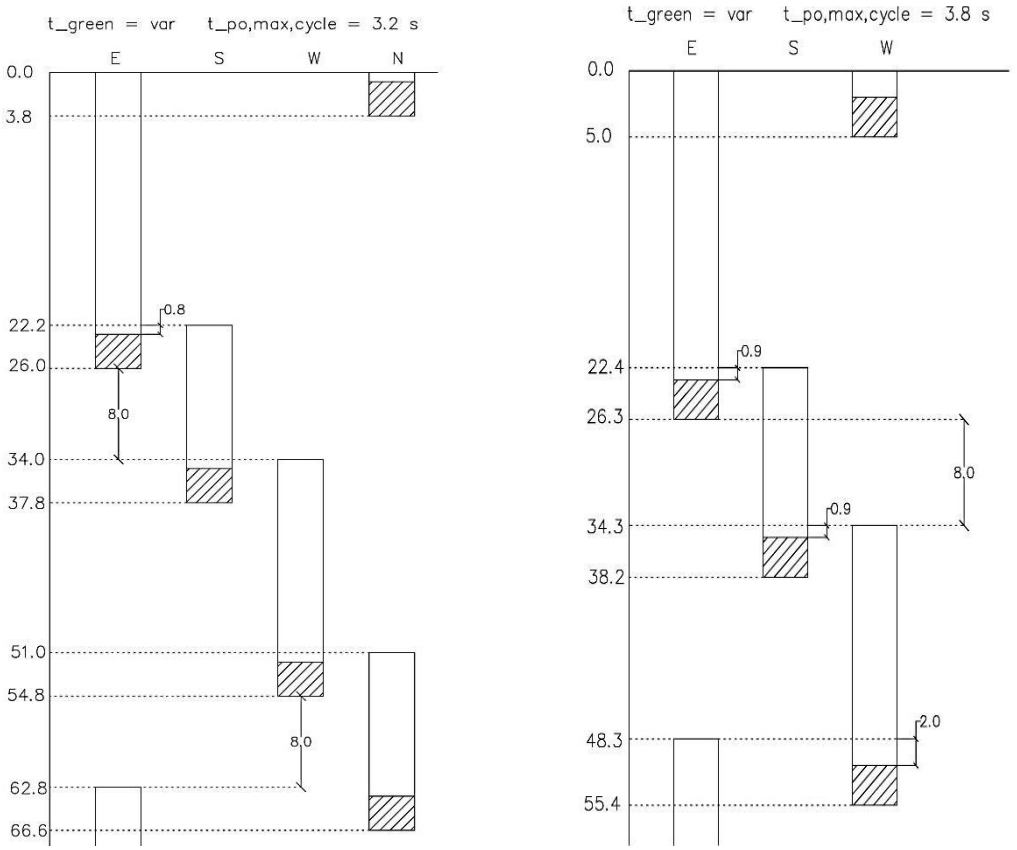


Figure 4-2 Control structures for the rotor roundabout with an inscribed radius of 12 m (left); and for the star roundabout with an inscribed radius of 12 m (right)

Dilemma of the cycle time

The maximum possible green phase overlap per hour is the product of the maximum possible green phase overlap per cycle and the amount of cycles per hour. The amount of cycles per hour in turn, depends on the cycle time. The presumption arises that the cycle time should be as short as possible, so as to obtain a green phase overlap per hour as long as possible. However, there is a drawback: the cycle time determines the duration of a green phase as well. As the duration of the green phase decreases, so does the saturation flow (to be shown in section 4.2.3). Therefore, if the cycle time becomes too short, the capacity of the roundabout might drop because of the low saturation flow.

Appendix J shows that the former influence is decisive. The cycle time has a minimum value, at which the green phase overlap per cycle can optimally be used: 47.2 s for the rotor roundabout with an inscribed radius of 12 m and equal green times for all legs. With a cycle time equal to or larger than 47.2 s, the green phase overlap per cycle is maximized to 3.2 s. The aggregated green time over all legs is (47.2 + 3.2) 50.4 s. With a green time per leg of (50.4 / 4) 12.6 s, the saturation flow is 1584 pcu/h (see the next section). If the cycle time increases, the duration of the green phase increases, and the saturation flow along with it. However, the capacity decreases, because the green phase overlap per hour decreases (as a consequence of the decreasing amount of cycles per hour).

4.2.3. Step 3: saturation flow

In the previous section, the cycle time has been calculated for which the capacity is maximized (62.8 s, for the demand patterns used in this project). From the structure in Figure 4-2 the effective green time per leg can be calculated (see Equation 4-1).

$$t_{eff.green,leg} = t_{green,leg} - t_{reaction} + t_{yellow,used} = t_{green,leg} + 1$$

Equation 4-1

where:

$t_{eff.green,leg}$ = duration of the effective green time in one phase per leg [s]
$t_{yellow,used}$ = used yellow time [s]
$t_{reaction}$ = reaction time [s]

During the effective green time, the entrance leg can serve traffic at saturation flow rate. The saturation flow rate depends on the effective green time, section J.6 quantifies the relationship, resulting in the following formula:

$$q_{sat,leg} = (t_{green,leg} - t_0)^{-1} * \int_{t_0}^{t_{eff.green,leg}} q_{runoff} dt$$

Equation 4-2

where:

q_{runoff} = actual flow of vehicles running off [pcu/h]
$q_{sat,leg}$ = actual saturation flow on a particular leg [pcu/h]
$t_{green,leg}$ = duration of the green phase of that leg [s]
$t_{eff.green,leg}$ = duration of the effective green time of that leg [s]
t_0 = start green phase [s]

For every leg, the effective green time has been calculated. Equation 4-2 computes the saturation flow on a leg by means of the effective green time.

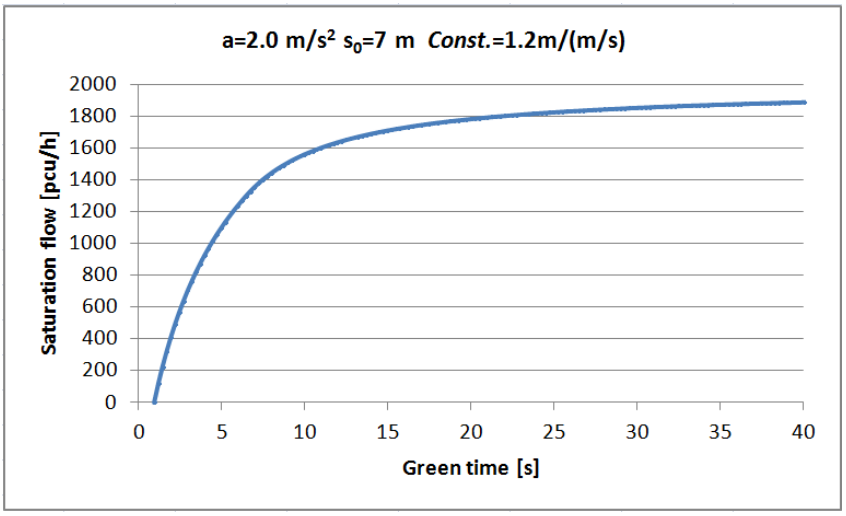


Figure 4-3 Saturation flow as a function of the green time

4.2.4. Step 4: capacity of the signalized rotor roundabout

The capacity is the product of the effective green time of a leg and the accessory saturation flow, aggregated over all legs. In formula:

$$C_{leg} = \frac{t_{green,leg}}{t_{cycle}} * q_{sat,leg} * n_{lanes,leg}$$

Equation 4-3

where:

C_{leg} = capacity of a leg on the signalized turbo roundabout [pcu/h]
$n_{lanes,leg}$ = amount of lanes serving traffic at saturation flow on that leg [-]
t_{cycle} = cycle time [s]

Amount of lanes: rotor roundabout

The amount of lanes serving traffic at saturation flow depends on the contribution of vehicles over the entrance lanes. This contribution in turn depends on the prevailing demand pattern. The lanes will most probably not serve traffic at saturation flow rate during the entire effective green time.

Figure 4-4 shows the distribution of traffic over the entrance lanes and the lane configuration on the rotor roundabout. The illustration shows the eastern leg; thanks to the symmetry of the rotor roundabout, this illustration also holds for the other legs. Based on this illustration, the distribution of traffic over the entrance lanes can be estimated [28]. The right-turning intensity is small; all right-turning vehicles will choose the right lane. Consequentially, all straight-ahead and left-turning vehicles will distribute over the middle and left lane; and the middle and left lane will only serve straight-ahead and left-turning vehicles. If the left-turning intensity is larger than the straight-ahead intensity (DP120 through DP200), all straight-ahead vehicles will choose the middle lane. If the left-turning intensity is smaller than the straight-ahead intensity (DP20 through DP100), the left lane will serve straight-ahead and left-turning vehicles.

This distribution of traffic over the lanes has implications for the rate of saturation of the lanes. Firstly, the right lane (serving only right-turning traffic streams) will probably never serve traffic at maximum saturation flow. The middle and left lane will only serve traffic at maximum saturation flow for DP20 through DP100. For DP120 through DP200, the left lane will serve left-turning vehicles at maximum saturation flow, and the middle lane will serve straight-ahead vehicles at a flow less than the maximum saturation flow. In fact, only in the first seconds of the effective green time, the middle lane will serve traffic at maximum saturation flow.

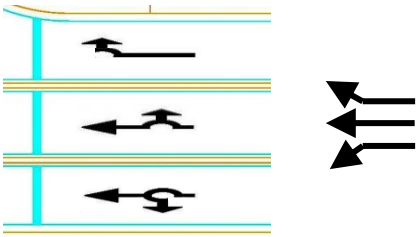


Figure 4-4 Entrance lane configuration on the rotor roundabout and the arrival demand pattern

Therefore, the number of lanes to be used in the capacity calculation is 2 for DP20 through DP100, and less than 2 for DP120 through DP200. For the latter set of demand patterns, the number of lanes depends on the ratio of the left-turning and straight ahead intensities. For DP200, the left lane will serve twice as

[28] *The estimation will be based on rational behaviour: a driver chooses the lane on which the queue of vehicles is smallest, given the constraint that that lane makes part of his route from origin to destination. However, sometimes drivers do not behave rationally. Irrational behaviour is hard to capture in a model and is out of the scope of this project.*

much traffic as the middle lane. By estimation, the middle lane will then serve traffic at saturation flow during half of the effective green time, and the left lane will serve traffic at saturation flow during the entire effective green time. In that case, the number of lanes is 1.5. Linearly interpolating, the number of lanes for DP120 is 1.9; for DP140 it is 1.8; for DP160 it is 1.7; for DP180 it is 1.6.

Amount of lanes: star roundabout

The star roundabout has three legs, therefore the demand patterns (see appendix B) are not symmetrical. This is illustrated by Figure 4-5.

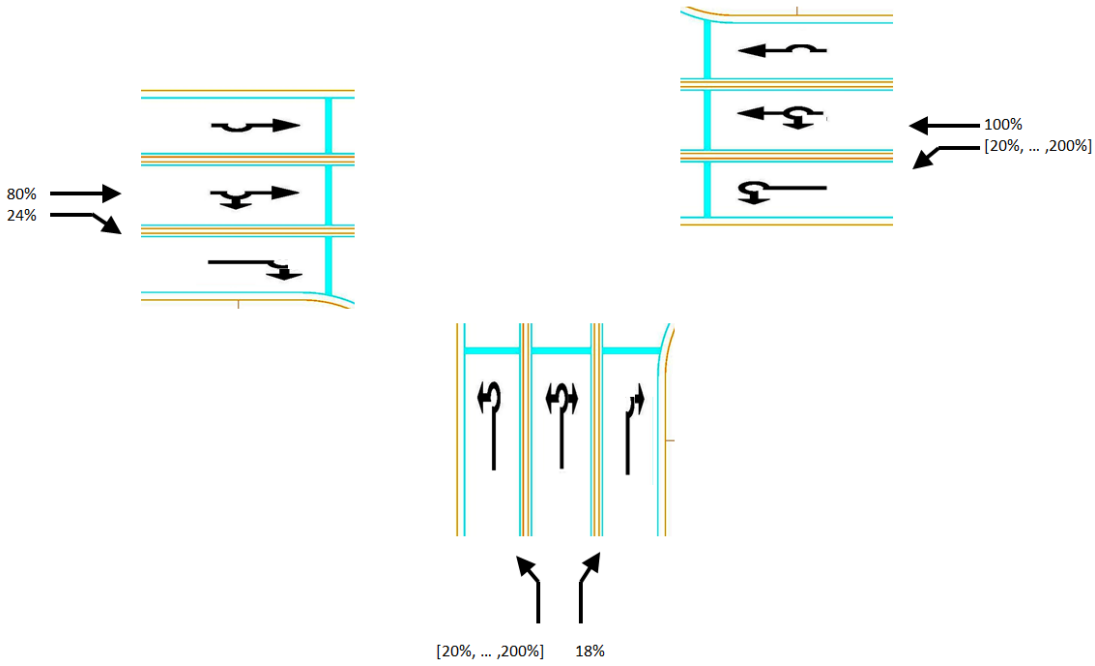


Figure 4-5 Entrance lane configuration on the star roundabout and the arrival demand pattern

By means of this figure, the distribution of vehicles on the lanes and the rate of saturation for each lane will be explored. With respect to the eastern leg: two lanes may serve vehicles going straight-ahead. Two lanes may serve left-turning vehicles. So for all demand patterns in which the left-turning intensities are between 0.5 times and 2 times the straight-ahead intensities (for DP60 through DP200), all three lanes serve traffic at maximum saturation. For DP20 and DP40, the left lane is undersaturated. The amount of lanes for DP20 is (2 + (20/50)) 2.4; the amount of lanes for DP40 is (2+ (40/50)) 2.8. With respect to the southern leg: the right lane becomes less saturated as the left-turning intensities increase. For DP40, all lanes are (more or less) saturated; the amount of lanes is 3. For DP20, the middle and left lanes are saturated for half of the effective green time; the amount of lanes is 2. For DP80, the middle and left lanes serve both twice as much traffic as the right lane; the amount of lanes is 2.5. For patterns DP120 through DP200, the share of the effective green time in which the right lane is saturated, is assumed to be negligible; the amount of lanes for these demand patterns is 2. With respect to the western leg: the middle and left lanes serve more or less twice as much traffic as the right lane, for all demand patterns. The amount of lanes for this leg is estimated to be 2.5.

Roundabout capacity

The roundabout capacity can be calculated by summing the capacity values of the legs:

$$C_{roundabout} = \sum_{all\ legs} C_{leg}$$

Equation 4-4

where:

$C_{roundabout}$ = capacity of the roundabout (pcu/h)

Table 4-3 (Table 4-4) shows an overview of the calculations in this section for the rotor roundabout with an inscribed radius of 12 m (20 m). Figure 4-6 shows the result of the capacity calculations graphically: the capacity of the rotor roundabout, depending on the demand pattern. Table 4-5, Table 4-6 and Figure 4-7 show the results for the star roundabout.

Table 4-3 Durations per leg of the rotor roundabout with an inscribed radius of 12 m

	Green time $t_{green,leg}$	Cycle time t_{cycle}	Eff. green time $t_{eff.green,leg}$	Saturation flow $q_{sat,leg}$	Amount of lanes $n_{lanes,leg}$	Leg capacity C_{leg}
	Figure 4-2	Figure 4-2	Equation 4-1	Equation 4-2	Figure 4-4	Equation 4-3
Leg E	23.0 s	62.8 s	24.0 s	1753 pcu/h	1.5 - 2.0	1005 - 1340 pcu/h
Leg S	12.6 s		13.6 s	1584 pcu/h	1.5 - 2.0	515 - 686 pcu/h
Leg W	17.8 s		18.8 s	1691 pcu/h	1.5 - 2.0	759 - 1012 pcu/h
Leg N	12.6 s		13.6 s	1584 pcu/h	1.5 - 2.0	515 - 686 pcu/h
					Roundabout capacity ->	2793 - 3724 pcu/h

Table 4-4 Durations per leg of the rotor roundabout with an inscribed radius of 20 m

	Green time $t_{green,leg}$	Cycle time t_{cycle}	Eff. green time $t_{eff.green,leg}$	Saturation flow $q_{sat,leg}$	Amount of lanes $n_{lanes,leg}$	Leg capacity C_{leg}
	Figure 4-2	Figure 4-2	Equation 4-1	Equation 4-2	Figure 4-4	Equation 4-3
Leg E	31.3 s	85.8 s	32.3 s	1812 pcu/h	1.5 - 2.0	974 - 1299 pcu/h
Leg S	17.6 s		18.6 s	1687 pcu/h	1.5 - 2.0	522 - 697 pcu/h
Leg W	24.5 s		24.5 s	1758 pcu/h	1.5 - 2.0	746 - 995 pcu/h
Leg N	17.6 s		18.6 s	1687 pcu/h	1.5 - 2.0	522 - 697 pcu/h
					Roundabout capacity ->	2765 - 3687 pcu/h

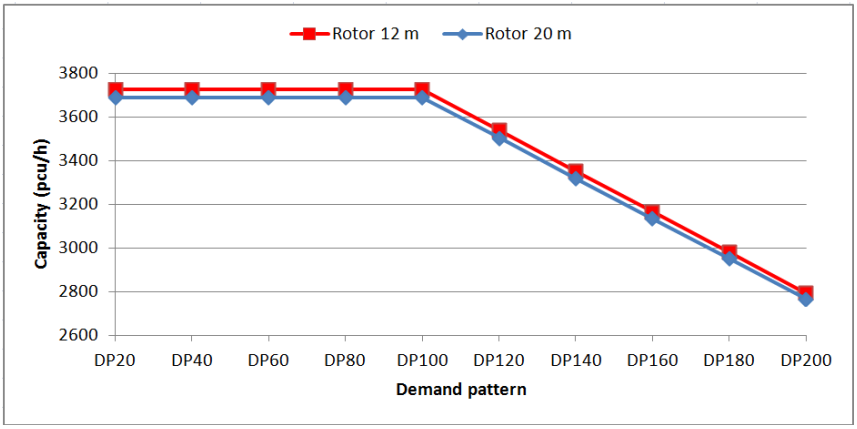


Figure 4-6 Result of the analytical approach: the capacity of the rotor roundabout

Table 4-5 Durations per leg of the star roundabout with an inscribed radius of 12 m

	Green time $t_{green,leg}$	Cycle time t_{cycle}	Eff. green time $t_{eff.green,leg}$	Saturation flow $q_{sat,leg}$	Amount of lanes $n_{lanes,leg}$	Leg capacity C_{leg}
	Figure 4-2	Figure 4-2	Equation 4-1	Equation 4-2	Figure 4-5	Equation 4-3
Leg E	23.3 s		24.3 s	1756 pcu/h	2.4 – 3.0	2120 - 2650 pcu/h
Leg S	12.8 s	48.3 s	13.8 s	1591 pcu/h	2.0 – 3.0	909 - 1364 pcu/h
Leg W	18.1 s		19.1 s	1695 pcu/h	2.0	1341 pcu/h
					Roundabout capacity ->	4370 - 5241 pcu/h

Table 4-6 Durations per leg of the star roundabout with an inscribed radius of 20 m

	Green time $t_{green,leg}$	Cycle time t_{cycle}	Eff. green time $t_{eff.green,leg}$	Saturation flow $q_{sat,leg}$	Amount of lanes $n_{lanes,leg}$	Leg capacity C_{leg}
	Figure 4-2	Figure 4-2	Equation 4-1	Equation 4-2	Figure 4-5	Equation 4-3
Leg E	30.0 s		31.0 s	1805 pcu/h	2.4 – 3.0	2122 - 2652 pcu/h
Leg S	16.8 s	63.3 s	17.8 s	1675 pcu/h	2.0 – 3.0	942 - 1413 pcu/h
Leg W	23.4 s		24.4 s	1756 pcu/h	2.0	1354 pcu/h
					Roundabout capacity ->	4417 - 5301 pcu/h

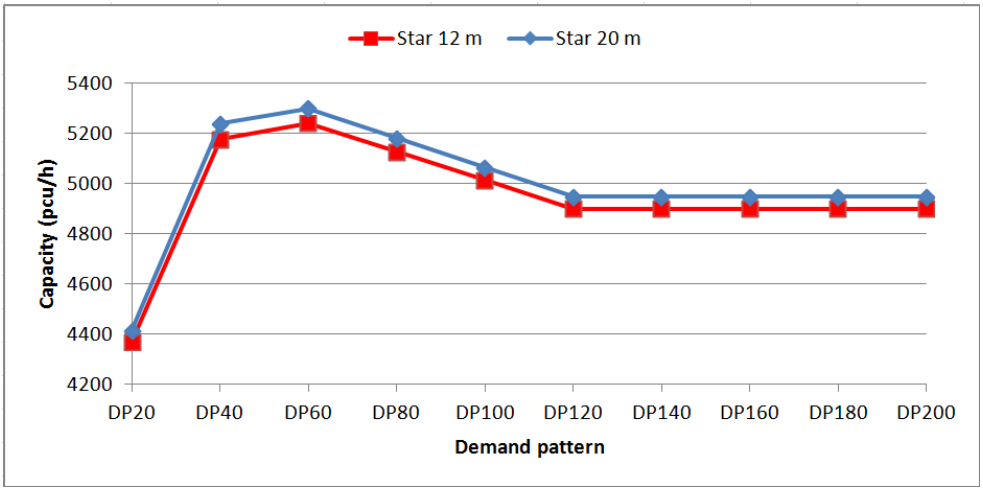


Figure 4-7 Result of the analytical approach: the capacity of the star roundabout

Saturation flow: validation

The estimations for the saturation flow are structurally lower than the saturation flow values estimated by in-field measurements presented in appendix C. Most likely, the differences are caused by the duration of the effective green times, these are probably lower on the signalized rotor and star roundabout than on the turbo circle (the in-field measurements have been performed on two turbo circles). The effective green time durations on the signalized rotor and star are shorter, because these intersection are equipped with a leg-by-leg control (four- or three-phase), while the turbo circle is equipped with a two-phase control.

4.3. VISSIM

This section presents the application of VISSIM to the signalized intersections invoked in this project, according to the plan addressed in section 3.2.3. VISSIM applies VRIGen and TrafCOD to generate a vehicle-actuated control. Therefore, the first section is devoted to the results from VRIGen. The following sections discuss the simulation results for every intersection type separately: respectively the signalized rotor roundabout (with inscribed radii of 12 m and 20 m); the signalized star roundabout (with inscribed radii of 12 m and 20 m); the partial turbo circle (with inscribed radii of 12 m and 20 m); the turbo circle

(with inscribed radii of 12 m, 20 m and 30 m); and the three-leg turbo circle (with inscribed radii of 12 m, 20 m and 30 m).

4.3.1. VRIGen: leg-by-leg control and two-phase control

Appendix K (VRIGen model development) shows the settings in the tabs of VRIGen, in order to produce the leg-by-leg control (result shown in Figure 4-8) and the two-phase control (result shown in Figure 4-9). The appendix also elaborates on the difficulty of invoking green phase overlap and the use of spare streams as a solution. VRIGen enables the user to generate the two-phase control without using spare streams.

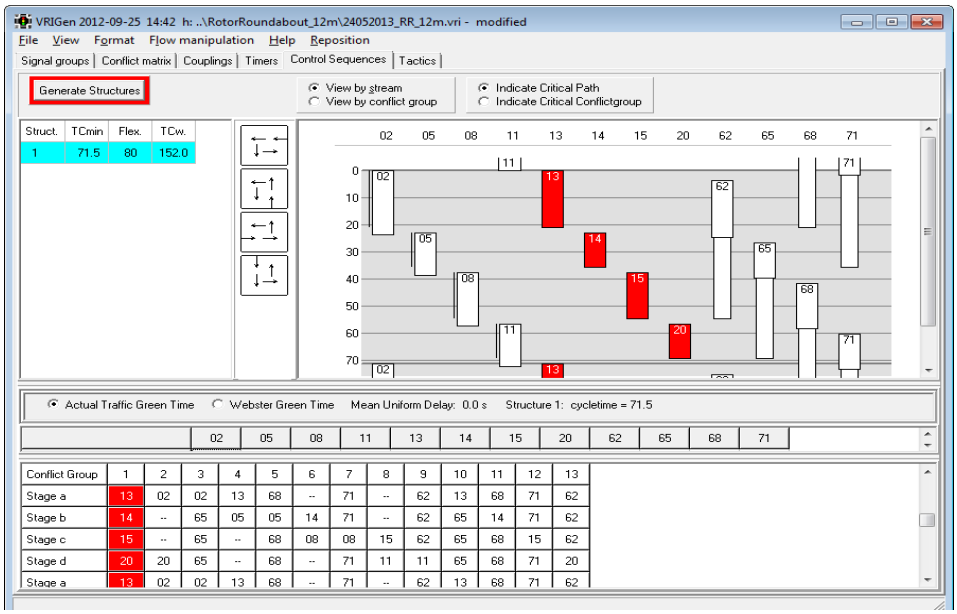


Figure 4-8 The control structure for the leg-by-leg control with phase overlap

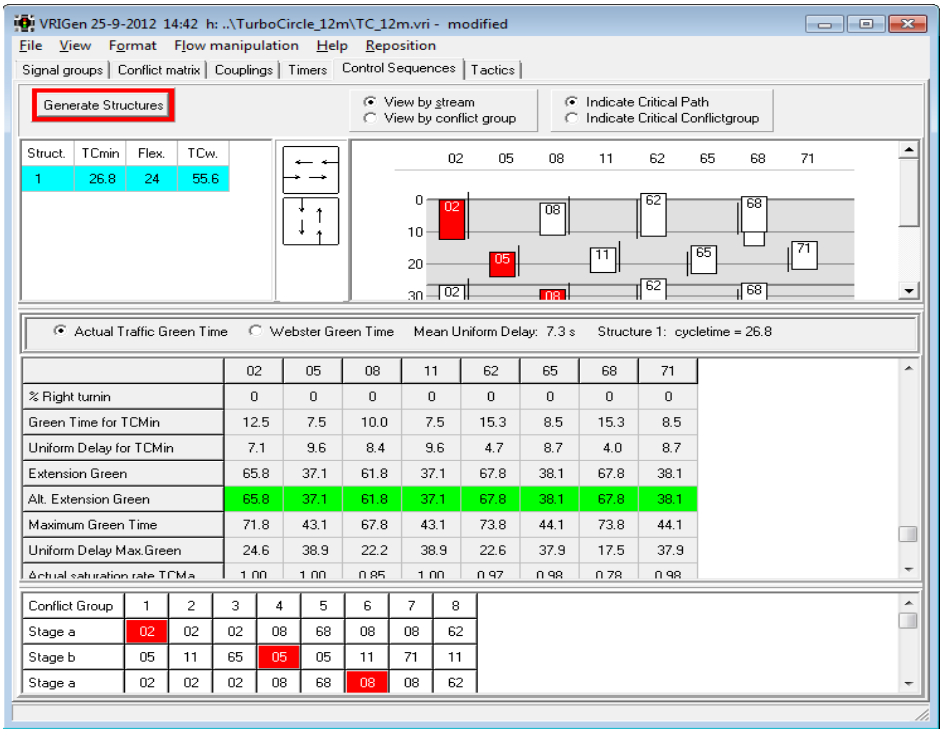


Figure 4-9 The control structure for the two-phase control

4.3.2. VISSIM: rotor roundabout, inscribed radius 12 m

The intermezzo in section 3.2.3 shows how VISSIM will be used to determine the capacity of the intersections invoked in this project. This section shows the results for the rotor roundabout with an inscribed radius of 12 m.

The diagrams in Figure 4-10 show that both lines for stream 02 start to increase simultaneously, this also holds for streams 05 and 08. The diagrams show that for the other streams, the queue length starts to build up earlier than the delay time. In conclusion, stream 02 is the restrictive stream on the leg E because the queue of stream 02 spills back on streams 01 and 03. This also holds for stream 05 with respect to 04 and 06; and for stream 08 with respect to 07 and 09. Therefore, the capacity of leg E is determined by stream 02 (t = 4,25 h; 3600 pcu/h); the capacity of leg S is determined by stream 05 (t = 4,5 h; 3800 pcu/h); and the capacity of leg W is determined by stream 08 (t = 4,5 h; 3800 pcu/h).

Northern leg: no saturation

The lines for the streams on leg N (stream 10, 11 and 12) do not show any saturation, because the lines do not start to increase within the shown interval (2.25 h through 6.0 h). The point of saturation of this leg takes event after t = 6.0 h. This is a remarkable observation, because the leg-by-leg control has been composed such, that no leg has preference over the other legs (see appendix K: VRIGen model development). VRIGen generated structures based on demand patterns which are equal to those applied in the dynamic assignment in VISSIM.

A possible explanation for the 'insatiable' leg N is the small traffic demand on that leg: merely 60% of the total demand on leg E (see appendix B: Demand patterns). The total traffic demand can be served within the maximally extended green phase, up to a total demand higher than 5000 pcu/h (at t = 6.0 h). However, this should also hold for leg S, where the total demand is also equal to 60% of the total demand on leg E. Figure 4-11 shows that the capacity lines of both legs do not coincide.

Due to the lack of sufficient explanation on the excessive capacity of the northern leg, the observations on this leg will be excluded from the capacity evaluation.

Overview of the saturation points

Table 4-7 presents the capacity values for all traffic streams, ordered per demand pattern (the first row shows the observations from Figure 4-10) [29]. The red values indicate the most restrictive traffic stream per leg. The last column presents an estimation for the total capacity of the intersection, that is the average of the restrictive streams. The restrictive streams on the northern leg have not been invoked in this average, because no queue has built up on this leg.

Figure 4-11 shows the capacity values from Table 4-7 graphically. Four lines represent the capacity values of the restrictive streams for every leg, but the first line represents the average value of legs E, S and W; that is the estimated capacity of the intersection (line Av capacity). The sixth line in Figure 4-11 (Av delay) represents the average delay time at capacity (averaged over all legs), projected to the secondary (left) vertical axis.

[29] *In the table, the moments of saturation in time have directly been 'translated' to capacity values by means of Figure 3-6.*

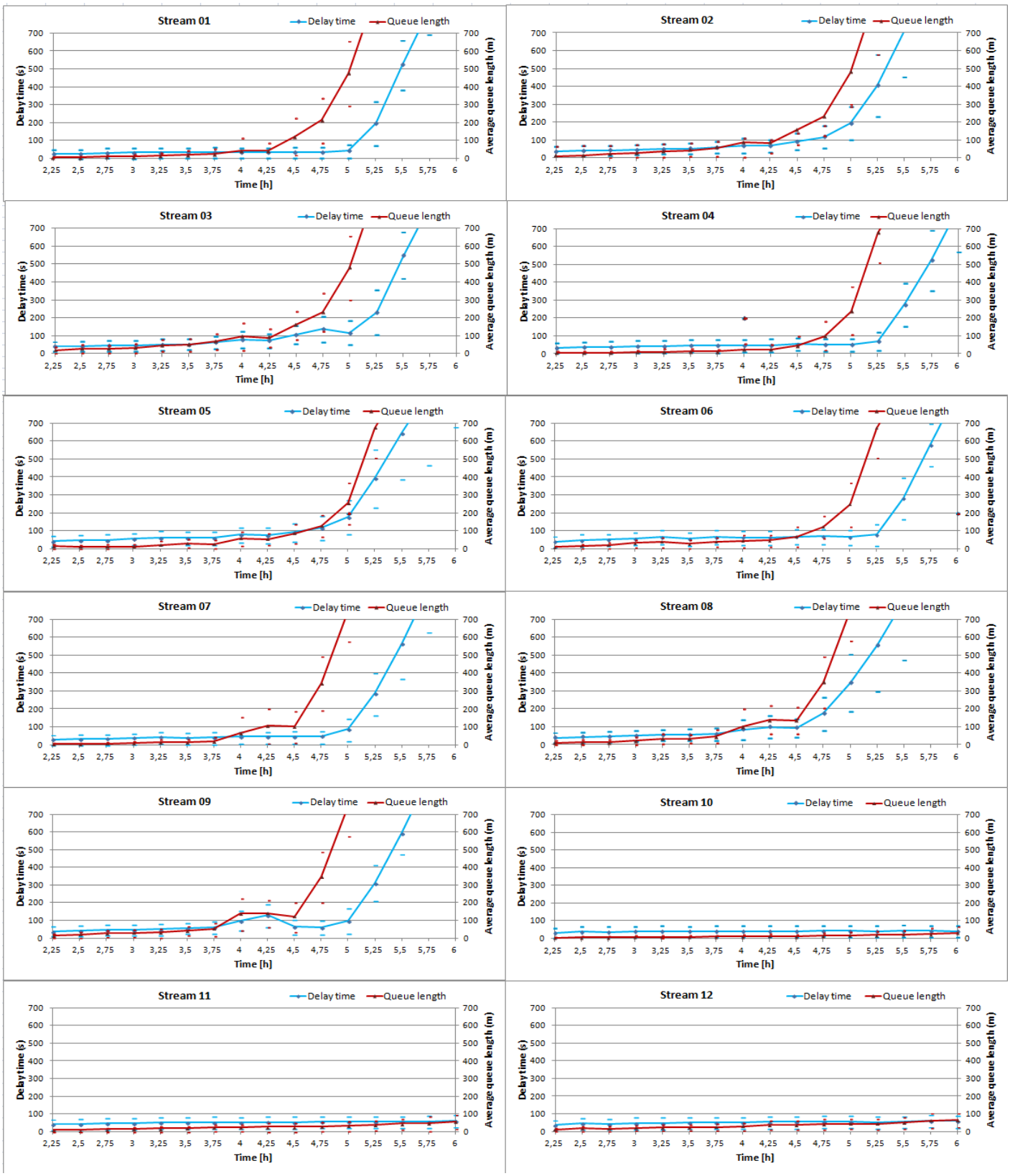


Figure 4-10 Diagrams of the delay time and the queue length on the rotor roundabout with inscribed diameter 12 m, demand pattern 20, all streams, averaged over all random seeds

Table 4-7 Rotor roundabout with an inscribed radius of 12 m: capacity values for every stream separately, per demand pattern (red values represent the constraining streams on the leg)

	Leg E			Leg S			Leg W			Leg N			
	01	02	03	04	05	06	07	08	09	10	11	12	AV
DP20	4200	3800	3600	4400	3800	4400	4000	3800	4000	5600	5200	6200	3733
DP40	4000	3200	3000	4600	4000	4600	4400	3200	4200	5800	5000	5000	3400
DP60	3800	3000	2600	4800	4000	4800	4400	3200	2800	5600	5000	4600	3133
DP80	3800	3000	3800	4600	3600	4200	4200	3400	4000	6000	5200	4600	3333
DP100	4200	3400	3600	5000	3800	3600	4600	3800	3800	6200	5200	4600	3600
DP120	4200	3600	3000	5000	3800	3200	4600	3800	3200	5800	5400	5000	3133
DP140	3800	3400	3000	4800	4000	3200	4200	3800	3000	5400	5000	4600	3067
DP160	3800	3400	2600	4400	3800	2400	4000	3600	3000	5000	4800	4400	2667
DP180	3600	3200	2400	4400	3600	2600	3800	3600	2400	5000	4400	4200	2467
DP200	3400	3000	2400	4200	3600	2600	3800	3400	2600	4600	4600	4400	2533

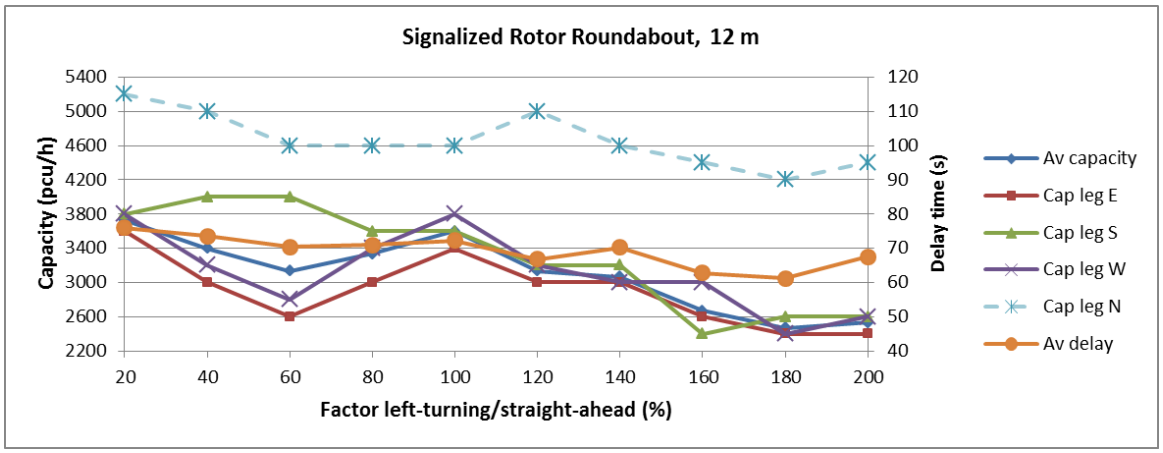


Figure 4-11 Rotor roundabout with an inscribed radius of 12 m: estimated capacity and average delay, as a function of the left-turning streams

Conclusions

Figure 4-11 yields that the capacity differs per leg, especially with respect to the demand patterns in which the straight-ahead streams are busier than the left-turning traffic streams (20% through 80%). An explanation for this observation is, that the traffic demand on legs S and N is merely 60% of the demand on leg E. These legs become saturated later than legs E and W, because the traffic demand is lower. This is also illustrated by the notion that the lines representing legs E and W coincide quite well, while the line representing leg S is structurally higher than the lines representing legs E and W.

4.3.3. VISSIM: rotor roundabout, inscribed radius 20 m

Table 4-8 shows the capacity values for every stream on the rotor roundabout, following from the delay time/queue length diagrams. From the table can be concluded that for demand patterns in which the straight-ahead streams are busier than the left-turning streams (DP20 through DP100), the straight-ahead streams are mostly restrictive. For demand patterns DP120 through DP200, the left-turning streams are mostly restrictive. The conclusion has also been drawn for the rotor roundabout with an inscribed radius of 12 m.

Table 4-8 Rotor roundabout with an inscribed radius of 20 m: capacity values for every stream separately

	Leg E			Leg S			Leg W			Leg N			
	01	02	03	04	05	06	07	08	09	10	11	12	AV
DP20	4400	3600	3600	5400	3400	3400	5200	3600	3600	6400	5600	5600	3533
DP40	4400	3600	3600	5400	4200	3800	5000	3800	3600	6400	6200	5800	3667
DP60	4200	3400	3200	5000	3800	3600	4600	3600	3000	6400	5600	5400	3267
DP80	4400	3800	4000	5400	4200	4400	4800	3800	4800	6400	6200	6400	3933
DP100	4600	4000	3800	5600	4400	4000	5200	4400	4400	6400	6400	6000	4067
DP120	4600	4200	3400	5600	4200	4000	5200	4200	3600	6400	6400	6000	3667
DP140	4400	4000	4800	5400	4400	4000	4800	4200	3600	6400	6400	5400	3867
DP160	4200	3800	3200	5200	4400	3600	4600	4200	3600	6400	6000	5400	3467
DP180	4000	3600	3000	4800	4400	3000	4400	4200	3200	6400	5800	5200	3067
DP200	4000	3600	2800	4800	4200	3000	4400	3800	3200	6200	5800	4800	3000

The restrictive streams (red values) have again been used to estimate the capacity of the signalized rotor roundabout, yielding the values in the most right column. Figure 4-12 shows the values graphically.

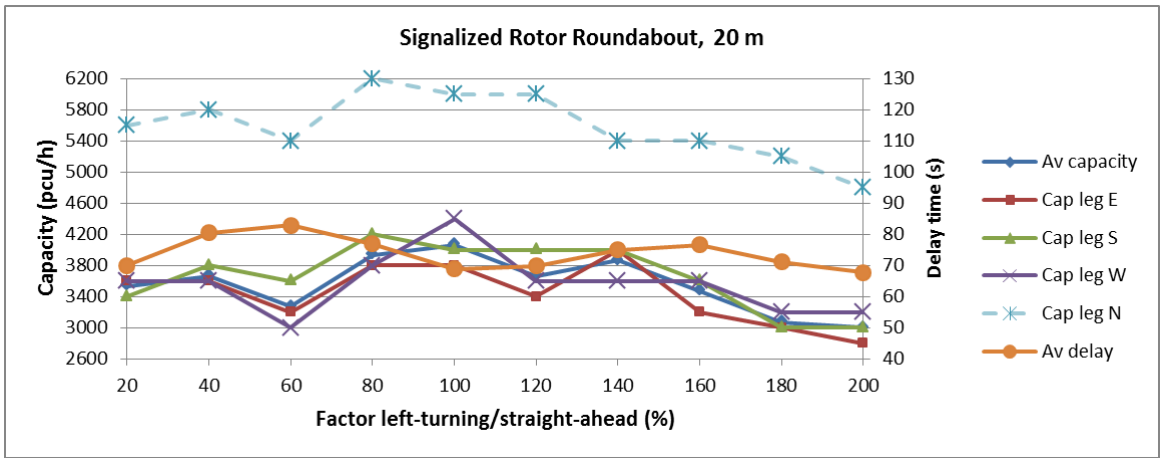


Figure 4-12 Rotor roundabout with an inscribed radius of 20 m: estimated capacity and average delay

Conclusions

Figure 4-12 yields the same conclusions as Figure 4-11.

4.3.4. VISSIM: star roundabout, inscribed radius 12 m

Figure 4-9 shows the capacity values for every stream on the star roundabout, following from the delay time/queue length diagrams. From the table can be concluded that for all demand patterns, the straight-ahead streams on legs E and W, and the left-turning stream on leg S are mostly restrictive.

The restrictive streams (red values) have again been used to estimate the capacity of the signalized star roundabout, yielding the values in the most right column. Figure 4-13 shows all values graphically.

Table 4-9 Star roundabout with an inscribed radius of 12 m: capacity values for every stream separately

	Leg E		Leg S		Leg W		
	02	03	04	06	07	08	AV
DP20	3400	3800	6800	6600	4200	3400	4467
DP40	4000	4600	6600	6400	5000	4200	4867
DP60	4200	4000	6400	6400	5400	4800	5067
DP80	3800	3800	6400	6200	6000	5400	5133
DP100	3600	3800	6400	6000	6600	5600	5067
DP120	3600	3600	6400	5800	6400	6000	5133
DP140	3800	4200	6000	5200	6400	6200	5067
DP160	4000	4200	5600	4800	6400	6200	5000
DP180	4200	4200	5400	4800	6600	6400	5133
DP200	4200	4200	5200	4400	6800	6400	5000

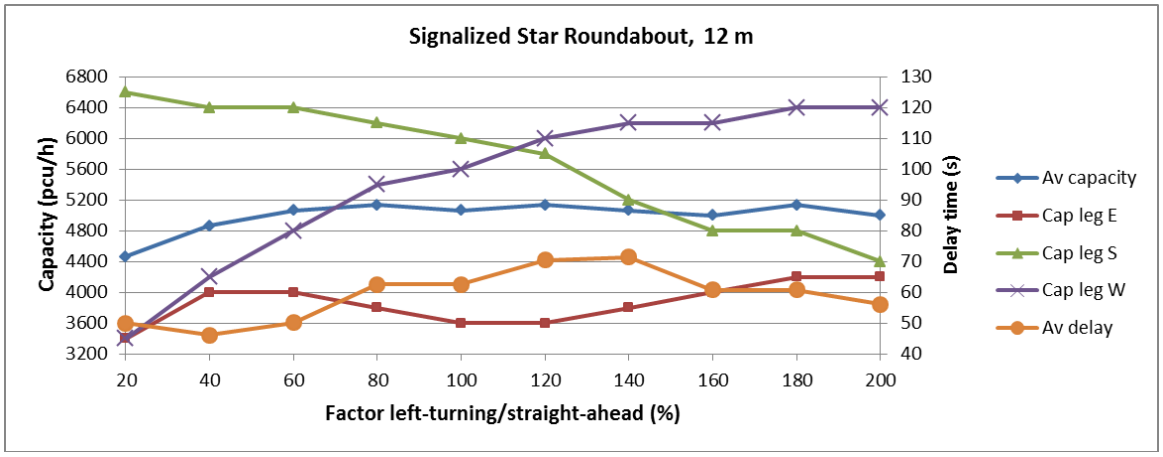


Figure 4-13 Star roundabout with an inscribed radius of 12 m: estimated capacity and average delay

Conclusions

Figure 4-13 yields that the capacity differs vastly per leg, with respect to all demand patterns. The capacity of leg E appears to be independent of the factor left-turning/straight-ahead streams and keeps a constant value between 3400 pcu/h and 4200 pcu/h. On the other hand, the capacity of the other two legs appears to depend on the factor left-turning/straight-ahead streams: the capacity of leg S decreases as the left-turning intensities increase, while the capacity of leg W increases as the left-turning intensities increase.

The major differences between the legs might be caused by the demand patterns for the three-leg intersections (see appendix B: Demand patterns). The patterns are constructed such, that the straight-ahead and right-turning traffic streams are constant, and the left-turning streams increase over the patterns (e.g. in DP20 the left-turning streams amount to 20% of the neighbouring straight-ahead stream,

etc.). In that case, the total demand per leg is constant for intersections with four legs, because every leg contains a left-turning stream. However, leg W on the star roundabout does not contain a left-turning stream. Therefore, the total demand on that leg decreases as the left-turning intensities increase. That explains why the capacity of leg W increases as the left-turning intensities increase: the saturation point is reached later because of a lower total demand on leg W.

4.3.5. VISSIM: star roundabout, inscribed radius 20 m

Similar to the star roundabout with an inscribed radius of 12 m, Table 4-10 shows that for all demand patterns, the straight-ahead streams on legs E and W, and the left-turning stream on leg S are mostly restrictive.

Table 4-10 Star roundabout with an inscribed radius of 20 m: capacity values for every stream separately

	Leg E		Leg S		Leg W		
	02	03	04	06	07	08	AV
DP20	4800	5200	9400	8800	5600	5000	6200
DP40	5400	5600	9000	8400	6200	5800	6533
DP60	4800	4800	8800	8000	6800	6000	6267
DP80	5400	5400	8000	7800	7000	6200	6467
DP100	4400	4400	6600	6400	6600	6000	5600
DP120	4000	4000	6600	5400	7400	6800	5400
DP140	4000	4200	6200	5200	7800	7200	5467
DP160	4000	4200	5600	4600	8000	7600	5400
DP180	4200	4400	5600	4600	8000	8000	5600
DP200	4400	4400	5600	4400	7400	8000	5400

The restrictive streams (red values) have again been used to estimate the capacity of the signalized star roundabout, yielding the values in the most right column. Figure 4-14 shows all values graphically.

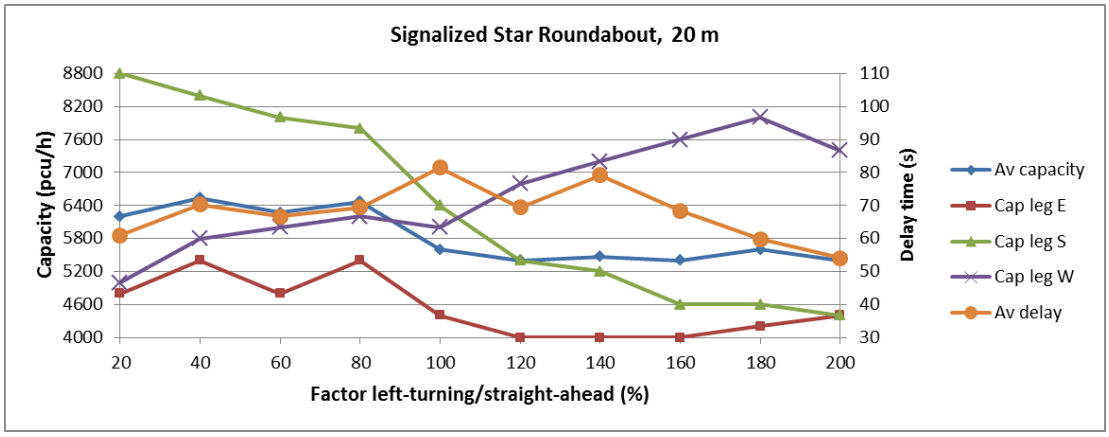


Figure 4-14 Star roundabout with an inscribed radius of 20 m: estimated capacity and average delay

Conclusions

Similar to the star roundabout with an inscribed diameter of 12 m, the capacities of the legs of this (larger) star roundabout differ vastly. Again, leg E has a fairly constant low capacity, whereas the capacity of leg S decreases as the left-turning intensities increase, and the capacity of leg W increases as the left-turning intensities increase.

4.3.6. VISSIM: partial turbo circle, inscribed radius 12 m

From Table 4-11 can be concluded that on all legs and for almost all demand patterns, the left-turning traffic stream is restrictive. This is in line with expectation, because the left-turning vehicles have to queue up on the partial turbo circle.

Table 4-11 Partial turbo circle with an inscribed radius of 12 m: capacity values for every stream separately

	Leg E			Leg S			Leg W			Leg N			
	01	02	03	04	05	06	07	08	09	10	11	12	AV
DP20	4800	5000	4600	4800	4800	5600	5600	6000	4800	4800	5200	5600	4733
DP40	4600	4600	3800	4400	4200	4200	5000	4800	3400	5400	5000	4000	3800
DP60	3600	3400	3000	4000	4200	3200	3800	3600	3000	4400	4400	3200	3067
DP80	4000	3800	3200	5800	4800	3600	4400	4000	3200	4800	4800	3600	3333
DP100	4000	3800	3000	4800	4400	3400	4400	4000	3200	4800	4400	3400	3200
DP120	3800	3600	2800	4600	4400	3200	4400	4400	3000	5000	4400	3400	3000
DP140	3800	3600	2800	4800	4800	3000	4200	4000	2800	5000	4800	2800	2867
DP160	3800	3800	2600	4600	4000	2800	4200	4200	2800	5000	5000	2800	2667
DP180	3600	3600	2400	4800	5200	2800	4000	4000	2800	4800	4600	2600	2667
DP200	3600	3600	2400	4600	4600	2600	3800	3800	2400	4800	4600	2600	2467

The restrictive streams (red values) have again been used to estimate the capacity of the partial turbo circle, yielding the values in the most right column. Figure 4-15 shows all values graphically.

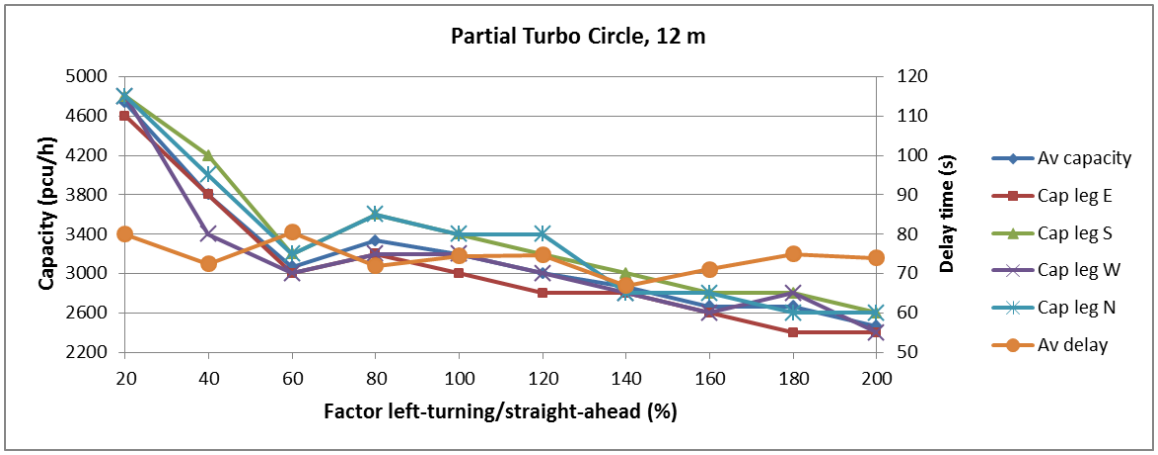


Figure 4-15 Partial turbo circle with an inscribed radius of 12 m: estimated capacity and average delay

Conclusions

The partial turbo circle has a high capacity for demand patterns with small left-turning intensities. The capacity lines representing the different legs coincide quite well, in contrast to the diagrams for the star roundabouts. Neither has leg N an extraordinary high capacity, in contrast to the diagrams for the rotor roundabouts.

4.3.7. VISSIM: partial turbo circle, inscribed radius 20 m

From Table 4-12 can be concluded that on all legs and for almost all demand patterns, the left-turning traffic stream is restrictive. This is in line with expectation.

Table 4-12 Partial turbo circle with an inscribed radius of 20 m: capacity values for every stream separately

	Leg E			Leg S			Leg W			Leg N			
	01	02	03	04	05	06	07	08	09	10	11	12	AV
DP20	5400	5400	5600	5000	5000	6000	6000	5800	6600	4800	5400	5800	5400
DP40	4800	4600	3800	4600	4400	4200	5200	5000	3800	5400	5400	4000	3933
DP60	4800	4600	3600	4800	5000	4200	5000	4800	3600	5800	5400	3800	3800
DP80	4400	3600	3600	5200	3800	4000	4000	3800	3600	4400	4400	3600	3667
DP100	4200	4000	3200	5400	5200	3600	4600	4200	3600	5400	5200	3600	3467
DP120	4200	4000	3200	5000	4600	3600	4400	4000	3200	5000	4600	3200	3333
DP140	4000	4000	2800	5200	4400	3200	4400	4400	3000	5200	5000	3200	3000
DP160	4000	4000	2600	4800	4200	2800	4400	4200	2800	5000	4400	2800	2733
DP180	3800	3800	2600	5000	4800	2600	4000	4000	2400	4800	4600	2800	2533
DP200	3600	3600	2400	4400	3800	2400	4000	4000	2400	4800	4600	2400	2400

The restrictive streams (red values) have again been used to estimate the capacity of the partial turbo circle, yielding the values in the most right column. Figure 4-16 shows all values graphically.

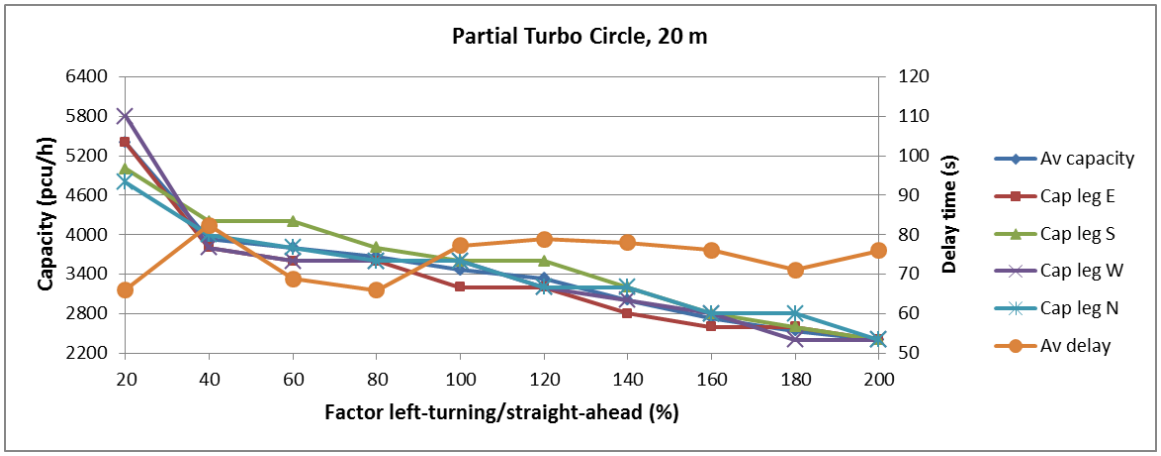


Figure 4-16 Partial turbo circle with an inscribed radius of 20 m: estimated capacity and average delay

Conclusions

Figure 4-16 yields the same conclusions as Figure 4-15.

4.3.8. VISSIM: four-leg turbo circle, inscribed radius 12 m

From Table 4-13 can be concluded that on all legs and for almost all demand patterns, the left-turning traffic stream is restrictive. This is in line with expectation.

Table 4-13 Turbo circle with an inscribed radius of 12 m: capacity values for every stream separately

	Leg E			Leg S			Leg W			Leg N			
	01	02	03	04	05	06	07	08	09	10	11	12	AV
DP20	9200	8800	9200	9800	8600	9800	9800	9200	9800	9800	8400	9800	8800
DP40	8400	8000	7000	10000	8600	9800	9400	8200	7200	10000	8400	9000	7533
DP60	7400	7000	5800	10000	9800	7800	8000	7200	6000	9600	8600	6200	6000
DP80	7000	6800	5600	8600	8600	7800	7200	6600	5600	8400	7800	6000	5733
DP100	6600	6400	5200	9400	9200	7600	7000	6400	5400	8000	7600	5600	5400
DP120	6400	6000	5200	7600	7600	8800	6800	6400	5400	7200	7000	5200	5267
DP140	6400	6000	5000	10000	9000	9200	6600	6200	5200	7400	7000	5000	5067
DP160	6200	5600	4800	9400	9400	8400	6600	6000	5400	6800	6200	5400	5200
DP180	5800	5400	4600	8800	8800	9200	6400	6200	5000	7000	6400	4800	4800
DP200	5600	5400	4600	9400	9400	8800	6000	5800	4800	6200	6600	4600	4667

The restrictive streams (red values) have again been used to estimate the capacity of the turbo circle, yielding the values in the most right column. Figure 4-17 shows all values graphically.

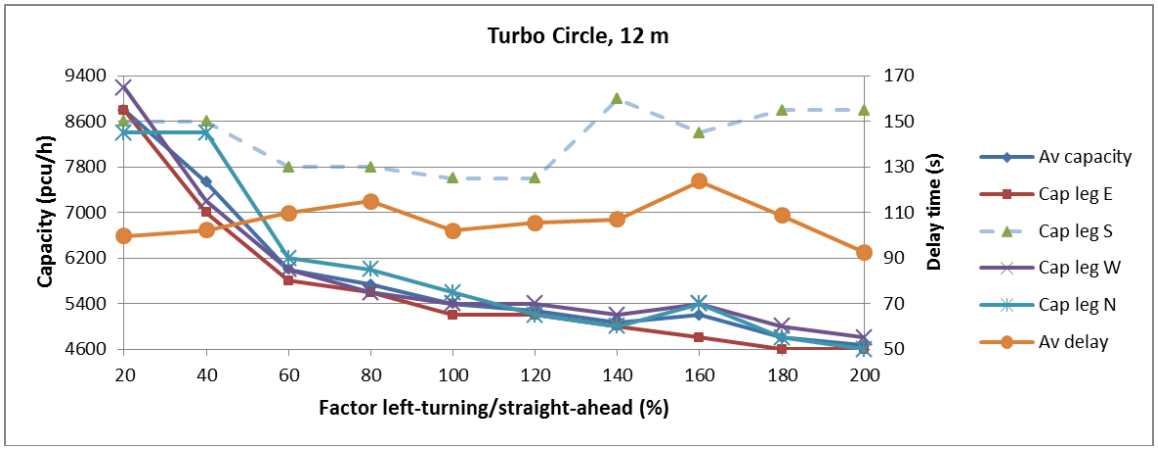


Figure 4-17 Turbo circle with an inscribed radius of 12 m: estimated capacity and average delay

Conclusions

The turbo circle has a high capacity for demand patterns where the left-turning intensities are low. The capacity lines representing the different legs coincide quite well, except for the line representing leg S. Just like leg N has a high capacity on the rotor roundabout, leg S has a high capacity on the turbo circle. Therefore, the observations on this leg are excluded from the capacity evaluation.

4.3.9. VISSIM: four-leg turbo circle, inscribed radius 20 m

Table 4-14 can be concluded that the left-turning traffic streams are generally restrictive. This is in line with expectation.

Table 4-14 Turbo circle with an inscribed radius of 20 m: capacity values for every stream separately

	Leg E			Leg S			Leg W			Leg N			
	01	02	03	04	05	06	07	08	09	10	11	12	AV
DP20	9200	8800	9200	10000	9200	10000	10000	8800	10000	10000	9000	9800	8950
DP40	8800	8000	7800	10000	8400	8600	10000	9800	7400	10000	8600	9400	8050
DP60	8000	7600	6800	9400	8800	7400	9600	9000	7000	10000	9000	7800	7250
DP80	7600	7200	6200	10000	9400	7200	9600	9000	6200	10000	9400	7400	6750
DP100	7200	7000	6000	9600	9200	6800	8000	7600	6600	9600	9000	6400	6450
DP120	7000	7000	6000	8800	8800	6800	7600	7400	6200	8800	8400	6800	6450
DP140	7000	6800	5800	8800	8600	6400	7800	7000	6000	8600	8400	6400	6150
DP160	6800	6600	5600	8800	9600	6200	7400	6800	5800	9000	8800	6400	6000
DP180	6600	6200	5200	9600	9200	6000	7400	7200	5800	9200	8800	6000	5750
DP200	6600	6000	5200	9800	9400	5800	7400	7000	5600	9000	8600	6000	5650

The restrictive streams (red values) have again been used to estimate the capacity of the turbo circle, yielding the values in the most right column. Figure 4-18 shows all values graphically.

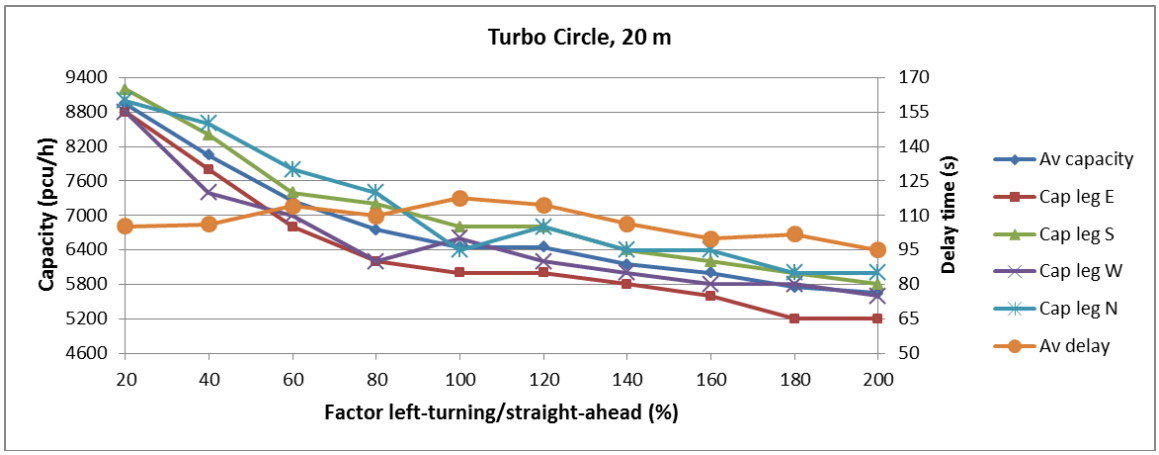


Figure 4-18 Turbo circle with an inscribed radius of 20 m: estimated capacity and average delay

Conclusions

The capacity lines representing the different legs coincide quite well (including leg S, in contrast with the turbo circle with an inscribed radius of 12 m). The lines representing legs E and W are structurally lower than the average capacity; the lines representing legs S and N are structurally higher than the average capacity. This is caused by the prevailing demand patterns, in which the total demand on legs S and N amounts to merely 60% of the total demand on leg E.

4.3.10. VISSIM: four-leg turbo circle, inscribed radius 30 m

Table 4-15 can be concluded that the left-turning traffic streams are generally restrictive. This is in line with expectation.

Table 4-15 Turbo circle with an inscribed radius of 30 m: capacity values for every stream separately

	Leg E			Leg S			Leg W			Leg N			
	01	02	03	04	05	06	07	08	09	10	11	12	AV
DP20	9200	8800	9200	10000	9200	10000	10000	10000	10000	9800	9000	9400	9250
DP40	8800	8200	8200	9600	8400	9600	10000	9800	9600	8400	8400	8400	8650
DP60	8400	7800	7200	9200	8400	9000	9800	8600	7200	10000	8000	9400	7700
DP80	7800	7200	6600	10000	9400	7800	9200	8800	6600	10000	9200	7200	7050
DP100	7600	7200	6400	8600	8600	7000	9200	8600	6400	8600	8400	6800	6650
DP120	7200	7000	6200	8600	8400	6800	9000	8400	6600	8600	8400	6800	6600
DP140	7200	7000	6200	8400	8200	6800	9000	8600	6400	8400	8400	6800	6550
DP160	7200	6800	6000	9600	9000	6200	7600	7200	6000	9400	9000	6400	6150
DP180	7000	6800	5800	9800	9400	5600	7200	7000	6000	9200	8800	6000	5850
DP200	6800	6600	5800	10000	9600	5600	7200	6800	5800	9800	9600	6000	5800

The restrictive streams (red values) have again been used to estimate the capacity of the turbo circle, yielding the values in the most right column. Figure 4-19 shows all values graphically.

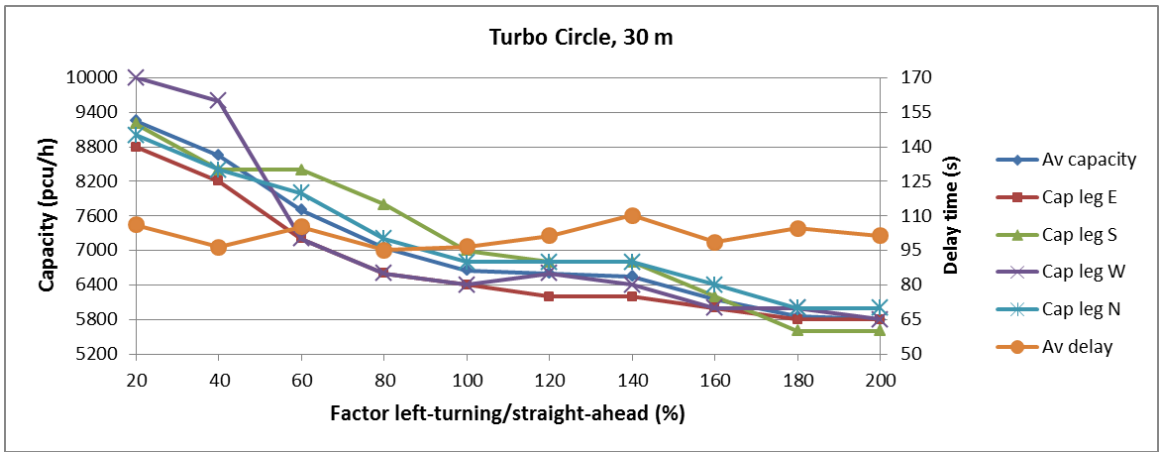


Figure 4-19 Turbo circle with an inscribed radius of 30 m: estimated capacity and average delay

Conclusions

Figure 4-19 yields the same conclusions as Figure 4-18.

4.3.11. VISSIM: three-leg turbo circle, inscribed radius 12 m

Similar to the signalized star roundabout, Table 4-16 shows that for all demand patterns, the straight-ahead streams on legs E and W, and the left-turning stream on leg S are mostly restrictive. The only difference with the star roundabout is, that stream 03 is restrictive on leg E for demand patterns with busy left-turning streams. This is in line with expectation, because on the three-leg turbo circle, vehicles in stream 03 have to queue up on the circle, in contrast with the signalized star roundabout.

Table 4-16 Three-leg turbo circle with an inscribed radius of 12 m: capacity values for every stream separately

	Leg E		Leg S		Leg W		
	02	03	04	06	07	08	AV
DP20	3600	3800	7400	7400	6000	5600	5533
DP40	3600	4000	8000	8000	6400	5800	5800
DP60	3800	4200	7800	8000	6600	6000	5867
DP80	4000	4400	8000	7600	6400	5800	5800
DP100	4200	4600	7200	6600	7200	6400	5733
DP120	4200	4200	6600	6000	7600	7200	5800
DP140	4400	4000	6400	5200	8000	7400	5533
DP160	4400	4000	5800	4600	8000	8000	5533
DP180	4400	4000	5400	4400	8000	8000	5467
DP200	4000	3800	5400	4400	8000	8000	5400

The restrictive streams (red values) have again been used to estimate the capacity of the three-leg turbo circle, yielding the values in the most right column. Figure 4-20 shows all values graphically.

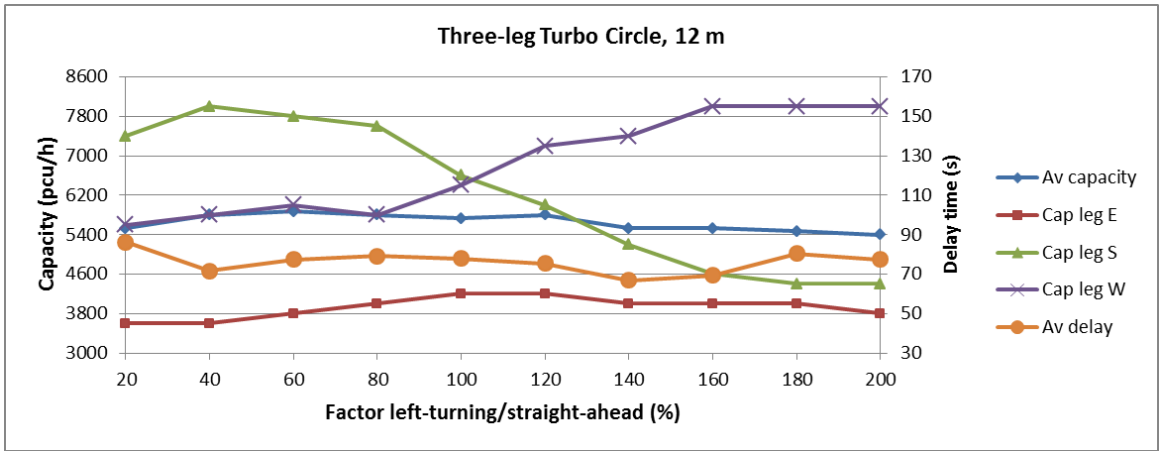


Figure 4-20 Three-leg turbo circle with an inscribed radius of 12 m: estimated capacity and average delay

Conclusions

Similar to the signalized star roundabout, the capacities of the legs of this three-leg turbo circle differ vastly. Again, leg E has a comparably constant low capacity, whereas the capacity of leg S decreases as the left-turning intensities increase, and the capacity of leg W increases as the left-turning intensities increase. This is caused by the demand patterns, in which the demand on leg W decreases, while the demand on the other legs increases.

A final interesting conclusion is that the average capacity of the three-leg turbo circle does not decrease as the left-turning intensities increase, according to Figure 4-20. This conclusion does not coincide with

the presumption in section 3.1., where the capacity of the three-leg turbo circle is presumed to decrease as the left-turning intensities increase, because the vehicles in stream 03 have to queue up on the circle. From visual observations of the VISSIM simulations and Table 4-16, the explanation can be drawn: the capacity of stream 02 constrains the capacity of leg E. Stream 02 is supplied with only one lane, with a sharp bend at the entrance to the circle [30]. This bottleneck imposes a capacity constraint on leg E; the capacity can be increased by supplying stream 02 with two lanes (four lanes on leg E).

4.3.12. VISSIM: three-leg turbo circle, inscribed radius 20 m

Again, Table 4-17 shows that for all demand patterns, the straight-ahead stream W, and the left-turning stream on leg S are mostly restrictive. Regarding leg E: the left-turning stream is restrictive for demand patterns with busy left-turning streams. This is in line with expectation.

Table 4-17 Three-leg turbo circle with an inscribed radius of 20 m: capacity values for every stream separately

	Leg E		Leg S		Leg W		
	02	03	04	06	07	08	AV
DP20	4800	4800	8000	9200	6200	5600	6133
DP40	4800	5200	8200	9200	6600	5800	6267
DP60	5000	5000	8000	9200	7000	6400	6467
DP80	4800	5000	8800	8200	7000	6400	6467
DP100	5200	5600	8000	7000	7400	6800	6333
DP120	5400	5000	7200	6200	8000	7800	6333
DP140	5000	4800	6800	5600	8400	8000	6133
DP160	5400	5200	6400	5600	9200	8800	6533
DP180	5600	4800	6000	4800	9200	9200	6267
DP200	6000	4800	5600	4800	8800	8800	6133

The restrictive streams (red values) have again been used to estimate the capacity of the three-leg turbo circle, yielding the values in the most right column. Figure 4-21 shows all values graphically.

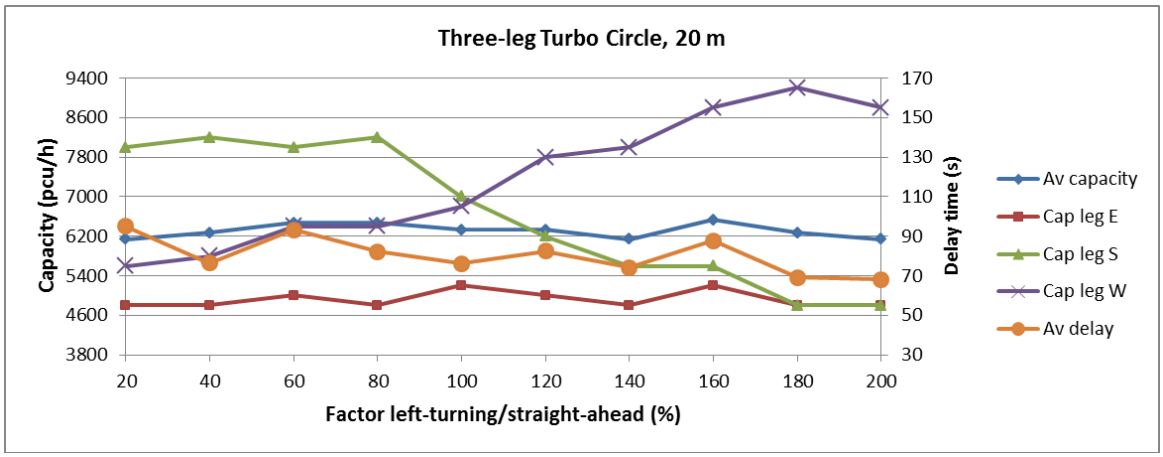


Figure 4-21 Three-leg turbo circle with an inscribed radius of 20 m: estimated capacity and average delay

[30] *This bend has a radius of 12 m. In VISSIM, the consequential speed reduction is simulated by a Reduced Speed Area with a speed limit of 25 km/h, see appendix L (VISSIM model development).*

Conclusions

Again, leg E has a comparably constant low capacity, whereas the capacity of leg S decreases as the left-turning intensities increase, and the capacity of leg W increases as the left-turning intensities increase.

4.3.13. VISSIM: three-leg turbo circle, inscribed radius 30 m

Again, Table 4-18 shows that for all demand patterns, the straight-ahead stream W, and the left-turning stream on leg S are mostly restrictive. Regarding leg E: the left-turning stream is restrictive for demand patterns with busy left-turning streams.

Table 4-18 Three-leg turbo circle with an inscribed radius of 30 m: capacity values for every stream separately

	Leg E		Leg S		Leg W		
	02	03	04	06	07	08	AV
DP20	5200	5600	7600	9600	6400	6400	6400
DP40	5400	5800	8600	8800	6800	6200	6733
DP60	5800	6000	9000	9800	6800	6600	7133
DP80	5800	6400	9400	8400	7200	6600	6933
DP100	6000	6600	8000	6800	7600	6800	6533
DP120	5800	5800	7200	6200	8000	7200	6400
DP140	6000	5400	6800	5600	9200	8600	6533
DP160	5600	5200	6400	5400	10000	8600	6400
DP180	5400	5200	6200	5200	10000	8800	6400
DP200	5000	4800	6000	5200	10000	9200	6400

The restrictive streams (red values) have again been used to estimate the capacity of the three-leg turbo circle, yielding the values in the most right column. Figure 4-22 shows all values graphically.

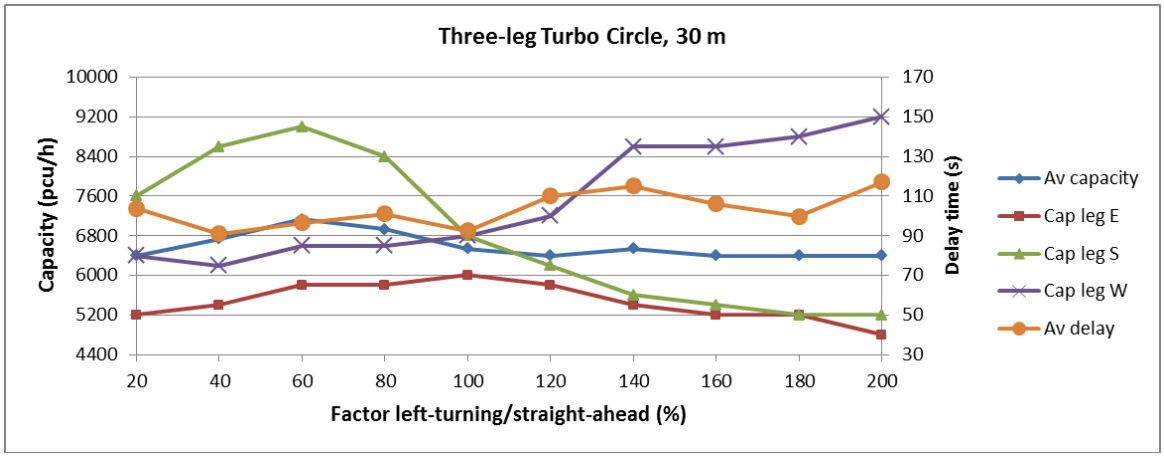


Figure 4-22 Three-leg turbo circle with an inscribed radius of 30 m: estimated capacity and average delay

Conclusions

Again, leg E has a comparably constant low capacity, whereas the capacity of leg S decreases as the left-turning intensities increase, and the capacity of leg W increases as the left-turning intensities increase.

4.4. Summary and conclusions

4.4.1. Un-signalized rotor and star roundabouts: results of the MSRV

The capacities of the signalized rotor and star roundabouts decrease as the left-turning intensities increase. The capacity of the rotor roundabout ranges from 2912 pcu/h to 4553 pcu/h. The capacity of the star roundabout ranges from 3676 pcu/h to 5075 pcu/h.

The delay time on the signalized rotor roundabout decreases as the left-turning intensities increase, while the delay time on the signalized star roundabout increases as the left-turning intensities increase (except for DP180 and DP200, where another leg constrains the capacity).

4.4.2. Signalized rotor and star roundabouts: results of the analytical approach

Duration of the maximum possible green phase overlap

The maximum possible green phase overlap per cycle depends on the geometrical design of the turbo roundabout and the acceleration behaviour of the first departing vehicle. The signalized rotor roundabout with an inscribed radius of 12 m (20 m) allows for a maximum possible green phase overlap of 3.2 s (5.2 s) per cycle. The signalized star roundabout with an inscribed radius of 12 m (20 m) allows for a maximum possible green phase overlap of 3.8 s (6.9 s) per cycle. These values for the green phase overlap do not depend on the duration of the green phase, but only on the geometrical design of the roundabout.

Capacity benefits thanks to the green phase overlap

There exists an optimal value for the cycle time duration, depending on the duration of the maximum possible green phase overlap per cycle, and the prevailing demand pattern. The capacity of the (symmetrical) rotor roundabout is maximized for the demand pattern in which all legs are equally (symmetrically) loaded. The capacity of the (asymmetrical) star roundabout is larger for the set of demand patterns applied in this project, than for the demand pattern in which all legs are equally loaded.

The optimum cycle time for the signalized rotor roundabout with an inscribed radius of 12 m is 47.2 s. Effectively, the green phase overlap offers the possibility of extending the aggregated effective green time per hour by 5% (3.2 / (24.0 + 13.6 + 18.8 + 13.6)), compared to the signalized rotor roundabout without any green phase overlap. For the signalized rotor roundabout with an inscribed radius of 20 m, this surplus is 6%. With respect to the signalized star roundabout, the green phase overlap offers a surplus of 7% (9%) for an inscribed radius of 12 m (20 m).

Consequently, the signalized turbo roundabout should be supplied with a static traffic control, in order to optimally use the green phase overlap.

Capacity of the signalized rotor roundabout

With the maximum possible green phase overlap, the capacity of the signalized rotor roundabout with an inscribed radius of 12 m (20 m) amounts to 3724 pcu/h (3687 pcu/h), depending on the demand pattern. The value decreases as the left-turning intensities increases, down to 2793 pcu/h (2765 pcu/h) for the demand pattern in which the left-turning intensities are twice as high as the straight-ahead intensities. This is caused by the fact that the arriving vehicles are unequally distributed on the entrance lanes.

The capacity of the rotor roundabout with an inscribed radius of 20 m is slightly smaller than the capacity of the rotor roundabout with an inscribed radius of 12 m. This is not in accordance with the presumption from section 3.1.3, stating that the larger the roundabout, the larger the distance between every pair of legs, the larger the green phase overlap, and thus the larger the capacity of the roundabout.

Apparently, the latter relationship is not correct: as the green phase overlap per cycle increases, the capacity of the roundabout does not necessarily increase. This is caused by the fact that in a clockwise leg-by-leg control, the green phases of two neighbouring legs may overlap, but the green phases of two opposite legs may not overlap. In fact, a time interval should separate both green phases, because the last vehicle in a left-turning stream needs time to cross the roundabout and clear the conflict area with the opposite leg. Therefore, in order to use the maximum green phase overlap offered by the distance between two neighbouring legs, the duration of the green phase of a leg has a lower boundary, equal to this time interval, plus the green phase overlap between two legs, plus the yellow time. This minimum green time determines the minimum cycle time.

As the inscribed radius increases, the green phase overlap per cycle increases. However, the minimum green time must increase as well, because the green phases of two opposite legs may not overlap. Therefore, the minimum cycle time increases. As the cycle time increases, the amount of cycles decreases, decreasing the green phase overlap per hour. This is the reason why the capacity of the larger rotor roundabout is slightly smaller than the capacity of the smaller roundabout.

Capacity of the signalized star roundabout

The capacity of the signalized star roundabout with an inscribed diameter of 12 m (20 m) amounts to 4900 pcu/h (4948 pcu/h). This is the capacity value for the demand pattern applied in this project, in which the left-turning intensities are higher than the straight-ahead intensities. For the demand pattern in which the left-turning intensities amount to 20% of the neighbouring straight-ahead intensities, the capacity is comparably low: 4370 pcu/h (4417 pcu/h), while the capacity is higher than 5014 pcu/h (5065 pcu/h) if that percentage differs from 40% through 100%. The capacity for DP20 is low, because the amount of lanes on the eastern leg is chosen comparably small (2.4). The capacity is maximized for DP60; the amount of lanes serving traffic at capacity is large.

4.4.3. Signalized intersections: results of VISSIM

The capacity evaluation by means of the simulations yields the values for the capacity and the delay time shown in Table 4-19.

Table 4-19 Capacity and delay time for every intersection type, resulting from the simulations

Intersection type	Inscribed radius	Capacity (pcu/h)	Delay time (s)
Signalized rotor roundabout	12 m	2500-3700	60-80
Signalized rotor roundabout	20 m	3000-4100	70-80
Signalized star roundabout	12 m	4500-5100	40-70
Signalized star roundabout	20 m	5400-6500	55-80
Partial turbo circle	12 m	2500-4700	70-80
Partial turbo circle	20 m	2400-5400	65-80
Turbo circle	12 m	4700-8800	90-120
Turbo circle	20 m	5700-9000	95-120
Turbo circle	30 m	5800-9300	95-110
Three-leg turbo circle	12 m	5400-5800	65-85
Three-leg turbo circle	20 m	6100-6500	70-95
Three-leg turbo circle	30 m	6400-7100	90-115

With regard to the signalized rotor roundabout: the capacity is optimized for the demand pattern in which the straight-ahead streams are equal to the left-turning streams. The capacity values per leg vary modestly for demand patterns in which the straight-ahead streams are busier than the left-turning streams. The simulations yield extraordinary high capacity values for leg N, the observations on this leg are therefore excluded from the capacity evaluation.

With regard to the signalized star roundabout and the three-leg turbo circle: the capacity values per leg vary substantially. Leg E has a low capacity, fairly constant over different demand patterns. The capacity of leg S decreases as the left-turning streams become busier, while the capacity of leg W increases as the left-turning streams become busier.

The major differences between the legs might be caused by the demand patterns for the three-leg intersections (see appendix B: Demand patterns). The patterns are constructed such, that the straight-ahead and right-turning traffic streams are constant, and the left-turning streams increase over the patterns (e.g. in DP20 the left-turning streams amount to 20% of the neighbouring straight-ahead stream, etc.). In that case, the total demand per leg is constant for four-leg intersections, because every leg contains a left-turning stream. However, the western leg on the star roundabout and the three-leg turbo circle does not contain a left-turning stream. Therefore, the total demand on that leg decreases as the left-turning intensities increase. That explains why the capacity of the western leg increases as the left-turning intensities increase: the saturation point is reached later because of a lower total demand on the western leg.

With regard to the (partial) turbo circle: the capacity of the intersection decreases as the left-turning intensities increases. This coincides with the presumption from chapter 2 (Literature review), where this is explained by the fact that left-turning vehicles have to queue up on the circle. The available queuing space on the circle thereby constraints the capacity of the intersection.

Moreover, the lines representing legs E and W are structurally lower than the average capacity; the lines representing legs S and N are structurally higher than the average capacity. This is caused by the prevailing demand patterns, in which the total demand on legs S and N amounts to merely 60% of the total demand on leg E.

5. Other performance indicators

The performance of the signalized turbo roundabout should be evaluated based on various performance indicators. So far, a lot of attention has been paid to the capacity of and delay times on the turbo roundabout. This chapter addresses the four other performance indicators: space requirement (first section), robustness (second section), traffic safety (third section) and environmental considerations (fourth section).

5.1. Space requirement

Appendix D (Geometrical designs) determines the space requirements of all intersections types invoked in this project. Table 5-1 presents an overview of inscribed and outer radii.

Table 5-1 Overview of the inscribed and outer radii

	Inscribed radius	Outer radius
Rotor roundabout	12 m	52 m
Rotor roundabout	20 m	64 m
Star roundabout	12 m	56 m
Star roundabout	20 m	68 m
Partial turbo circle	12 m	66 m
Partial turbo circle	20 m	77 m
Four-leg turbo circle	12 m	79 m
Four-leg turbo circle	20 m	91 m
Four-leg turbo circle	30 m	106 m
Three-leg turbo circle	12 m	65 m
Three-leg turbo circle	20 m	76 m
Three-leg turbo circle	30 m	92 m

5.2. Robustness

Robustness indicates the performance of an intersection if the prevailing traffic demand pattern differs from the pattern for which the intersection was designed. Robustness can be assessed on a long term (a persistent change of the prevailing demand pattern) and on a short term (an irregularity such as an crash on or near the intersection). This study pays attention to the effect of the combination of traffic control and demand pattern on the capacity of the signalized turbo roundabout. Therefore, changes in the demand pattern (temporary and persistent) will be considered.

Section 4.2.2 showed that the cycle time of the traffic control on the signalized turbo roundabout influences the capacity. The cycle time duration has an optimum value, for which the capacity is maximized. Therefore, the signalized turbo roundabout is not as robust as the un-signalized turbo roundabout: a deflection from the cycle time yields a lower capacity. Consequentially, the signalized turbo roundabout should be equipped with a fixed-time control, but such a control generally leads to unnecessary delay times (Muller, 1997).

The (partial) turbo circle also has a drawback on the criterion of robustness. Due to the two-phase control, the left-turning vehicles have to queue up on the circle. Therefore, the available queuing space yields a capacity constraint. If, for some reason, the left-turning stream from (one of) the entrance leg(s) increases, the intersection might become oversaturated.

In conclusion, both the signalized turbo roundabout and the (partial) turbo roundabout showcase a drawback with respect to this criterion. The un-signalized rotor and star roundabouts are more robust than the other intersections.

5.3. Traffic safety

This section on traffic safety consists of two parts. The first part will present a comparison of the conventional intersection and the roundabout. This part is based on literature and concludes that the roundabout is safer than the conventional intersection. The second part considers the consequences of traffic signals on roundabouts, based on rational considerations (or: expert judgment of the author). These considerations will result in a set of hypotheses; proposals for future research.

5.3.1. Comparison of the conventional intersection and the roundabout

Fortuijn (2013) and the SWOV (2012) state that the roundabout is safer than the conventional (non-circular) signalized intersection. The SWOV quantifies the difference: the single-lane roundabout offers a safety benefit of ca. 46% less severe casualties, compared to the conventional signalized roundabout. This safety benefit is caused by two considerations:

- the roundabout has less (potential) conflicts, thus reducing the psychological load imposed by the complex driving task;
- the average speed on the roundabout is lower. Therefore, the potential energy in case of an accident is smaller and the probability of severe casualties less.

The driving task on a roundabout is less complex compared to the conventional intersection, because there are less (potential) conflicts, illustrated by Figure 5-1. While entering the conventional intersection, the driver has to pay attention to two (for right-turning movements), five (for left-turning movements), or six conflicting streams (for straight-ahead movements). The road user has to pay attention to all of the conflicting streams simultaneously, this requires a substantial load of visual information to be processed in a limited amount of time, accompanied by the need for large head turns. While entering the roundabout, the road user only has to pay attention to one conflicting stream; a small head turn is required to obtain the required visual information.

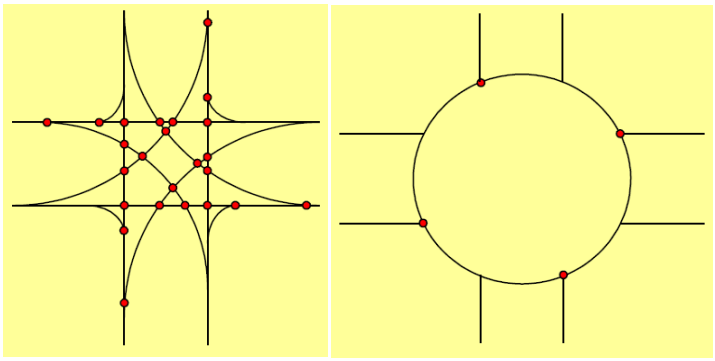


Figure 5-1 [31] The amount of (potential) conflicts is lower on a roundabout, compared to the conventional intersection (subtracted from SWOV, 2012, p.3)

Another aspect reducing the driving task on the roundabout is the complexity, caused by the amount of lanes. On a conventional intersection, drivers have to choose a lane before entering the intersection. This is a task on the manoeuvring level (Michon, 1987); the route choice on the strategic level should already have been made. Therefore, the route signs should meet the driver's information requirements. On the single-lane roundabout, lane choice is irrelevant because there is only one lane. The route choice can be made later; on the roundabout.

The lane and route choice are more complex on the (multi-lane) rotor and star roundabouts. If the environment is unfamiliar to the driver, the lane choice before entering the roundabout may be complex.

[31] *The red dots indicate (potential) conflict points.*

To reduce complexity, the road environment should be sufficiently recognizable and predictable; the route signs play an important role.

5.3.2. Consequences of traffic signals on the roundabout

Traffic signals do not change the amount of conflict points, however, they may alter the nature of the conflict points. In the case of un-protected conflicts, most road users consciously pay attention to the conflicting streams. In the case of protected conflicts, many road users blindly rely on the traffic signal and refuse (purposely or not) to pay attention to the conflicting streams. This may reduce the perceived task load, but may also worsen traffic safety on the roundabout. This presumption is solely based on a rational consideration of microscopic behaviour, and needs therefore to be studied.

Traffic signals might relieve the perceived driving task, because the driver does not have to pay attention to the conflicting stream anymore. Instead, he can focus his attention to the lane choice while keeping an eye on the traffic signal. However, the perceived driving task will probably be aggravated if the traffic signals are turned off or show flashing yellow. In that case, the driver has to pay attention to the lane choice and the conflicting stream, and he might also wonder why the traffic signal is installed aside the road, requiring part of his limited attention.

One of the most important causes for crashes on signalized intersections in general, is red light negation (Muller, 1997, p.168). When a traffic signal turns from green to yellow, the approaching drivers have to decide whether to yield or to drive through. On the one hand, if a driver decides to yield and a following driver wishes to drive through, a head-tail collision is likely to occur. On the other hand, a hurried driver observing the yellow light, might decide to accelerate in order to enter the intersection just within the yellow phase. He might in fact cross the red light; in that case, there is a chance that the clearance time is not long enough to prevent a crash with a fastly accelerating conflicting vehicle in a stream in the next stage. Therefore, red light negation might be a second argument for the statement that traffic signals influence traffic safety on a roundabout negatively. A topic for further research is the question whether this argument also holds signalized (turbo) roundabouts.

Traffic signals may also influence the speed on the roundabout. As indicated in the former paragraph, a hurried driver may accelerate in order to enter the intersection just within the yellow phase. Consequently, the (maximum) speed on a roundabout may increase, and therefore the potential energy in case of a crash may increase. The probability of a crash is considerable in that case, because the driver crosses the yellow light, or the first second(s) of the red light. Again, this presumption is solely based on rational considerations; the influence on traffic safety depends on a variety of factors.

From these considerations, a set of hypotheses for future research results:

1. The un-signalized roundabout is inherently safer than the signalized roundabout;
2. The perceived driving task is more complex on un-signalized roundabout than on signalized roundabouts;
3. A) Drivers approaching an un-signalized roundabout pay consciously attention to traffic on the roundabout;
3. B) Drivers approaching a signalized roundabout do not pay consciously attention to traffic on the roundabout;
4. A) Red light negation on signalized roundabouts occurs to such an extent, that traffic safety worsens;
4. B) Head-tail collisions on signalized roundabouts occur to such an extent, that traffic safety worsens.
5. The average and maximum speed on a signalized roundabout are higher than the average and maximum speed on an un-signalized roundabout.

Appendix L presents LED-technology; this novelty might reduce the complexity of the signalized turbo roundabout, and increase clarity and traffic safety. A direct relationship between the hypotheses and LED-illumination does not exist.

5.4. Environmental considerations

The final performance indicator is environmental burden. The literature (a.o. Fortuijn, 2013) indicates that the un-signalized roundabout yields environmental benefits compared to signalized intersections. An explanation is that the amount of stops at signalized intersections is generally higher than the amount of stops at un-signalized intersections. Therefore, vehicles have to decelerate and accelerate more often at signalized intersections; un-signalized roundabouts yield reduced air pollution and noise. Therefore, the signalized intersections perform worse than un-signalized intersections in general.

5.5. Summary and conclusions

Indicator space requirement: Table 5-2 presents an overview of the space requirement of the intersection invoked in this project. Indicator robustness: the signalized intersections perform worse than un-signalized intersections. The signalized turbo roundabout has an optimum cycle time; any deflection from this cycle time results in a lower capacity. Therefore, the signalized turbo roundabout is sensitive to sudden (temporary) changes in traffic demand. On the (partial) turbo circle, traffic has to queue up on the circle. These intersections are therefore sensitive to a sudden (temporary) increase in left-turning intensities. Indicator safety: traffic signals may worsen traffic safety on a roundabout, because they probably alter the nature of the (potential) conflicts on the roundabout. In particular, on an un-signalized roundabout drivers pay consciously attention to the conflicting stream, but on a signalized roundabout many drivers blindly rely on the traffic signal, probably. Therefore, the signalized intersections are generally presumed to perform worse than un-signalized intersections, because the (potential) conflicts on signalized intersections presumably have a fundamentally different nature than the (potential) conflicts on un-signalized intersections. Moreover, the maximum speed on signalized intersections is probably higher than the average speed on un-signalized intersections, decreasing safety. Indicator environment: the signalized intersections perform worse than un-signalized intersections, because in general, vehicles have to decelerate and accelerate more often at signalized intersections; un-signalized roundabouts yield reduced air pollution and noise. Table 5-2 presents an overview of the conclusions.

Table 5-2 Performance of four-leg intersections, resulting from the simulations

Intersection type	Space requirement		Robust-ness	Safety	Environ-ment
	Inscribed	outer			
Un-signalized rotor roundabout	12 m	52 m	+	+	+
Un-signalized rotor roundabout	20 m	64 m	+	+	+
Un-signalized star roundabout	12 m	56 m	+	+	+
Un-signalized star roundabout	20 m	68 m	+	+	+
Signalized rotor roundabout	12 m	52 m	-	-	-
Signalized rotor roundabout	20 m	64 m	-	-	-
Signalized star roundabout	12 m	56 m	-	-	-
Signalized star roundabout	20 m	68 m	-	-	-
Partial turbo circle	12 m	66 m	-	-	-
Partial turbo circle	20 m	77 m	-	-	-
Turbo circle	12 m	79 m	-	-	-
Turbo circle	20 m	91 m	-	-	-
Turbo circle	30 m	106 m	-	-	-
Three-leg turbo circle	12 m	65 m	-	-	-
Three-leg turbo circle	20 m	76 m	-	-	-
Three-leg turbo circle	30 m	92 m	-	-	-

6. Conclusions

This chapter describes the findings of this project in the first section; the findings comprise the results of the capacity models. From these findings, the conclusions will be drawn in the second section. The conclusions aim to answer the research question, inquiring for the applicability range of the signalized turbo roundabout. Primarily, the capacity determines the applicability ranges, and secondarily, the other performance indicators will be invoked in the second section. In the third section, the implications will be formulated, distinguishing between implications for scientific research and implications for professional traffic engineering. Finally, the fourth section presents an overview of recommendations for further research.

6.1. Findings from the application of the models

This section presents the findings from this study. They will be presented in diagrams, in which the capacity results of the three applied models are shown. That way, the un-signalized rotor roundabout will be compared with the signalized rotor roundabout firstly. Next, the (un-)signalized rotor roundabout will be compared with the (partial) turbo circle. Likewise, the un-signalized star roundabout will be compared with the signalized star roundabout, and the (un-)signalized star roundabout will be compared with the three-leg turbo circle.

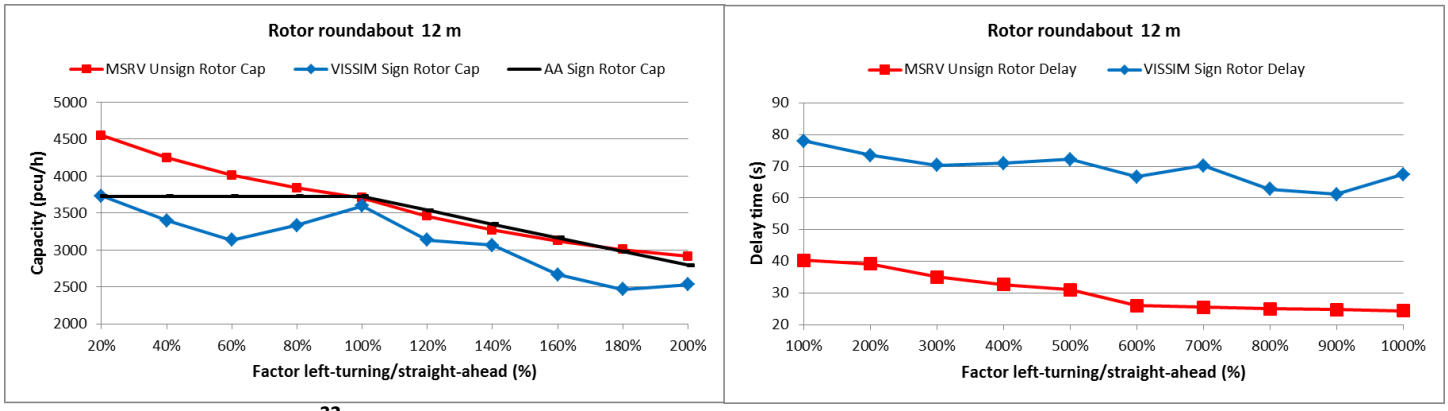


Figure 6-1 [32] (Un-)signalized rotor roundabout with an inscribed radius of 12 m: capacity and delay time

Rotor roundabout: signalized vs. un-signalized

Figure 6-1 and Figure 6-2 show the capacity of and delay time on the (un-)signalized rotor roundabout with inscribed radii of 12 m and 20 m. Regarding the comparison between the capacity of the un-signalized rotor roundabout (MSRV) and the capacity of the signalized rotor roundabout (the analytical approach and VISSIM), the diagrams show that the un-signalized rotor roundabout with an inscribed radius of 12 m offers a higher capacity than the signalized rotor roundabout with an inscribed radius of 12 m [33], while the delay time more than doubles. The capacity of the signalized rotor roundabout with an inscribed radius of 20 m might is 0 pcu/h to 500 pcu/h higher than the capacity of the un-signalized rotor

[32] *Chapter 7 (Reflection) argues that the lines representing the AA and VISSIM underestimate the capacity, because the green phase overlap is underestimated. Also, chapter 7 presents three reasons why the line representing VISSIM underestimates the capacity: 1) the presence of route choice in the VISSIM network; 2) the poor modelling of green phase cut-off criteria by TrafCOD; and 3) the choice for vehicle-actuated control.*

[33] *The capacity results of the analytical approach and VISSIM do not entirely coincide, but in general they are equal to or lower than the capacity results of the MSRV.*

roundabout with the same radius, only for demand patterns in which the left-turning streams are busier than the straight-ahead streams. In contrast, the delay time more than doubles.

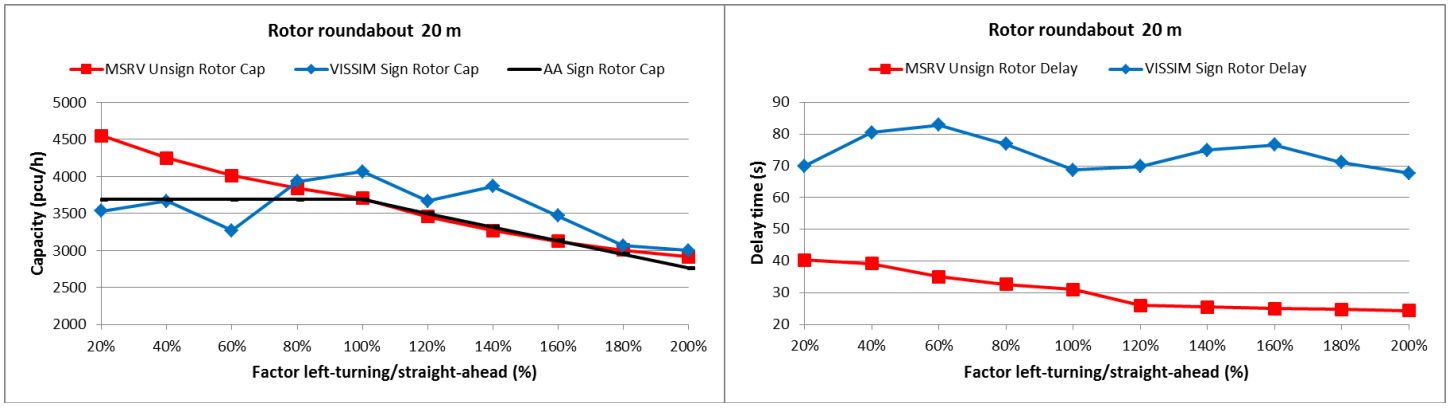


Figure 6-2 (Un-)signalized rotor roundabout with an inscribed radius of 20 m: capacity and delay time

Signalized rotor roundabout vs. (partial) turbo circle

Figure 6-3 shows the comparison of (un-)signalized rotor roundabout with an inscribed radius of 20 m and the partial turbo circle with inscribed radii of 12 m and 20 m, based on the criteria of capacity and delay time. The diagrams show that the partial turbo circle has a lower capacity than the (un-)signalized rotor roundabout. Only for low left-turning intensities, the partial turbo circle with an inscribed radius of 20 m might offer a higher capacity. The delay times on the rotor roundabout and the partial turbo circle are comparable.

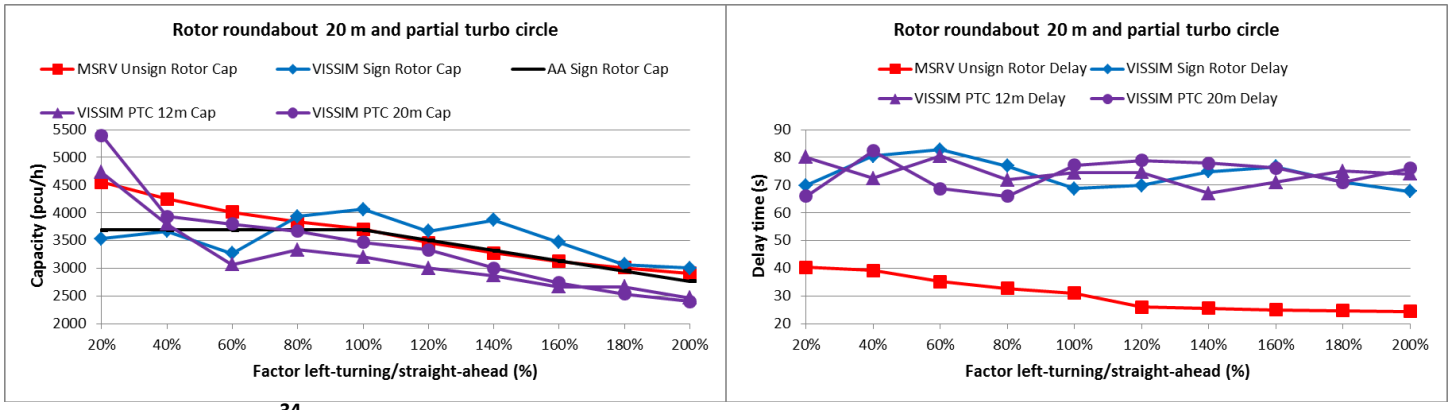


Figure 6-3 [34] (Un-)signalized rotor roundabout with an inscribed radius of 20 m and the partial turbo circle (PTC) with inscribed radii of 12 m and 20 m: capacity and delay time

Figure 6-4 shows the comparison of the (un-)signalized rotor roundabout with an inscribed radius of 20 m and the turbo circle with inscribed radii of 12 m, 20 m and 30 m, based on the criteria of capacity and delay time. The diagrams show that the turbo circle has a structurally higher capacity than the rotor roundabout. The difference between the capacities of the turbo circles with inscribed radii of 20 m and 30 m is not large.

[34] *Chapter 7 (Reflection) presents three reasons why the lines representing the partial turbo circle underestimate the capacity: 1) the presence of route choice in the VISSIM network; 2) the poor modelling of green phase cut-off criteria by TrafCOD; and 3) the poor modelling of the joint delay in the two-phase control.*

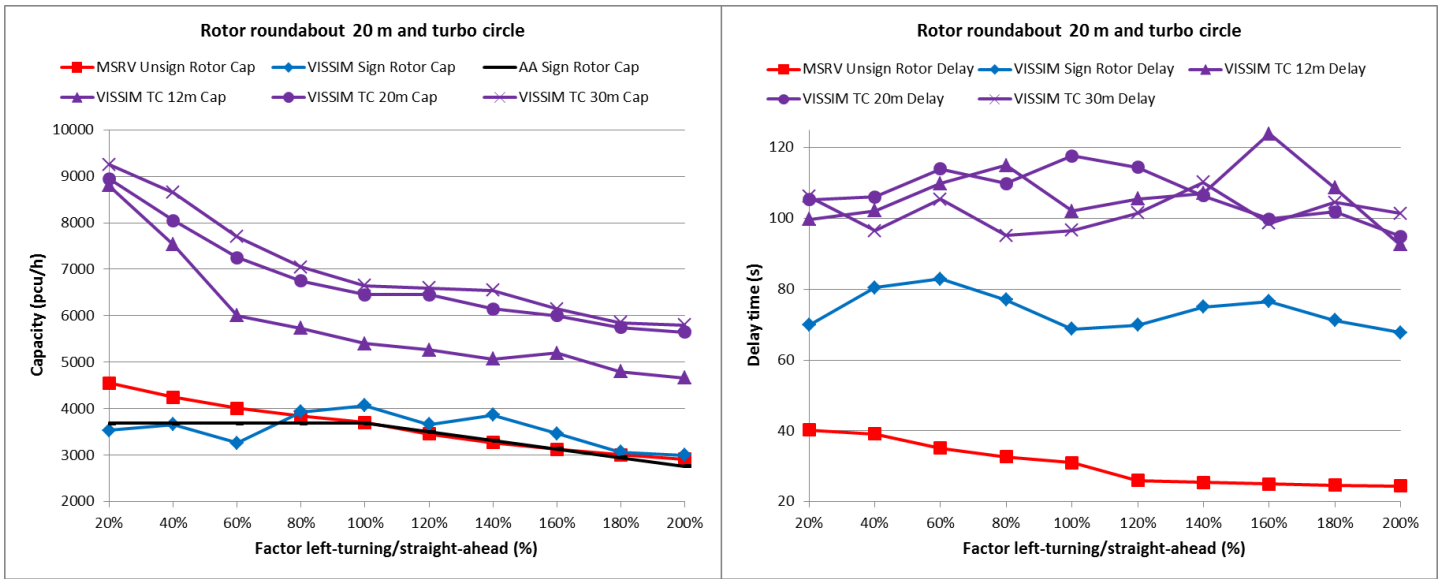


Figure 6-4 (Un-)signalized rotor roundabout with an inscribed radius of 20 m and the turbo circle (TC) with inscribed radii of 12 m, 20 m and 30 m: capacity and delay time

Star roundabout: signalized vs. un-signalized

Figure 6-5 and Figure 6-6 show the capacity of and delay time on the (un-)signalized star roundabout with inscribed radii of 12 m and 20 m. Regarding the comparison between the capacity results, the diagrams show that the capacities of the signalized star roundabouts with an inscribed radius of 12 m (20 m) are 0 pcu/h to 1300 pcu/h (0 pcu/h to 2100 pcu/h) larger than the capacities of the un-signalized star roundabouts with the same radii [35]. However, the delay time nearly doubles.

The results of the analytical approach and VISSIM with respect to the star roundabout with an inscribed radius of 20 m do not coincide: the lines differ by 500 pcu/h to 1600 pcu/h. Expecially with respect to DP20 through DP80, the differences are large. An explanation for these differences has not been found [36].

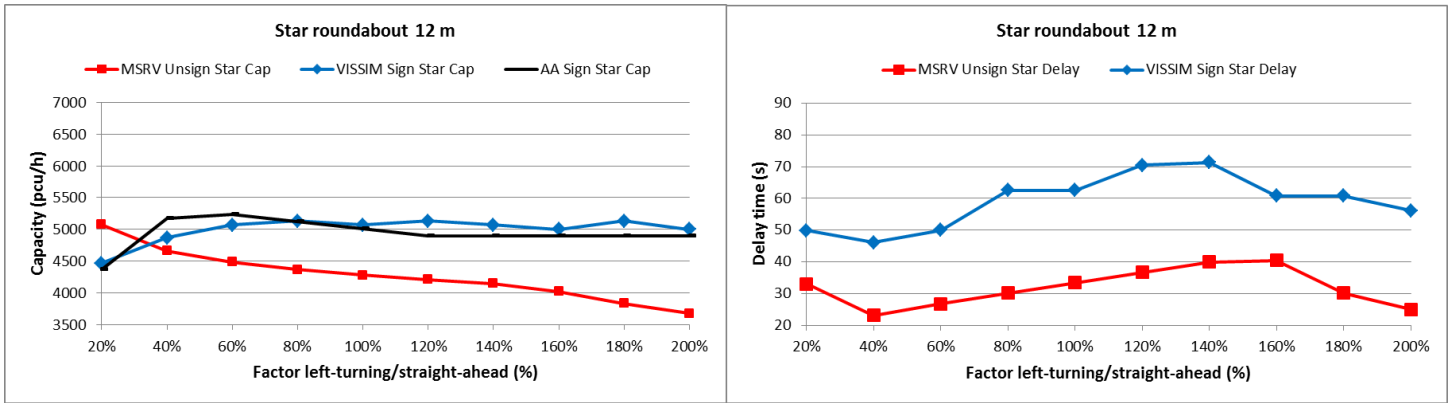


Figure 6-5 (Un-)signalized star roundabout with an inscribed radius of 12 m: capacity and delay time

[35] *The capacity results of the analytical approach and VISSIM do not entirely coincide with respect to the star roundabout with an inscribed radius of 20 m, but in general they are higher than the capacity results of the MSRV.*

[36] *However, the lines representing both models are higher than the line representing the MSRV. So the lack of explanation does not question the conclusion (next section) that the signalized star roundabout has a higher capacity than the un-signalized star roundabout.*

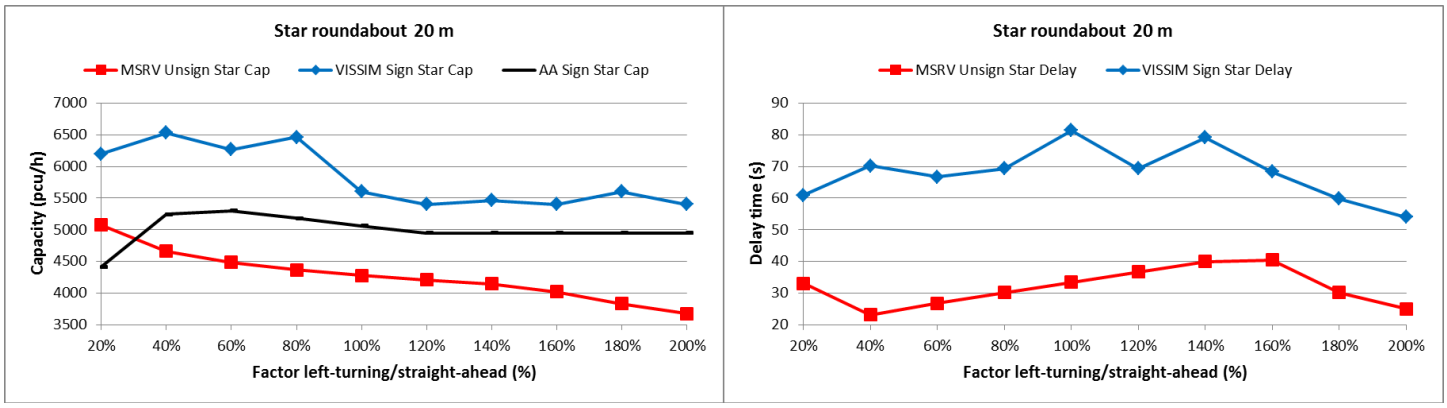


Figure 6-6 (Un-)signalized star roundabout with an inscribed radius of 20 m: capacity and delay time

Signalized star roundabout vs. three-leg turbo circle

Figure 6-7 shows the comparison of the (un-)signalized star roundabout with an inscribed radius of 20 m and the three-leg turbo circle with inscribed radii of 12 m, 20 m and 30 m, based on the criteria of capacity and delay time. The diagrams show that the capacities of the star roundabout with an inscribed radius of 20 m and the three-leg turbo circle with an inscribed radius of 12 m are approximately equal for demand patterns in which the left-turning streams are busier than the straight-ahead streams.

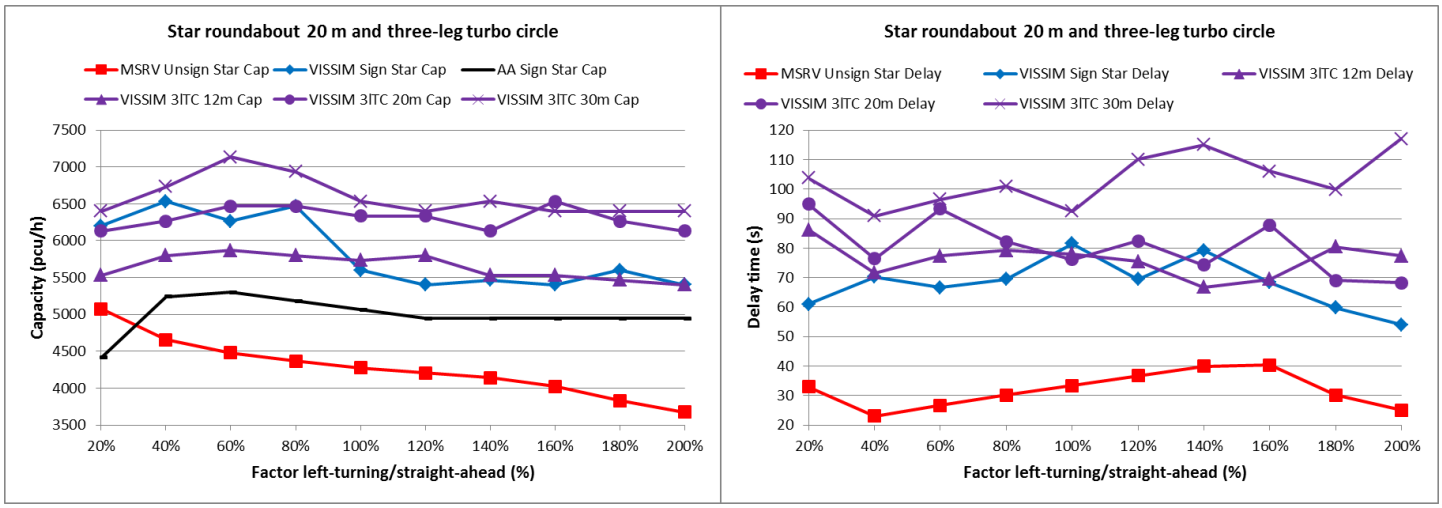


Figure 6-7 (Un-)signalized star roundabout with an inscribed radius of 20 m and the three-leg turbo circle (3ITC) with inscribed radii of 12 m, 20 m and 30 m: capacity and delay time

6.2. Conclusions

From the findings in the previous section, a part of the conclusions will be drawn in the first sub section. These conclusions result directly from the results of the models, and are most relevant to the research question. However, they are not the only conclusions. The second section will pay attention to conclusions on the fundamentals of the models that have been applied. Finally, the conclusions with respect to traffic control will be stated.

6.2.1. Conclusions with respect to the application of the models: results

This study evaluated the intersections by means of six performance criteria. Table 6-1 and Table 6-2 present the performance of the intersections on these criteria. The space requirements have been determined based on the geometrical designs in appendix D. The capacity values and delay times have

been calculated by means of the MSRV, the analytical approach and VISSIM. Chapter 5 elaborated on the performance indicators robustness, safety and environmental considerations. The performance is indicated by means of + and -, because chapter 5 made general statements and formulated presumptions. These performance indicators are subject to future research.

Four-leg intersections

From the evaluation can be concluded that the un-signalized rotor roundabout is always preferred over the signalized rotor roundabout (equal space requirements but higher capacity, lower delay time, better safety and robustness, less environmental burden). Only in situations where the left-turning streams are larger than the straight-ahead streams, the signalized rotor roundabout with an inscribed radius of 20 m offers a slightly higher capacity (see Figure 6-2). Regarding the other criteria, the applicability range of the signalized rotor roundabout is very small.

On all criteria, the partial turbo circle performs worse than the signalized rotor roundabout. Only in situations in which the left-turning intensities are very low (ca. 20% of the straight-ahead streams), the partial turbo circle offers a higher capacity than the signalized rotor roundabout. This is primarily due to the fact that the partial turbo circle contains only one lane for the left-turning streams; the queuing space is small. The turbo circle contains two lanes; offering a higher capacity.

Table 6-1 Performance of four-leg intersections

Intersection type	Space requirement		Capacity (pcu/h)			Delay	Robustness	Safety	Env.
	Inscribed	outer	MSRV	VISSIM	AA	(s)			
Un-signalized rotor roundabout	12 m	52 m	3700 ± 800			33 ± 8	+	+	+
Un-signalized rotor roundabout	20 m	64 m	3700 ± 800			33 ± 8	+	+	+
Signalized rotor roundabout	12 m	52 m		3100 ± 600	3300 ± 500	70 ± 10	-	-	-
Signalized rotor roundabout	20 m	64 m		3600 ± 600	3300 ± 500	75 ± 5	-	-	-
Partial turbo circle	12 m	66 m		3600 ± 1100		75 ± 5	-	-	-
Partial turbo circle	20 m	77 m		3900 ± 1500		73 ± 8	-	-	-
Turbo circle	12 m	79 m		6700 ± 2000		105 ± 15	-	-	-
Turbo circle	20 m	91 m		7400 ± 1700		110 ± 10	-	-	-
Turbo circle	30 m	106 m		7600 ± 1800		100 ± 10	-	-	-

Three-leg intersections

The signalized star roundabout offers a higher capacity than the un-signalized star roundabout (nevertheless, its performance on the other criteria is worse).

An interesting conclusion from Figure 6-7 is that the capacity of the three-leg turbo circle does not decrease as the left-turning intensities increase. This conclusion does not coincide with the presumption in section 2.3.2, where the capacity of the three-leg turbo circle is presumed to decrease as the left-turning intensities increase, because the vehicle in stream 03 have to queue up on the circle. From visual observations of the VISSIM simulations and Table 4-16, Table 4-17 and Table 4-18, the explanation can be drawn: the capacity of stream 02 constrains the capacity of leg E. Stream 02 is supplied with only one lane, with a sharp bend at the entrance to the circle [37]. This bottleneck imposes a capacity constraint on leg E; the capacity can be increased by supplying stream 02 with two lanes (four lanes on leg E).

The three-leg turbo circles with inscribed radii of 20 m and 30 m offer a higher capacity than the signalized star roundabout. The capacity of the three-leg turbo circle was in this project mainly restricted

[37] *This bend has a radius of 12 m. In VISSIM, the consequential speed reduction is simulated by a Reduced Speed Area with a speed limit of 25 km/h, see appendix L (VISSIM model development).*

by the capacity of the eastern leg. Providing stream 02 with two lanes instead of one lane, would probably raise the capacity of the three-leg turbo circle.

Table 6-2 Performance of three-leg intersections

Intersection type	Space requirement		Capacity (pcu/h)			Delay	Robustness	Safety	Env.
	Inscribed	outer	MSRV	VISSIM	AA	(s)			
Un-signalized star roundabout	12 m	56 m	4400 ± 700			30 ± 5	+	+	+
Un-signalized star roundabout	20 m	68 m	4400 ± 700			30 ± 5	+	+	+
Signalized star roundabout	12 m	56 m		4800 ± 300	4800 ± 400	55 ± 15	-	-	-
Signalized star roundabout	20 m	68 m		6000 ± 600	4800 ± 400	70 ± 10	-	-	-
Three-leg turbo circle	12 m	65 m		5600 ± 200		75 ± 10	-	-	-
Three-leg turbo circle	20 m	76 m		6300 ± 200		80 ± 10	-	-	-
Three-leg turbo circle	30 m	92 m		6800 ± 400		100 ± 10	-	-	-

6.2.2. Conclusions with respect to the models

VRIGen and the leg-by-leg control

This project applied VRIGen to generate the control structures of the leg-by-leg control and the two-phase control. The leg-by-leg control can be generated by VRIGen in the 'common' way, as shown in chapter 3 (Experimental design). However, the phase overlap cannot be included in the leg-by-leg control in that way (the green phases of the main signal group and the following interception signal group start simultaneously). As a solution, this project invoked spare streams in VRIGen (these are streams that do not exist in reality).

VISSIM drawback: usage of approach lanes

Section 5.3 (Capacity modeling: VISSIM) elaborates on some microscopic behavioural characteristics of the drivers in the model. A point of concern is the driver's lane choice behaviour when approaching a traffic signal. In reality, when a driver approaches a red traffic light, he will most likely check which lanes offer the possibility to proceed on his route, and then choose for the lane on which the queue of waiting vehicles is shortest. However, in VISSIM this behaviour is not being modelled.

The VISSIM model contains a route choice for right-turning and straight-ahead vehicles. VISSIM deals with this route choice by assigning an equal amount of vehicles to each route. Consequentially, vehicles in the model are assigned an entrance lane randomly (according to the route) while entering the network, so situations might occur in which one entrance lane contains a (long) queue, while another lane leading to the same destination is left unoccupied. Consequently, the model adopts a highly inefficient lane choice behaviour. This is one of the drawbacks of VISSIM: approaching vehicles do not consider the actual queue length on each of the approach lanes, while in reality drivers do. With respect to this project: a pragmatic solution has been applied by means of edge closure, described in section 3.2.3.

6.2.3. Conclusions with respect to control structures

Traffic controls and applicability to the turbo roundabout and circle

Due to the presence of choice lanes, the turbo roundabout only allows for a leg-by-leg control. The turbo roundabout can be adjusted such, that the two-phase control can be applied to the turbo roundabout; the results are the partial turbo circle (adjusted rotor roundabout) and the three-leg turbo circle (adjusted star roundabout). The (partial) turbo circle and the three-leg turbo circle are suitable for the two-phase control, because the circle provides queuing space for left-turning vehicles.

Optimum cycle time

By means of the analytical approach, an optimum cycle time duration was calculated in section 4.2 (Capacity modelling: analytical approach), for both the rotor and star roundabout with inscribed radii of 12 m and 20 m. For this optimum cycle time duration, the green phase overlap per hour within the traffic control is maximized, and therefore the capacity of the turbo roundabout is maximized.

6.3. Implications

The conclusions yield implications to both future scientific research and professional traffic engineering (practical cases). This section states the implications.

6.3.1. Implications for scientific research

This study concluded that the rotor roundabout does not benefit from traffic signals. With respect to future research, it is not sensible to study the combination of four-leg turbo roundabouts and traffic signals any longer (section 3.1.2 stated that if traffic signals do not benefit the rotor roundabout, they will certainly not benefit smaller four-leg turbo roundabouts).

The partial turbo circle has a lower capacity than the rotor roundabout. The delay times of the rotor roundabout and the partial turbo circle are comparable. The space requirements of the rotor roundabout with an inscribed radius of 20 m and the partial turbo circle with an inscribed radius of 12 m are comparable. Based on this comparison, further research into the partial turbo circle is not recommendatory.

This study also concluded that traffic signals are advantageous to the star roundabout. Therefore, it is sensible to further study the combination of the three-leg turbo roundabouts (star roundabout and smaller three-leg turbo roundabouts; see section 3.1.2). The three-leg turbo circles offer a higher capacity than the signalized star roundabout, but performs worse on the other indicators. Therefore, the three-leg turbo circle should be subject to further research. Section 6.4 presents a number of proposals for future research.

6.3.2. Implications for professional traffic engineering

In general, the signalized rotor roundabout should not be invoked in any variant study, because it offers less capacity than the un-signalized rotor roundabout, while the space requirements is larger. The same holds for the partial turbo circle. However, it might be sensible to invoke the partial turbo circle in variant studies into situations where the left-turning intensities are small, such as the junction of a secondary road and a provincial road.

The signalized star roundabout offers a higher capacity than the un-signalized star roundabout, but performs worse on the other indicators (except for space requirement). Therefore, the signalized star roundabout may be invoked in any variant study. An alternative would be to construct star roundabouts in principle without traffic signals, and signalize them once the traffic demand has grown such, that the capacity is no longer sufficient [38]. The three-leg turbo circle may also be invoked in any variant study; it requires more space than the (un-)signalized star roundabout, but offers a higher capacity.

[38] *In that case, the road authority should also be recommended to search for a new intersection solution with a higher capacity, because the capacity of the star roundabout only grows by 0 pcu/h to 1800 pcu/h, depending on the demand pattern.*

6.4. Future research

This section presents an overview of the proposals for further investigation that have been made throughout the study. Proposals have been made with respect to: the fundamentals of the analytical approach and VISSIM; the (intermediate) results of the application of the models to the intersections; research into traffic safety; research into LED illumination; and topics outside the scope of this study.

6.4.1. Fundamentals of the models

Behaviour of first vehicle

In appendix G, the maximum possible green phase overlap for the leg-by-leg control is calculated by means of the distance between two consecutive stop lines (e.g. the stop lines joining streams 02 and 62). Next, a simple model has been applied for the first vehicle departing from stop line 02: the vehicle accelerates at 2,5 m/s^2. This number is based on field observations by Grontmij (2001). The first vehicle decelerates at 2.0 m/s^2, in order to stop in front of the stop line 62.

In reality, the first vehicle departing from stop line 02, will notice the red interception signal of stream 62 at a certain moment (probably while waiting for signal 02 to turn green). Here, behavioural characteristics on decision taking and perception thresholds are relevant, and these are not invoked in the simple model described above. In order to estimate the green phase overlap reliably, this behaviour should be studied.

With respect to this project: the acceleration rate 2,5 m/s^2 is a rather high value, so the estimation of the phase overlap is conservative. Moreover, the road user behaviour on the signalized turbo roundabout is highly uncertain, because it is an intersection type still unknown to the road user. Possibilities to perform behavioural measurements are limited. For these two reasons, the decision is taken to base the estimation of the phase overlap on this value, and excluding a detailed behavioural study.

A future study could focus on the microscopic behaviour of a driver-vehicle combination, departing from the main signal and approaching the interception signal. A research question could be: what is the travelled distance as a function of time, and what factors determine this function? A variety of factors may be included, like: characteristics of the driver (age, gender, aggressiveness, sober or drunk, etc.), characteristics of the vehicle (age, mass, brand, etc.), characteristics of and familiarity with the environment, etc.

Functions and distributions in VISSIM

In section L.2 (VISSIM model development; Base data) the development of the VISSIM models has been described. VISSIM combines several microscopic behavioural models to simulate traffic on a network. To do so, VISSIM uses a set of input parameters, of which most can be expressed as distributions or functions of speed. These functions and distributions need to be calibrated.

In this project, the default settings in VISSIM have been discussed and compared with settings used by the Dutch private consultancy companies Oranjewoud, Grontmij and Goudappel Coffeng, and the German consultancy company Pöyry. Based on this comparison, a set of functions and distributions has been recommended in this project. These recommendations are solely based on *expert judgment*: common sense of the author. The recommended functions and distributions are subject to future research. Due to lack of data resources and time, the input parameters have not been validated in this project.

6.4.2. (Intermediate) results of the models

Validation of the results

This project produced capacity values for the signalized rotor and star roundabout, and the (partial) turbo circle. These intersection solutions have not been implemented in practice (yet). Therefore, it is not

possible to gather data from the field and implement them in the models to be used. Validation of the models and calibration towards a specific case is not possible in this project. It is recommendatory to validate the results by means of field measurements once the intersection types have been constructed in practice.

Optimal traffic control for the turbo roundabout

In section 4.2 (Capacity calculation; analytical approach) a control with an optimal cycle time duration was calculated. For this optimal duration, the phase overlap per hour within the traffic control is maximized, and therefore the capacity of the turbo roundabout is maximized. VISSIM applies a suboptimal control, because the green periods are extended according to the prevailing arrival pattern.

Principally, the optimal control is a fixed-time control. The capacity of the turbo roundabout is maximized with a fixed-time control, but generally the delay times in a fixed-time control are larger than the delay times in a vehicle-actuated control. Therefore, a semi-actuated traffic control should be designed that combines the advantages of both controls. During saturated conditions, the control should apply the optimum cycle time duration, so to serve the goal of maximizing capacity. During under-saturated conditions, the control should become vehicle-actuated, so to serve the goal of minimizing delay times.

Check the driving curve

In appendix D (Geometrical designs), the geometrical characteristics of the signalized turbo roundabout and the (partial) turbo circle have been elaborated on. The resulting designs have been used to measure the size of the circle, the length of various roadway segments, and other characteristics. The designs have been made by means of guidelines from the literature (a.o. CROW, 1998 and Fortuijn, 2013).

In this project, the designs have not been checked on their compatibility with various vehicle types: does the geometrical design offer sufficient space for carrying the driving curve of all vehicles with access to the public roads? In common practice, the design of a new road segment will be checked by means of software packages such as AutoTURN, in order to investigate whether all types of vehicles with access to public roads are able to cross the road segment. It is assumed that the guidelines used in this project are sufficient to design fully compatible traffic circles, but investigating the geometrical designs in this project by means of AutoTURN might indicate the need for some (minor) adjustments to the designs.

6.4.3. Consequences to traffic safety

Section 5.3 formulated several considerations and presumptions with respect to the consequences of traffic signals on safety. This resulted in a set of hypotheses; a proposal for future research:

1. The un-signalized roundabout is inherently safer than the signalized roundabout;
2. A) Drivers approaching an un-signalized roundabout pay consciously attention to traffic on the roundabout;
2. B) Drivers approaching a signalized roundabout do not pay consciously attention to traffic on the roundabout;
3. A) Red light negation on signalized roundabouts occurs to such an extent, that traffic safety worsens;
3. B) Head-tail collisions on signalized roundabouts occur to such an extent, that traffic safety worsens.
4. The average and maximum speed on a signalized roundabout are higher than the average and maximum speed on an un-signalized roundabout.

6.4.4. LED illumination

Road user's perception of LED illumination

Appendix L addresses the possibility of equipping the signalized turbo roundabout and circle with LED illumination. From this appendix, the following hypotheses result, subjects for future research:

1. A) LED pavement markings relieve the mental workload while crossing the intersection.
1. B) LED pavement markings enhance the clarity and predictability of the road environment.
2. When a stream is not in the green phase, the accessory LED modules should be turned off, rather than showing red.
3. A) LED illumination can substitute the function of the wide roadway dividers on the turbo circle. The function is to conduct the road user while crossing the intersection, and to minimize the amount of erroneous manoeuvres.
3. B) LED illumination can substitute the function of the roundabout shields. The function is to warn approaching drivers of a discontinuity in the driving coarse, already at considerable distance from the intersection.
3. C) LED illumination can substitute the function of the route signs with respect to the manoeuvring level (the arrows on the route signs). The function with respect to the manoeuvring level is to inform approaching drivers about how to cross the intersection.

Economical applicability of LED illumination

In order to assess the range of applicability of the LED modules on signalized turbo roundabouts and (partial) turbo circles, a cost-benefit analysis can be carried out. Here, the monetary costs of installing the LED modules should be weighed against the societal costs of (fatal) injuries resulting from a lack of guidance on the intersection. The guideline OEI (Eijgenraam, 2000) presents tools to perform such a cost-benefit analysis.

6.4.5. Topics outside the scope of this study

Smaller turbo roundabout types

Section 3.1.2 motivated why only the rotor and star roundabouts are invoked in this study: they are the largest turbo roundabout types. The section proposed to study the effect of traffic signals on smaller types if it would appear that traffic signals influence the rotor and star roundabout beneficially. This project draws the conclusions that traffic signals influence the rotor roundabout negatively, however, their influence on the capacity of the star roundabout is beneficial. Therefore, the influence of smaller three-leg turbo roundabouts should be investigated as well. Section 2.1 shows the other (smaller) three-leg turbo roundabouts: the three-leg knee roundabout, the three-leg egg roundabout, the three-leg basic turbo roundabout and the three-leg spiral roundabout.

Invoke slow traffic streams

The project studied intersection outside the urban area; slow traffic streams were not invoked in the project. However, on intersection inside the urban area, slow traffic streams are often present. Therefore, the influence of slow traffic streams on the six indicators should be investigated.

Other demand patterns

This project applied a specific set of demand patterns; the patterns differ only with respect to the left-turning intensities (see appendix B: Demand patterns). The calculations by means of the analytical approach (section 4.2: Analytical capacity modelling) showed that the capacity of the signalized turbo roundabout (with a leg-by-leg control) depends on the ratio of the main directions and secondary directions. In particular, the demand patterns have a ratio 08/02 of 80% and 05/02 (and 11/02) of 60%. When all ratios are 100% (equally loaded legs), the capacity is maximized. Apparently, the capacity of the signalized turbo roundabout depends on the prevailing demand pattern. Extending the project with an investigation by means of a wide variety of demand patterns can be recommended.

7. Reflection

In this chapter, the author reflects on the research process of the study that has been performed.

The research was not a linear process

The report of a research project should have a clear and transparent structure; the contents should be easily comprehensible to the reader. Therefore, the report does not reflect the process of the study, which often contains a lot of feedback processes. This aim has been pursued in this report: to systematically present all steps.

An example to illustrate a feedback loop in the research process, can be taken by section 3.1.4, where the choice for demand patterns has been made. This choice has been made in an early stage of the research: before applying the three models to the turbo roundabouts. In the choice, it was assumed that the demand pattern does not influence the capacity of the signalized turbo roundabout, equipped with a leg-by-leg control. By logical reasoning, it was already assumed that the capacity of a traffic circle equipped with a two-phase control depends on the left-turning intensities; therefore a set of demand patterns was chosen which only differ with respect to the left-turning intensities. However, while applying the analytical approach, the author realized that the distribution of traffic demand over the legs also influences the capacity of the leg-by-leg control [37]. Therefore, the capacity of the signalized turbo roundabouts is higher for demand patterns in which the legs are equally loaded, than for the demand patterns used in this project, where the demand on leg W amounts to 80% of the demand on leg E, and the demands on legs N and S amount 60% of the demand on leg E.

Another example of a feedback loop can be found in section 3.1.3. There, the choice was made to invoke the signalized rotor roundabout with inscribed radii of 12 m and 20 m. The upper boundary was chosen because the space requirement of that rotor roundabout is equal to the space requirement of the smallest partial turbo circle. The partial turbo circle was assumed to have a higher capacity, because it is equipped with a two-phase control, which was presumed to be more efficient than the leg-by-leg control on the rotor roundabout. However, the partial turbo circle appeared to have a lower capacity than the signalized rotor roundabout with an inscribed radius of 20 m, concluding from the VISSIM simulations. Therefore, it would have been sensible to also invoke the rotor roundabout with an inscribed radius larger than 20 m. However, from the analytical approach appears that the capacity of the rotor roundabout with an inscribed radius of 12 m is slightly larger than the capacity of the rotor roundabout with an inscribed radius of 20 m. In that sense, it is not sensible to also invoke larger rotor roundabouts.

Fundamentals of the model or application of the model?

In the early stages of the research project, no clear distinction was made between the fundamentals of the three models and the application of those models. As a consequence, the report was not clearly structured: both aspects were mixed together. The audience (consisting of the members of the graduation committee) had trouble to comprehend the main aim of the research: to assess the models or to assess the turbo roundabouts, by applying the models. In a later stage, this distinction has been introduced in the report. It would have been more efficient to have made this distinction in an earlier stage.

[37] *If a the demand on a particular leg is larger than on the other legs, the green time for that leg needs to be extended; therefore the cycle time needs to be extended and consequentially, the maximum green phase overlap per hour decreases, decreasing the capacity*

Proposal for improving the application of the analytical approach and VISSIM: green phase overlap

The analytical approach and VISSIM can be improved reviewing the clearance time calculation in appendix E. Based on the geometrical design of the rotor and star roundabouts, the clearance time has been calculated. For instance, Figure E-2 shows how the locations of the stop lines determine the entrance time and the exit time. Based on that example, the clearance time has been calculated to be -1.8 s, rounded to 0.0 s for legal safety considerations. The models are applied to the rotor and star roundabouts with the same configuration of the stop lines.

However, the fact that the clearance time is negative, indicates the possibility to increase the exit time. In Figure 4-2, that means that the stop line of stream 12 may be placed somewhere upstream from the indicated location. This replacement has consequences for the maximum possible green phase overlap, calculated in appendix G. In particular, if the stop line were to be replaced upstream, length A in Figure G-2 increases, and so does the maximum green phase overlap.

In conclusion, the green phase overlap estimated in appendix G is too short; the geometrical design of the roundabout offers a higher green phase overlap. Again, the author lacks time resources to repair this shortcoming, unfortunately.

Proposal for improving the application of VISSIM: removing route choice

Appendix L (VISSIM model development) explains that the lanes leading to and on the turbo roundabout are modelled by a separate link. This choice has been made, because vehicles are not allowed to change lanes on the turbo roundabout. However, this approach induces a route choice in the VISSIM network (explained in section 3.2.3). As a solution, two edges had to be closed, but this solution is suboptimal (a static solution to a dynamic problem).

A sound solution would be to remove the route choice from the network. This can be done by modelling the lanes on the circulatory roadway by means of one link, consisting of two lanes. VISSIM offers the possibility to prohibit drivers to change lanes on a link. Then, the drivers in the network would have no route choice, because there is one single route consisting of links with multiple lanes. This project applies networks with route choice, because there are multiple routes consisting of links with one lane.

Unfortunately, the author lacks time resources to repair this shortcoming. However, next simulations from the author's hand will not contain unnecessary route choice anymore.

Proposal for improving the application of VISSIM: cut-off criteria for the green phase

The capacity curves in section 4.3 show excessively high values for particular legs (leg N on the rotor roundabout and leg S on the turbo circle with an inscribed radius of 12 m). As described in the conclusions accompanying the curves, the excessively high values could not be explained. However, visual assessment of the simulations in a later stage of the project inspired the author to formulate a presumption.

Presumably, the large differences are caused in the process of green time assignment by TrafCOD. This presumption is solely based on excluding other possible explanations for the differences. The author excluded these explanations by thoroughly examining the input into the VRIGen and VISSIM models, and finally concluding that leg S and leg N are exactly identical with respect to the minimum green time and maximum extension green time in VRIGen, the geometrical design in VISSIM and the demand pattern in VISSIM and VRIGen. Therefore, the capacity differences between leg N and leg S cannot be explained by the input to the models.

To the other's knowledge, only one explanation remains: the process of green time assignment by TrafCOD. The structure in VRIGen prescribes a minimum green time duration and a maximum extension green time duration for every stream (which are identical for leg N and leg S); TrafCOD chooses a green time duration between these borders. On the rotor roundabout (equipped with a leg-by-leg control),

TrafCOD chooses a green time duration for leg N which is structurally higher than the green time duration for leg S, for some unknown reason. Essentially, this presumption yields the question: based on which criteria does TrafCOD cut-off the green phase? The author assumed that the green phase is cut-off if the detector is not occupied anymore (there is no traffic demand) or if the maximum extension green time is reached. However, in the perspective of the identical leg N and leg S, this does not explain the capacity differences.

Unfortunately, the author lacks knowledge of the fundamentals of TrafCOD and C++ (the programming language of TrafCOD) to thoroughly examine the cause for the capacity differences.

Proposal for improving the application of VISSIM: static or vehicle-actuated control?

This project applied TrafCOD to generate a vehicle-actuated control in the VISSIM simulations. In the perspective of appendix H, where optimum (static) controls have been designed, this choice seems illogical, because the capacity of the leg-by-leg control is maximized for a certain static control. However, this choice has been made for two reasons: 1) it is common practice among traffic engineers to invoke vehicle-actuated control systems in models and practice and 2) by means of a vehicle-actuated control, the delay times in under-saturated conditions can be decreased.

The VISSIM simulations presumably yield too low capacity estimations for the signalized rotor and star roundabout, because the vehicle-actuated leg-by-leg controls assign green time durations which are longer than the durations in the optimized structures in appendix H. This presumption is based on the notion that the maximum extension green time durations in VRIGen are longer than the durations in the optimized control structures, and the notion that TrafCOD will extend the green time maximally in saturated conditions.

Therefore, the choice for applying static controls in this project would have been more sensible, because the static and vehicle-actuated controls are essentially the same in saturated conditions, if the maximum extension green times in VRIGen were manually adapted to the values found in appendix H. In case of the static control, the delay times in under-saturated conditions are over-estimated, but this project was only interested in the saturated conditions: the capacity and delay times in saturated conditions.

Proposal for improving the application of VISSIM: joint delay in the two-phase control

Figure 6-4 shows the capacity of the turbo circle with inscribed radii of 12 m, 20 m and 30m; resulting from the VISSIM simulations. Fortuijn (2013: 341) calculated the capacity of the turbo circle analytically. The VISSIM results do not coincide with the results from Fortuijn (2013). The most important difference is the fact that the capacity of the turbo circle according to Fortuijn is constant for demand patterns in which the left-turning intensities are smaller than or equal to the straight-ahead intensities (DP20 through DP100), while in Figure 6-4, the capacity lines decrease in the range from DP20 through DP100 (and beyond).

In order to understand the cause for this difference, the notion of *joint delay* (Dutch: *aansluitverlies*) should be clarified. Fortuijn (2013: 330) explains the joint delay as the unused green time at an interception signal, caused by the time gap between the passage of the last vehicle in the queue of left-turning vehicles and the first departing vehicle in a straight-ahead stream. For instance, at the moment stream 65 obtains green, the queued vehicles from streams 69 and 09 will pass the signal, and then the vehicles in stream 05. The time gap between the passage of the last vehicle in the queue from stream 09 and the first vehicle in stream 05 is the joint delay.

In the analytical calculations, Fortuijn invoked a constant joint delay: 2 s. In the VISSIM simulations, the joint delay is variable, this probably causes the difference between the capacity lines. In the VISSIM network, the detector for stream 69 is located just stream upward of the stop line. As soon as this detector is cleared, stream 69 obtains yellow and red, and the green phase for stream 05 commences.

Here, the joint delay occurs. That means that the joint delay does not occur if the queue in front of signal 65 is so short, that the last vehicle does not occupy the detector on stream 69. For demand patterns with low left-turning intensities, the left-turning queues are shorter than for other demand patterns. Therefore, the capacity is higher for demand patterns with low left-turning intensities: the joint delay occurs less often in the simulations (with different random seeds) for demand patterns with low left-turning intensities.

Visual assessment of the VISSIM simulations raises the presumption that the joint delay is overestimated in the VISSIM simulations; it is larger than 2 s, as assumed by Fortuijn (2013). Furthermore, the notion that the joint delay only occurs if the queue has reached the detector in front of signal 69, yields the conclusion that the results depend on the way of modeling. Indeed, if the detector is being moved upstream, the joint delay decreases, but the chance of occurrence also decreases.

References

Allen, T.M., Lunenfeld, H., Alexander, G.J. (1971). Driver information needs. Highway Research Record, 366: 102-15.

Arem, B. van, Kneepkens, W.E. (1992). Capacities and Delays at Roundabouts in The Netherlands. Delft/Arnhem: Institute of Spatial Organization TNO, Traffic and Transportation Unit; Rijkswaterstaat Directie Gelderland.

Arem, B. van, Traag, W.J.M. (1993). De Rotonde Verkenner. *Een Literatuurstudie*. Delft/Arnhem: INRO-TNO afdeling Verkeer en Vervoer, Rijkswaterstaat Directie Gelderland.

Baan, D. de (2013). Aantal 'gespotte' turborotondes. Published on www.dirkdebaan.nl/locaties.html. Consulted at 03/12/2013.

Beinum, A.S. van (2007). Prestatieanalyse van de Turborotonde. *Systematische benadering van de relatie tussen geometrisch ontwerp en capaciteit*. Den Haag: Technische Universiteit Delft, Witteveen+Bos.

Branston, D, Zuylen, H. van (1978). The Estimation of Saturation Flow, Effective Green Time and Passenger Car Equivalents at Traffic Signals by Multiple Linear Regression. Elsevier Ltd., published on www.sciencedirect.com, consulted at 03/12/2013.

Bundesanstalt für Straβenwesen, Federal Highway Research Institute (2000). German Highway Capacity Manual. 2nd edition. Bochum, Germany.

Bureau Goudappel Coffeng (1987). Evaluatie Verkeerslichtenregelingen rotondes. In opdracht van Rijkswaterstaat, Dienst Verkeerskunde. Kenmerk RWE/593/13/Bn. Deventer, 5 oktober 1987.

Chen, P., Nakamura, H., Asano, M. (2011). Saturation Flow Rate Analysis for Shared Left-turn Lane at Signalized Intersections in Japan. Procedia Social and Behavioral Sciences 16 (2011) 548-559. Furo-cho, Japan: Nagoya University.

CROW (1996). Richtlijn Ontruimingstijden Verkeersregelinstallaties. Publicatie 111. Ede: CROW.

CROW (1998). Eenheid in rotondes. *Publicatie 126*. Ede: CROW.

CROW (2006). Handboek Verkeerslichtenregelingen. *Publicatie 213*. Ede: CROW.

CROW (2008). Turborotondes. *Publicatie 257*. Ede: CROW.

Eijgenraam, C.J.J., Koopmans, C.C., Tang, P.J.G., Verster, A.C.P. (2000). Evaluatie van Grote Infrastructuurprojecten: Leidraad voor Kosten-Baten Analyse. *Onderzoeksprogramma Economische Effecten Infrastructuur*. Ministerie van Verkeer en Waterstaat; Ministerie van Economische Zaken.

Elling, R., Andeweg, B., Jong, J. de, Swankhuisen, C. (2005). Rapportagetechniek. 3e druk. Groningen/Houten: Wolters Noordhoff

Florida Department of Tranportation (1996). Florida Roundabout Guide.

Fortuijn, L.G.H. (2000). Rotonde-pijlmarkering. Verkeerskundige Werkdagen 2000. Ede: CROW.

Fortuijn, L.G.H. (2008). Capacities Turbo Roundabouts. Non-published presentation at *Provincie Zuid-Holland*, January 28, 2008.

Fortuijn, L.G.H. (2009). Turbo Roundabouts. *Design Principles and Safety Performance*. Washington D.C., Transportation Research Record: Journal of the Transportation Research Board, No. 2096, pp. 16-24.

Fortuijn, L.G.H. (2011). Guest lecture CT3711, 22 maart 2011. *Ontwikkeling van de turborotonde en turboplein*.

Fortuijn, L.G.H. (2013). Turborotonde en Turboplein: Ontwerp, Capaciteit en Veiligheid. Delft, TRAIL Research School.

Granneman (2011). Effect van Verkeerslichten op Turborotondes. Den Haag/Rotterdam: Technische Universiteit Delft, Witteveen+Bos.

Grontmij (2001). Afwikkeling Eerste Deel Wachtrij. *Onderzoek naar het vertrek van voertuigen bij verkeerslichten*. De Bilt: Grontmij Verkeer & Infrastructuur.

Hoogendoorn, S.P. (2011). VK4821 Traffic Flow Theory and Simulation. Delft: University of Technology, faculty of Civil Engineering and Geosciences, section Transportation and Traffic Engineering.

Horst, A.R.A. van der, Groenewoud, M.C.L., Martens, M.H., Franx, E.C.J. (2008). Evaluatie geregelde turbopleinen. TNO-rapport TNO-DV 2008 C006. Soesterberg: TNO.

Inter Traffic Systems. http://www.intertrafficsystems.nl/. *Website of a company producing LED units in asphalt pavements*. Latest consulted at April 8, 2013.

Michon, J.A. (1985). A critical view of driver behaviour models: What do we know, what should we do? In: L. Evans and R. Schwing (*eds*), Human Behaviour and Traffic Safety. New York: Plenum Press, 485-520.

Muller, T.H.J. (1997). College VK4820 Verkeersafwikkeling Deel B Signalized Intersections. Delft: Technische Universtiteit Delft, Faculteit der Civiele Techniek, Sectie Verkeerskunde.

Muller, T.H.J., Dijker, T., Furth, P.G. (2004). Red Clearance Intervals: Theory and Practice. Presented at TRB January 2004.

Muller, T.H.J., Hegyi, A., Salomons, M., Zuylen, H.J. van (2011). CT4822-09 Traffic Management and Control. *Approaches for Urban and Freeway Traffic*. Delft: TU Delft, faculty of Civil Engineering and Geosciences, section Transport and Planning.

ROA (1991). Richtlijnen voor het Ontwerp Autosnelwegen. Hoofdstuk II Alignement. Rijkswaterstaat, Dienst Verkeerskunde. Den Haag, SDU uitgeverij.

RVV (1990). *Reglement Verkeersregels en Verkeerstekens*. Den Haag: Ministerie van Verkeer en Waterstaat. Koninkrijk der Nederlanden Staatsblad 459, oktober 1990 en wijziging Staatsblad 268, mei 1999.

Provincie Zuid-Holland (2013). Meerstrooksrotondeverkenner. Den Haag, provincie Zuid-Holland.

PTV Vision (2011). VISSIM 5.30-05 User Manual. Karlsruhe: PTV Planung Transport Verkehr AG.

Rijkswaterstaat (2001). Regeling Verkeerslichten d.d. 28 augustus 2001. Staatscourant, nummer 169 d.d. 3 september 2001. Rapportnummer lbw-3750. Rotterdam: Ministerie van Verkeer en Waterstaat, Directoraat-Generaal Rijkswaterstaat, Adviesdienst Verkeer en Vervoer.

Romph, E. de (2012). Lecture slides *CIE5802 Advanced Transportation Modelling*, guest lecture. December 17, 2012. Delft: Delft University of Technology.

Salomons, A.M. (2012). Lecture slides *CIE4822 Traffic Management and Control.* Lectures on VRIGen, TrafCOD and VISSIM. June, 2012. Delft: Delft University of Technology.

Siegloch, W. (1973). Die Leistungsermittlung an Knotenpunkten ohne Lichtsignalsteuerung. Schriftenreihe Straβenbau und Straβenverkehrstechnik no. 154.

SWOV (2006). *Eds:* Harris, S., Vorst, A. van der. SWOV Verkeersveiligheidstermen Nederlands-Engels en Engels-Nederlands, *Een Overzicht van Verkeersveiligheids-, Verkeers-, en Algemene Onderzoekstermen*. Leidschendam, Stichting Wetenschappelijk Onderzoek Verkeersveiligheid. Reportnumber D-99-6.

SWOV (2006), *Eds:* Wegman, F., Aarts, L. Advancing Sustainable Safety. *National Road Safety Outlook for 2005-2020*. Leidschendam, The Netherlands: SWOV Institute for Road Safety Research.

SWOV (2012). SWOV Factsheet Roundabouts. Leidschendam, The Netherlands: SWOV Institute for Road Safety Research.

Theeuwes, J., Horst, R. van der, Kuiken, M. (2012). Designing Safe Road Systems. *A Human Factors Perspective.* Surrey (UK): Ashgate Publishing Limited.

Transportation Research Board (2010a). Roundabouts: An Informational Guide. *National Cooperative Highway Research Program Report 672*. 2nd edition. Washington D.C.: Transportation Research Board of the National Academies, U.S. Department of Transportation, Federal Highway Administration.

Transportation Research Board (2010b). Highway Capacity Manual, fifth edition. D.C.: Transportation Research Board of the National Academies, U.S. Department of Transportation, Federal Highway Administration.

Verhaeghe, R.J. (2007). Reader *CT4831 Data, Modelling & Decision Making*. Delft, Delft University of Technology, Faculty of Civil Engineering and Geosciences.

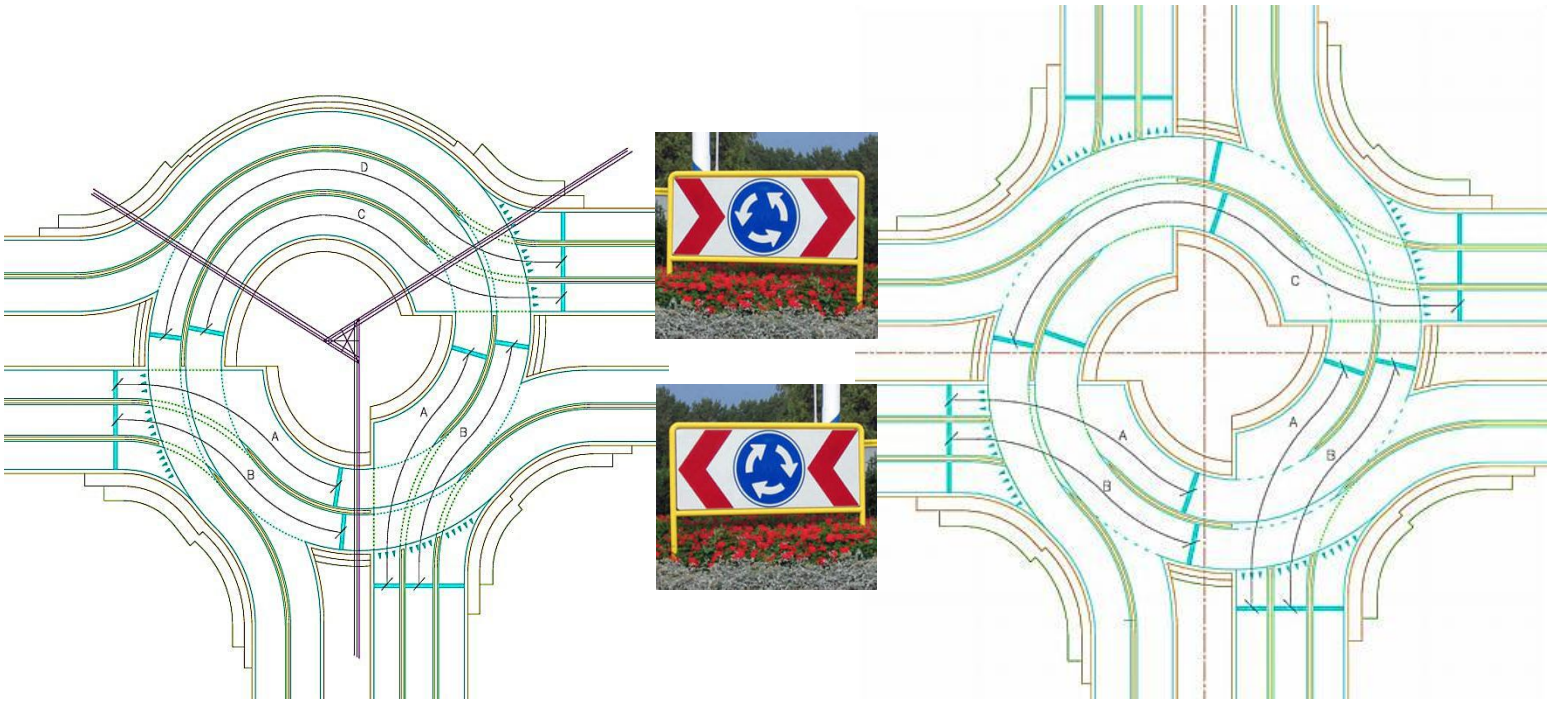
Wickens, C.D. (1984). Engineering Psychology and Human Performance. Columbus, OH: Bell and Howell.

Wu, N. (2001). A Universal Procedure for Capacity Determination at Unsignalized (Priority-Controlled) Intersections. Transportation Research Part B 35 (2001) 593-623.

SIGNALIZED TURBO ROUNDABOUTS

A Study into the Applicability of Traffic Signals on Turbo Roundabouts

Appendices



Rogier R.M. Hoek
July, 2013

TU Delft Delft University of Technology

Table of contents

Appendix A: Discussion of the terminology 109
A.1. Signalized turbo roundabout 109
A.2. Partial turbo circle 109
A.3. Black box approach 109
A.4. Traffic demand and traffic supply 110

Appendix B: Demand patterns 111
B.1. Choice for demand patterns 111
B.1.1. Motivation 111
B.1.2. Variable: left-turning intensity 112
B.2. Overview of demand patterns 112

Appendix C: Saturation flow, field measurements 115
C.1. Saturation flow: highly variable 115
C.2. HCM formula 115
C.3. Saturation flow measurements in The Netherlands 117

Appendix D: Geometrical designs 121
D.1. Lane narrowing 121
D.2. Curvature of entrance and exit legs 123
D.3. Location of the stop lines 125
D.4. Minimum inscribed radius 128
D.5. Rotor roundabout 128
D.5.1. Turboblock 128
D.5.2. Roundabout design 130
D.5.3. Space requirement 132
D.5.4. Length of the segments 132
D.6. Star roundabout 132
D.6.1. Turboblock 133
D.6.2. Roundabout design 134
D.6.3. Space requirement 135
D.6.4. Length of the segments 136
D.7. Partial turbo circle 136
D.7.1. Turboblock 137
D.7.2. Circle design 138
D.7.3. Space requirement 140
D.8. Four-leg turbo circle 140
D.8.1. Turboblock 140

D.8.2. Circle design 142
D.8.3. Space requirement 144
D.8.4. Length of the segments 144
D.9. Three-leg turbo circle 144
D.9.1. Turboblock 145
D.9.2. Circle design 147
D.9.3. Space requirement 148

Appendix E: Clearance time calculation 149
E.1. General method 149
E.2. Application to the rotor roundabout 150

Appendix F: Simplified acceleration model 153
F.1. Description of acceleration behaviour 153
F.1.1. Waiting for the red light 153
F.1.2. Accelerating from standing still 153
F.1.3. Perceiving the interception signal 154
F.1.4. Deciding to accelerate or decelerate 154
F.2. Summary: acceleration behaviour 154
F.3. Constraint of the acceleration length 154
F.4. Maximum phase overlap 155
F.5. Sensitivity analysis 156

Appendix G: Green phase overlap calculation 157
G.1. Input: geometrical design 157
G.2. Calculation of the green phase overlap 158

Appendix H: Control structures for the turbo roundabout 161
H.1. Minimum cycle time 161
H.1.1. Based on the minimum green time 161
H.1.2. Time lag between two opposite legs 161
H.1.3. Adjusting the structure for the green phase overlap 162
H.2. Influence of unequally loaded entrance legs 163

Appendix J: Cycle time optimization 165
J.1. Dilemma of the cycle time 165
J.2. Geometrical design and green phase overlap 165
J.3. Minimum cycle time 166
J.4. Effective green time 169
J.5. Cycle time and phase overlap per hour 169
J.6. Effective green time and saturation flow 170

J.7. Cycle time and capacity 172
J.8. Results 173

Appendix K: VRIGen model development 175
K.1. VRIGen: overview of the tabs 175
K.2. Four-phase leg-by-leg control – without spare streams 175
K.2.1. Signal groups 175
K.2.2. Conflict matrix 176
K.2.3. Couplings 177
K.2.4. Timers 178
K.2.5. Control sequences 179
K.2.6. Tactics 180
K.2.7. Resulting control program 180
K.3. Four-phase leg-by-leg control – with spare streams 180
K.3.1. Spare streams – the strategy 181
K.3.2. Signal groups 181
K.3.3. Conflict matrix 182
K.3.4. Couplings 182
K.3.5. Timers 182
K.3.6. Control sequences 184
K.3.7. Tactics 184
K.3.8. Resulting control program 184
K.4. Troubleshooting 185
K.4.1. Description of the problem 185
K.4.2. Cause of the problem 185
K.4.3. Solution to the problem 186
K.5. Three-phase leg-by-leg control – with spare streams 186
K.5.1. Signal groups 186
K.5.2. Conflict matrix 187
K.5.3. Couplings 188
K.5.4. Timers 188
K.5.5. Control sequences 188
K.5.6. Tactics 188
K.5.7. Resulting control program 188
K.6. Four-leg two-phase control 189
K.6.1. Conflict matrix 189
K.6.2. Couplings 189
K.6.3. Resulting control program 192

K.7. Three-leg two-phase control 193

Appendix L: VISSIM model development 195
L.1. Network 195
L.1.1. Links and connectors 195
L.1.2. Nodes and parking lots 197
L.1.3. Signal heads and detectors 197
L.1.4. Reduced speed areas 199
L.1.5. Priority rules 202
L.2. Base data 204
L.2.1. Vehicle Types 204
L.2.2. Vehicle Classes 205
L.2.3. Functions, Maximum Acceleration 206
L.2.4. Functions, Desired Acceleration 208
L.2.5. Functions, Maximum Deceleration 210
L.2.6. Functions, Desired Deceleration 212
L.2.7. Distributions, Desired Speed 214
L.2.8. Distributions, Power and Weight 217
L.2.9. Driving Behaviour 218
L.2.10. Link Behaviour Types 221
L.3. Traffic demand 221
L.3.1. Vehicle composition 221
L.3.2. .fma-files 221
L.4. Signal control 222
L.4.1. Connection between TrafCOD and VISSIM 222
L.5. Evaluation 223
L.5.1. Travel time 223
L.5.2. Queue length 224

Appendix M: LED illumination 225
M.1. Why LED illumination? 225
M.2. Pavement LEDs: state of affairs 225
M.3. Lay-out of the LED markings 226
M.4. LEDs and functionalities of the turbo roundabout 229
M.4.1. Start of the inner circulatory roadway 229
M.4.2. Roadway dividers vs. LEDs 230
M.4.3. Roundabout shields 231
M.4.4. Design of the route signs 232
M.5. Hypotheses for future research 233

Appendix A: Discussion of the terminology

This appendix explains and motivates the choices for using the terminology *signalized turbo roundabout* and *partial turbo circle*. Moreover, the a discussion on the name of the *black box approach* will be addressed. Finally, the use of the terminology *traffic demand* and *traffic supply* in this document will be addressed.

A.1. Signalized turbo roundabout

The turbo roundabout has a closed definition. Fortuijn (2013, p.47) describes nine characteristics of the turbo roundabout (see Figure 1-6 in the introduction); if a roundabout does not meet these requirements, it is not a turbo roundabout. From these characteristics follows that a signalized roundabout is strictly not a turbo roundabout. It is not even a roundabout, because circulatory traffic does not have priority by traffic rule; instead, traffic signals manage the priority assignment on the intersection. However, in this project the turbo roundabouts will be simulated with traffic signals. The correct terminology would then be 'signalized traffic circle', because the traffic circle is the first type in the hierarchy over the roundabout (see Figure 1-2 in the introduction) which allows for traffic signals. However, that phrase indicates a wide range of intersection types; it is not clear what intersection type is meant exactly. Therefore, this paper uses the terminology *signalized turbo roundabout*. Although this is strictly not correct, this choice has been made out of pragmatism.

A.2. Partial turbo circle

Section 3.1.3 described how to adjust the turbo roundabout, in order to make it suitable for the two-phase control. The adjustment consists of removing the choice lanes. When the circulatory lanes offering a choice are removed, the intersection is strictly not a turbo roundabout anymore, because the lane offering a choice is part of the definition of the turbo roundabout (Fortuijn, p.47). It complies to all characteristics of the turbo circle, all but one. The turbo circle accommodates all directions with separate roadways. On the partial turbo circle (see Figure 2-7), the right lane serves both the right-turning traffic stream and the straight-ahead traffic stream. Therefore it is not a turbo circle; the terminology *partial turbo circle* will be chosen.

A.3. Black box approach

This project applies the *black box approach* to calculate the capacity of the signalized turbo roundabouts analytically. The method and its name are adopted from Fortuijn (2013).

The *black box approach* carries this name, because it is developed along the lines of the general idea of the black box, depicted in Figure 2-9. The internal traffic process on the roundabout is not being considered, but regarded as the transfer characteristics. The name of the *black box approach* is not undisputed. Opponents argue that the method opens up the *black box* of the roundabout, because the phase overlap – and therefore the length of the circulatory road stretch between two legs – needs to be calculated. Proponents argue that the phrase *black box* does not refer to the roundabout itself, but to the internal traffic process on the signalized roundabout, which is not regarded by the method.

This project applies the *black box approach* to a high level of detail. Where Fortuijn estimated the green phase overlap based on assumptions, this project calculates the green phase overlap. Furthermore, control structures are being constructed by means of which the minimum cycle time, the effective green time per leg and the capacity of the signalized rotor and star roundabouts can be calculated. Therefore, the name *black box approach* is not applicable anymore; the name *analytical approach* will be used.

A.4. Traffic demand and traffic supply

This terminology is often confused, especially in Dutch engineering practice. However, the literature prescribes clearly how to use the terminology. This section serves to reveal the way this terminology is used in this document: corresponding to the literature (Sanders *et al.*, 2008; Van Arem *et al.*, 2013).

The literature distinguishes two markets within the integrated transportation system: the transport market and the traffic market (see Figure A-1). In the transport market, the demand for transfers (passengers as well as freight) is confronted with the supply of transport services. The transport services are offered by the transport means (e.g. car, train, airplane). In the traffic market, the demand for transport services is confronted with the traffic services. The traffic services consist of the infrastructure, by means of which the transport services can perform the transfers (e.g. roads, railways, airports). Effectively, the transport services are the supply-side in the transport market, and the demand side in the traffic market.

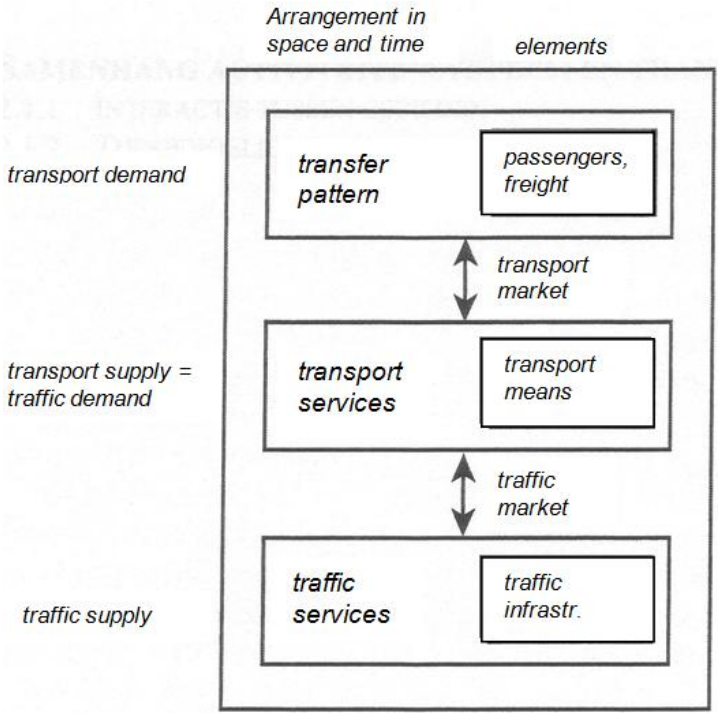


Figure A-1 The integrated traffic and transport system (Van Arem *et al.*, 2013, p.13)

This report applies the terminology strictly; only the traffic market is relevant. In particular, a (signalized) roundabout offers a traffic service, quantified by the capacity. The transport service (the demand side) consists of the traffic that uses the roundabout (e.g. cars, trucks, buses), quantified by the total traffic demand or volume.

Appendix B: Demand patterns

The capacity calculations in this project are based on a set of demand patterns. This appendix motivates which demand patterns will be applied.

B.1. Choice for demand patterns

Fortuijn (2013, p.143) chose the demand patterns shown in Table B-1 to compare the turbo circle with the conventional signalized intersection. The horizontal axis represents the ratio of the traffic flows from directions 02 and 08 (these are the main, primary directions with the largest intensities), the vertical axis represents the ratio of the traffic flows from directions 05 and 02 (05 and 11 are the secondary directions, their traffic flows are equal). The ratio of the right-turning flows w.r.t. the straight-ahead flows [38] is 0.3. The ratio of the left-turning flows w.r.t. the straight-ahead flows [39] takes on ten values: the set [0.2, 0.4, 0.6, 0.8, 1.0, 1.2, 1.4, 1.6, 1.8, 2.0].

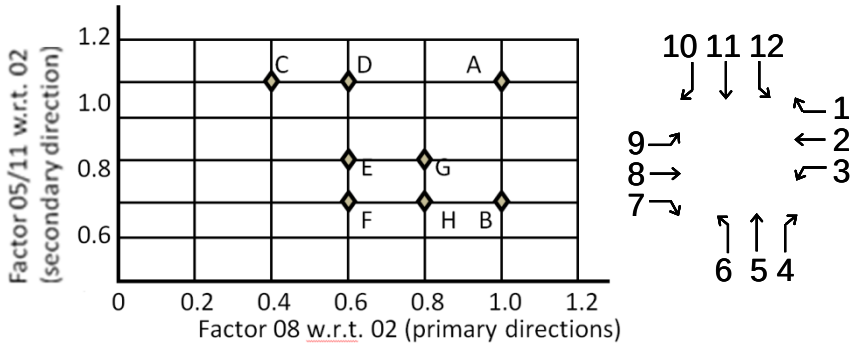


Table B-1 Traffic demand patterns to be applied on the turbo roundabout types

B.1.1. Motivation

In principle, these demand patterns should also be used in this project. The reason for this choice is that the project can be regarded as an offspring of Fortuijn (2013). Indeed, the four intersection types will be investigated in way comparable to Fortuijn's investigation. Moreover, this approach enables the possibility to reliably compare the results of Fortuijn (2013) with the outcomes of this project. Besides, Fortuijn motivates his choice for these demand patterns as follows. The novelty of the turbo intersections needs to be assessed by means of as much demand patterns as possible, in order to evaluate the performance as well as possible. Table B-1 in combination with the set of values for the left-turning intensities, represents all relevant patterns. The right-turning traffic flow is set at one (low) constant value, because the right-turning flows are generally of minor importance to the capacity of intersections.

If these demand patterns will all be applied in this project, the capacities have to be calculated based on 80 demand patterns. If per type a set of five diameters will be evaluated, then 1600 models are to be calculated. This seems rather excessive, and it is not sensible to apply all eight demand patterns in Table B-1. The (non-signalized) rotor roundabout and star roundabout do not have any significant directions (Fortuijn, 2009); both roundabouts serve all directions equally well, or: all straight-ahead flows (directions 02, 05, 08 and 11) have equivalent capacities. When these turbo roundabouts are being compared with signalized turbo roundabouts, it does not make sense to apply a demand pattern A (equal flows for the straight-ahead traffic), because then the models will show an overestimation of the capacity of the un-signalized turbo roundabouts. In reality, a demand pattern with exactly the same intensities for the straight-ahead flows will rarely occur. Fortuijn (2013) presents the capacity of the turbo circle as a

[38] *These are the ratios 01/02, 04/05, 07/08 and 10/11*
[39] *These are the ratios 03/02, 06/05, 09/08 and 12/11*

function of the demand pattern in appendix G.4. These graphs show that the turbo circle has the highest capacity under demand pattern A, with equal left-turning and straight-ahead intensities (9700 pcu/h). The turbo circle has the lowest capacity under demand patterns B, C, F and H (circa 8200 pcu/h). Pattern G yields a modest capacity (8800 pcu/h, see Figure B-1), therefore demand pattern G will be used in this project.

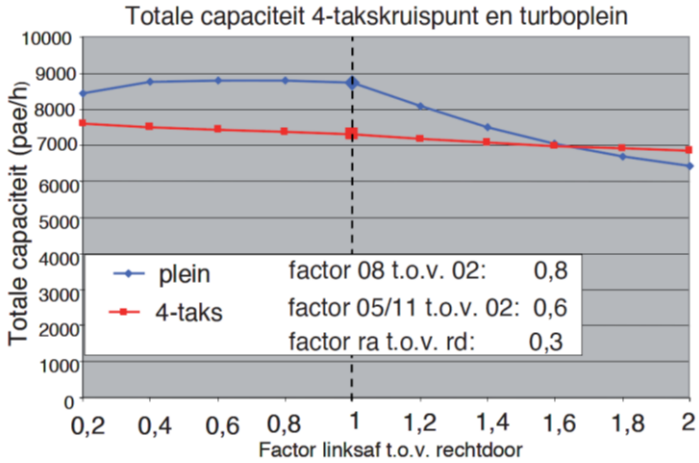


Figure B-1 Fortuijn (2013) plotted eight of these diagrams, with different demand patterns

B.1.2. Variable: left-turning intensity

As discussed in section 3.1.4, the diameter of the turbo circle influences the capacity of the left-turning traffic flows, because the available queuing space on the turbo circle depends on the diameter. The diameter of the signalized turbo roundabout influences the total capacity, not only the capacity of the left-turning traffic flows, because it is equipped with a leg-by-leg control (as illustrated, the larger the diameter, the larger the phase overlap, the larger the green time in one hour, the larger the capacity). Therefore, the left-turning intensities will be varied. The set of ten values for the left-turning flows in Fortuijn (2013) will be adopted in this project.

B.2. Overview of demand patterns

Effectively, the following demand patterns result:

Table B-2 Traffic demand patterns for the four-leg intersections

Demand pattern		Traffic stream											
		01	02	03	04	05	06	07	08	09	10	11	12
		30%	100%		30%	100%		30%	100%		30%	100%	
DP20	Left 20%	0,30	1,00	0,20	0,18	0,60	0,12	0,24	0,80	0,16	0,18	0,60	0,12
DP40	Left 40%	0,30	1,00	0,40	0,18	0,60	0,24	0,24	0,80	0,32	0,18	0,60	0,24
DP60	Left 60%	0,30	1,00	0,60	0,18	0,60	0,36	0,24	0,80	0,48	0,18	0,60	0,36
DP80	Left 80%	0,30	1,00	0,80	0,18	0,60	0,48	0,24	0,80	0,64	0,18	0,60	0,48
DP100	Left 100%	0,30	1,00	1,00	0,18	0,60	0,60	0,24	0,80	0,80	0,18	0,60	0,60
DP120	Left 120%	0,30	1,00	1,20	0,18	0,60	0,72	0,24	0,80	0,96	0,18	0,60	0,72
DP140	Left 140%	0,30	1,00	1,40	0,18	0,60	0,84	0,24	0,80	1,12	0,18	0,60	0,84
DP160	Left 160%	0,30	1,00	1,60	0,18	0,60	0,96	0,24	0,80	1,28	0,18	0,60	0,96
DP180	Left 180%	0,30	1,00	1,80	0,18	0,60	1,08	0,24	0,80	1,44	0,18	0,60	1,08
DP200	Left 200%	0,30	1,00	2,00	0,18	0,60	1,20	0,24	0,80	1,60	0,18	0,60	1,20

Figure B-2 and Figure B-3 illustrate the demand patterns.

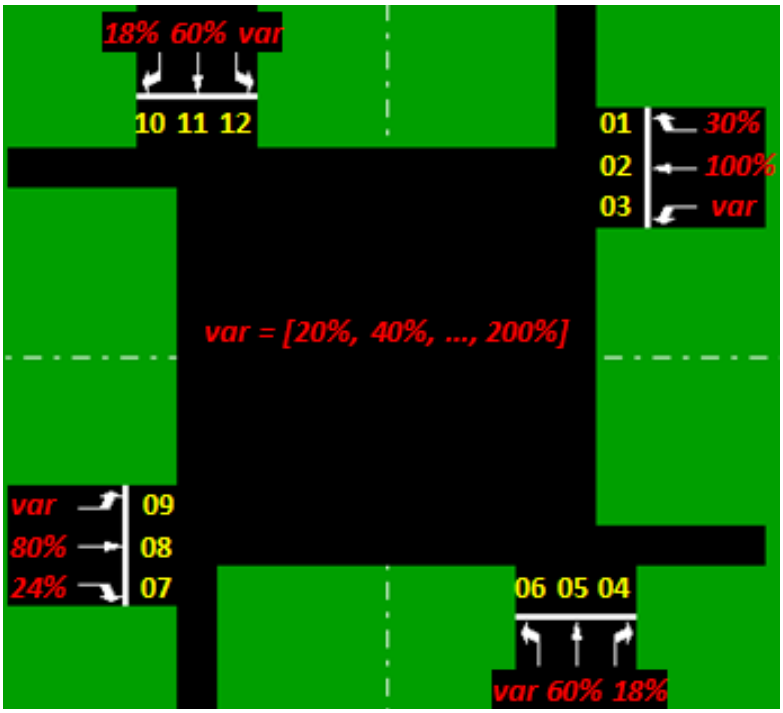


Figure B-2 Illustration of the demand patterns for the four-leg intersections

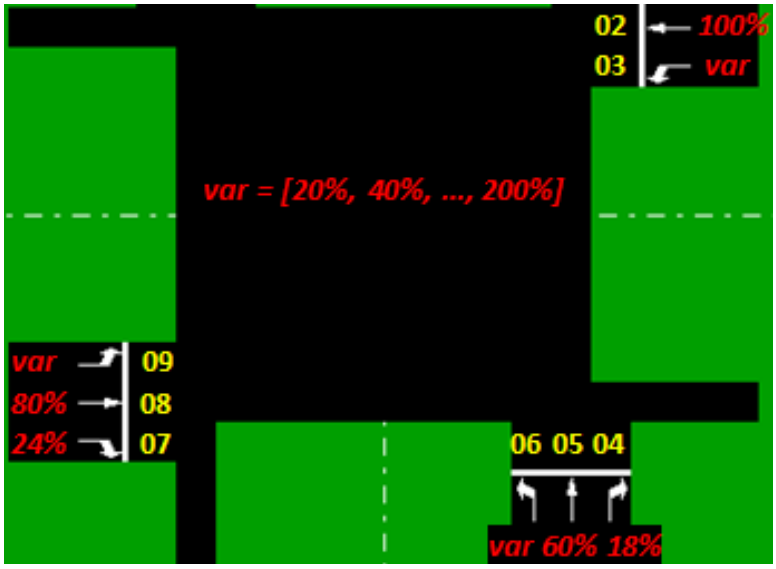


Figure B-3 Illustration of the demand patterns for the three-leg intersections

Appendix C: Saturation flow, field measurements

This appendix determines the values for the saturation flow [40] to be used in this project. The saturation flow is an input variable to the black box approach. The first section indicates that the saturation flow is highly variable. Therefore, it needs to be determined carefully. Basically, there are two ways to determine the saturation flow: by means of a model (the HCM formula) and field measurements. Both methods are addressed separately in the second and third sections; the second section motivates why the HCM formula is not recommended for application to this project.

C.1. Saturation flow: highly variable

As mentioned in section 2.4.2, Fortuijn (2013: 115) estimated the saturation flow to be ca. 1750 pcu/h, he did not motivate this choice. However, recent field measurements show that this value is not a constant; it depends on the site characteristics of the location, such as the number of lanes, lane width, the slope of the road stretch and the demand pattern (right- and left-turning movements). The saturation flow even appears to differ per culture. In The Netherlands, the value of 1750 pcu/h is a commonly accepted value, however in Japan, the saturation flow is measured in the range of 1500 to 1600 pcu/h (Chen *et al.*, 2011). This gives rise to the presumption that the saturation flow is highly variable and demands further investigation.

Moreover, the saturation flow depends on the duration of the green time period per cycle: the longer the (undisturbed) green time, the higher the saturation flow (Branston and Van Zuylen, 1978). A common explanation is that the queue of vehicles waiting to cross the stop line accelerates (just after) the moment it gets green. So as the green time proceeds, the queued vehicles drive faster. For high velocities, this means that the average time headway decreases, and the saturation flow increases (this relation is quantified in section J.6. Therefore, it is important to perform field measurements of the saturation flow. In (scientific) projects, this is part of the common procedure of investigating or reconstructing intersections. This project will use results from Dutch field measurements, to be explained in section C.3.

C.2. HCM formula

The Highway Capacity Manual (TRB, 2010b) offers the following formula for estimating the saturation flow:

$$s = n_{lanes} f_w f_{HV} f_g f_p f_{bb} f_a f_{RT} f_{LT} s_0$$

Equation C-1

where:

s = saturation flow
n_{lanes} = number of lanes
f_w = adjustment factor for lane width
f_{HV} = adjustment factor for heavy vehicles
f_g = adjustment factor for grade
f_p = adjustment factor for parking facilities
f_{bb} = adjustment factor for bus blockage
f_a = adjustment factor for area type
f_{RT} = adjustment factor for right turning movements
f_{LT} = adjustment factor for left turning movements
s_0 = basic saturation flow

[40] *In Dutch: afrijcapaciteit*

The Highway Capacity Manual recommends to use a basic saturation flow slightly higher than Fortuijn used for motivating the black box approach: 1800 pcu/h. The HCM also recommends to use the following values for the adjustment factors, based on model validation. The Swedish manual (CAPCAL) and the German method (Harders) also validated Equation C-1; the differences for the adjustment factors are small (Muller *et al.*, 2011).

n_{lanes} = 3 The rotor and star roundabout contain three lanes on every approaching leg.
f_w = 1.03 The approaching lanes are wider than 4.0 m.
f_{HV} = 0.91 This factor is site specific. The normative truck share outside the urban area used in The Netherlands is 20% (this project considers roundabouts outside the urban area, see section 3.1).
f_g = 1.00 This factor is site specific. Assumption: the roundabouts to be investigated do not contain a grade on the approaching legs.
f_p = 1.00 By definition, parking manoeuvres do not occur on roundabouts (FDOT, 1996).
f_{bb} = 1.00 This factor is site specific. Assumption: no stopping buses on the approaching legs.
f_a = 1.00 This project investigates roundabouts outside the urban area (see section 3.1).
f_{RT} = 0.85 There are no permitted conflicts on the signalized turbo roundabout.
f_{LT} = 0.95 The middle lane serves the left-turning and straight-ahead streams. This value presents the worst case scenario. Depends on the prevailing traffic demand.
s_0 = 1800 pcu/h

The HCM formula presents a saturation flow of ca. 1400 pcu/h per lane. Compared to values used in other studies and Dutch traffic engineering practice, this value is very low. The value cannot be used in this project. The HCM formula is subject to the following drawbacks, and is therefore inapplicable to this project.

Drawback 1: calibrated for non-circular intersections

The HCM formula was calibrated for conventional, non-circular intersections. The applicability to turbo roundabouts is therefore disputable, especially with regard to the adjustment factor for lane width f_w. The circulatory roadways have different widths: the inner roadway is widest and the outer roadway is narrowest (see appendix D: Geometrical designs). The larger the diameter of the roundabout, the narrower the swept path of the normative truck, the narrower the approach legs can be. Furthermore, the turbo roundabout contain multiple curves for all directions, while the non-circular intersection only contains curves for the left and right turning lanes; one curve each. Presumably, the curves affect the driving behaviour on the roundabout and thereby the saturation flow.

Drawback 2: interception signals

If roundabouts are equipped with traffic signals, interception signals need to be installed in order to secure the conflict areas between the entrance legs and the circulatory roadways (Fortuijn, 2013, p.114). The interception signals join traffic streams 62 through 72 (see Figure C-1). They aim to intercept slow vehicles on the roundabout and vehicles making a U-turn (as far as that is possible on turbo roundabouts, without changing lanes). Crashes between these vehicles and vehicles from conflicting streams would not be prevented by the traffic control if the interception signals are absent.

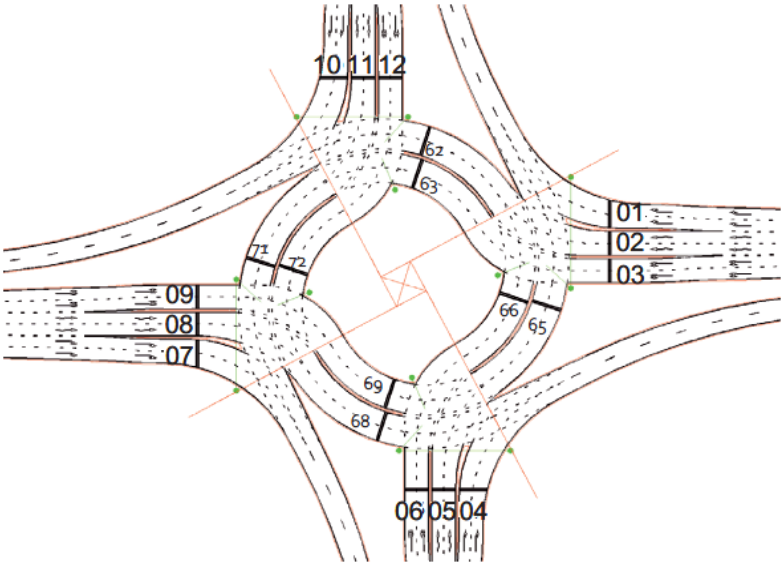


Figure C-1 Standard coding of traffic streams (subtracted from Fortuijn, 2013, p. 130)

The second drawback of the HCM-formula is that it does not take into account these interception signals. If a traffic stream gets green, the front vehicles start accelerating. The acceleration of the left-turning vehicles might be low if the front drivers see that the interception light still shows red. The HCM-formula assumes acceleration at the desired acceleration rate, therefore the formula might overestimate the saturation flow.

Drawback 3: the model is validated for American occasions

The HCM-formula cannot be applied directly to Dutch case studies, because it is validated for American occasions. A variety of arguments can be mentioned: American and Dutch vehicles in general have different characteristics; the driving culture is very different; Dutch and American road environments are often very different, etc.

Drawback 4: the model is validated quite a long time ago

Nowadays, vehicles are equipped with more powerful engines. Due to the developments in the automotive industry, the average performance and acceleration of vehicles have improved.

C.3. Saturation flow measurements in The Netherlands

The influence of the interception signals on the turbo roundabout and turbo circle is hard to include in a model. It largely depends on psycho-physiological aspects, such as driver awareness and attention, anticipation, familiarity with the area, etc. From that point of view, estimations from field measurements are more reliable than any model, because the field measurements take into account the mentioned aspects and all other aspects of which traffic engineers are ignorant.

At the moment of this writing (July 2013), two turbo circles have been realized in practice which are suitable to make measurements. The turbo circles are located in The Netherlands, province of South-Holland: the intersection Doenkadeplein N209/N471 and the intersection Tolhekplein N470/N471 (see Figure C-2). Measurements have been performed on these intersections by the governmental institution Province of South-Holland (PZH) in the month October 2012. Table C-1 shows an example of the raw data (part of the measurements performed on October 10, 2012). Table C-2 shows the values averaged over all days, both intersections, per traffic stream.

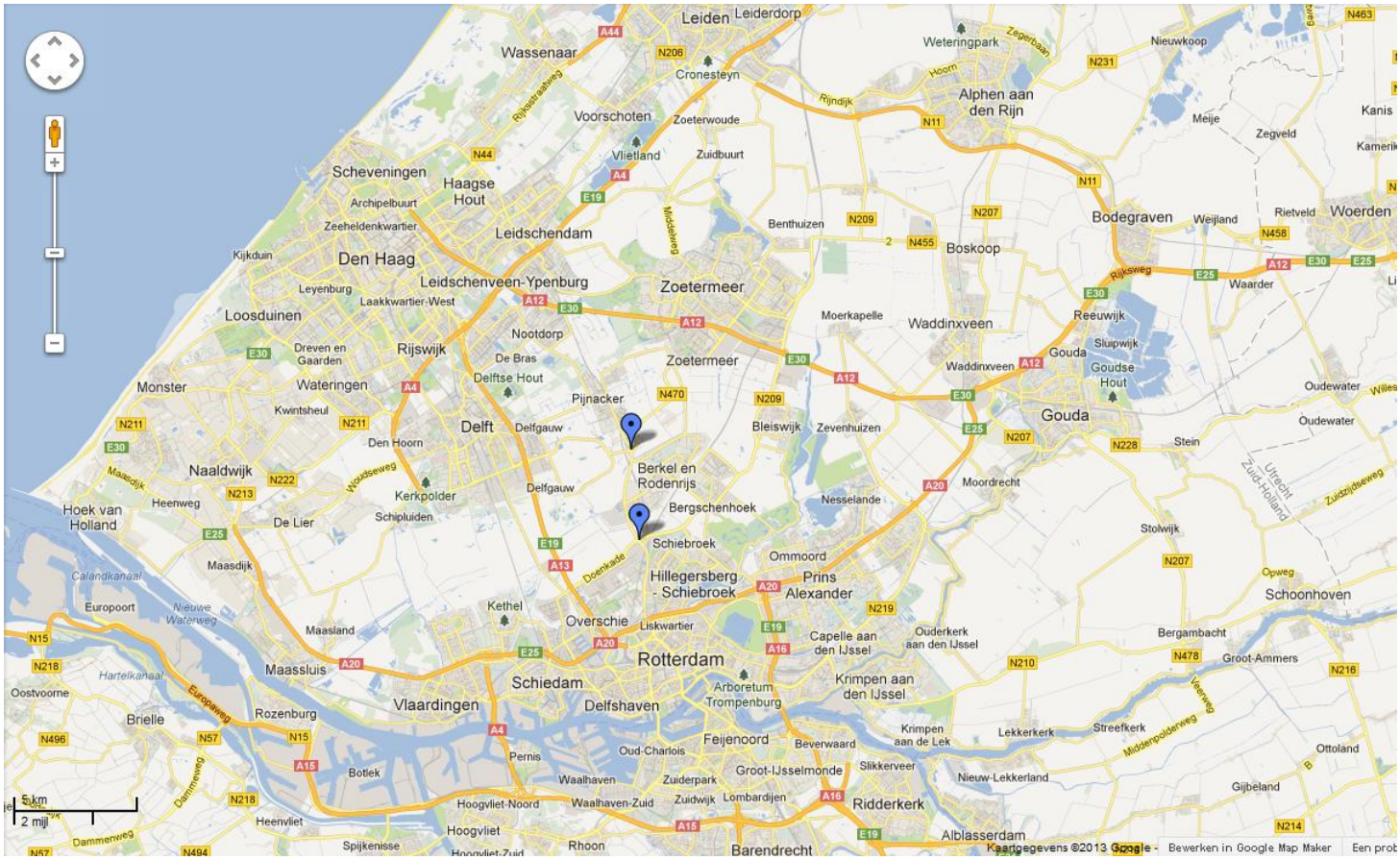


Figure C-2 Locations of the Tolhekplein (northern bubble) and the Doenkadeplein (southern bubble)

Table C-2 shows the saturation flow measurements at both intersections. The values for the Doenkadeplein are averaged over eight days in October 2012, the values for the Tolhekplein are averaged over 12 days in October 2012. The weekend days have been excluded. Moreover, these values are based on measurements during the peak periods (07h00 – 09h00 and 16h00 – 18h00).

This project includes intersections with different lane configurations. Therefore, the data from Table C-2 will be translated into values for the right-turning lanes, straight-ahead lanes and left-turning lanes separately:

lanes right-turning	1852 pcu/h
lanes straight ahead	1891 pcu/h
lanes left-turning	1843 pcu/h

The average saturation flow at the interception signals is 2077 pcu/h.

Table C-1 Example of the raw saturation flow data, courtesy of the Province of South-Holland

Afrijcapaciteit
Locatiecode: 0904 N209 N471 Doenkadeplein Berkel en Rodenrijs
Periode: ma 01-10-2012
Objecttype: Rijstroken
Alle getoonde waarden zijn uitgedrukt in pae/uur per rijstrook.

Van	Tot	01.1	02.1	02.2	03.1	03.2	07.1	08.1	08.2	09.1	09.2	62.1	62.2	65.1	65.2	68.1	68.2	71.1	71.2	Geselec-teerde rijstroken
15:00	15:15	1664	1676	2197	1431	1916	1787	1705	1905	1735	2057	1812	2356	1788	2262	1829	2069	1767	1953	1838
15:15	15:30	1670	1612	2004	1549	1902	1829	1564	2349	1630	2062	1854	2183	1868	2199	1719	2677	2011	1937	1852
15:30	15:45	1694	1870	2001	1562	1886	1513	1605	2042	1577	2026	1882	2134	1987	2071	1786	2215	1861	2257	1836
15:45	16:00	1740	1791	1974	1536	1944	1580	1681	1663	1611	1984	1979	2017	2012	2442	1920	2084	1922	2237	1865
	15:00-16:00	1692	1737	2044	1520	1912	1677	1639	1990	1638	2032	1882	2173	1914	2244	1814	2261	1890	2096	1848
16:00	16:15	1766	1702	2106	1652	1895	1592	1741	2099	1733	2002	1898	2455	2026	2056	1964	2746	1836	1955	1893
16:15	16:30	1788	1754	1894	1607	2172	1618	1623	1895	1620	1862	1909	2098	2007	2234	1980	2206	1838	1999	1871
16:30	16:45	1806	1804	2017	1888	1982	1899	1851	2100	1800	1893	1969	2197	1906	2253	2033	2189	2090	2248	1928
16:45	17:00	1758	1972	2111	1721	2112	1822	1857	2056	1886	1828	2101	2119	2071	2347	2027	2355	1978	2232	1963
	16:00-17:00	1780	1808	2032	1717	2040	1733	1768	2038	1760	1896	1969	2217	2003	2223	2001	2374	1936	2109	1914
17:00	17:15	1734	1678	2099	1647	2061	1771	1755	2163	1909	1905	2046	2264	2025	2355	2191	2491	2035	2121	1965
17:15	17:30	1744	1723	2125	1820	2017	1842	1843	2006	1697	1667	1913	2282	2035	2419	2183	2077	2092	2206	1962
17:30	17:45	1764	1491	2043	1790	2054	1826	1788	2002	1986	1794	1841	2246	2109	2093	2058	2199	2091	2176	1943
17:45	18:00	1760	1642	2104	1700	2012	1929	1828	2099	1931	1945	1813	2337	1956	2205	2122	2169	1894	2084	1949
	17:00-18:00	1751	1634	2093	1739	2036	1842	1804	2068	1881	1828	1903	2282	2031	2268	2139	2234	2028	2147	1955
18:00	18:15	1757	1755	1961	1705	1918	1847	1805	1939	1929	2019	1988	2187	2121	2181	2121	2175	2148	2250	1961
18:15	18:30	1743	1610	1930	1688	1970	1808	1794	1882	1823	2038	2147	2164	2120	2202	2014	2090	1885	2105	1911
18:30	18:45	1712	1843	1897	1713	1970	1789	1699	2076	1799	2039	2097	2079	1774	2242	1958	2329	1779	2033	1907
18:45	19:00	1753	1720	1981	1698	1970	1771	1553	2201	1754	2039	2013	2938	1869	2195	1691	2380	1757	1969	1913
	18:00-19:00	1741	1732	1942	1701	1957	1804	1713	2025	1826	2034	2061	2342	1971	2205	1946	2244	1892	2089	1923
Periode	00:00-24:00	1761	1679	1999	1586	1965	1770	1690	2010	1737	2093	1907	2277	1910	2201	1973	2275	1891	2066	1879

Table C-2 Saturation flow measurements, averaged per traffic stream

Doenkadeplein			**Tolhekplein**		
Direction	Sat flow	St dev	Direction	Sat flow	St dev
01.1	1798	117	01.1	1752	131
02.1	1754	73	02.1	1802	110
02.2	2013	94	02.2	2055	146
03.1	1705	82	03.1	1809	62
03.2	1916	101	03.2	1999	58
04.1	1695	110	04.1	1870	115
04.2	1938	97	04.2	2057	134
05.1	1851	75	05.1	1776	80
05.2	2020	100	05.2	1922	109
06.1	1739	77	06.1	1752	81
07.1	1763	104	07.1	2142	159
08.1	1730	84	08.1	1850	108
08.2	2044	81	08.2	1949	130
09.1	1778	85	09.1	1810	106
09.2	1932	99	09.2	2017	147
10.1	1736	134	10.1	1767	75
11.1	1837	55	11.1	1715	102
11.2	2022	63	11.2	1911	56
12.1	1775	76	12.1	1758	78
12.2	1835	82	12.2	1971	75
62.1	1948	70	62.1	2137	120
62.2	2212	92	62.2	1952	94
65.1	1998	97	65.1	2107	160
65.2	2247	70	65.2	2003	115
68.1	2014	98	68.1	2136	199
68.2	2246	112	68.2	1943	74
71.1	1968	69	71.1	2196	78
71.2	2189	80	71.2	1932	39

Appendix D: Geometrical designs

This appendix addresses the details on the geometrical designs of the intersections to be modelled in this project. The appendix is written such that the reader with basic skills of AutoCAD can reproduce the designs. The first section describes a directive prescribing the permitted lane narrowing on a turbo roundabout and turbo circle. The second section pays attention to the radii of the curves connecting the entrance and exit legs to the circulatory roadways. The third section describes the locations of the stop lines on the turbo roundabout and circle. The remarks in these three section all apply to the turbo roundabout and circle in general. The fourth section states the lower boundary of the inscribed radius of the turbo roundabouts and circles. The following five sections pay attention to the geometry of the specific intersection types. These sections structured are equally: firstly, the turboblock will be described, based on section D.1. Secondly, the design will be finished by adding the entrance and exit legs, based on section D.2, and the stop lines, based on section D.3. Thirdly, the space requirements of each intersection type will be stated. Finally, some geometrical characteristics (length of the circulatory road segments) will be measured from the design; that information is necessary input for the analytical approach (described in section 4.2).

The geometrical designs of the turbo roundabouts and circles are described for two reasons. They are necessary input for the VISSIM simulations (see appendix J: VISSIM model development) and the space requirement – a criterion for assessing the performance of the intersection types – can be stated accurately.

D.1. Lane narrowing

Because the circulatory roadways 'fan out' (characteristic of the design: Fortuijn, 2013), the radius of the circle to be driven by a vehicle crossing a turbo intersection increases. In order to reduce the required space and velocity on the roundabout (lower speed improves traffic safety), the width of the circulatory roadways should decrease as vehicles proceed on the roundabout. The minimum required width of the roadway can be calculated by means of Dutch design guidelines (CROW, 1998 and ROA, 1991). These guidelines present the following formula for the outer radius of the swept path as a function of the inscribed radius and the vehicle dimensions:

$$R_{outer} = \sqrt{\left[\sqrt{\{(R_{inner} + ½BO)^2 + (WO + KA)^2 - KA^2\}} + ½BT\right]^2 + (WT + VT)^2}$$

Equation D-1

where:

R_{outer} = outer radius of the swept path
R_{inner} = inscribed radius of the swept path
BO = width of the trailer
WO = width of the trailer's wheel base
KA = distance between the king-pin and the truck's rear-end
BT = width of the truck
WT = width of the truck's wheel base
VT = front overhang

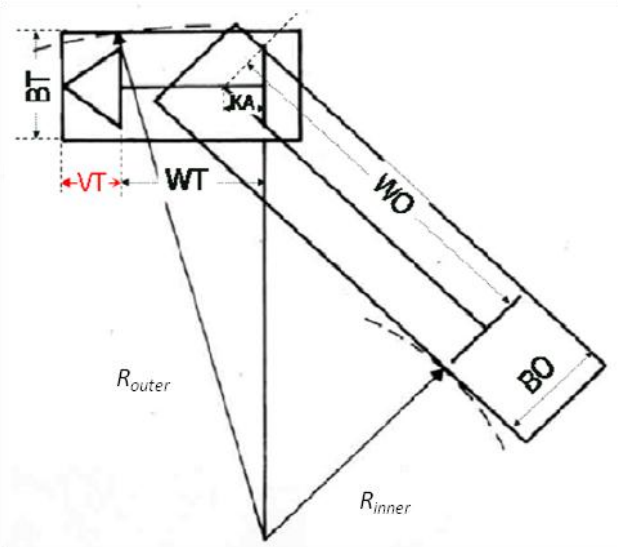


Figure D-1 Dimensions of the truck-trailer combination (taken from Fortuijn, 2013, p.241)

The dimensions of the truck-trailer combination are illustrated by Figure D-1. Table D-1 presents the quantification of three normative vehicle types: the vehicle without exemption, the 22-m vehicle and the vehicle with exemption.

Table D-1 Dimensions of the normative vehicle types

	Without exemption	22-m vehicle	With exemption
BO	2.55 m	2.55 m	2.55 m
WO	7.80 m	9.58 m	11.40 m
KA	0.60 m	0.60 m	0.60 m
BT	2.45 m	2.45 m	2.45 m
WT	3.40 m	3.70 m	3.70 m
VT	0.00 m	0.00 m	0.00 m

The value for *VT* will be chosen 0 m, because the front overhang does not influence the swept path of the wheels (Fortuijn, 2013, p.241). This statement and the formula are based on Figure D-1.

Vehicles without exemption: vehicles without exemption should be able to cross the intersection using the roadway only. For instance, under the condition of outer radius R_{outer}= 12.50 m, the inscribed radius should not exceed R_{inner}= 5.30 m.

22-m vehicles: vehicles with a length of 22 m should be able to cross the intersection using one roadway and the truck apron. For instance, under the condition of outer radius R_{outer}= 14.50 m, the inscribed radius should not exceed R_{inner}= 6.50 m.

Vehicles with exemption: vehicles with exemption (for instance due to an obligation to follow a specific route with indivisible cargo) should be able to cross the intersection using one roadway, the truck apron and the hard shoulder. For instance, under the condition of outer radius R_{outer}= 16.50 m, the inscribed radius should not exceed R_{inner}= 7.50 m.

By means of Equation D-1 and the dimensions of the normative vehicles, the turboblocks of the turbo roundabouts and circles will be designed in the following sections. But first, this appendix deals with two general design aspects which apply to every turbo roundabout and turbo circle in this project: the curvature of the entrance and exit legs, as well as the location of the stop lines.

D.2. Curvature of entrance and exit legs

On the turbo roundabouts and circles, the entrance and exit legs are connected to the circulatory roadways by curves which have identical inscribed radii for all intersection types. These radii are prescribed by the Dutch design guideline CROW publication 126 *Eenheid in rotondes* (CROW, 1998, p.41) and have typical values: 12 m for the entrance legs and 15 m for the exit legs.

With these typical values, the radii of all curves in the connection between an entrance leg and the circulatory roadway, and all curves in the connection between an exit leg and the circulatory roadway are determined. They can be calculated by means of Equation D-1 and the dimensions of the normative vehicles. For instance, the normative vehicle without exemption making a curve with inscribed radius 12 m, needs an outer radius of 17.30 m; this is the outer radius of the right entrance lane. A normative 22-m vehicle (making use of the truck apron) needs an inscribed radius of 10.50 m, under the condition of outer radius 17.30 m. A normative vehicle with exemption (making use of the hard shoulder) needs an inscribed radius of 8.80 m, under the condition of outer radius 17.30 m.

These values and the values for the other curves are presented in Figure D-2. They are calculated by means of Equation D-1 and apply to the rotor and star roundabout. The partial turbo circle and the turbo circle (three- and four-leg) have different lane configurations, and therefore different entrance and exit curvature. The entrance and exit curves of these intersection types are illustrated by Figure D-3 and Figure D-4.

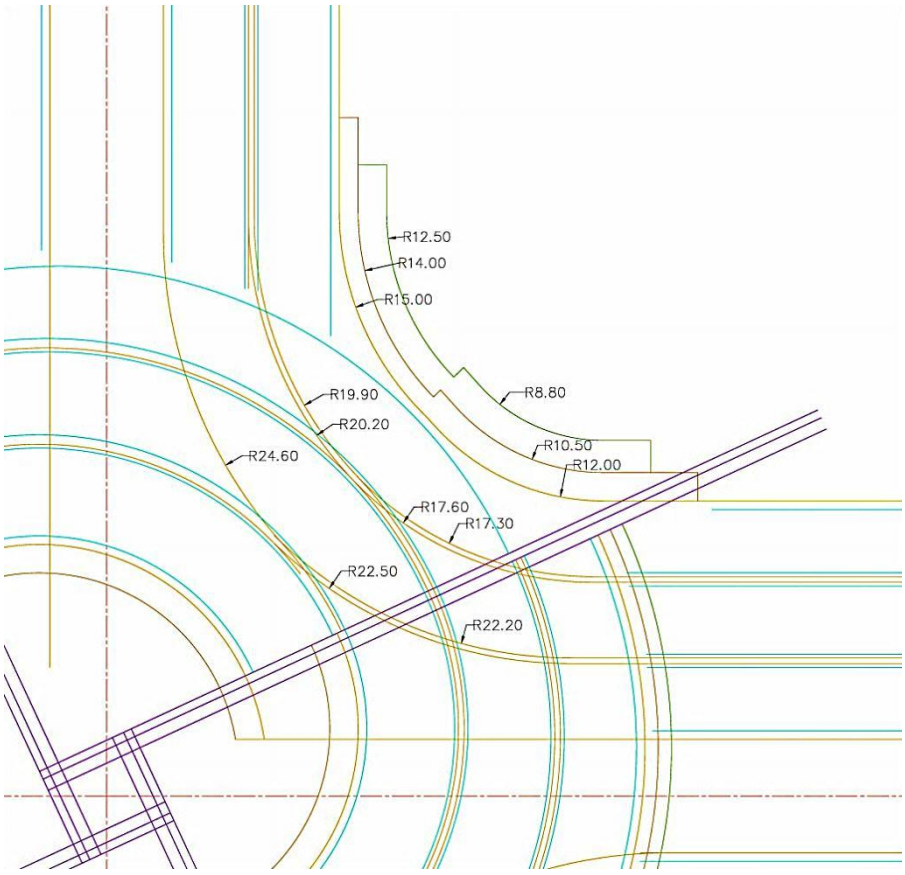


Figure D-2 Geometrical design of an entrance and exit leg on the rotor and star roundabout

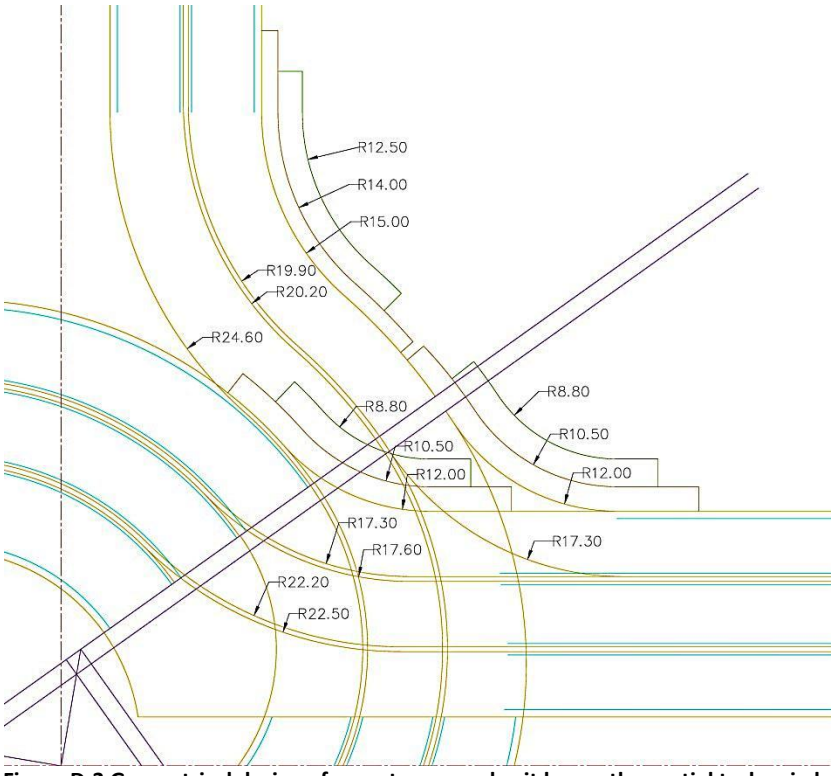


Figure D-3 Geometrical design of an entrance and exit leg on the partial turbo circle

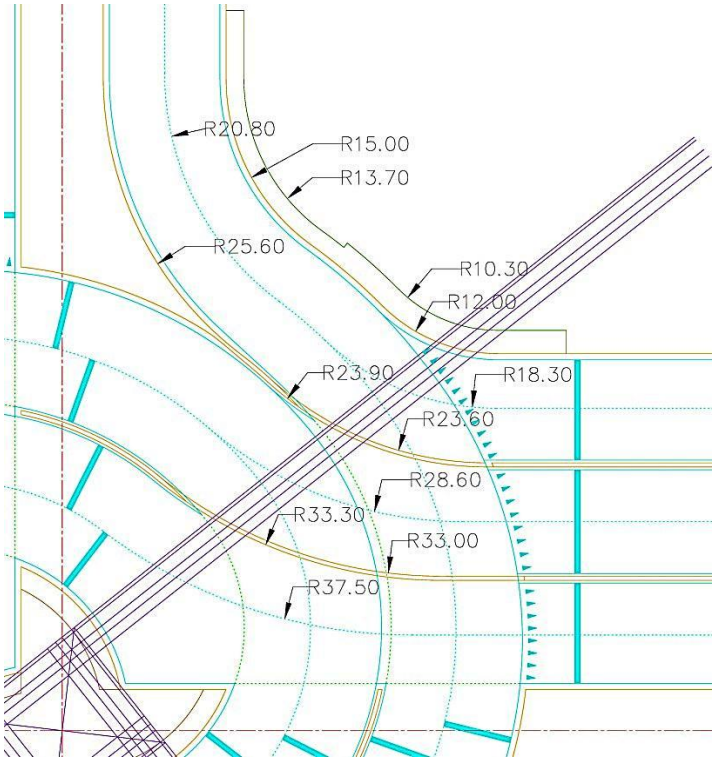


Figure D-4 Geometrical design of an entrance and exit leg on the turbo circle

On the turbo circle, the entrance, exit and circulatory roadways consist of multiple lanes (see Figure D-4). That means that two trucks might accelerate next to each other onto the turbo circle; one on the right

lane and one on the left. If those vehicles comply to the dimensions of the normative 22-m vehicle, the truck on the left lane can use the truck apron, but the truck on the right lane cannot. For this reason, the lanes on the turbo circle should be designed to accommodate a 22-m vehicle.

Eenheid in Rotondes also prescribes typical values with respect to the width of the lanes on the entrance and exit legs: 4 m for the entrance legs and 4.50 m for the exit legs (CROW, 1998, p.41).

Another design aspect of interest is the width of the splitter island. *Eenheid in Rotondes* presents a typical value of 5.00 m, for roundabouts with single-lane exit legs. The turbo roundabouts and circles in this project contain double-lane exit legs. Therefore, a splitter island width of 6.00 m will be applied to the turbo roundabouts and circles in this project.

D.3. Location of the stop lines

The location of the stop lines affect the traffic control to be applied to the turbo roundabouts and circles. In particular, this geometrical characteristic determines the distance from the stop line to the conflict area of a couple of conflicting traffic streams. Therefore, they affect the clearance time for the couple of conflicting streams in question (for more details, see appendix H: VRIGen model development).

In this section, the location of the stop lines will be determined based on field observations. The position of the traffic signals determine the position of the stop lines. Figure D-5 indicates the locations of the turbo circles that have already been constructed in The Netherlands (time of writing: June 2013); the geometry of the stop lines will be designed based on those turbo circles. Figure D-6 shows a part of the Doenkadeplein, the distance between the stop line and the traffic signal is indicated for directions 01, 02, 03, 65 and 66. Table D-2 shows the distances for all directions on the Doenkadeplein and the Tolhekplein.

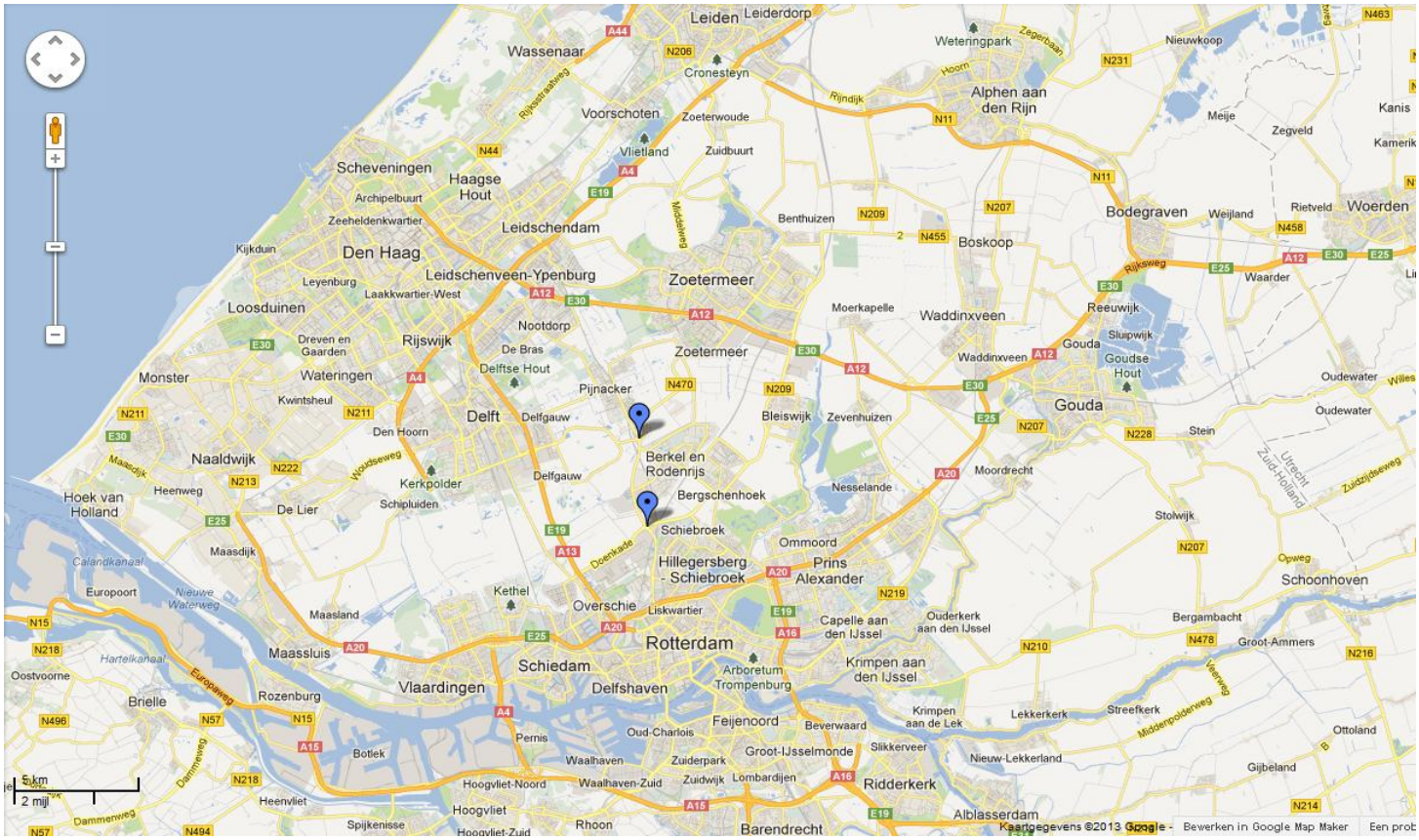


Figure D-5 Locations of the Tolhekplein (northern bubble) and the Doenkadeplein (southern bubble)

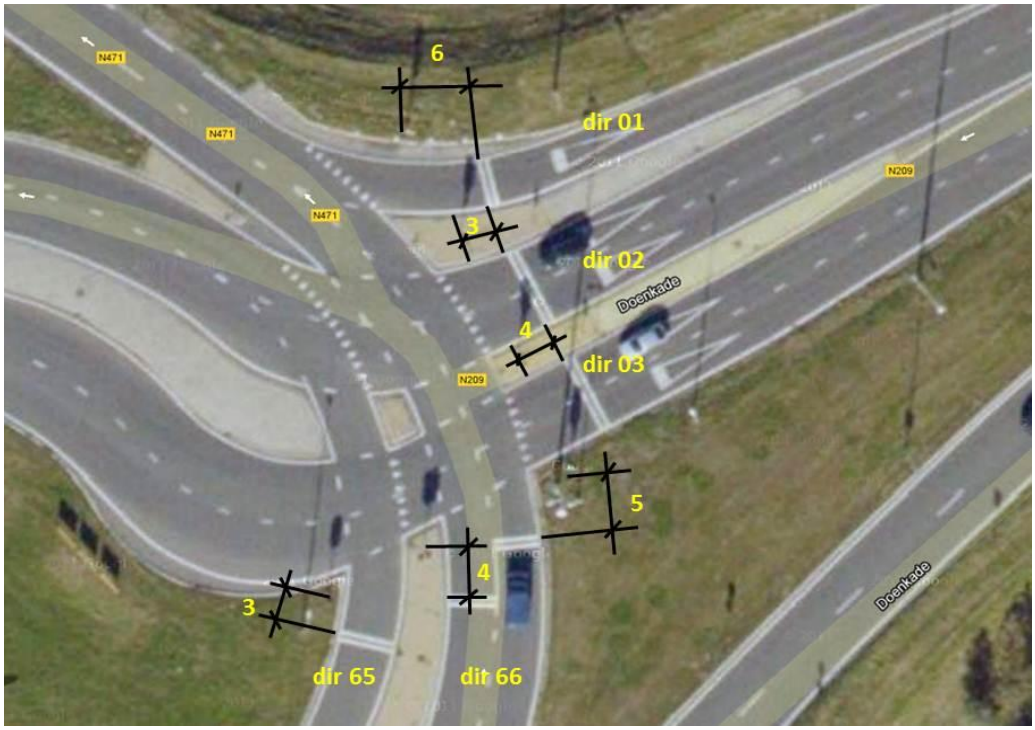


Figure D-6 Distances (in meters) between stop lines and signals on the Doenkadeplein

Table D-2 Distances between stop lines and signals [41]

	Doenkadeplein		Tolhekplein	
	distance	# lanes	distance	# lanes
01	6/3	1	4/4	1
02	3/4	2	4/4	2
03	4/5	2	5/4	2
04	8/3	2	4/4	2
05	4/3	2	4/4	2
06	4/4	1	5/4	2
07	4/5	1	5/6	2
08	4/4	2	6/5	2
09	6/4	2	6/6	1
10	3/5	1	6/7	1
11	3/3	2	6/6	1
12	4/3	2	6/6	1
62	3/5	2	5/5	2
63	4/3	2	5/5	2
65	4/5	2	5/5	2
66	3/8	1	5/5	2
68	4/3	2	5/5	2
69	2/4	2	11/5	1
71	3/3	2	5/5	2
72	3/3	2	11/5	1

[41] *For every direction (single- and double-lane), two sigal are installed. The two distance are presented, divided by a slash ("/") where the number in front of the slash presents the distance between the stop line (of the left lane) and the left signal; the number after the slash presents the distance between the stop line (of the right lane) and the right signal.*

From the picture and the table, the following conclusions can be drawn:

- The traffic signals for directions 01 through 12 are located on the entrance legs. The distance between the signal and the roadside of the circulatory lanes is 1 m, as a minimum.
- The traffic signals for directions 62 through 72 are located on the circulatory roadways. The distance between the signal and the roadside of the entrance leg is 1 m, as a minimum.
- The minimum distance between the stop line and the signal for directions 01 through 12 is 3 m.
- The distance between the stop line on the (right) lane of the outer circulatory roadway and the traffic signal on the splitter island is at least 3 m, preferably 5 m.
- The distance between the stop line on the (left) lane of the outer circulatory roadway and the traffic signal between the inner and the outer roadway ranges arbitrarily between 3 and 5 m.
- The distance between the stop line on the (left) lane of the inner circulatory roadway and the traffic signal on the middle island is arbitrary (range of 2 through 11 m).

From these conclusions, the following choices will be made for the geometrical design of the signalized turbo roundabouts:

- The minimum distance between the traffic signals on the entrance legs and the roadside of the circulatory roadway is 1 m.
- The minimum distance between the traffic signals on the circulatory roadways and the roadside of the entrance legs is 1 m.
- The minimum distance between the traffic signals on the entrance legs and the stop lines is 3 m.
- The minimum distance between the traffic signals on the circulatory roadways and the stop lines is 3 m.

In conclusion, the distance between the stop lines and the roadsides is 4 m, for all directions (see Figure D-7).

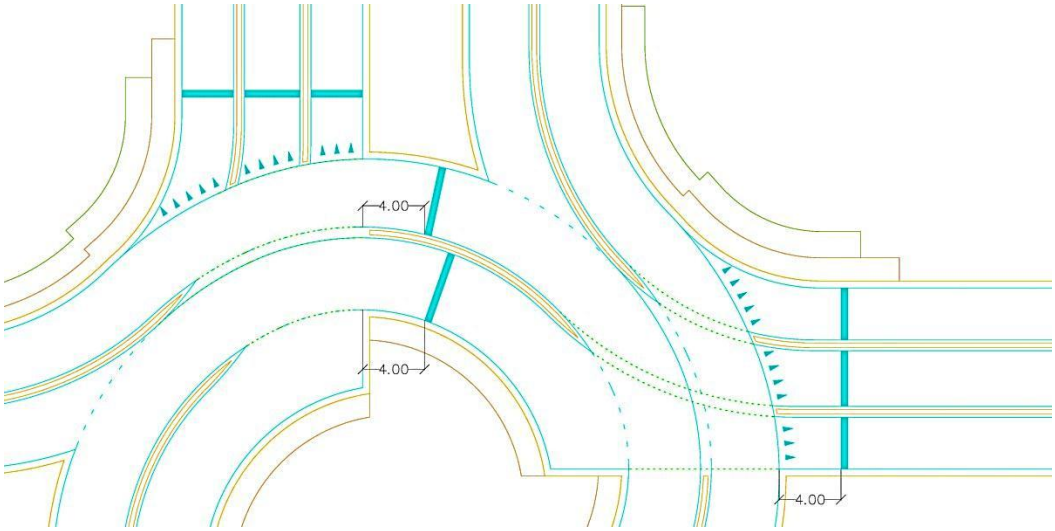


Figure D-7 Positions of the stop lines

This design of the stop lines is in accordance with the *Regeling Verkeerslichten* (Rijkswaterstaat, 2001), a Dutch legislative policy document on the design of traffic signals. For this project, the relevant prescriptions are:

- The horizontal distance between the edge of the signal and the edge of the roadway shall be at least 0.60 m (clause 17);
- The horizontal distance between the signal at the side of the roadway and the stop line of the corresponding roadway shall be at least 3 m (clause 19);
- The horizontal distance between the signal over the roadway and the stop line of the corresponding roadway shall be at least 12 m and at maximum 20 m (clause 20);

- If a lane is equipped with a signal at the side of the roadway and a signal over the roadway, the horizontal distance between both signals and the stop line of the corresponding roadway shall be at least 3 m (clause 21).

D.4. Minimum inscribed radius

The value for the minimum inscribed radius should be chosen as small as possible, because in that case, the required space of the turbo roundabout is minimized. On the other hand, the inscribed radius should not be too small, because it influences the driving curve of the straight-ahead and left-turning vehicles. A small central island yields a fairly straight driving curve for the straight-ahead vehicles, increasing the speed of these vehicles.

In this dilemma, an optimum can be found by means of Dutch design guidelines (CROW, 1998, p.40). According to that document, the desired speed in the curves of the intersection depends on the radius of the driving curve according to the following relationship (CROW, 1998, p.40):

$$v_{desired} = 7.4 * \sqrt{R_{curve}}$$

Equation D-2

where:
$v_{desired}$ = desired speed [km/h];
R_{curve} = radius of the driving curve [m].

When applying an inscribed radius of 12 m to the turbo roundabout, the average speed will be about 25 km/h, which is regarded a safe speed on a turbo roundabout. The value 12 m will be used as the lower bound for the set of diameters to be applied on the signalized turbo roundabouts.

D.5. Rotor roundabout

This section deals with the design of the rotor roundabout. Firstly, the turboblock will be designed based on section D.1. Secondly, the rotor roundabout will be finished based on sections D.2 and D.3. Finally, the space requirement of the rotor roundabout and some important dimensions will be stated. The rotor roundabout will be designed with two values for the inscribed diameter: 12 m and 20 m.

D.5.1. Turboblock

On the rotor roundabout, the inner circulatory lanes start opposite of an entrance leg. The rotor roundabout has four legs, that means that the circulatory roadways need to 'fan out' by the width of the inner circulatory roadway over the length of a quarter segment. In order to secure a smooth driving curve, the geometrical design of the rotor roundabout consists of circles with four different centre points. Therefore, four translation axis are necessary which make angles of 90 degrees with respect to each other (see Fortuijn, 2013, appendix E).

Circulatory roadway narrowing

Inner roadway: the inner roadway has inscribed radius 12 m. A vehicle without exemption should be able to make a left-turn via the inner roadway. By means of the dimensions of the vehicle without exemption and Equation D-1, one can calculate the corresponding roadway width: 5.26 m, rounded off to 5.30 m. The inner roadway covers the distance of a quarter of a segment. It starts 5.30 m wide, and does not narrow, because at the start and at the end of the quarter segment, the radius is still 12 m. The truck apron on the central island has to accommodate for a 22-m vehicle. With outer diameter (12+5.30) 17.30 m, the inscribed radius must be 10.50 m. This means that the truck apron on the middle island is 1.50 m wide.
Middle roadway: the middle roadway has inscribed radius (12+5.30+0.30) 17.60 m (the roadway divider between two roadways is 0.30 m wide). It has to accommodate for a vehicle without exemption. By

means of Equation D-1 the width of the middle roadway can be calculated: 4.60 m. The middle roadway narrows from 5.05 m [42] to 4.60 m.

Outer roadway: the outer roadway has inscribed radius (17.60+4.60+0.30) 22.50 m. It has to accommodate for a vehicle without exemption, and the entrance and exit curves are equipped with truck aprons to accommodate for 22-m vehicles, and a hard shoulder to accommodate for vehicles with exemption. In that case, the outer roadway is 4.20 m wide. The outer roadway narrows from 4.85 m (the width of the end of the middle roadway plus 0.25 m) to 4.20 m. The width of the truck apron (accommodating the normative 22-m vehicle) is 0.70 m and the hard shoulder (accommodating the normative vehicle with exemption) is 0.70 m wide. The narrowing of the outer roadway is probably not important, because the outer roadway has left the roundabout long before it has reached the reduced width, so the curve widening at the exit leg is more important. This remark also applies to the truck apron and the hard shoulder.

The previous calculations are structurally shown in Table D-3. Figure D-8 shows a section of the circulatory roadways at the start of an inner roadway. Table D-4 shows the roadway narrowing for the rotor roundabout with an inscribed radius of 20 m. The roadway narrowing is illustrated by the turboblock in Figure D-9 and the detail in Figure D-10.

Table D-3 Roadway narrowing of the rotor roundabout with inscribed radius 12 m

Roadway		*Radius*		*Start width*		*End width*		
Truck apron		10.50 m		1.50 m		1.50 m		
Inner	R1	12.00 m	WS1	5.30 m	WE1	5.30 m		
Middle	R2	17.60 m	WS2	5.05 m	WE2	4.60 m	A	0.45 m
Outer	R3	22.50 m	WS3	4.85 m	WE3	4.20 m	B	0.65 m
Truck apron	R4	26.70 m		0.70 m		0.70 m		
Hard shoulder		27.40 m		0.70 m		0.70 m		

Table D-4 Roadway narrowing of the rotor roundabout with inscribed radius 20 m

Roadway		*Radius*		*Start width*		*End width*		
Truck apron		19.20 m		0.80 m		0.80 m		
Inner	R1	20.00 m	WS1	4.40 m	WE1	4.40 m		
Middle	R2	24.70 m	WS2	4.15 m	WE2	4.10 m	A	0.05 m
Outer	R3	29.10 m	WS3	4.35 m	WE3	3.90 m	B	0.45 m
Truck apron	R4	33.00 m		0.50 m		0.50 m		
Hard shoulder		33.50 m		0.60 m		0.60 m		

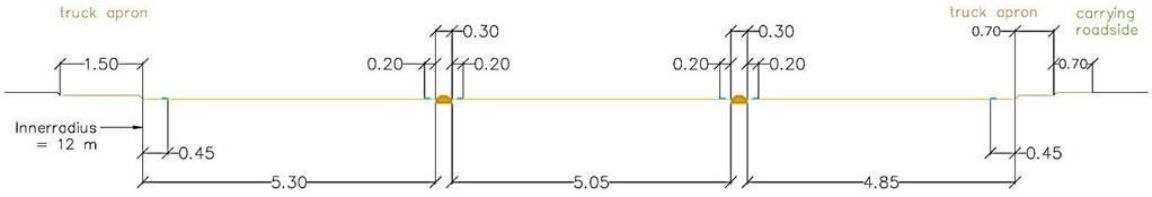


Figure D-8 Section of the rotor roundabout with inscribed radius 12 m

[42] *The middle roadway connects at the start to the inner roadway; the inner roadway is 0.25 m wider than the middle roadway because it contains a hard shoulder.*

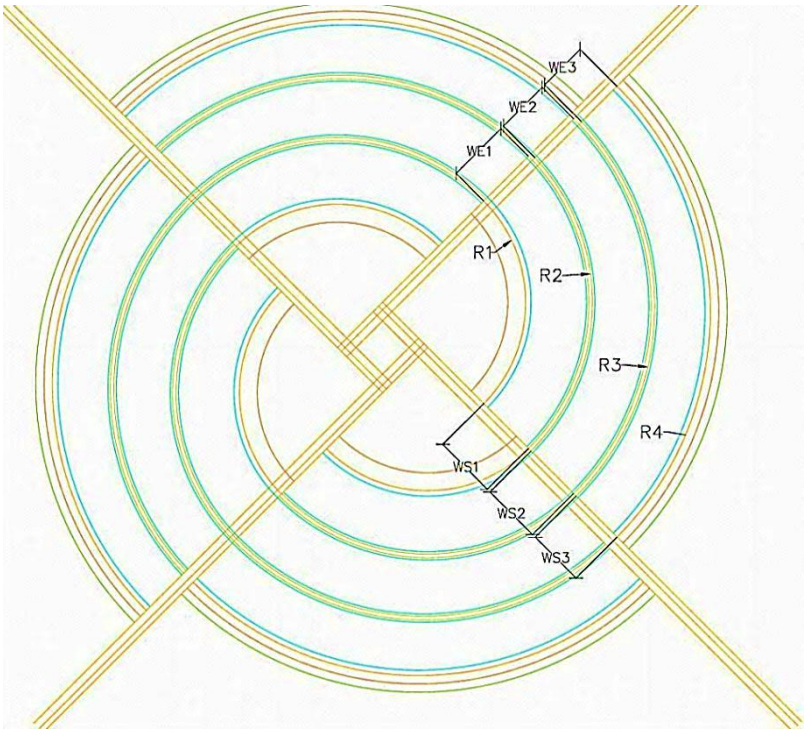


Figure D-9 Turboblock of the rotor roundabout

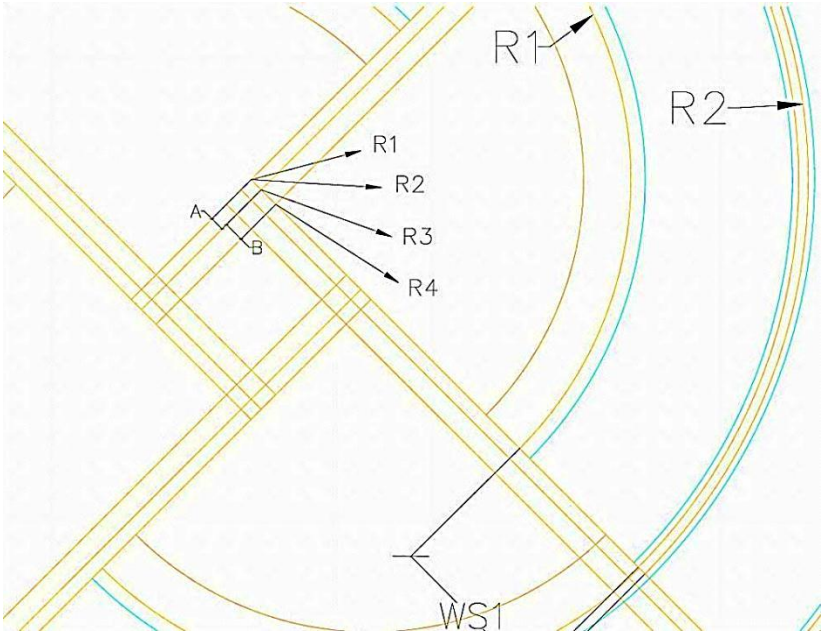


Figure D-10 Detail of the turboblock of the rotor roundabout

D.5.2. Roundabout design

The turboblock is the base for the roundabout design. The entrance and exit legs need to be connected to the circulatory roadways in the turboblock, by means of the curvature described in section D.2. Figure D-11 and Figure D-12 show the designs of the rotor roundabout with inscribed radii of 12 m and 20 m.

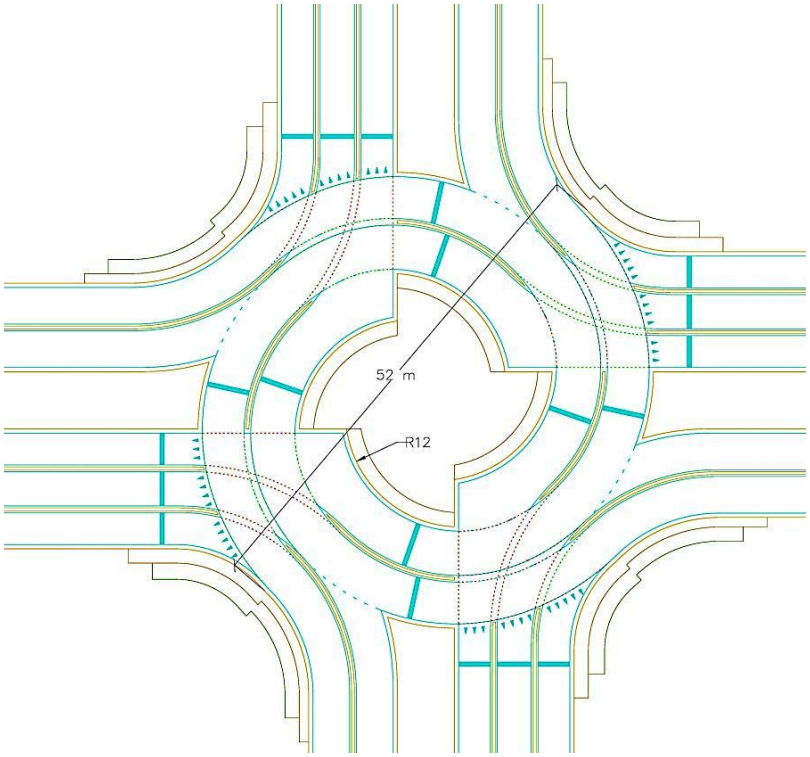


Figure D-11 The design of the rotor roundabout with an inscribed radius of 12 m

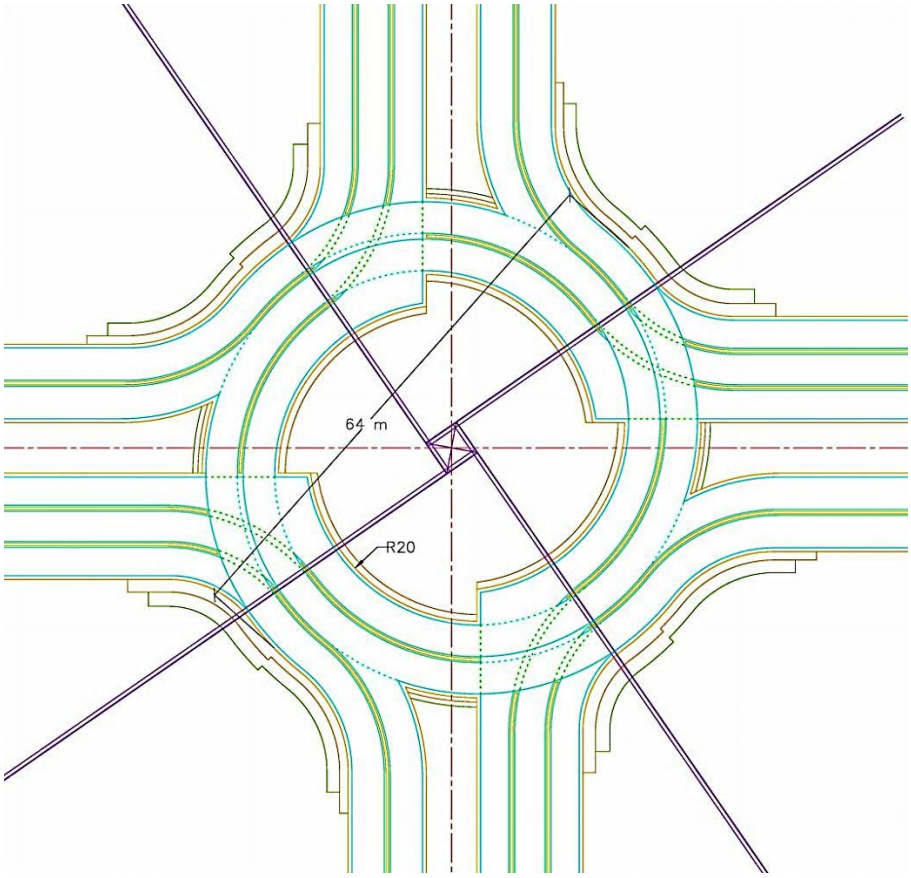


Figure D-12 The design of the rotor roundabout with an inscribed radius of 20 m

D.5.3. Space requirement

Figure D-11 and Figure D-12 show the outer diameters of both rotor roundabouts, Table D-5 presents an overview. This table will be used in later stages of the project.

Table D-5 Overview of the inscribed and outer diameters of the rotor roundabout

	Inscribed radius	Outer radius
Rotor roundabout	12 m	52 m
Rotor roundabout	20 m	64 m

D.5.4. Length of the segments

Section 4.2 describes the analytical approach, a method to calculate the capacity of a signalized turbo roundabout analytically. A necessary input for this method is the length of the road segments between every pair of main signal and interception signal (e.g. traffic streams 02 and 62). The road segments are indicated in Figure D-13. Table D-6 quantifies the lengths for the rotor roundabouts with inscribed diameters of 12 m and 20 m.

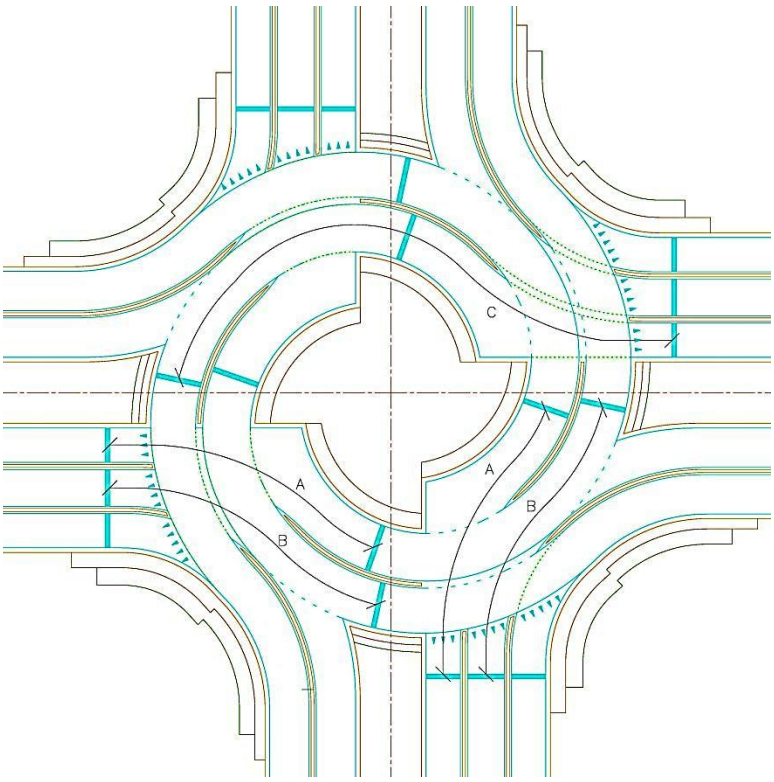


Figure D-13 Indication of the length of circulatory road segments, input for the analytical approach

Table D-6 Values for A and B for the rotor roundabout

Inscribed radius	A	B	C
12 m	29 m	31 m	55 m
20 m	38 m	38 m	82 m

D.6. Star roundabout

This section deals with the design of the star roundabout. Firstly, the turboblock will be designed based on section D.1. Secondly, the star roundabout will be finished based on sections D.2 and D.3. Finally, the space requirement of the star roundabout and some important dimensions will be stated. The star roundabout will be designed with two values for the inscribed diameter: 12 m and 20 m.

D.6.1. Turboblock

The star and rotor roundabout have nearly identical turboblocks. The only major difference is the amount of translation axes. While the rotor roundabout has four translation axis, the star roundabout has three translation axes, because the inner circulatory lane needs to 'fan out' by the width of a lane over the length of one third of the entire circle (effectively, the translation axis make angles of 120 degrees with respect to each other). This is caused by the facts that the star roundabout has three legs and the inner legs start opposite of an entrance leg.

The results of the calculations by means of Equation D-1 are shown in Table D-7 and Table D-8. Figure D-14 shows a section of the circulatory roadways at the start of an inner roadway, for the star roundabout with an inscribed radius of 12 m. The roadway narrowing is illustrated by the turboblock in Figure D-15 and the detail in Figure D-16.

Table D-7 Roadway narrowing of the star roundabout with inscribed radius 12 m

Roadway		*Radius*		*Start width*		*End width*		
Truck apron		10.50 m		1.50 m		1.50 m		
Inner	R1	12.00 m	WS1	5.30 m	WE1	5.30 m		
Middle	R2	17.60 m	WS2	5.05 m	WE2	4.60 m	A	0.30 m
Outer	R3	22.50 m	WS3	4.85 m	WE3	4.20 m	B	0.43 m
Truck apron	R4	26.70 m		0.70 m		0.70 m		
Hard shoulder		27.40 m		0.70 m		0.70 m		

Table D-8 Roadway narrowing of the star roundabout with inscribed radius 20 m

Roadway		*Radius*		*Start width*		*End width*		
Truck apron		19.20 m		0.80 m		0.80 m		
Inner	R1	20.00 m	WS1	4.40 m	WE1	4.40 m		
Middle	R2	24.70 m	WS2	4.15 m	WE2	4.10 m	A	0.03 m
Outer	R3	29.12 m	WS3	4.35 m	WE3	3.90 m	B	0.30 m
Truck apron	R4	33.17 m		0.50 m		0.50 m		
Hard shoulder		33.67 m		0.60 m		0.60 m		

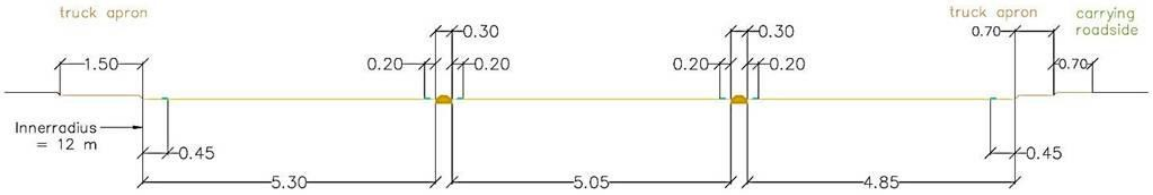


Figure D-14 Section of the star roundabout with inscribed radius 12 m

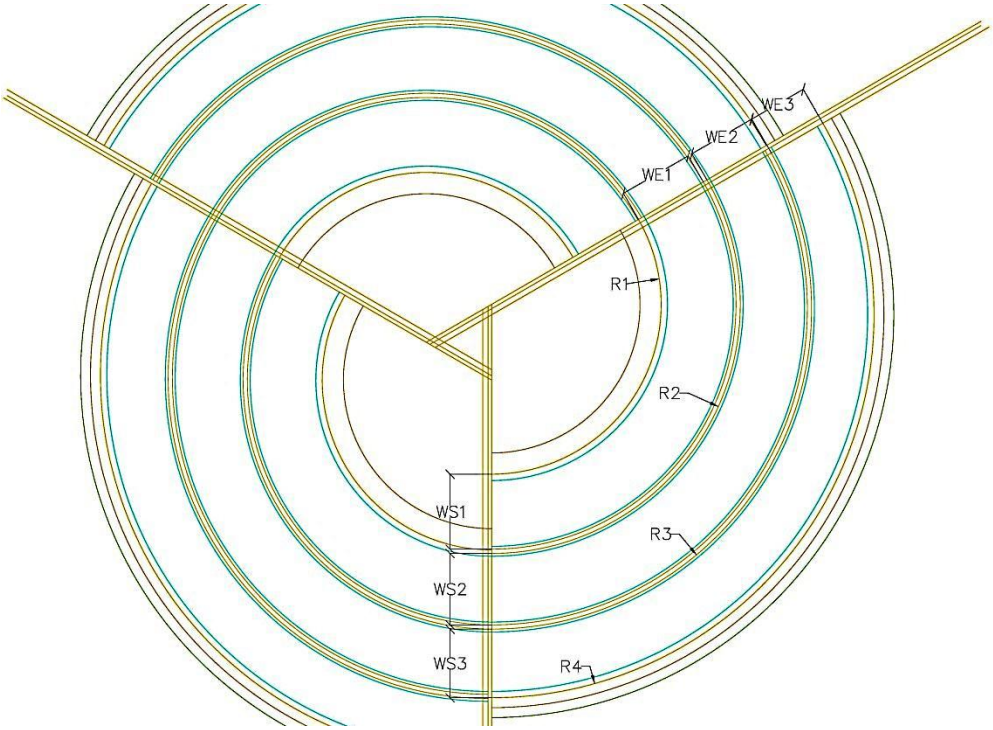


Figure D-15 Turboblock of the star roundabout

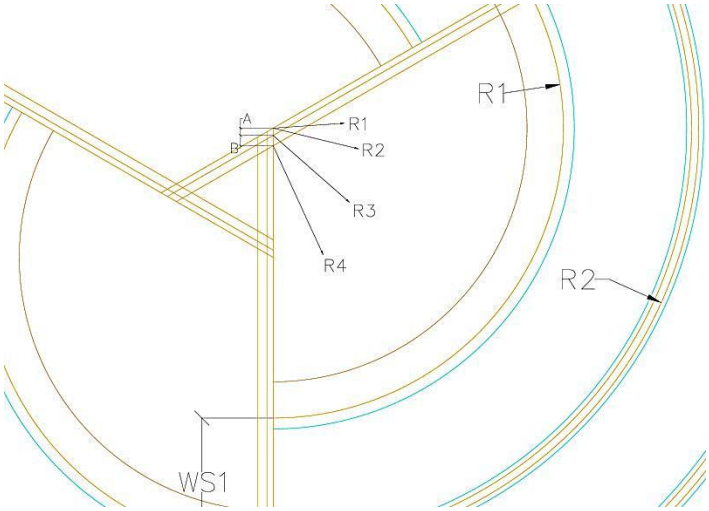


Figure D-16 Detail of the turboblock of the star roundabout

D.6.2. Roundabout design

The turboblock is the base for the roundabout design. The entrance and exit legs need to be connected to the circulatory roadways in the turboblock, by means of the curvature described in section D.2. Figure D-17 and Figure D-18 show the designs of the star roundabout with inscribed radii of 12 m and 20 m.

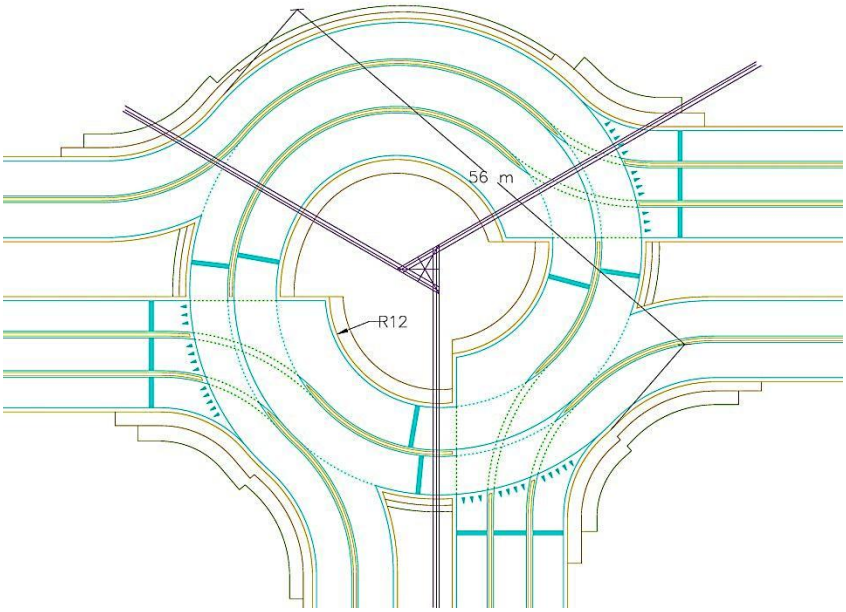


Figure D-17 The design of the star roundabout with an inscribed radius of 12 m

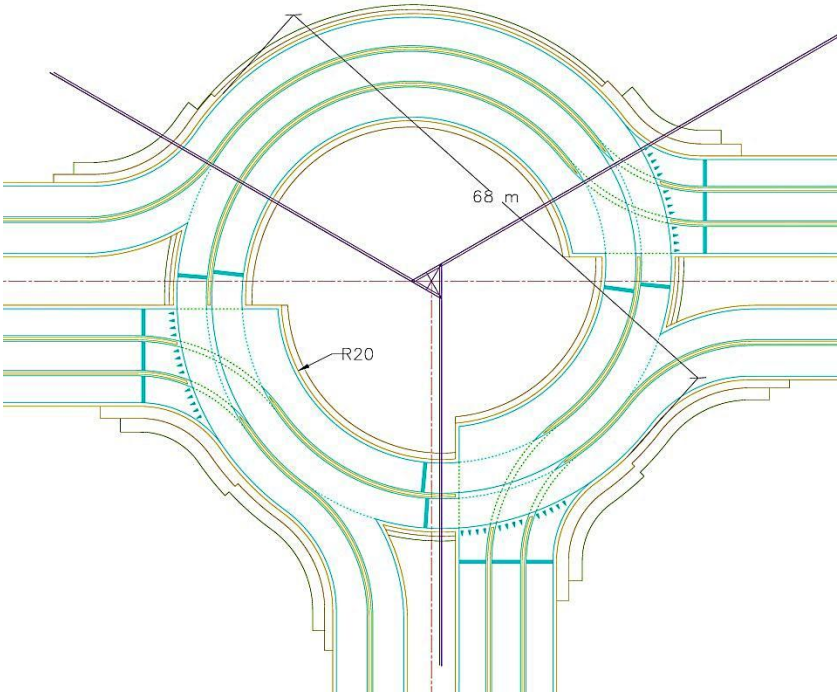


Figure D-18 The design of the star roundabout with an inscribed radius of 20 m

D.6.3. Space requirement

Figure D-17 and Figure D-18 show the outer diameters of both star roundabouts, Table D-9 presents an overview. This table will be used in later stages of the project.

Table D-9 Overview of the inscribed and outer diameters of the star roundabout

	Inscribed radius	Outer radius
Star roundabout	12 m	56 m
Star roundabout	20 m	68 m

D.6.4. Length of the segments

Section 4.2 describes the analytical approach, a method to calculate the capacity of a signalized turbo roundabout analytically. A necessary input for this method is the length of the road segments between every pair of main signal and interception signal (e.g. traffic streams 02 and 62). The road segments are indicated in Figure D-19. Table D-10 quantifies the lengths for the star roundabouts with inscribed diameters of 12 m and 20 m.

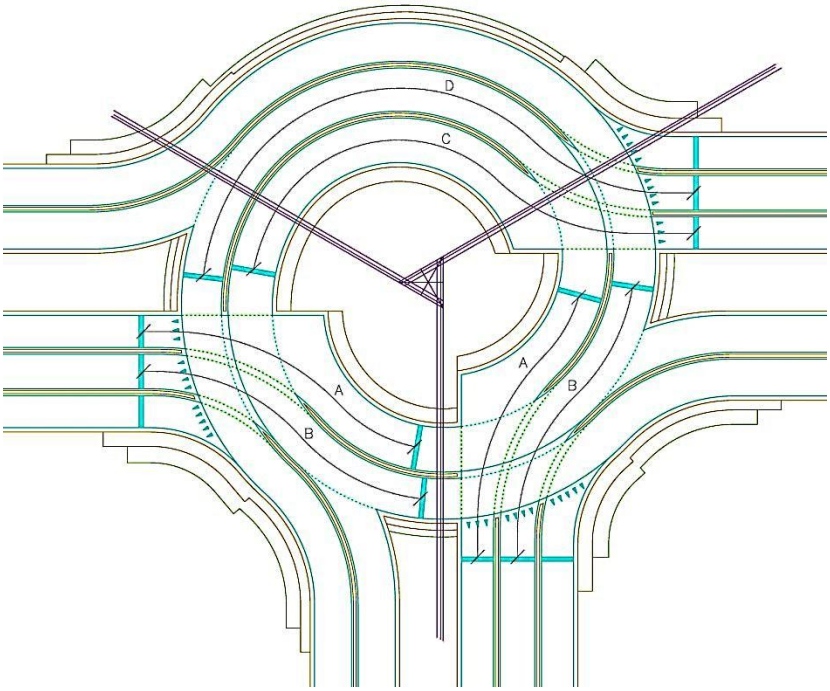


Figure D-19 Indication of the length of circulatory road segments, input for the analytical approach

Table D-10 Values for A, B, C and D for the star roundabout

Inscribed radius	A	B	C	D
12 m	31 m	33 m	54 m	64 m
20 m	41 m	42 m	76 m	84 m

D.7. Partial turbo circle

This section deals with the design of the partial turbo circle [43]. Firstly, the turboblock will be designed based on section D.1. Secondly, the partial turbo circle will be finished based on sections D.2 and D.3. Finally, the space requirement of the partial turbo circle and some important dimensions will be stated. The partial turbo circle will be designed with two values for the inscribed diameter: 12 m and 20 m.

[43] *The partial turbo circle was created from the desire to adjust the rotor roundabout, such that it is suitable for a two-phase traffic control. The adjustment consisted of removing the choice lanes (see the main report).*

D.7.1. Turboblock

The partial turbo circle and the rotor roundabout have nearly identical turboblocks. The only major difference is the extent to which the inner circulatory roadway has to 'fan out'. While on the rotor roundabout the inner circulatory roadway needs to 'fan out' by the width of one roadway over an angle of 90 degrees, on the partial turbo circle the inner circulatory roadway needs to 'fan out' by the width of two roadways over an angle of 90 degrees.

Circulatory roadway narrowing

Inner roadway: the inner roadway on the partial turbo circle is identical to the inner roadway on the rotor roundabout, except for the fact that it 'fans out' to a larger extent. It has an inscribed radius of 12 m, a width of 5.30 m (not narrowing) and a truck apron of 1.50 m wide.
Middle roadway: the middle roadway has an inscribed radius of 17.60 m and a width of 4.60 m. It is identical to the middle roadway on the rotor roundabout, except for the fact that it does not narrow on the partial turbo circle, because it does not connect to the inner roadway.
Outer roadway: the outer roadway has an inscribed radius of 22.50 m and a width of 4.20 m. On the partial turbo circle – contrary to the rotor roundabout – it narrows from 5.05 m [44] to 4.20 m.

The results of the calculations by means of Equation D-1 are shown in Table D-11 and Table D-12. Figure D-20 shows a section of the circulatory roadways at the start of an inner roadway, for the partial turbo circle with an inscribed radius of 12 m. The roadway narrowing is illustrated by the turboblock in Figure D-21 and the detail in Figure D-22.

Table D-11 Roadway narrowing of the partial turbo circle with inscribed radius 12 m

Roadway		*Radius*		*Start width*		*End width*		
Truck apron		10.50 m		1.50 m		1.50 m		
Inner	R1	12.00 m	WS1	5.30 m	WE1	5.30 m		
Middle	R2	17.60 m	WS2	4.60 m	WE2	4.60 m	A	
Outer	R3	22.50 m	WS3	5.05 m	WE3	4.20 m	B	0.85 m
Truck apron	R4	26.70 m		0.70 m		0.70 m		
Hard shoulder		27.40 m		0.70 m		0.70 m		

Table D-12 Roadway narrowing of the partial turbo circle with inscribed radius 20 m

Roadway		*Radius*		*Start width*		*End width*		
Truck apron		19.20 m		0.80 m		0.80 m		
Inner	R1	20.00 m	WS1	4.40 m	WE1	4.40 m		
Middle	R2	24.70 m	WS2	4.00 m	WE2	4.00 m	A	
Outer	R3	29.00 m	WS3	4.40 m	WE3	3.80 m	B	0.60 m
Truck apron	R4	32.80 m		0.60 m		0.60 m		
Hard shoulder		33.40 m		0.60 m		0.60 m		

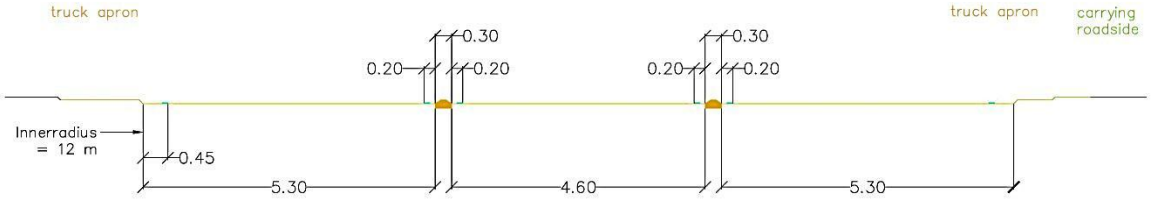


Figure D-20 Section of the partial turbo circle with inscribed radius 12 m

[44] *The outer roadway connects at the start to the inner roadway; the inner roadway is 0.25 m wider than the outer roadway because it contains a hard shoulder.*

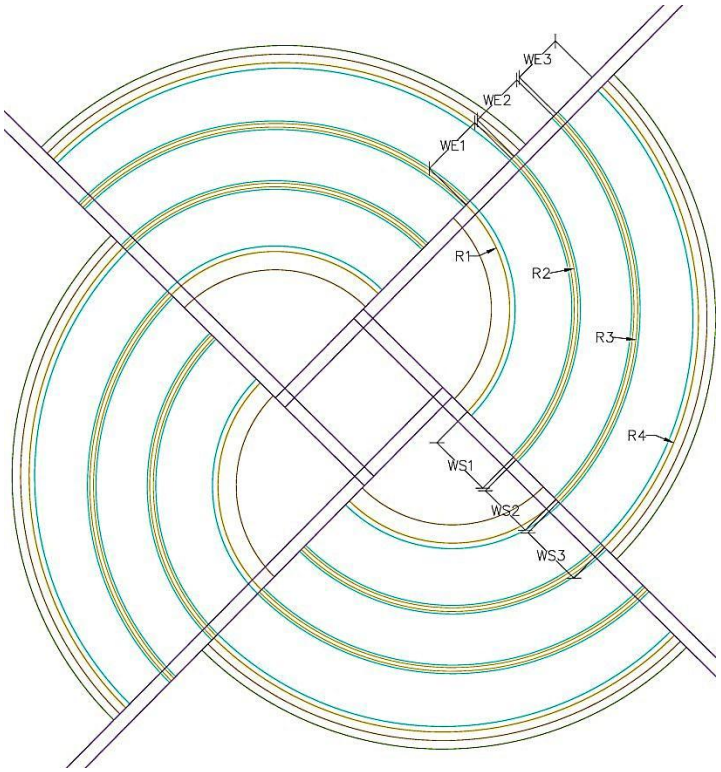


Figure D-21 Turboblock of the partial turbo circle

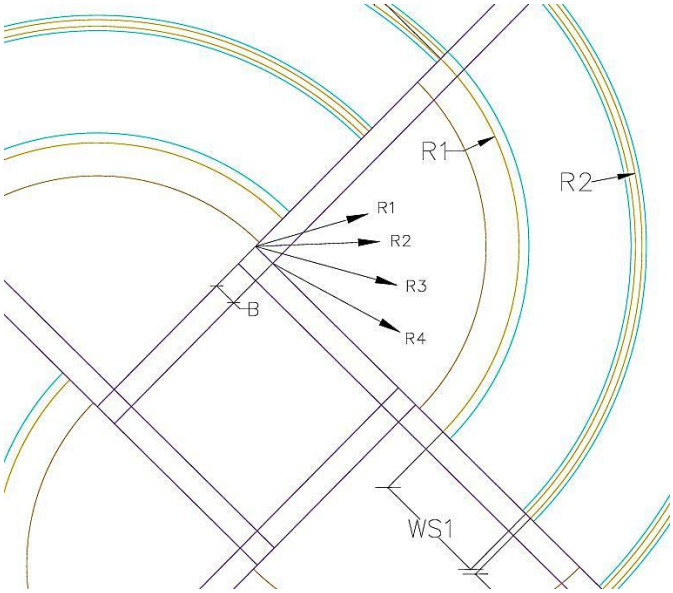


Figure D-22 Detail of the turboblock of the partial turbo circle

D.7.2. Circle design

The turboblock is the base for the circle design. The entrance and exit legs need to be connected to the circulatory roadways in the turboblock, by means of the curvature described in section D.2. Figure D-23 and Figure D-24 show the designs of the partial turbo circle with inscribed radii of 12 m and 20 m.

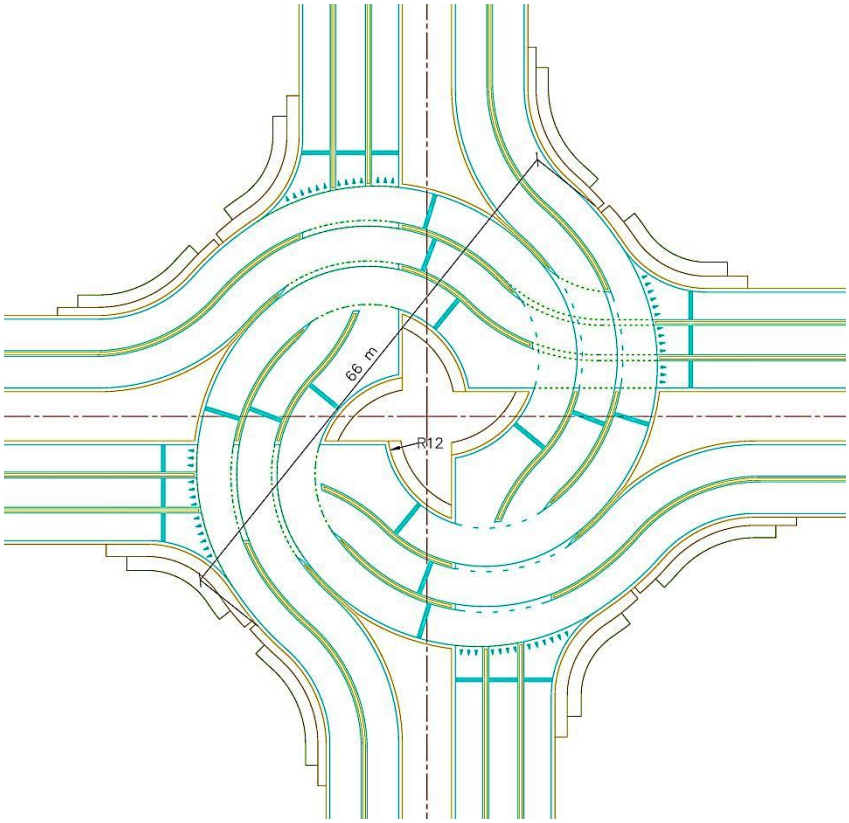


Figure D-23 The design of the partial turbo roundabout with an inscribed radius of 12 m

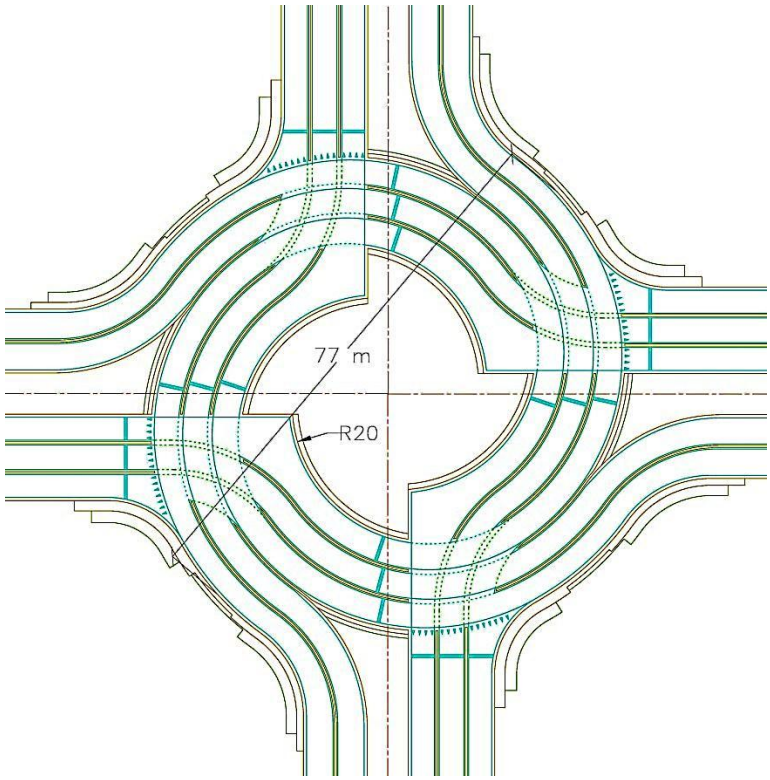


Figure D-24 The design of the partial turbo roundabout with an inscribed radius of 20 m

D.7.3. Space requirement

Figure D-23 and Figure D-24 show the outer diameters of both partial turbo circles, Table D-13 presents an overview. This table will be used in later stages of the project.

Table D-13 Overview of the inscribed and outer diameters of the partial turbo circle

	Inscribed radius	Outer radius
Partial turbo circle	12 m	66 m
Partial turbo circle	20 m	77 m

D.8. Four-leg turbo circle

This section deals with the design of the four-leg turbo circle. Firstly, the turboblock will be designed based on section D.1. Secondly, the turbo circle will be finished based on sections D.2 and D.3. Finally, the space requirement of the turbo circle will be stated. The turbo circle will be designed with three values for the inscribed diameter: 12 m, 20 m and 30 m.

D.8.1. Turboblock

The algorithm for designing the turboblock of the turbo circle is similar to that of the rotor roundabout. The only major difference is the fact that every roadway on the turbo circle contains two lanes. That means that two trucks might accelerate next to each other onto the turbo circle; one on the right lane and one on the left. If those vehicles comply to the dimensions of the normative 22-m vehicle, the truck on the left lane can use the truck apron, but the truck on the right lane cannot. For this reason, the lanes on the turbo circle should be designed to accommodate a 22-m vehicle.

The results of the calculations by means of Equation D-1 are shown in Table D-14, Table D-15 and Table D-16. Figure D-25 shows a section of the circulatory roadways at the start of an inner roadway, for the turbo circle with an inscribed radius of 12 m. The roadway narrowing is illustrated by the turboblock in Figure D-26 and the detail in Figure D-27.

Table D-14 Roadway narrowing of the turbo circle with inscribed radius 12 m

Roadway		*Radius*		*Start width*		*End width*		
Truck apron		10.50 m		1.50 m		1.50 m		
Inner 1st	R1	12.00 m	WS1	5.30 m	WE1	5.30 m		
Inner 2nd	R2	17.30 m	WS2	5.40 m	WE2	5.40 m		
Middle 3rd	R3	23.00 m	WS3	5.05 m	WE3	4.80 m	A	0.25 m
Middle 4th	R4	27.80 m	WS4	5.40 m	WE4	4.50 m	B	0.90 m
Outer 5th	R5	32.60 m	WS5	4.80 m	WE5	4.20 m	C	0.60 m
Outer 6th	R6	36.80 m	WS6	4.75 m	WE6	4.00 m	D	0.75 m
Hard shoulder	R7	40.80 m		0.60 m		0.60 m		

Table D-15 Roadway narrowing of the turbo circle with inscribed radius 20 m

Roadway		*Radius*		*Start width*		*End width*		
Truck apron		19.00 m		1.00 m		1.00 m		
Inner 1st	R1	20.00 m	WS1	5.10 m	WE1	5.10 m		
Inner 2nd	R2	25.10 m	WS2	4.70 m	WE2	4.70 m		
Middle 3rd	R3	30.10 m	WS3	4.85 m	WE3	4.30 m	A	0.55 m
Middle 4th	R4	34.40 m	WS4	4.70 m	WE4	4.10 m	B	0.60 m
Outer 5th	R5	38.80 m	WS5	4.30 m	WE5	4.00 m	C	0.30 m
Outer 6th	R6	42.80 m	WS6	4.35 m	WE6	3.80 m	D	0.55 m
Hard shoulder	R7	46.60m		0.50 m		0.50 m		

Table D-16 Roadway narrowing of the turbo circle with inscribed radius 30 m

Roadway		*Radius*		*Start width*		*End width*		
Truck apron		0.60 m		0.60 m		0.60 m		
Inner 1st	R1	30.00 m	WS1	4.40 m	WE1	4.40 m		
Inner 2nd	R2	34.40 m	WS2	4.10 m	WE2	4.10 m		
Middle 3rd	R3	38.80 m	WS3	4.15 m	WE3	4.00 m	A	0.15 m
Middle 4th	R4	42.80 m	WS4	4.10 m	WE4	3.80 m	B	0.30 m
Outer 5th	R5	46.90 m	WS5	4.00 m	WE5	3.70 m	C	0.30 m
Outer 6th	R6	50.60 m	WS6	4.05 m	WE6	3.70 m	D	0.55 m
Hard shoulder	R7	54.30 m		0.30 m		0.30 m		

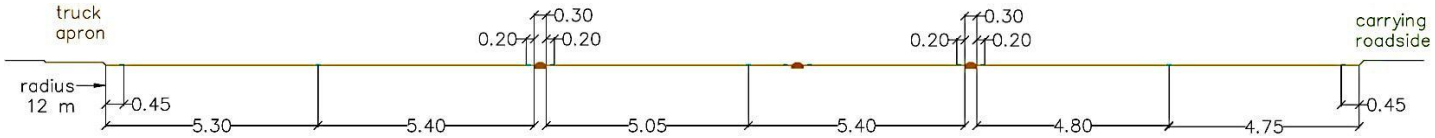


Figure D-25 Section of the turbo circle with inscribed radius 12 m [45]

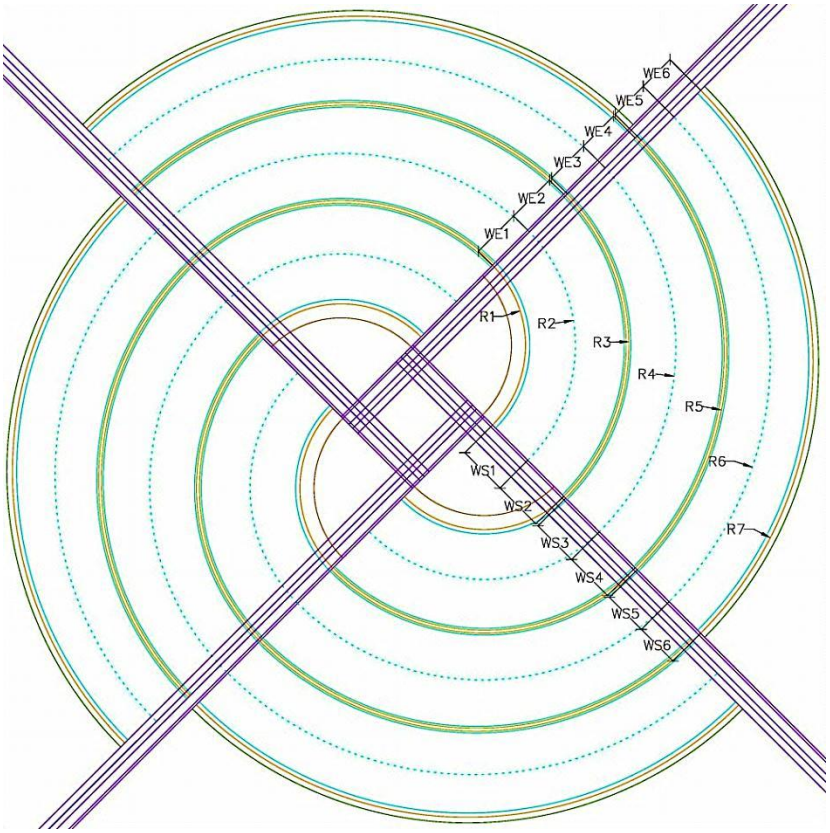


Figure D-26 Turboblock of the turbo circle

[45] *The drawing contains a roadway divider on the fourth lane. Of course, it does not belong there. There reader is begged pardon for this deficiency.*

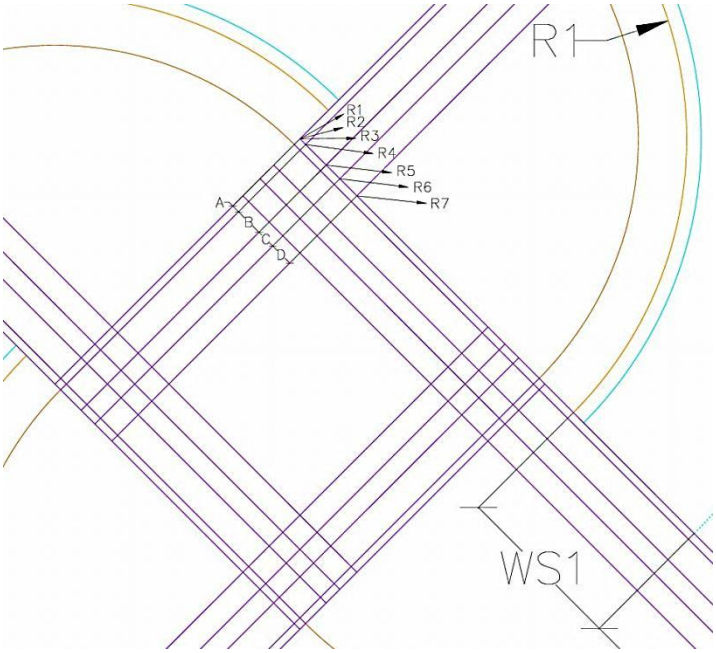


Figure D-27 Detail of the turboblock of the turbo circle

D.8.2. Circle design

The turboblock is the base for the circle design. The entrance and exit legs need to be connected to the circulatory roadways in the turboblock, by means of the curvature described in section D.2. Figure D-28, Figure D-29 and Figure D-30 show the designs of the turbo circle with inscribed radii of 12 m, 20 m and 30 m.

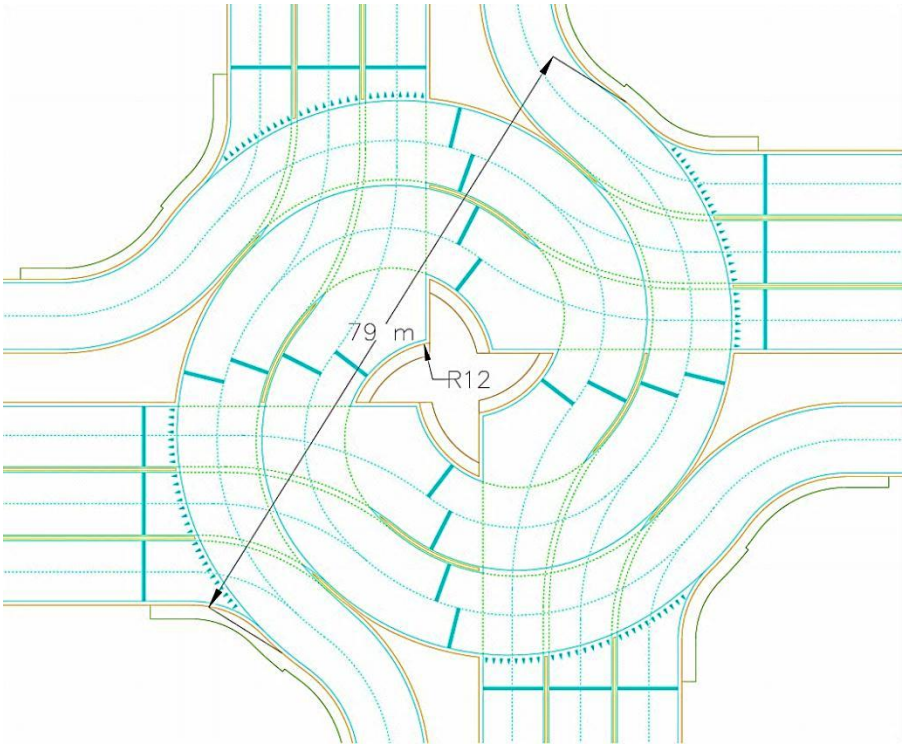


Figure D-28 The design of the turbo circle with an inscribed radius of 12 m

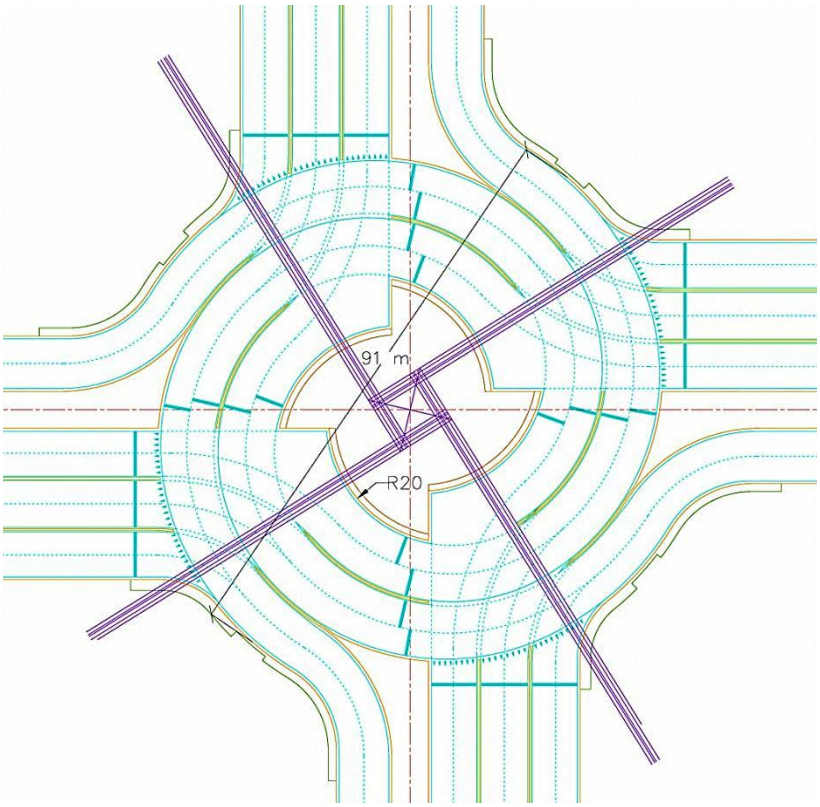


Figure D-29 The design of the turbo circle with an inscribed radius of 20 m

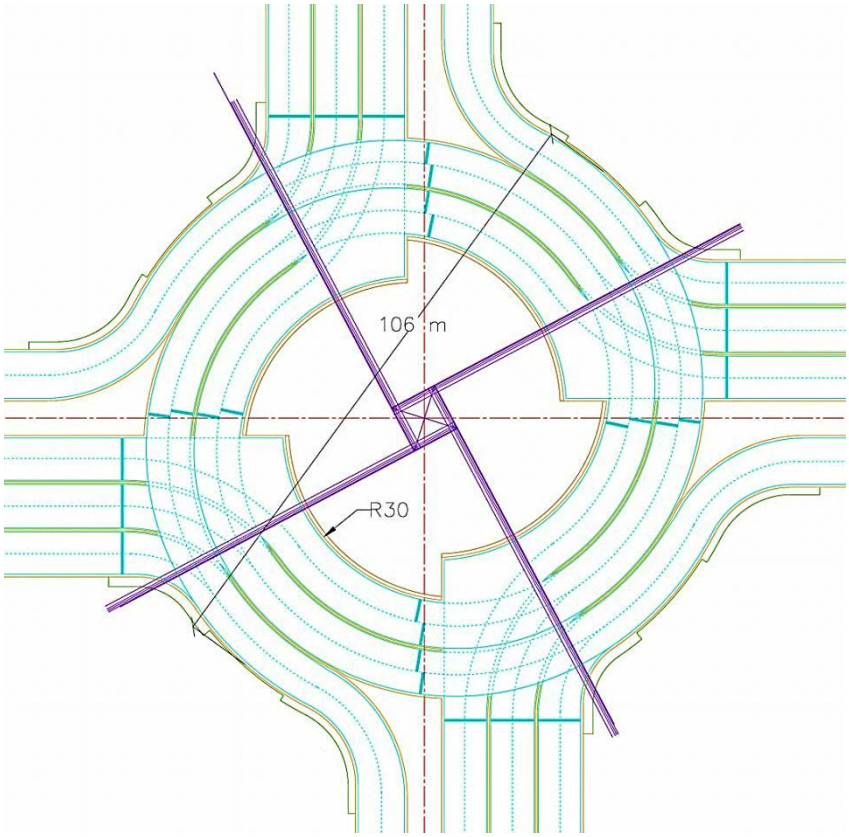


Figure D-30 The design of the turbo circle with an inscribed radius of 30 m

D.8.3. Space requirement

Figure D-28, Figure D-29 and Figure D-30 show the outer diameters of the turbo circles, Table D-17 presents an overview. This table will be used in later stages of the project.

Table D-17 Overview of the inscribed and outer diameters of the turbo circle

	Inscribed radius	Outer radius
Turbo circle	12 m	79 m
Turbo circle	20 m	91 m
Turbo circle	30 m	106 m

D.8.4. Length of the segments

In the development of the most suitable traffic control (see appendix H: VRIGen model development), the length of some road segments on the turbo circles are necessary input for the clearance time calculation. The road segments are indicated in Figure D-31. Table D-18 quantifies the lengths for the turbo circles with inscribed diameters of 12 m, 20 m and 30 m.

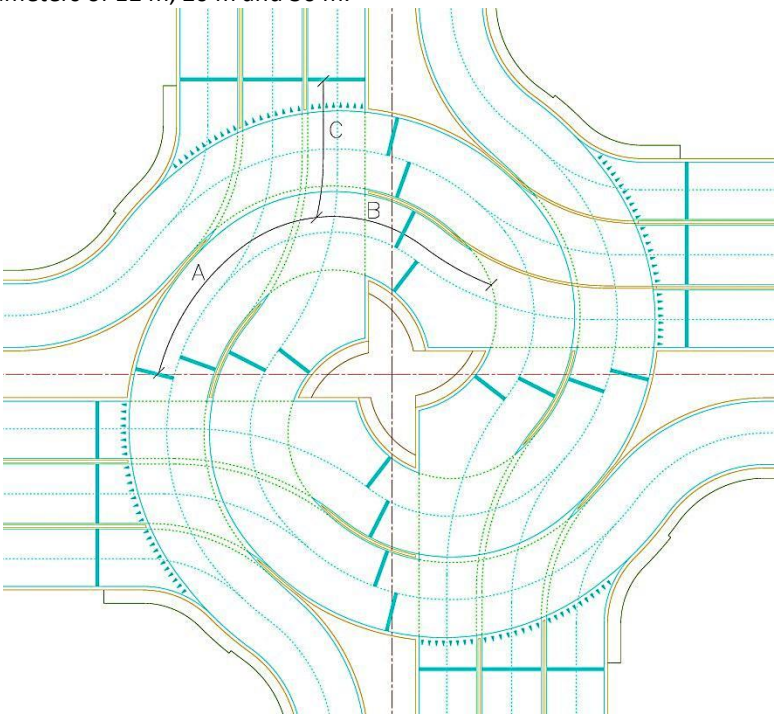


Figure D-31 Indication of the length of circulatory road segments, input for the analytical approach

Table D-18 Values for A and B for the turbo circle

Inscribed radius	A	B	C
12 m	31 m	14 m	15 m
20 m	43 m	36 m	15 m
30 m	55 m	50 m	15 m

D.9. Three-leg turbo circle

This section deals with the design of the three-leg turbo circle. Firstly, the turboblock will be designed based on section D.1. Secondly, the three-leg turbo circle will be finished based on sections D.2 and D.3. Finally, the space requirement of the three-leg turbo circle will be stated. The three-leg turbo circle will be designed with three values for the inscribed diameter: 12 m, 20 m and 30 m.

D.9.1. Turboblock

The algorithm for designing the turboblock of the three-leg turbo circle is similar to that of the star roundabout. The only major difference is the fact that every roadway on the three-leg turbo circle contains two lanes. The repercussions for the three-leg turbo circle are the same as those for the four-leg turbo circle: the lanes on the three-leg turbo circle should be designed to accommodate a 22-m vehicle.

The results of the calculations by means of Equation D-1 are shown in Table D-19, Table D-20 and Table D-21. Figure D-32 shows a section of the circulatory roadways at the start of an inner roadway, for the three-leg turbo circle with an inscribed radius of 12 m. The roadway narrowing is illustrated by the turboblock in Figure D-33 and the detail in Figure D-34.

Table D-19 Roadway narrowing of the three-leg turbo circle with inscribed radius 12 m

Roadway		*Radius*		*Start width*		*End width*		
Truck apron		10.50 m		1.50 m		1.50 m		
1st lane	R1	12.00 m	WS1	5.30 m	WE1	5.30 m		
2nd lane	R2	17.30 m	WS2	4.60 m	WE2	4.60 m	A	
3rd lane	R3	22.20 m	WS3	5.05 m	WE3	4.20 m	B	0.57 m
4th lane	R4	26.68 m	WS4	4.85 m	WE4	4.00 m	C	0.57 m
Hard shoulder		31.56 m		0.60 m		0.60 m		

Table D-20 Roadway narrowing of the three-leg turbo circle with inscribed radius 20 m

Roadway		*Radius*		*Start width*		*End width*		
Truck apron		19.20 m		0.80 m		0.80 m		
1st lane	R1	20.00 m	WS1	4.40 m	WE1	4.40 m		
2nd lane	R2	24.40 m	WS2	4.10 m	WE2	4.10 m		
3rd lane	R3	28.80 m	WS3	4.15 m	WE3	3.90 m	A	0.17 m
4th lane	R4	32.78 m	WS4	4.35 m	WE4	3.70 m	B	0.43 m
Hard shoulder		36.90 m		0.50 m		0.50 m		

Table D-21 Roadway narrowing of the three-leg turbo circle with inscribed radius 30 m

Roadway		*Radius*		*Start width*		*End width*		
Truck apron		29.40 m		0.60 m		0.60 m		
1st lane	R1	30.00 m	WS1	3.80 m	WE1	3.80 m		
2nd lane	R2	33.80 m	WS2	3.70 m	WE2	3.70 m		
3rd lane	R3	37.80 m	WS3	3.55 m	WE3	3.55 m	A	0.00 m
4th lane	R4	41.35 m	WS4	3.95 m	WE4	3.50 m	B	0.30 m
Hard shoulder		45.40 m		0.40 m		0.40 m		

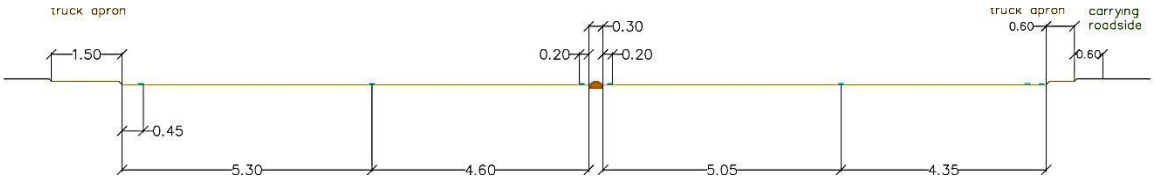


Figure D-32 Section of the three-leg turbo circle with inscribed radius 12 m

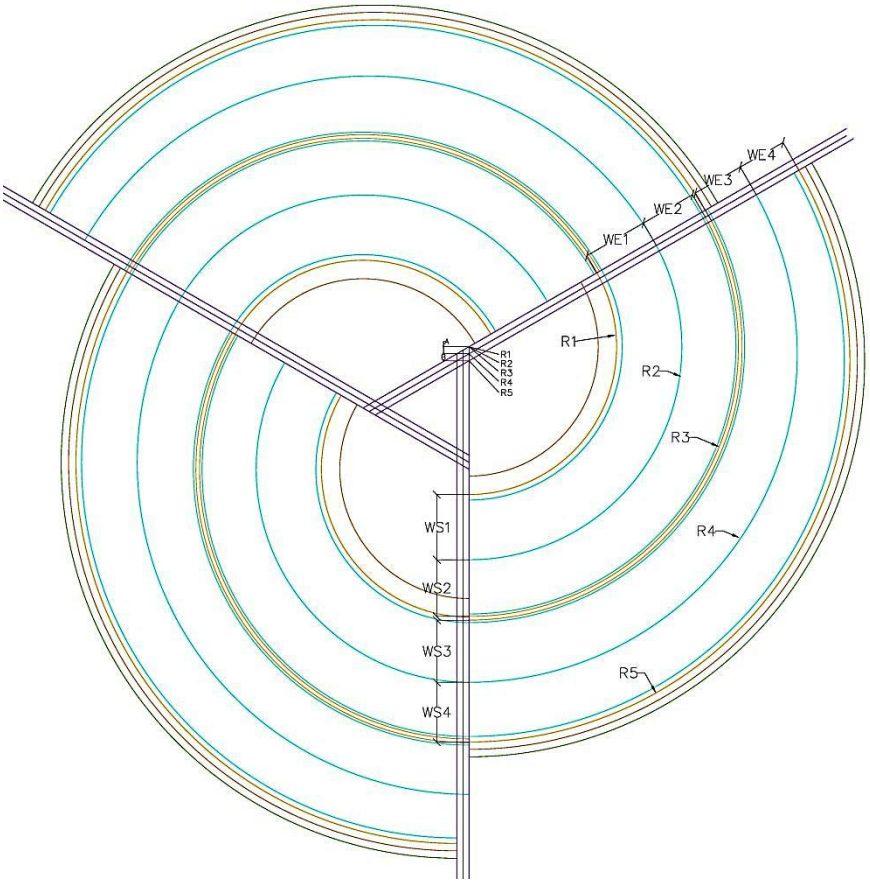


Figure D-33 Turboblock of the three-leg turbo circle

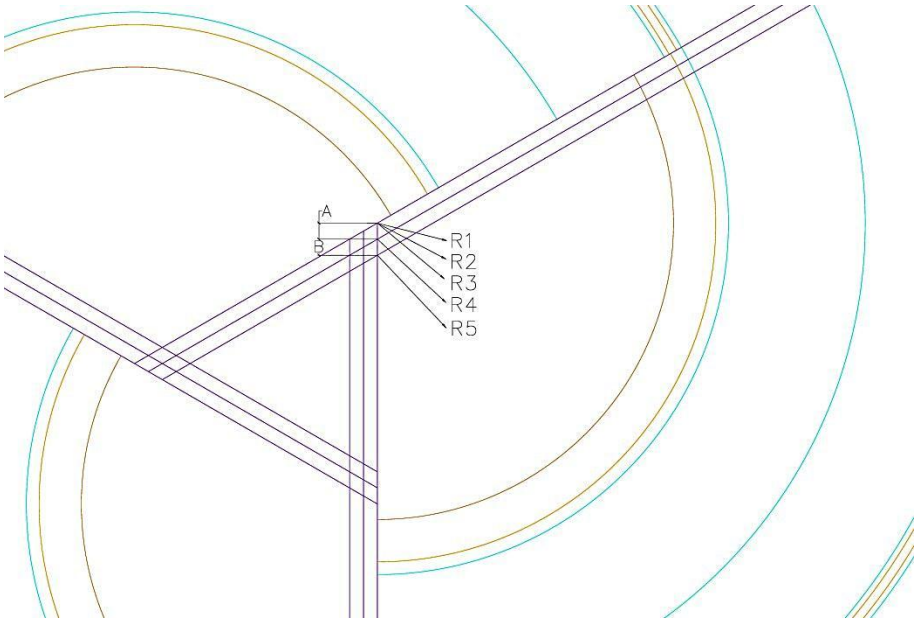


Figure D-34 Detail of the turboblock of the three-leg turbo circle

D.9.2. Circle design

The turboblock is the base for the circle design. The entrance and exit legs need to be connected to the circulatory roadways in the turboblock, by means of the curvature described in section D.2. Figure D-35, Figure D-36 and Figure D-37 show the designs of the three-leg turbo circle with inscribed radii of 12 m, 20 m and 30 m.

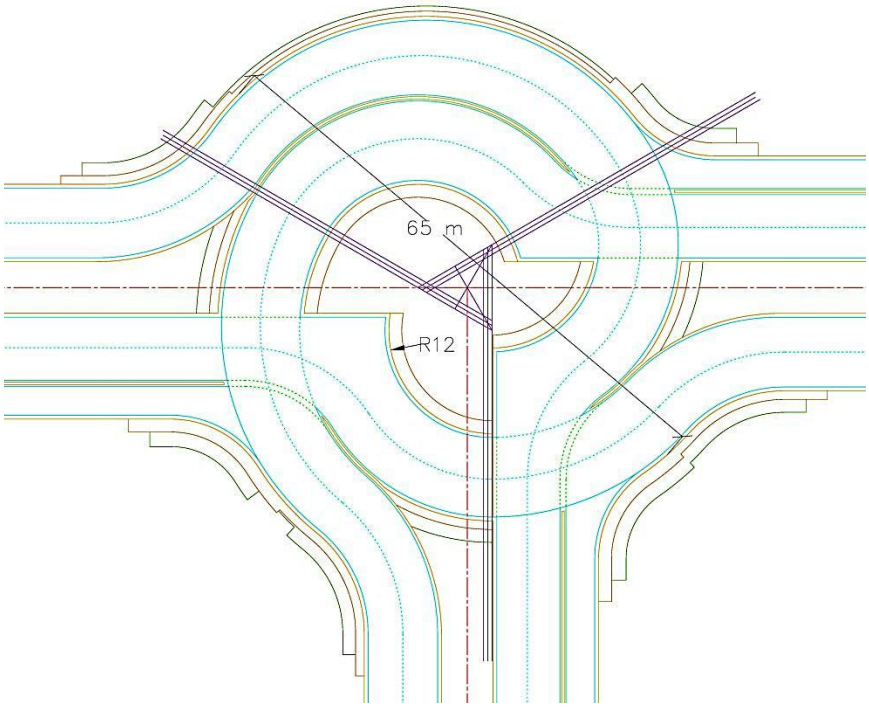


Figure D-35 The design of the three-leg turbo circle with an inscribed radius of 12 m

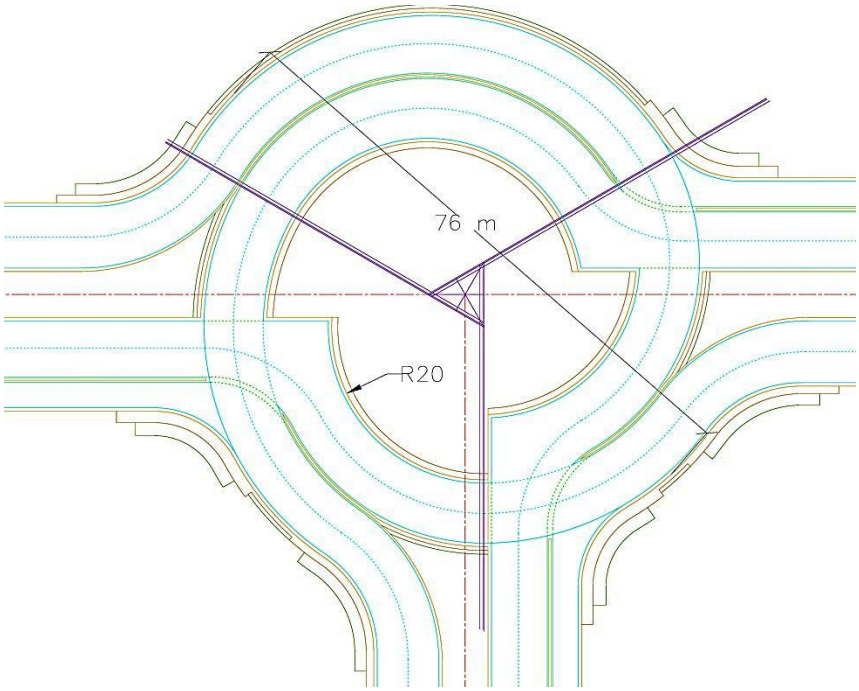


Figure D-36 The design of the three-leg turbo circle with an inscribed radius of 20 m

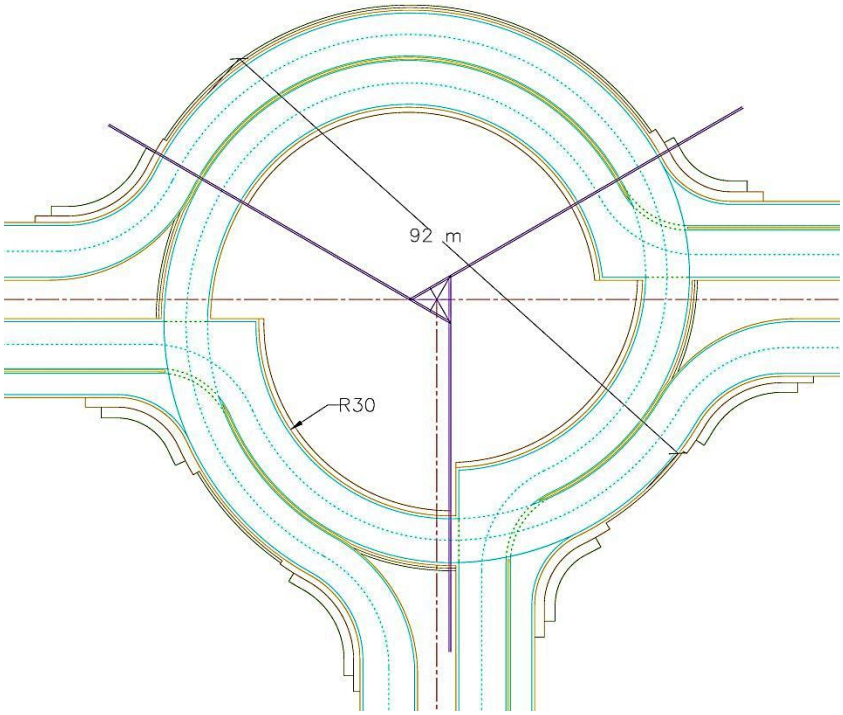


Figure D-37 The design of the three-leg turbo circle with an inscribed radius of 30 m

D.9.3. Space requirement

Figure D-35, Figure D-36 and Figure D-37 show the outer diameters of the three-leg turbo circles, Table D-22 presents an overview. This table will be used in later stages of the project.

Table D-22 Overview of the inscribed and outer diameters of the three-leg turbo circle

	Inscribed radius	Outer radius
Three-leg turbo circle	12 m	65 m
Three-leg turbo circle	20 m	76 m
Three-leg turbo circle	30 m	92 m

Appendix E: Clearance time calculation

An input parameter for the analytical approach is the clearance time of the conflicts consisting of a main signal (e.g. 02) and the conflicting interception signal (e.g. 65). An input parameter for VRIGen is a conflict matrix with all clearance times on the intersection. This appendix explains how the clearance time can be calculated.

In the first section, the general method by Muller *et al.* (2004) will be addressed. The second section applies the method to the rotor roundabout with an inscribed radius of 12 m; all clearance times on that intersection appear to be 0 s. The appendix concludes that this holds for all intersections invoked in this project.

E.1.General method

Clearance times can be calculated by means of the method of Muller *et al.* (2004). The method is represented by the following equations, it is based on the definitions of entrance and exit distance illustrated by Figure E-1.

$$t_{clearance} = t_{exit} - t_{entrance}$$

Equation E-1

$$t_{exit} = \frac{s_{exit}}{v_{exit}}$$

Equation E-2

$$t_{entrance} = \begin{cases} t_r + \sqrt{\dfrac{2 * s_{entrance}}{a_{acc} - a_{dec}}} & if \ \ s_{entrance} \leq s_{critical} \\ t_r + \dfrac{s_{entrance}}{v_{max}} + \dfrac{v_{max}}{2 * (a_{acc} - a_{dec})} & if \ \ s_{entrance} \geq s_{critical} \end{cases}$$

Equation E-3

$$s_{critical} = \frac{v_{max}^2}{2 * (a_{acc} - a_{dec})}$$

Equation E-4

where:

$t_{clearance}$	= clearance time between two conflicting streams (indicated as *conflict group*) [s]
t_{exit}	= exit time; the first stream needs the exit time to clear the conflict area [s]
$t_{entrance}$	= entrance time; in which a vehicle in the second stream can reach the conflict area [s]
s_{exit}	= distance that a vehicle from the first stream has to cover in order to clear the conflict area, see Figure E-1
v_{exit}	= speed at which a vehicle from the first stream clears the conflict area [m/s]
t_r	= reaction time [s]
$s_{entrance}$	= the distance between the stop line of the second stream and the closest point of the conflict area [m]
a_{acc}	= acceleration rate [m/s^2]
a_{dec}	= deceleration rate [m/s^2]
v_{max}	= the maximum speed with which a vehicle enters the intersection [m/s]
$s_{critical}$	= critical distance taking into account the influence of the speed limit on the intersection

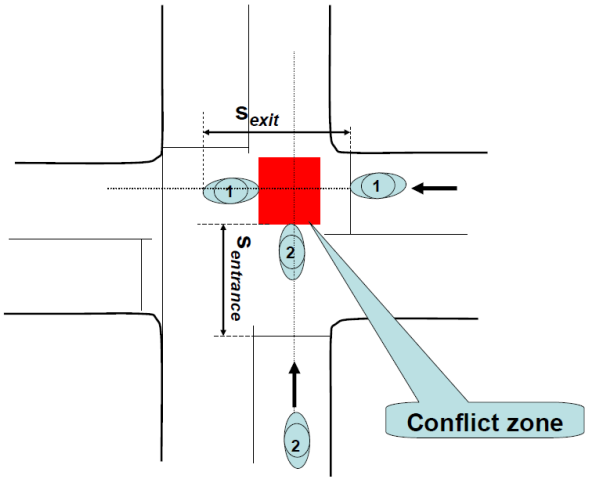


Figure E-1 The clearance time calculation is based the geometrical design of the intersection (taken from Muller *et al.*, 2004)

In Muller *et al.* (2004), a calibration was invoked with respect to the value $a_{acc} - a_{dec}$ which can be seen as a measure of driver aggressiveness. The calibration was performed by means of data gathered on intersections in the Dutch municipalities of Haarlem and Delft and yielded a value of 2.4 m/s^2. The authors note that this value is well below the capacities of the present-day vehicles and human comfort and suggest that in investigations lacking calibration, a value in the range of 2.5 to 3.0 m/s^2 should be applied. In this project, this recommendation will be obeyed.

With respect to the other variables: v_{max} is bound to the prevailing speed limit on the intersection. For safety reasons, v_{exit} should represent the velocity of a slow vehicle leaving the conflict area. The reaction time t_r will be estimated to be one second, as estimated in appendix F (Simplified acceleration model).

E.2.Application to the rotor roundabout

Figure E-2 illustrates the conflict areas on the rotor roundabout, together with the stop lines joining the main and interception signals. The conflict area 12/63 is most significant, because this conflict (first 12 green, then 63 green) has the largest exit distance and a small entrance distance, and therefore yields the largest clearance time (see Equation E-1). This conflict determines the clearance time 11/62 in VRIGen, because signals 10, 11 and 12 are together represented by 11 and 62 and 63 are represented together by 62 (see the previous section).

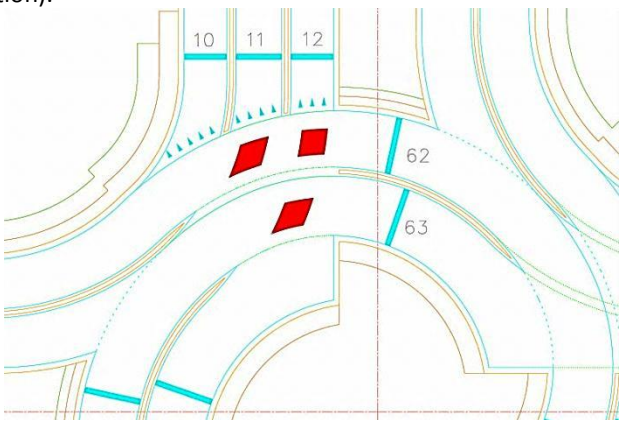


Figure E-2 Conflict areas between the northern leg and the circulatory roadways

The distance from the stop line joining direction 12 and the conflict area is 11 m, this is the exit distance. The distance from the stop line joining direction 63 and the conflict area is 7 m, this is the entrance distance. Assuming:

v_{exit} = 25 km/h
t_r = 1 s
$a_{acc} - a_{dec}$ = 2.5 m/s^2
v_{max} = 50 km/h

yields:

t_{exit} = 1.6 s
$t_{entrance}$ = 3.4 s
$t_{clearance}$ = -1.8 s

The (negative) clearance time is set to zero, for safety considerations (Muller *et al.*, 2004). This calculation also counts for the other three conflicts on the roundabout. Applying Muller *et al.* (2004) to the rotor roundabout with inscribed radii of 12 and 20 m, the star roundabout with inscribed radii of 12 and 20 m, the (partial) turbo circle and the three-leg turbo circle with any inscribed radius yields the same clearance times. The cause for this is the choice for the location of the stop lines, motivated by means of field observations and legislation in section D.3. There, the distance between the stop line of any stream and the roadside of any conflicting stream is chosen to be 4 m.

Appendix F: Simplified acceleration model

Section 3.2.2 describes the analytical approach as a means of calculating the capacity of a signalized turbo roundabout analytically. One of the input parameters for this method is an acceleration model, by which the first vehicle accelerating from standing still at a stop line can be modelled. This appendix explains the details of the acceleration model.

The model is called 'simplified', because it does not take into account the cognitive-psychological influence of the interception signals. The next section explains that the perception of the interception signals might influence the acceleration behaviour, and therefore the saturation flow. It also explains that extensive research is necessary, in order to model this influence properly. The acceleration model is 'simplified', meaning that the extensive research has not been carried out; several assumptions are to be made and defended.

F.1. Description of acceleration behaviour

This section describes the basic behaviour of a vehicle accelerating from standing still at a stop line to its preferred speed.

F.1.1. Waiting for the red light

The simplified model in this appendix considers a vehicle approaching a traffic signal indicating red. The red phase does not end until the vehicle has stopped in front of the stop line. The time interval the vehicle stands still influences the attention level of the driver. For instance, if the red phase persists quite long (longer than, say, one minute) the driver will start to pay attention at other objects in his vicinity than the traffic signal. In that case, his reaction time increases. On the other hand, a hurried driver may start yelling at the traffic signal and intends to accelerate as soon as the light turns green. In that case, his reaction time will be quite short.

This simplified model applies one single value for the reaction time. This value is set to one second, based on extensive field measurements in various parts of The Netherlands (Grontmij, 2001). This means that in this model, the time interval between start green of the signal and the vehicle starting to accelerate, is one second.

F.1.2. Accelerating from standing still

The rate of acceleration of a vehicle highly depends on a number of factors. A few examples are: characteristics of the driver (age, gender, physical condition, mood, aggressiveness, etc), the characteristics of the car (age, engine power, weight, etc.), the slope of the road segment on which the vehicle accelerates, etc. Consequentially, the acceleration is also highly variable.

This simplified acceleration model again applies one single value for the acceleration. This values is based on the same source (Grontmij, 2001) and is set to 2.5 m/s^2. This value is assumed to be constant over time. Logically, the acceleration rate decreases as the vehicle speed increases. However, in this project the value is taken to be constant because in the calculation of the phase overlap, the acceleration distance (the distance between main signal and interception signal) is quite short. On that short distance, the driver accelerates to a speed of ca. 30 km/h, see the next sections. For such low speeds, the acceleration rates can be chosen a constant value, without reducing the reliability of the acceleration model, presumably.

F.1.3. Perceiving the interception signal

The driver accelerates from the main signal on the entrance leg of the turbo roundabout to the interception signal of one of the circulatory roadways on the turbo roundabout. In the case of a clockwise leg-by-leg control with phase overlap, the interception signal still shows red at the moment the main signal turns green. After a certain time interval (equal to the phase overlap), the interception signal shows green. Presumably, the first driver accelerating from the main signal focusses his attention on the interception signal hoping it will turn green very soon. Therefore, the time interval between start green of the interception signal and the driver's decision to proceed accelerating (called the perception time) is probably shorter than the one second reaction time explained in the previous section. There are no field measurements available on this perception time. Therefore, the quantification of the perception time will be based on expert judgment: half a second.

Of course, this value also differs over drivers. Moreover, drivers who are familiar with the intersection will notice that the interception signal will turn green shortly after the main signal has turned green. From psychological literature (Zimbardo *et al.*, 2007), the conclusion can be drawn that people who are expecting the green light, their perception time is substantially smaller than the perception time of people without this expectation.

F.1.4. Deciding to accelerate or decelerate

After the perception of the green interception signal, the driver will proceed to accelerate. This model assumes that the value of the acceleration rate is again 2.5 m/s^2. If the driver perceives a red signal, he will decide to decelerate. The deceleration rate differs over drivers and environmental conditions. Based on Grontmij (2001), the deceleration rate is assumed to be 2.0 m/s^2. In that case, the vehicle instantly changes from the acceleration phase to the deceleration phase. Consequentially, the velocity-time diagram of the vehicle shows a triangular shape.

F.2. Summary: acceleration behaviour

All previous remarks can be summaried as follows:

- Vehicle stops in front of the stop line;
- Main signal turns green;
- Vehicle starts to accelerate after one second of reaction time;
- Vehicle accelerates at a constant rate of 2.5 m/s^2 up to a maximum speed of 40 km/h;
- Interception signal turns green;
- Driver perceives the interception signal after a 0.5 s of perception time;
- Vehicle proceeds acceleration at 2.5 m/s^2 or starts decelerating at 2.0 m/s^2;
- If decelerating, the vehicle stops in front of the stop line joining the interception signal.

F.3. Constraint of the acceleration length

By means of this simplified acceleration model, the duration of the acceleration phase t_x can be calculated, such that the first vehicle only accelerates or decelerates. The time t_x at which the driver quits accelerating and starts decelerating, depends on the length of the road stretch between the stop lines joining the main signal and the interception signal. For instance, if the length between both signals is 25 m, the vehicle accelerates at 2.5 m/s^2 over the first 12.2 m in 3.1 s. Then the vehicle decelerates over the remaining 12.8 m in 3.6 s to standstill. Effectively, t_x is equal to 3.1 s plus the reaction time (one second) minus the perception time (a half a second).

Equation F-1, Equation F-2 and Equation F-3 represent the simplified acceleration model in mathematical expressions of the acceleration-time diagram, the velocity-time diagram and the distance-time diagram. Figure F-1 shows the diagrams graphically.

$$a = \begin{cases} 2.5 \; for \; t < t_x \\ 2.0 \; for \; t > t_x \end{cases}$$

Equation F-1

$$v = \begin{cases} 2.5t \; for \; t < t_x \\ -2t \; for \; t > t_x \end{cases}$$

Equation F-2

$$s = \begin{cases} 1.25t^2 & for \; t < t_x \\ -t^2 + 4.5t_x \; for \; t > t_x \end{cases}$$

Equation F-3

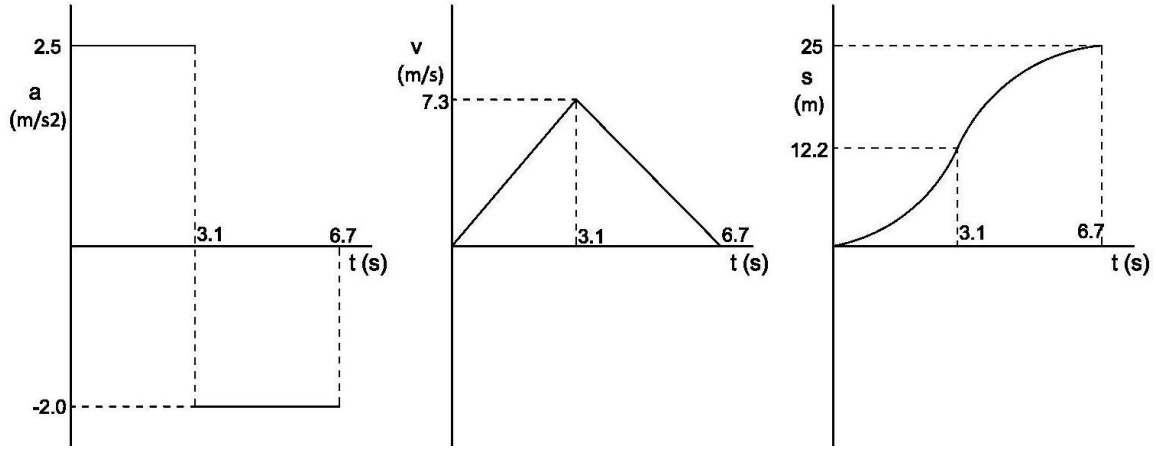


Figure F-1 Acceleration-time, velocity-time and distance-time diagrams for the example

F.4. Maximum green phase overlap

As explained in the main report, the maximum green phase overlap is the time interval in which the legs in two subsequent phase of the leg-by-leg control can have green simultaneously. The traffic control should be designed, such that the maximum phase overlap is maximized. The simplified acceleration model has shown that the maximum value depends on the geometry of the roundabout (i.e. the length over which the first vehicle accelerates). In order to prevent the vehicle from entering the deceleration phase, the interception signal should turn green t_x seconds after the main signal has turned green. The maximum green phase overlap can be calculated based on t_x [46], adjusted for the reaction time, perception time and yellow time of the predecessor stage (3 s). Table F-1 shows some values for the phase overlap, dependent on the acceleration length. These values are used as input for the analytical approach in section 4.2.

[46] *Assuming that the clearance time between the end green of the leg in the predecessor phase and the start green of the interception signal is zero. Appendix K (VRIGen model development) will show that this is indeed the case.*

Table F-1 Acceleration length and maximum possible green phase overlap [47]

	Acc. Length	t_x	Phase overlap
Example	25 m	3.1 s	0.6 s
Rotor roundabout, 12 m	29 m	3.3 s	0.8 s
Rotor roundabout, 20 m	38 m	3.8 s	1.3 s
Star roundabout, 12 m, E-S and S-W	31 m	3.4 s	0.9 s
Star roundabout, 12 m, W-E	54 m	4.5 s	2.0 s
Star roundabout, 20 m, E-S and S-W	41 m	3.9 s	1.4 s
Star roundabout, 20 m, W-E	76 m	6.6 s	4.1 s

F.5.Sensitivity analysis

The sensitivity analysis consists of varying the acceleration and deceleration rates, and check the effect on the phase overlap. Table F-2 and Figure F-2 show the sensitivity analysis. The horizontal straight line indicates t_x = 3.1 s, this represents the combination of acceleration and deceleration rates chosen (2.5 m/s^2 and 2.0 m/s^2 resp.). The chosen combination seems reasonable; not optimistic, neither conservative.

Table F-2 Values for t_x for varying acceleration and deceleration rates, acceleration length 25 m

Deceleration rate	Acceleration rate	t_x
2.5 m/s^2	3.0 m/s^2	2.9 s
2.5 m/s^2	2.5 m/s^2	3.3 s
2.5 m/s^2	2.0 m/s^2	3.8 s
2.5 m/s^2	1.5 m/s^2	4.7 s
2.0 m/s^2	3.0 m/s^2	2.7 s
2.0 m/s^2	2.5 m/s^2	3.1 s
2.0 m/s^2	2.0 m/s^2	3.6 s
2.0 m/s^2	1.5 m/s^2	4.5 s
1.5 m/s^2	3.0 m/s^2	2.5 s
1.5 m/s^2	2.5 m/s^2	2.8 s
1.5 m/s^2	2.0 m/s^2	3.4 s
1.5 m/s^2	1.5 m/s^2	4.2 s

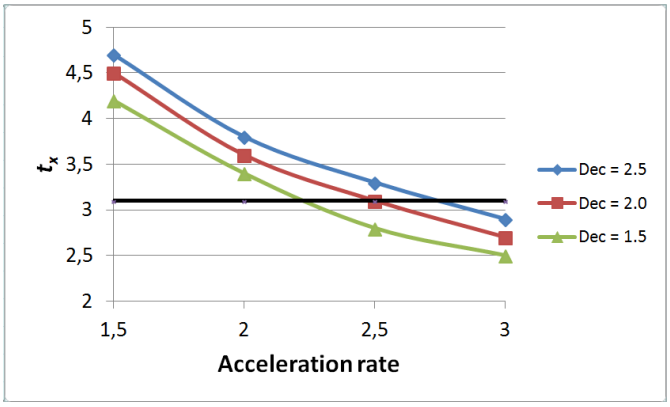


Figure F-2 Visualization of the sensitivity analysis in Table F-2

[47] *The star roundabout has two values for phase overlap, because it contains two legs in subsequent control phases which make an angle of 180 degrees; the other legs make angles of 90 degrees. E-S is the phase transition from leg East to leg South (90 degrees); S-W is the transition from leg South to leg West (90 degrees); W-E is the transition from leg West to leg East (180 degrees). The values for the acceleration length result from appendix D (Geometrical designs), recorded in Table D-6 and Table D-10.*

Appendix G: Green phase overlap calculation

The green phase overlap is an input parameter to the analytical approach, as well as to VRIGen. This appendix shows how the green phase overlap can be calculated. Green phase overlap can only be incorporated in the leg-by-leg control, applied to the rotor and star roundabouts in this project. Therefore, the green phase overlap will be calculated for the rotor and star roundabouts.

G.1. Input: geometrical design

In order to calculate the green phase overlap, the geometrical design of the intersections should be determined. This topic is addressed in appendix D (Geometrical designs), Figure G-1 and Figure G-2 show the result for the rotor and star roundabouts. The indicated dimensions A, B, C and D are necessary for calculating the green phase overlap (in the next paragraphs). In particular, A and B indicate the length which the first departing vehicles have to cover in order to reach the conflict area with the first conflicting streams. Length C indicates the length which the last vehicle in stream 03 has to cover in order to reach the conflict area with the last conflicting streams.

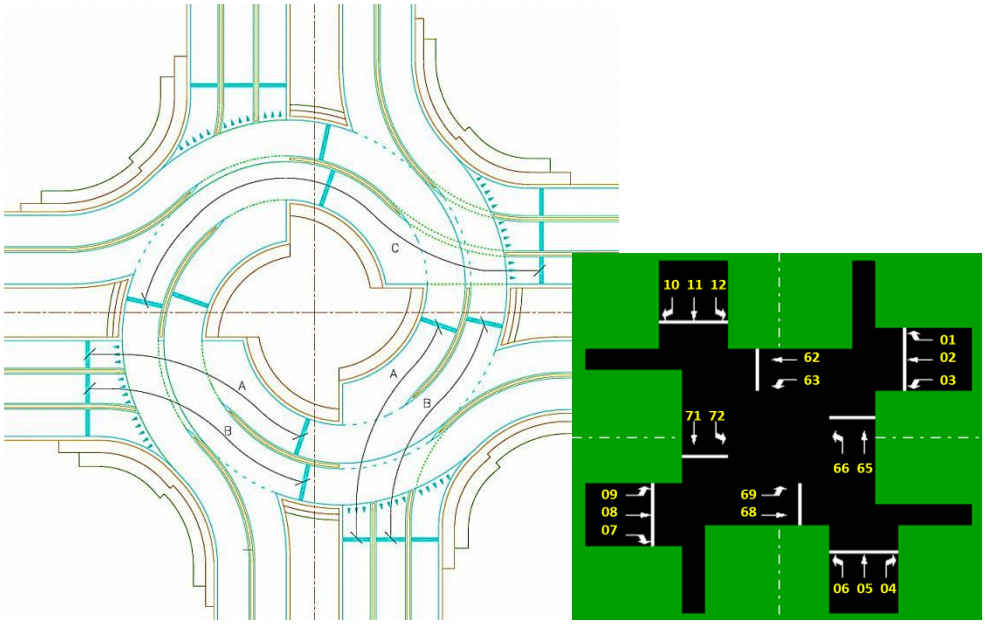


Figure G-1 Geometrical design of the rotor roundabout and standard coding of traffic streams

Table G-1 Values for A and B for the rotor roundabout

Inner radius	A	B	C
12 m	29 m	31 m	55 m
20 m	38 m	38 m	82 m

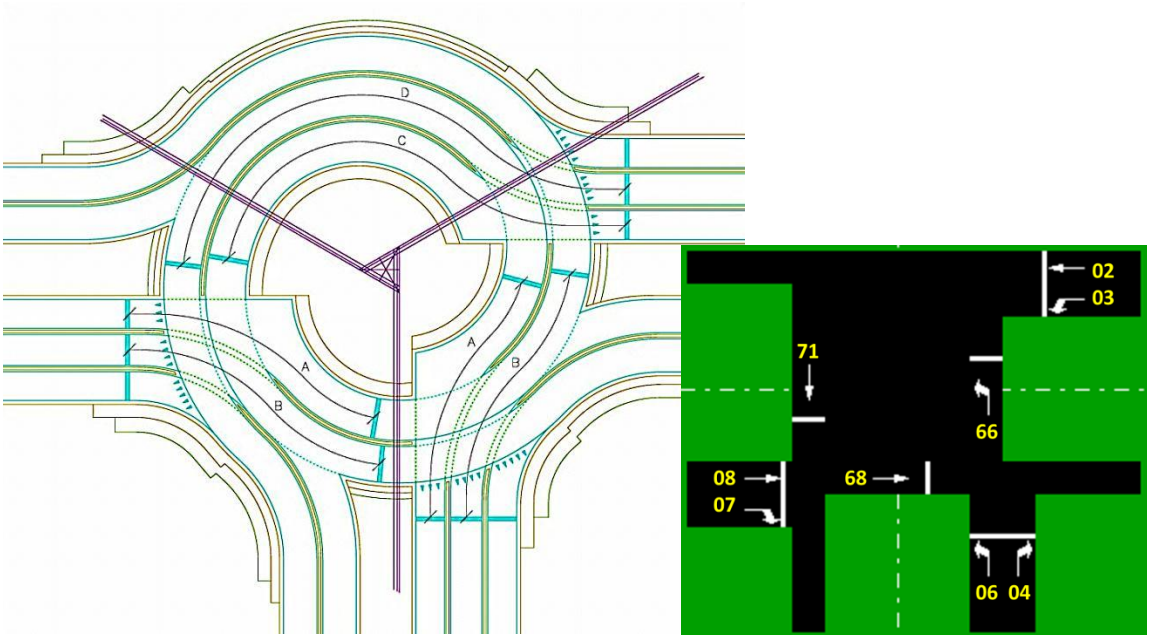


Figure G-2 Geometrical design of the star roundabout and standard coding of traffic streams

Table G-2 Values for A, B, C and D for the star roundabout

Inner radius	A	B	C	D
12 m	31 m	33 m	54 m	64 m
20 m	41 m	42 m	76 m	84 m

G.2. Calculation of the green phase overlap

Section 2.3.1 introduced the definition of green phase overlap:

The green phase overlap is the time interval in which two legs in subsequent stages can obtain green simultaneously.

This can be illustrated by means of Figure G-1. In the phase transition from the phase in which the eastern leg obtains green to the phase in which the southern leg obtains green, the signal on leg S turns green while leg E still obtains green (or yellow). Stream 65 still shows red, in order to secure the conflict area between leg E and stream 65. Stream 65 turns green as soon as the yellow phase of leg E has ended, because the clearance time of this conflict is zero seconds (see the intermezzo at the end of this section).

Consequentially, the first departing vehicle in stream 05 starts accelerating while interception signal 65 still shows red. Presumably, the first vehicle will start to decelerate after it started to accelerate in order to stop in front of the stop line joining stream 65. That would mean that a shockwave of decelerating vehicles would be initiated, moving upstream on the entrance lane. The shockwave reduces the saturation flow on the entrance lane. Therefore, the time lag between start green of 05 and start green of 65 should be optimized, such that signal 65 turns green before the driver decides to start decelerating, in order to prevent the vehicle from decelerating and a shockwave to occur. As a consequence, the duration of the green phase overlap depends on the length of the road stretch and the acceleration of the first departing vehicle. Here, already a simplified acceleration model has been formulated, appendix F (Simplified acceleration model) elaborates on the details of the presumptions and calculations with respect to the green phase overlap. In that appendix, the first departing vehicle is assumed to accelerate at 2.0 m/s^2 and decelerate at 2.5 m/s^2. The result of that appendix consists of the optimized green phase

overlap [48] ; the time interval between start green of the main signal and start green of the interception signal is calculated to be 3.8 s. This value needs to be corrected for the yellow phase in order to obtain the green phase overlap, see Table G-3.

Table G-3 Acceleration length and maximum possible green phase overlap (SG = start green)

		Acc. Length	SG main signal - SG interception signal	Green phase overlap
Rotor roundabout, 12 m	A =	29 m	3.8 s	0.8 s
Rotor roundabout, 20 m	A =	38 m	4.3 s	1.3 s
Star roundabout, 12 m, E-S and S-W	A =	31 m	3.9 s	0.9 s
Star roundabout, 12 m, W-E	C =	54 m	5.0 s	2.0 s
Star roundabout, 20 m, E-S and S-W	A =	41 m	4.4 s	1.4 s
Star roundabout, 20 m, W-E	C =	76 m	7.1 s	4.1 s

The green phase overlap on the rotor roundabout with an inscribed radius of 12 m is (3.8 s – 3.0 s) 0.8 s per phase transition; that is (4 x 0.8) 3.2 s per cycle. This value is called the *maximum green phase overlap per cycle*, because it is maximum duration allowed by the geometrical design of the turbo roundabout.

On the star roundabout, the green phase overlap is not equal for every phase transition, as it is for the rotor roundabout. The road stretch between the western and eastern leg (distance C in Figure G-2) is longer than the other road stretches, therefore the green phase overlap in the phase transition between these legs can be longer. Table G-3 shows the durations of the green phase overlaps of all phase transitions.

All considerations in this section can be summarized in the flow diagram of Figure G-3.

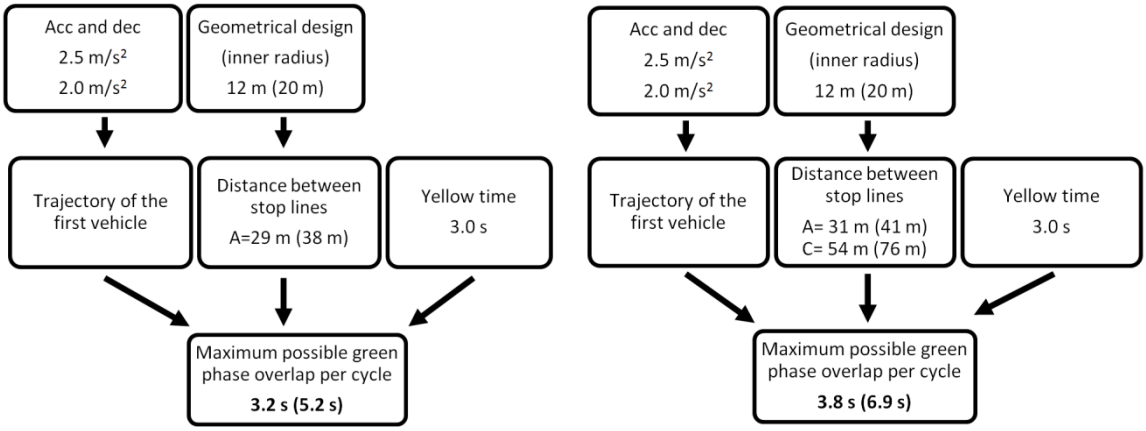


Figure G-3 Calculation of the green phase overlap on the rotor roundabout (left) and star roundabout (right)

[48] *These values included the yellow time, so these are not the green phase overlap.*

Appendix H: Control structures for the turbo roundabout

The clockwise leg-by-leg control structure for the rotor and star roundabouts will be calculated in this appendix. The green phase overlap calculated appendix G, is an important input variable. As a start, the structure with the minimum cycle time will be constructed based on the minimum duration of the green phase. This results in a control structure with equal green phase durations. These durations will be adjusted according to the demand patterns used in this study.

H.1. Minimum cycle time

In this section, the minimum cycle time will be calculated, because the capacity of the roundabout is optimized when the cycle time is minimized. Firstly, a preliminary structure will be constructed, solely based on the minimum green time. Next, two adjustments will be made to this preliminary structure.

H.1.1. Based on the minimum green time

The value for the minimum green time is chosen to be 3.0 s (CROW, 2006). Figure H-1 shows the phase diagram for the case in which the minimum green time is assigned to all legs. The green phase of leg E lasts from t = 0.0 s to t = 3.0 s (minimum green time). Afterwards, the yellow phase lasts for 3.0 s. The maximum possible green phase overlap on the rotor roundabout with an inscribed diameter of 12 m is 0.8 s, so leg S obtains green at t = 3.0 – 0.8 = 2.2 s [49]. This way, the complete phase diagram can be constructed. The minimum cycle time is 8.8 s.

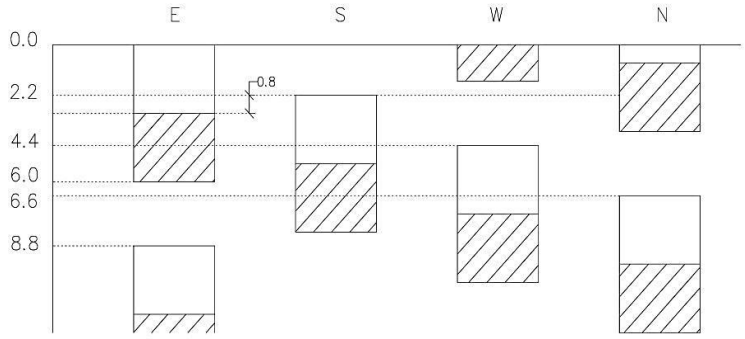


Figure H-1 Preliminary phase diagram with minimum green times (vertical axis: time, dashed areas: yellow phases)

H.1.2. Time lag between two opposing legs

Figure H-1 shows that three legs obtain green simultaneously. This is not possible in the leg-by-leg control on the rotor roundabout, because two opposing legs may not appear in the same phase (this also counts for the star roundabout, for the transition from leg E to leg W). For instance, if signal group 03 on leg E obtains green, signal groups 63 and 71 should also obtain green [50]. 71 conflicts with 08, so the green phases of leg E and leg W may not overlap. Indeed, the left-turning vehicles need time to cross the roundabout, so there should be a time lag between the end of the green phase of leg E and start green of leg W. This time lag can be calculated by means of the following formula [51]:

[49] *The yellow phase, in the figure indicated with the dashed area, lasts for 3.0 s.*

[50] *Else the left-turning vehicles would have to queue on the roundabout. This should be avoided because queuing left-turning vehicles might block the circulatory roadway for the straight-ahead vehicles.*

[51] *This formula applies to the last vehicles passing the green phase. They have already reached their desired speed, therefore an acceleration or deceleration phase should not be considered.*

$$t_{E-W} = \frac{d_{03-71}}{v_{roundabout}}$$

Equation H-1

where:

t_{E-W} = time lag between the end of the green phase of leg E and start green of leg W [s]
d_{03-71} = distance between stop line 3 on leg E and stop line 71 [m]
$v_{roundabout}$ = velocity of the last vehicle in stream 03 on the roundabout [m/s]

On the rotor roundabout with an inscribed radius of 12 m, d_{03-71} amounts to 55 m. Assuming $v_{roundabout}$ is 25 km/h, t_{E-W} amounts to 8 s. Figure H-2 shows the phase diagram including legs E and W. The minimum cycle time can be calculated to be 28 s.

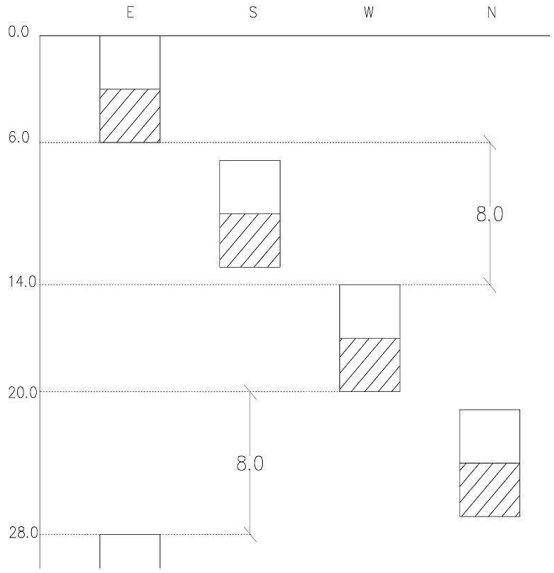


Figure H-2 Phase diagram with minimum time lag between legs E and W

H.1.3. Adjusting the structure for the green phase overlap

Figure H-2 indicates another notion: the green phase overlap diminishes. The green phase overlap for the smallest rotor roundabout was calculated to be 3.2 s per cycle. However, adding the green phase of leg N and S in Figure H-2 with green time 6 s, the green phase overlap becomes negative: (4 x -1 s) -4 s per cycle. In conclusion, if the green time is chosen minimally, then the green phase overlap offered by the roundabout cannot be used.

Figure H-3 shows three phase diagrams with different green times. The left phase diagram is again characterized by the minimum green time. In that case, the green phase of the following leg can start 1 s after the end of the green phase of the predecessor leg. The cycle time is 28 s. The middle diagram shows the case in which the green phase of the following leg can start at the moment the green phase of the predecessor leg ends. In that case, the green time is 8 s and the cycle time is 32 s. In the left phase diagram, the green time is (0.8 + 3.0 + 8.0 + 0.8) 12.6 s. The green phase overlap is (4 legs x 0.8 s) 3.2 s and the cycle time is 47.2 s.

In conclusion, the absolute minimum cycle time is 28.0 s. Up to a cycle time of 47.2 s, the traffic control does not optimally use the green phase overlap offered by the geometry of the roundabout.

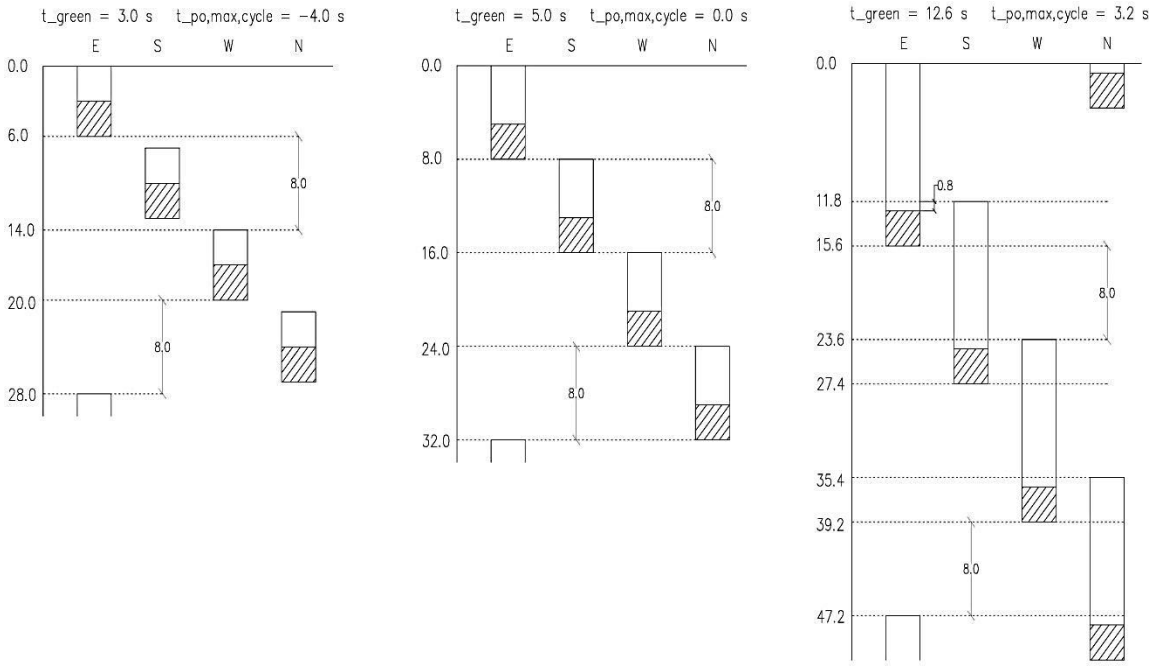


Figure H-3 Phase diagrams for three different minimum green times

H.2. Influence of unequally loaded entrance legs

Figure H-3 illustrates how the minimum cycle time for which the maximum possible green phase overlap is used, can be calculated. However, the diagrams are somewhat misleading; all legs obtain an equal duration of the green phase. Such a traffic control is suitable for situations in which the entrance legs are equally loaded (the traffic demand is equal for every leg). But this project considers demand patterns in which the ratio leg W/E is 0.8 (main directions); the ratio leg S/E is 0.6 (secondary direction); and the ratio leg N/E is 0.6 (secondary direction), see appendix B (Demand patterns). Consequentially, the duration of the green phase for leg W should be 80% of that of leg E, and the duration of the green phase for leg S and leg N should be 60% of that of leg E (neglecting the influence of the saturation flow, which increases as the duration of the green phase increases, see section **Fout! Verwijzingsbron niet gevonden.**).

Figure H-4 shows the result: the duration of the green phase of leg E is 23.0 s, that of leg W is 17.8 s and those of leg S and leg N is 12.6 s. The duration of the cycle time is 62.8 s. The maximum possible green phase overlap per cycle is: 3.2 s in a cycle time of 62.8 s.

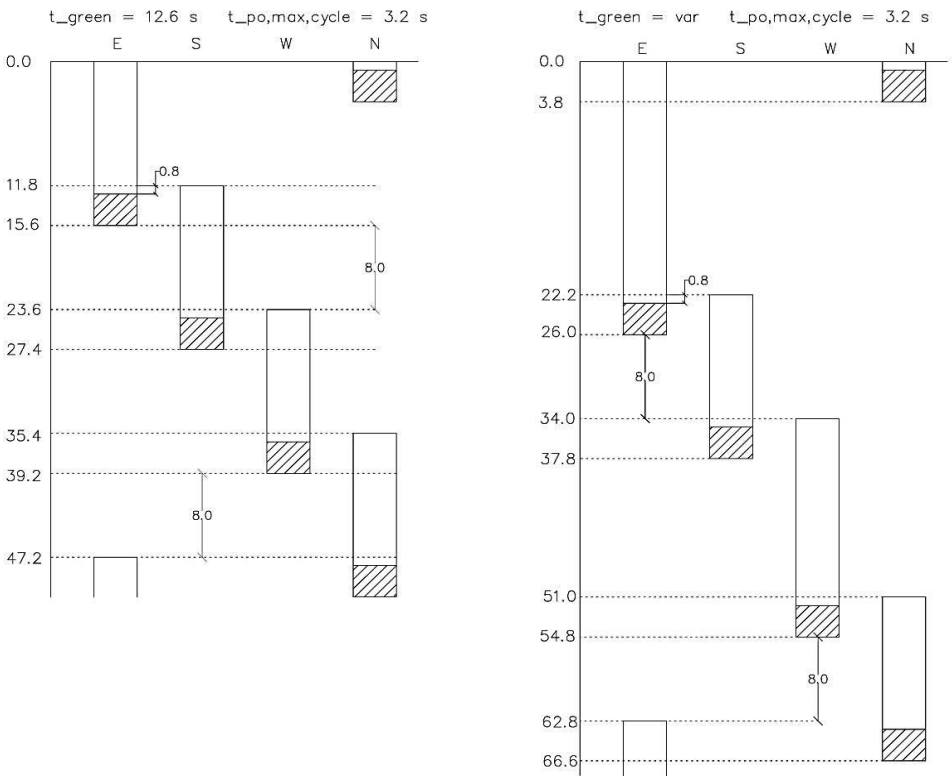


Figure H-4 Rotor roundabout with an inscribed radius of 12 m; cycle for optimal use of the green phase overlap (left) and cycle with unequal green times (right)

Likewise, the control structure with the shortest cycle time for the star roundabout can be constructed, Figure H-5 shows the result.

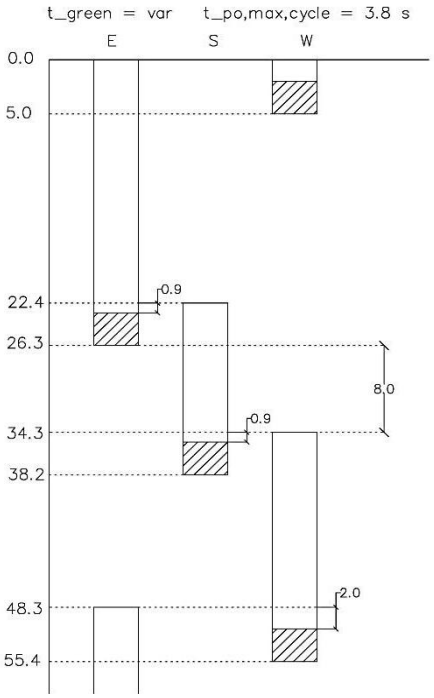


Figure H-5 Star roundabout with an inscribed radius of 12 m; cycle for optimal use of the green phase overlap with unequal green times (right)

Appendix J: Cycle time optimization

This appendix aims to explain the ambiguous relationship between the cycle time and the capacity, and to catch it in a flow diagram. The first section presents an introduction to the ambiguous relationship in the form of a dilemma. The second section addresses the influence of the geometrical design of the turbo roundabout on the green phase overlap, explained in appendix G. The influence of the cycle time is added in the third section, explained in appendix H. The fourth section addresses the calculation of the effective green time, which is input to the calculation of the saturation flow in the sixth section. The relationships between the cycle time and the phase overlap per hour is explained in the fifth section. Finally, the influence of the cycle time on the capacity of the turbo roundabout will be presented in the form of a graph (quantitative) and a diagram illustrating relationships (qualitative). At the end of the appendix, a flow diagram will be presented with the chosen values for the presented parameters.

J.1. Dilemma of the cycle time

The four-phase clockwise leg-by-leg control is suitable for the signalized rotor roundabout. This control allows for green phase overlap: a certain time lag in which two legs in subsequent phases obtain green simultaneously. Effectively, the green phase overlap increases the aggregated green time per cycle and thereby increases the capacity. Therefore, the green phase overlap should be maximized in order to maximize the capacity of the turbo roundabout.

The green phase overlap is constant per cycle, to be explained in section J.2. As a consequence, the green phase overlap per hour depends on the amount of cycles per hour, and therefore on the cycle time duration. The green phase overlap per hour in turn, influences the capacity of the roundabout (the larger the green phase overlap, the larger the capacity; to be illustrated in section J.7). Apparently, the cycle time influences the capacity of the turbo roundabout via the green phase overlap per hour, and therefore the cycle time has an optimum value.

However, the cycle time also influences the duration of the green phases within the traffic control. The duration of the green phase influences the saturation flow positively, to be illustrated in section J.6.

Notice the following relationship. As the green time decreases, the cycle time decreases and the number of cycles per hour increases. Therefore the green phase overlap per hour increases and so does the capacity. However, as the green time decreases, the saturation flow decreases as well, and so does the capacity. Via these basic notions, the optimum value for the cycle time – at which the capacity of the roundabout is maximized – will be calculated in the coming sections.

J.2. Geometrical design and green phase overlap

An important aspect of the black box approach is the notion of green phase overlap, described in section 2.3.1. Applying green phase overlap to a signalized turbo roundabout, is only possible thanks to the circulatory road segment between two legs in subsequent control phases. The length of this road segment is illustrated by Figure G-1, length A. The larger the inscribed radius of the turbo roundabout, the larger length A [52]. The first departing vehicle at the stop line uses this length to accelerate and decelerate if the interception signal shows red; this behaviour is described in the acceleration model in appendix F (Simplified acceleration model). In this model, the variables of the acceleration and deceleration rate determine the trajectory *[x,t]* of the first departing vehicle.

[52] *In this appendix, length A will be denoted with d_{02-62} in order to express that this is the distance between stop lines 02 and 62.*

In conclusion, the green phase overlap depends on two factors: the geometrical design of the turbo roundabout (cq. the inscribed radius) and the acceleration and deceleration behaviour of the first departing vehicle. Figure J-1 illustrates these relationships.

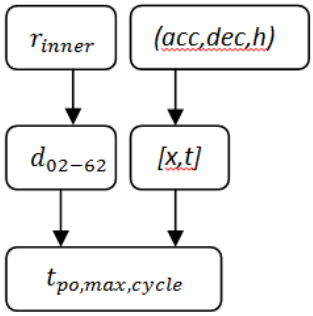


Figure J-1 Relationship between the geometrical design and the maximum phase overlap (parallel to Figure G-3)

J.3. Minimum cycle time

As noted, the cycle time influences the capacity of the turbo roundabout and therefore has to be optimized (assuming that one desires to maximize the capacity). The cycle time is constrained to a lower boundary. This boundary can be calculated by constructing the control structure with thr minimum green time, this has been done in appendix H (Control structures for the turbo roundabout). The considerations in that section are captured by the following overview:

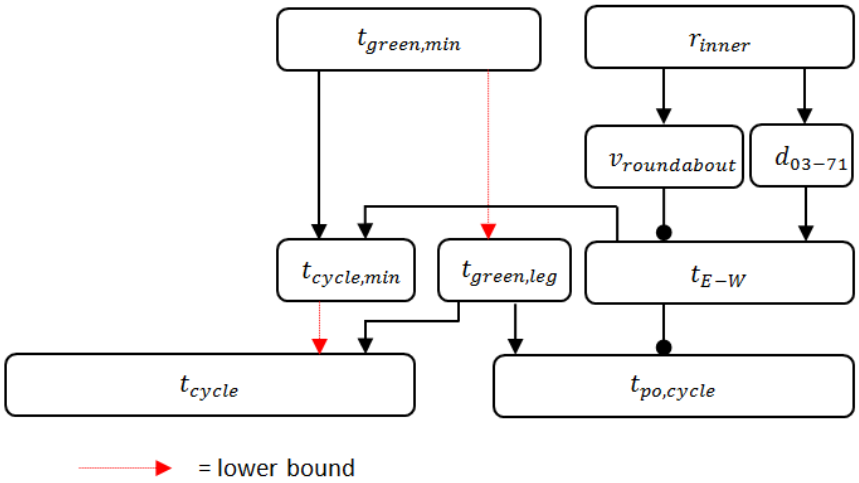


Figure J-2 Relationship among the minimum green time, minimum cycle time and phase overlap per cycle

Figure J-3 through Figure J-6 show the optimized traffic control structures for the rotor and star roundabout with inscribed radii of 12 m and 20 m.

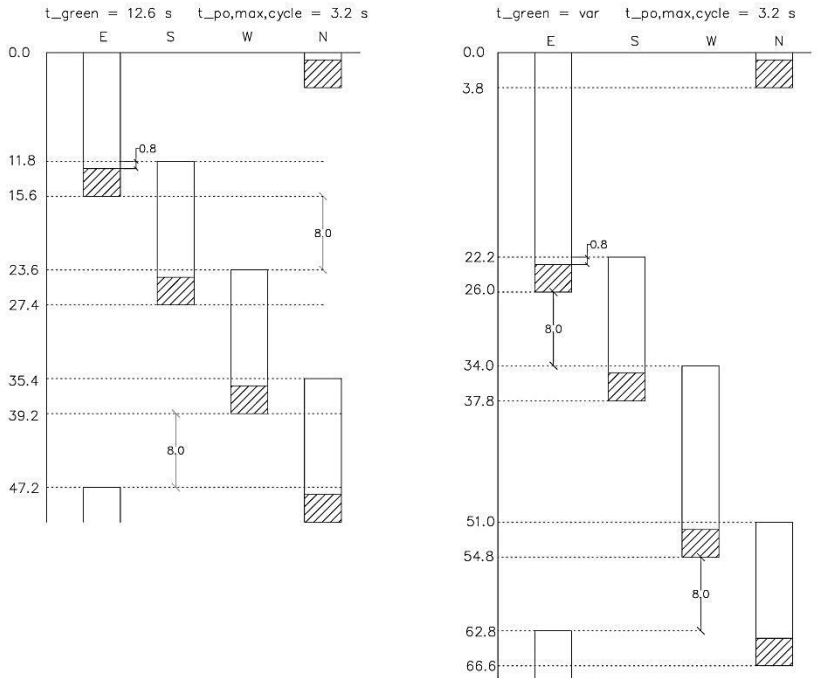


Figure J-3 Rotor roundabout with an inscribed radius of 12 m; cycle for optimal use of the phase overlap (left) and cycle with unequal green times (right)

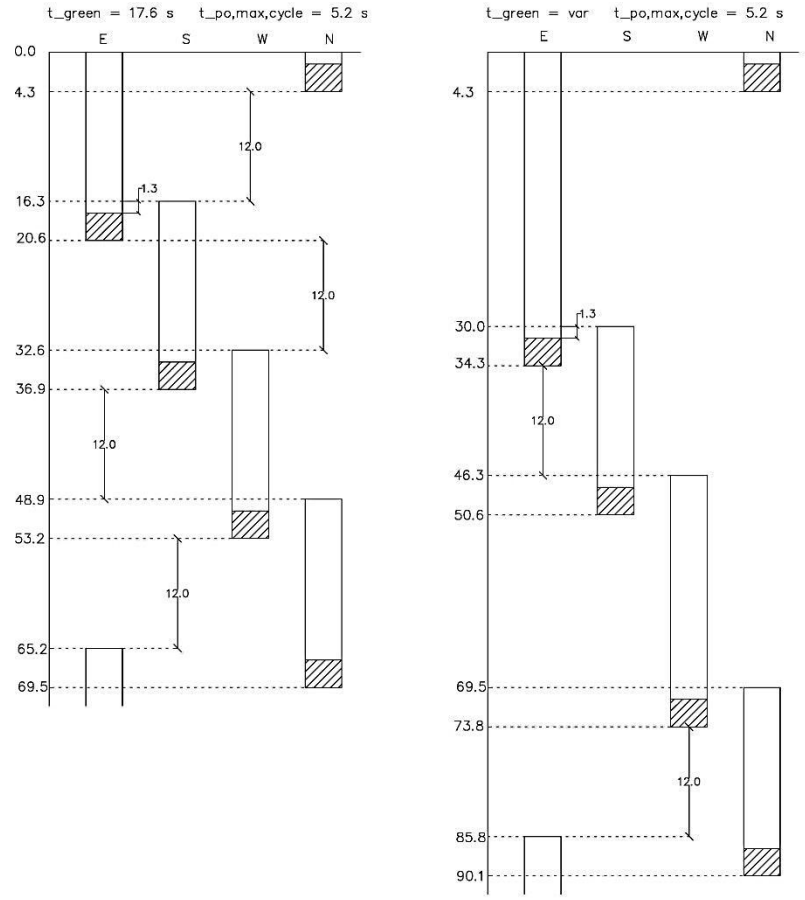


Figure J-4 Rotor roundabout with an inscribed radius of 20 m; cycle for optimal use of the phase overlap (left) and cycle with unequal green times (right)

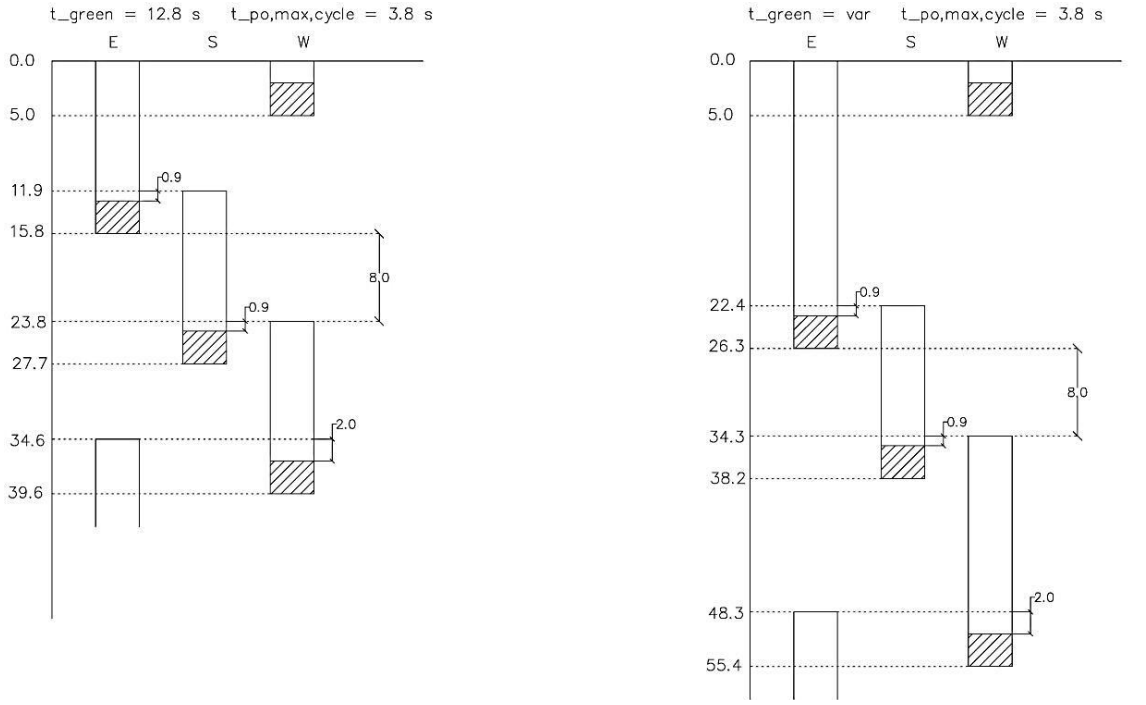


Figure J-5 Star roundabout with an inscribed radius of 12 m; cycle for optimal use of the phase overlap (left) and cycle with unequal green times (right)

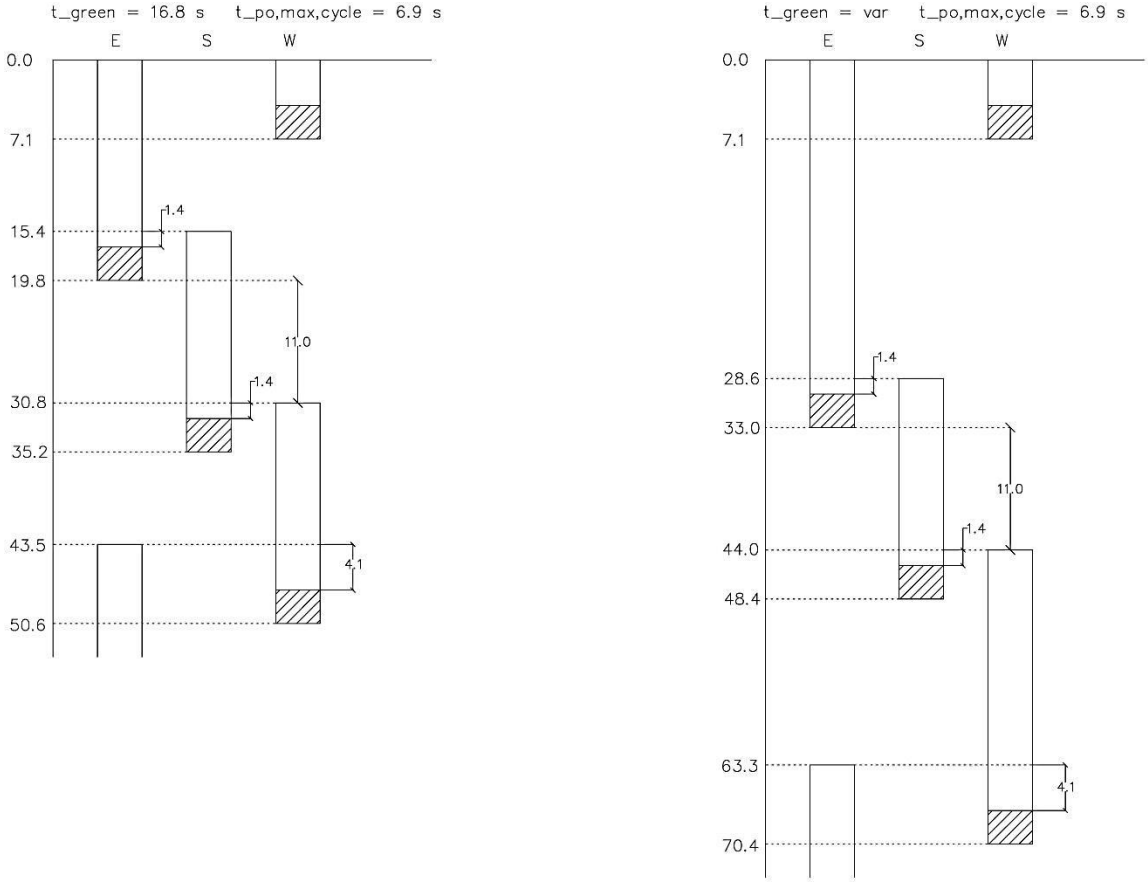


Figure J-6 Star roundabout with an inscribed radius of 20 m; cycle for optimal use of the phase overlap (left) and cycle with unequal green times (right)

J.4. Effective green time

The cycle time can be determined by constructing the control structure with the shortest cycle time, using the maximum possible green phase overlap entirely. The effective green time per leg can also be calculated from the structure. The general formula in Equation J-1 shows the variables influencing the effective green time. The green phases in the structures in the previous section can be converted to effective green times by subtracting the unused yellow time.

$$t_{eff.green,leg} = t_{green,leg} - t_{reaction} + t_{yellow,used} = t_{green,leg} + 1$$

Equation J-1

where:

$t_{eff.green,leg}$ = duration of the effective green time per leg [s]
$t_{yellow,used}$ = used yellow time [s]
$t_{reaction}$ = reaction time [s]

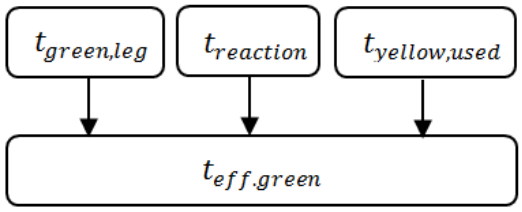


Figure J-7 Relationship between the green time and the cycle time

J.5. Cycle time and phase overlap per hour

Section J.1 showed that the maximum possible phase overlap per cycle depends on the geometrical design of the roundabout (i.e. the inner radius and the amount of legs) and the behaviour of the first vehicle. The previous section showed that the maximum possible phase overlap cannot entirely be used if the cycle time is smaller than 47.2 s.

The phase overlap per hour can be calculated if the number of cycles per hour is known, which in turn depends on the cycle time:

$$n_{cycles} = \frac{3600}{t_{cycle}}$$

Equation J-2

$$t_{po,hour} = t_{po,cycle} * n_{cycles}$$

Equation J-3

where:

$t_{po,hour}$ = phase overlap per hour, allowed by the geometrical design [s]
$t_{po,cycle}$ = phase overlap per cycle, allowed by the geometrical design [s]
n_{cycles} = number of cycles per hour [-]
t_{cycle} = cycle time [s]

The boundary conditions of the minimum cycle time needs to be added to the equations (see appendix H). These conditions are:

- the cycle time cannot be shorter than 28 s;
- the maximum possible phase overlap per cycle cannot by optimally used for cycle times between 28 s and 47.2 s.

Figure J-8 illustrates the maximum possible phase overlap per hour as a function of the cycle time. The maximum possible phase overlap per hour is maximized for a cycle time of 47.2 s, because:

- the maximum possible phase overlap per cycle cannot by optimally used for cycle times between 28 and 47.2 s;

- the maximum possible phase overlap per hour cannot by optimally used for cycle times longer than 47.2 s (longer cycle time -> less cycles per hour -> less phase overlaps per hour).

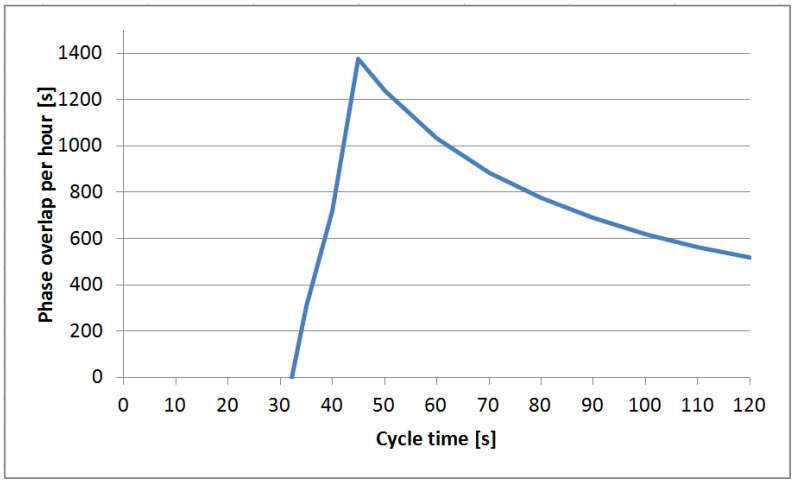


Figure J-8 Aggregated phase overlap per hour as a function of the cycle time

These considerations are captured by the following overview:

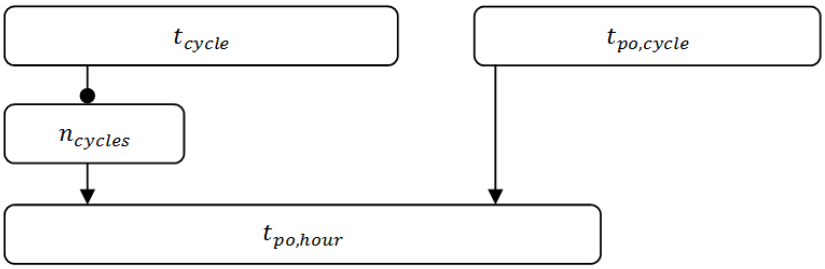


Figure J-9 Relationship among the cycle time, the phase overlap per cycle and the phase overlap per hour

J.6. Effective green time and saturation flow

In order to quantify the relationship between the effective green time and the saturation flow (Figure J-10), the traffic flow from the stop line should be regarded. The trajectories of queued vehicles accelerating from standing still can be analyzed by means of the following elementary equations:

$$v = \int a\,dt = a * t$$

Equation J-4

$$d = \int v\,dt = v * t$$

Equation J-5

By means of these equations, the trajectory of the first departing vehicle will be determined. By means of the car-following model to be described below, the trajectories of the following vehicles will be determined, on basis of which the saturation flow can be expressed as a function of time.

The elementary car following behaviour of an individual vehicle can be described by means of the following elementary formula's:

$$s_{desired} = s_0 + Const.* v$$

Equation J-6

$$h = \frac{s}{v}$$

Equation J-7

$$q_{runoff} = \frac{3600}{h}$$

Equation J-8

where:

d = travelled distance [m]
a = actual acceleration [m/s^2]
v = actual speed [m/s]
h = time headway [s]
s = actual distance headway, assumed to be equal to the desired distance headway [m]
$s_{desired}$ = desired distance headway [m]
s_0 = average gross distance headway while standing still [m]
$Const.$ = constant value; influence of the speed on the desired distance headway [m/(m/s)]

Expressing the saturation flow in terms of time, one obtains a graph like Figure J-10. The amount of vehicles running off can be expressed as a function of time:

$$q_{runoff} = \frac{3600at}{s_0 + Const.\,at}$$

Equation J-9

This formula presents the flow running off at a certain time moment. It would be too optimistic to calculate the saturation flow simply by filling in the green time and then use that value to calculate the roundabout capacity, because the acceleration period (in which the saturation flow is lower, starting from 0 pcu/h) is then neglected. The saturation flow q_{sat} at a certain moment can be calculated by dividing the total amount of vehicles that runs off during the effective green time (that is the integral of q_{runoff} over the effective green time; the second part of Equation J-10) by the duration of the green phase (the first part of Equation J-10).

$$q_{sat} = (t_{green} - t_0)^{-1} * \int_{t_0}^{t_{eff.green}} q_{runoff}\,dt$$

Equation J-10

where:

q_{runoff} = actual flow of vehicles running off [pcu/h]
q_{sat} = actual saturation flow [pcu/h]
t_{green} = duration of the green phase [s]
$t_{eff.green}$ = duration of the effective green time [s]
t = duration of the green phase [s]
t_0 = start green [s]

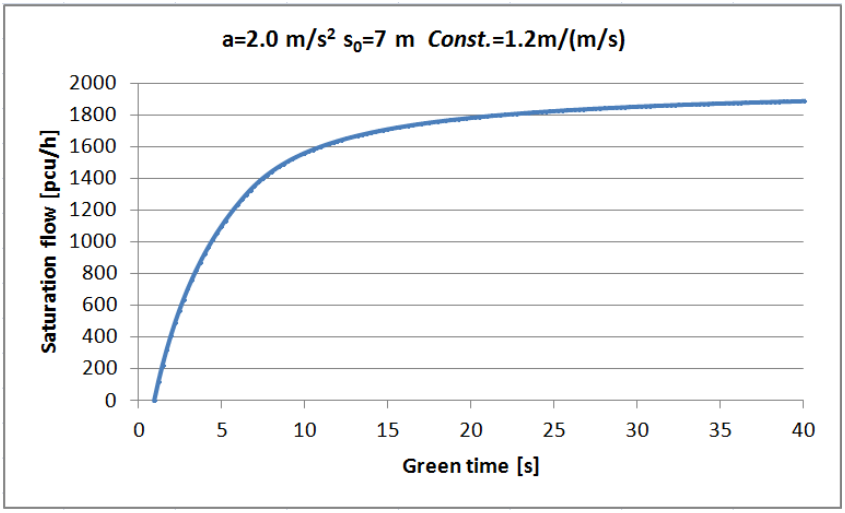


Figure J-10 Saturation flow as a function of the effective green time

These considerations are captured by the following overview:

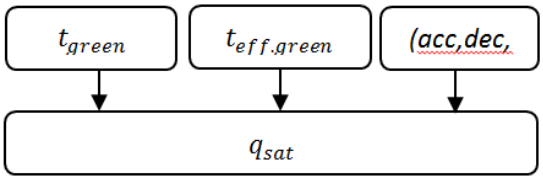


Figure J-11 Relationship among the green time, microscopic behaviour and saturation flow

J.7. Cycle time and capacity

Now, the capacity of the signalized turbo roundabout can be expressed in terms of the maximum phase overlap per hour (allowed by the geometrical design) and the saturation flow (determined by the green time):

$$C = t_{eff.green} * q_{sat} * n_{lanes}$$

Equation J-11

where:

C = capacity of the signalized turbo roundabout [pcu/h]

This formula presents the capacity per lane; the results needs to be multiplied by the number of lanes per leg. The number of lanes will be chosen to be 2, despite the fact that the rotor and star roundabout have three lanes on each entrance legs. The reason for this is that the right lane of the approaching legs of the rotor roundabout is used only by right-turning traffic. Now the question arises: if the rotor roundabout will be signalized, will the green time for the right lane entirely be used? Only if the right-turning flows are large, the answer to this question is yes, but in this project the right-turning flows are merely 30% of the straight-ahead flows (see appendix B: Demand patterns). Section 4.2.4 addresses the amount of lanes to be invoked on the rotor and star roundabouts.

From the previous explanations follows that the maximum possible phase overlap increases as the cycle time decreases (shorter cycle time -> more cycles per hour -> more phase overlaps per hour -> longer maximum possible phase overlap per hour). However, it also follows that the saturation flow increases as the cycle time increases (longer cycle time -> longer green time -> higher saturation flow). In conclusion, the cycle time influences the capacity negatively via the phase overlap and positively via the saturation flow. Presumably, an optimum exists for the duration of the cycle time, Equation J-11 allows to calculate

the optimum for this dilemma. This optimum is exactly at a cycle time of 47.2 s; the cycle time at which the phase overlap can optimally be used (see appendix H). Figure J-12 illustrates this calculation.

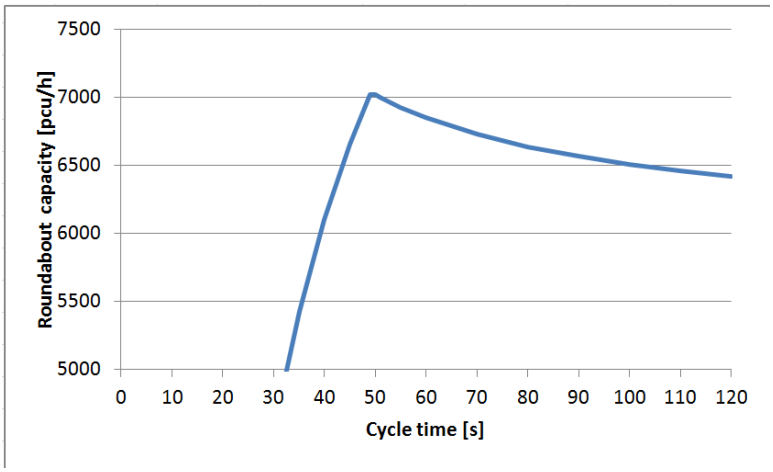


Figure J-12 Roundabout capacity as a function of the cycle time

Now the dilemma from the first section can be settled. In that dilemma, the cycle time influences the capacity in two ways. On the one hand, if the cycle time decreases, the amount of cycles per hour increases, and so do the phase overlap per hour and the capacity. On the other hand, if the cycle time decreases, the effective green time per leg decreases, the average saturation flow decreases and so does the capacity. The former influence is decisive: the influence of the effective green time duration on the saturation flow is less important than the influence of the phase overlap per hour.

These considerations are captured by the following overview:

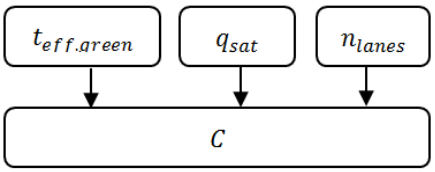


Figure J-13 Relationship between the green time and the cycle time

J.8. Results

This chapter presented overviews, which can be combined to Figure J-14.

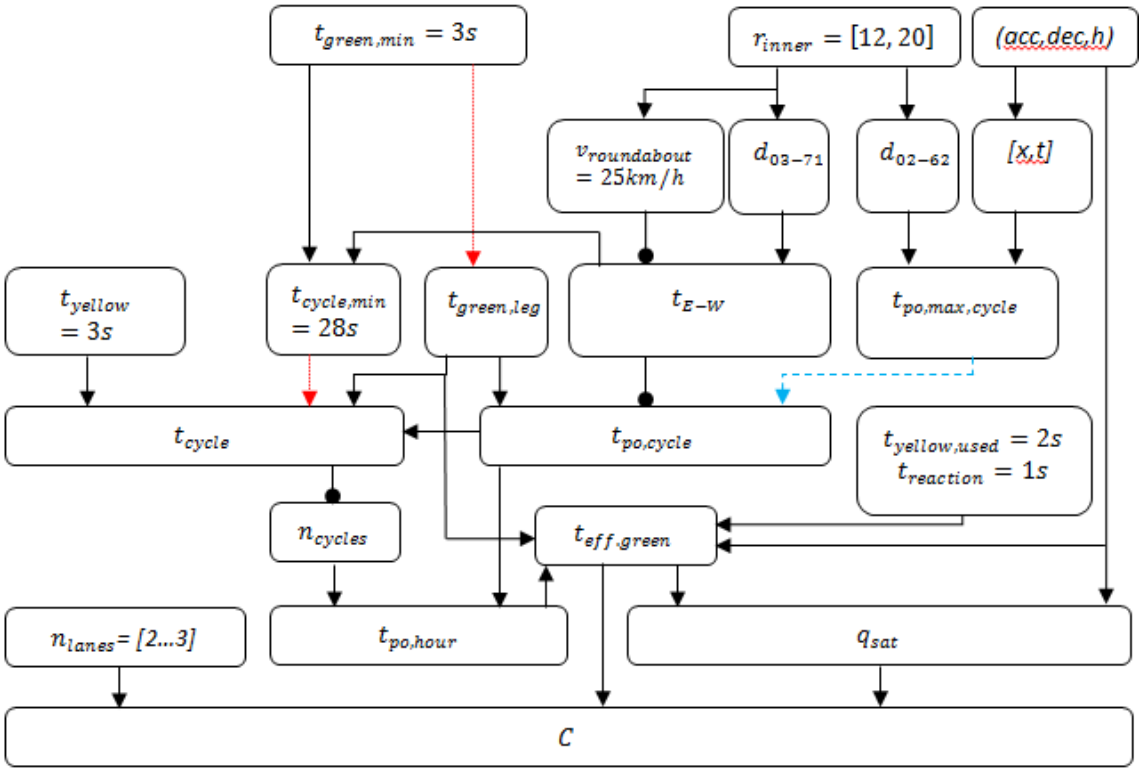


Figure J-14 Relationship among the variables determining the capacity

In the overview:

(acc,dec,h) = characteristics of microscopic driving behaviour: acceleration, deceleration, time headway
C = capacity of the signalized turbo roundabout [pcu/h]
d_{02-62} = distance between stop line 02 on the eastern leg and stop line 62 [m]
d_{03-71} = distance between stop line 03 on the eastern leg and stop line 71 [m]
n_{cycles} = number of cycles per hour [-]
n_{legs} = amount of approaching legs [-]
q_{sat} = saturation flow [pcu/h]
r_{inner} = inner radius of the signalized turbo roundabout [m]
$t_{po,cycle}$ = actual phase overlap per cycle [s]
$t_{po,hour}$ = actual phase overlap per hour [s]
$t_{po,max,cycle}$ = maximum possible phase overlap per cycle, allowed by the geometrical design [s]
$t_{po,max,hour}$ = maximum possible phase overlap per hour, allowed by the geometrical design [s]
t_{E-W} = time lag between the end of the green phase of the eastern leg and start green of the western leg [s]
t_{cycle} = cycle time [s]
$t_{cycle,min}$ = minimum cycle time [s]
t_{green} = duration of the green time per leg [s]
$t_{green,min}$ = minimum duration of the green time per leg [s]
$t_{yellow,unused}$ = unused yellow time [s]
$v_{roundabout}$ = velocity of the last vehicle in stream 03 on the roundabout [m/s]
[x,t] = trajectory of the first vehicle in the queue

Appendix K: VRIGen model development

This appendix describes the development of the models in VRIGen applied in this project. It describes all choices and results in such a way, that the reader with basic knowledge of VRIGen should be able to reproduce the models.

In the first section, the tabs in the user interface of VRIGen will be addressed. Then, the settings in all tabs in VRIGen for modelling the four-phase leg-by-leg control (for the signalized rotor roundabout) will be explained. Running VRIGen will then result in a traffic control pattern. The second section concludes that the phase overlap cannot be modelled in the 'common' way by means of VRIGen; the third section shows that this is possible if spare streams are invoked. Section K.4 describes a problem to be noticed during the simulations in VISSIM, along with a solution to it. The fifth section shows the settings in all tabs in VRIGen for creating the three-phase leg-by-leg control (for the signalized star roundabout), this will also be done with help of spare streams. Sections K.6 and K.7 deal with the two-phase traffic controls for the four-leg turbo circle and the three-leg turbo circle respectively.

K.1. VRIGen: overview of the tabs

The user interface of the software program VRIGen consists of six tabs, in which the user builds the traffic control step-by-step. In the first tab, all signal groups – a (set of) traffic stream(s) – present on the intersection have to be indicated. In the second tab, the conflict matrix has to be defined, with all clearance times determined by the geometrical design of the intersection. The third tab allows to invoke couplings: a pair of signal groups can be coupled such, that they obtain green simultaneously. This is relevant to the signalized turbo roundabout and turbo circle, because a main signal and the successive interception signal should obtain green simultaneously. In the fourth tab, the minimum and maximum durations of the sub green phases, the yellow phase and the red phase have to be indicated per traffic stream. In the fifth tab produces the output: the control sequence, calculated by VRIGen. The sixth tab allows to indicate cut-off conflicts, this tab does not change the control sequence.

K.2. Four-phase leg-by-leg control – without spare streams

This section shows how to create a four-phase leg-by-leg traffic control by means of VRIGen. As a start, this will be done in the 'common way', i.e. without using spare streams. At the end of the section, the conclusion will be drawn that phase overlap cannot be modelled this way.

K.2.1. Signal groups

The first tab in VRIGen contains the signal groups. Figure K-1 shows the signal groups on the rotor roundabout to be applied in this model.

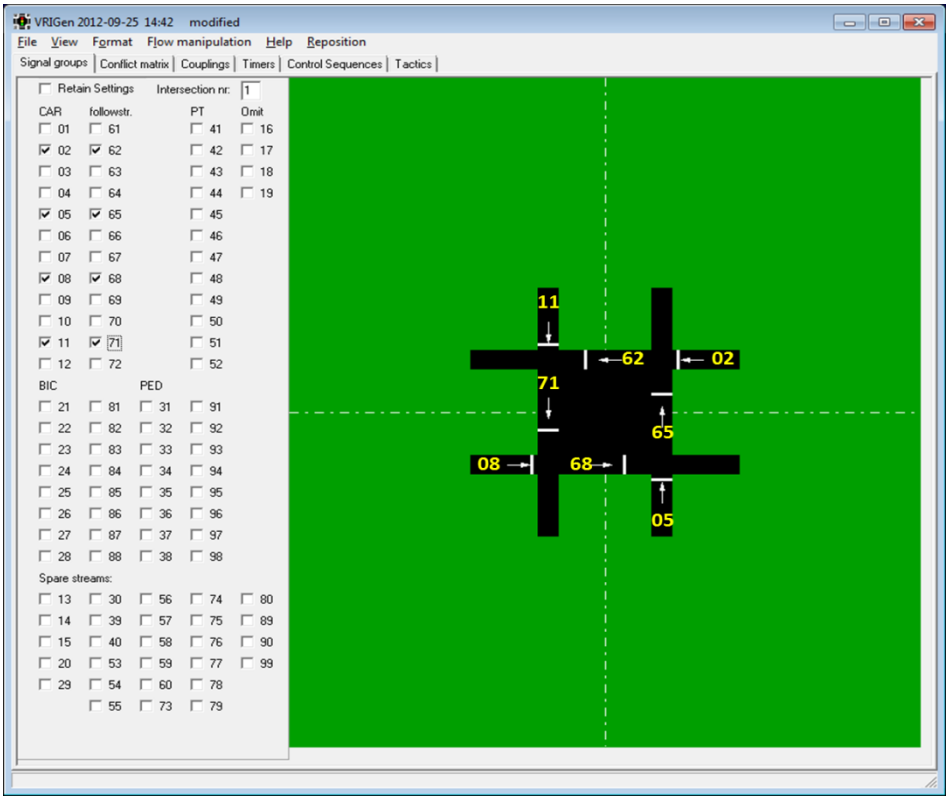


Figure K-1 Traffic streams on the rotor roundabout

Already an important choice has been made in this tab. In reality, the rotor roundabout invokes all main signal groups (01 through 12) and all interception signal groups (62 through 72). However, in this project only streams 02, 05, 08, 11, 62, 65, 68 and 71 will be invoked. This choice has been made in order to simplify the structure and thereby reduce the computation time. The choice is legitimate, because in a leg-by-leg control, a phase serves all traffic streams on one leg, and all streams on a leg are served in one phase. For instance, streams 01, 02 and 03 are served in one phase simultaneously, and in one phase only. Therefore, it is legitimate to represent streams 01, 02 and 03 in stream 02 (02 is chosen randomly).

Moreover, the traffic control should assure that each pair of neighbouring interception signals show green simultaneously. This constraint should be set out of psychological considerations: for example, if a driver in stream 62 obtains green in his stream, but sees a red signal for stream 63, he may get confused because the roadways for 62 and 63 are directly next to each other. Representing 62 and 63 in the same signal group prevents this problem.

K.2.2. Conflict matrix

With the conflict matrix only containing the physical conflicts, VRIGen produces a two-phase control, similar to the two-phase control for the turbo circle. However, the desired result consists of a leg-by-leg control. The cause is that VRIGen 'has not been told yet' that the rotor roundabout cannot store any left-turning vehicles on the circle [53]. This problem can be solved by adding imaginary conflicts to the conflict matrix, such that the leg-by-leg control is the only possible outcome.

[53] *The rotor roundabout contains a choice lane at every exit leg. In case of a two-phase control, the choice lane causes the queuing left-turning vehicles to block the path for the straight-ahead streams. So due to the presence of the choice lane, the rotor roundabout only allows for a leg-by-leg control.*

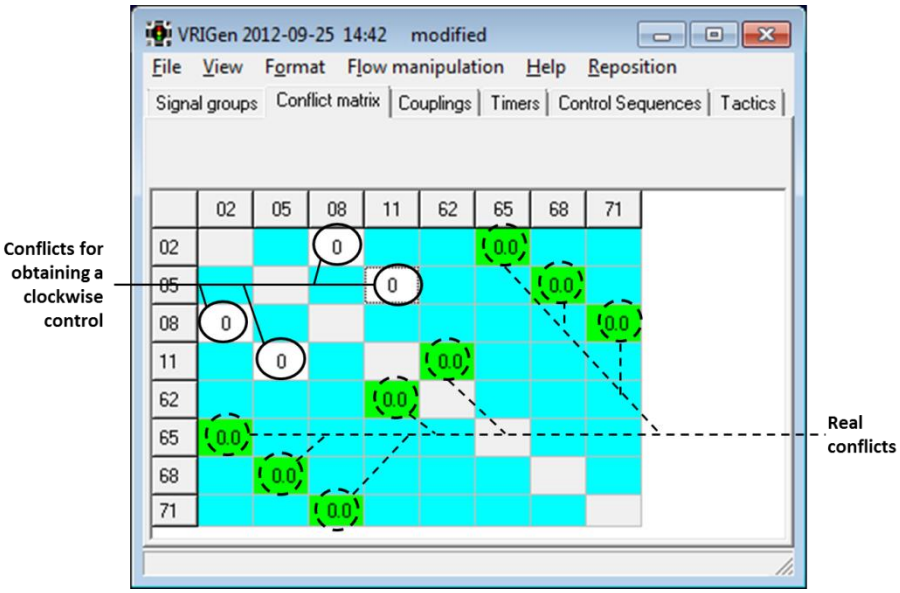


Figure K-2 Conflict matrix

The conflict matrix needs to be adjusted, such that directions 02 and 08 do not appear in the same stage. This can be done by adding a conflict between directions 62/08 (and the equivalent conflicts on the other three segments), or by adding a conflict between directions 02/08. Again: these are not physical conflicts, but the conflicts assure that VRIGen produces a leg-by-leg control. The second solution direction (conflict 02/08) will be chosen, see Figure K-2. The second solution is better, because the first solution yields problems with respect to the phase overlap. For example, if the conflict 62/08 would be added, 62 and 08 will not be allowed to obtain green simultaneously. This yields no problems for the phase in which the western leg has green, but it does yield problems for the phase transition from the southern leg to the western leg. Signal group 62 and the southern leg appear in the phase, because 62 serves the left-turning traffic from the southern leg (i.e. 62 is fed by the left-turns from 65, which is in turn fed by the left-turns from 05). That means that 62 should have green, as long as 05 has green. However, as soon as 08 obtains green, 62 obtains red. Consequently, the green phase 05 and 08 cannot overlap in that case. Therefore, the first solution (conflict 62/08) is not satisfactory.

The conflicts 02/08 and 05/11 have been added with clearance times set to zero, see Figure K-2. The reason is that these conflicts are added in order to prevent a pair of signal groups to appear in the same phase. They have not been added to create a time gap between two phases.

In appendix E, the clearance times of the physical conflicts have been calculated to be 0 s.

K.2.3. Couplings

The phase overlap can be incorporated in the Couplings tab, by means of the first four couplings [54] (02/62, 05/65, 08/68 and 11/71, see Figure K-3). The value for *TYveh* indicates the time interval the green phase of the following stream starts earlier than the green phase of the predecessor stream. If this value is negative, the green phase of the following stream starts later than the predecessor stream. On a rotor roundabout with an inscribed radius of 12 m, the green phase overlap per transition is 0.8 s. Adding the yellow time, the phases should overlap 3.8 s in the final structure (i.e. the time lag between start green 02 and start green 62, etc.), as calculated in the main report. The value *TYveh* for these couplings needs to be set to -3.8 s.

[54] *At the end of this section, it will be noted that the phase overlap cannot be incorporated this way.*

Moreover, four extra couplings need to be added in order to assure that in the resulting phase diagrams, directions 63 and 71 appear in the same phase (vehicles in stream 03 should obtain green at stop line 03, 63 and 71 in the same phase, else they need to queue up on the roundabout – which is not allowed on the signalized turbo roundabout). This cannot simply be done via a coupling 62/71, because if the other three couplings (65/62, 68/65 and 71/68) are to be added, all interception signals are coupled and the clockwise leg-by-leg control would be excluded from the results. Alternatively, 62 and 71 appear in the same phase via a coupling 02/71. The same holds for couplings 05/62, 08/65 and 11/68 [55].

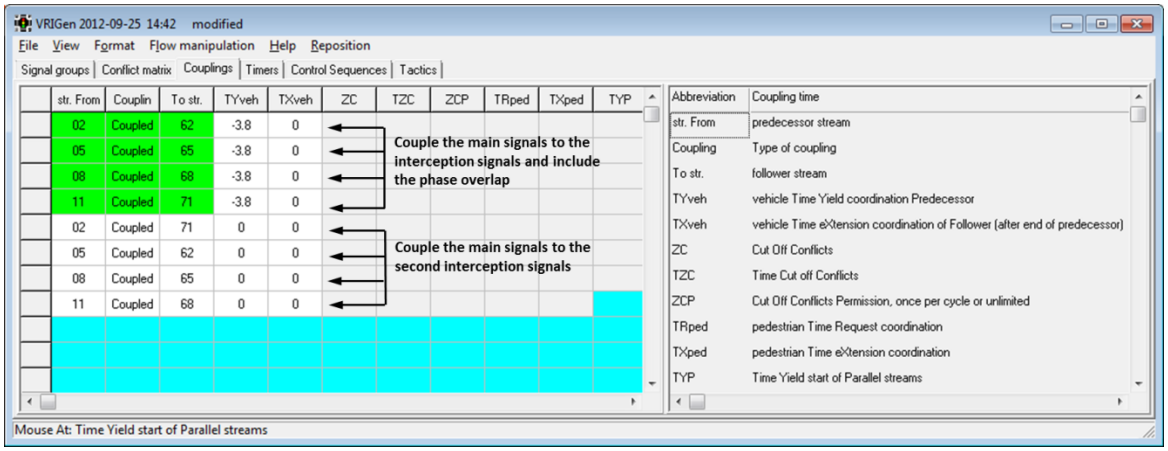


Figure K-3 Couplings for the rotor roundabout with inner radius 12 m

K.2.4. Timers

In the tab Timers, the user can adjust the duration of the green, yellow and red phases, and the green sub phases (e.g. fixed green time). There is no reason to change the default settings in this tab, except for the Yellow use. These values are set to 2.0 s (default 1.0 s), in accordance with Muller (2011, lecture notes CIE4822 p.66).

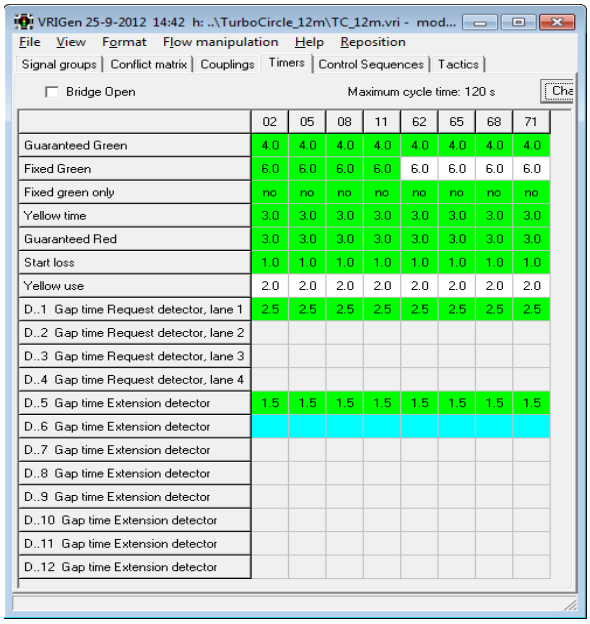
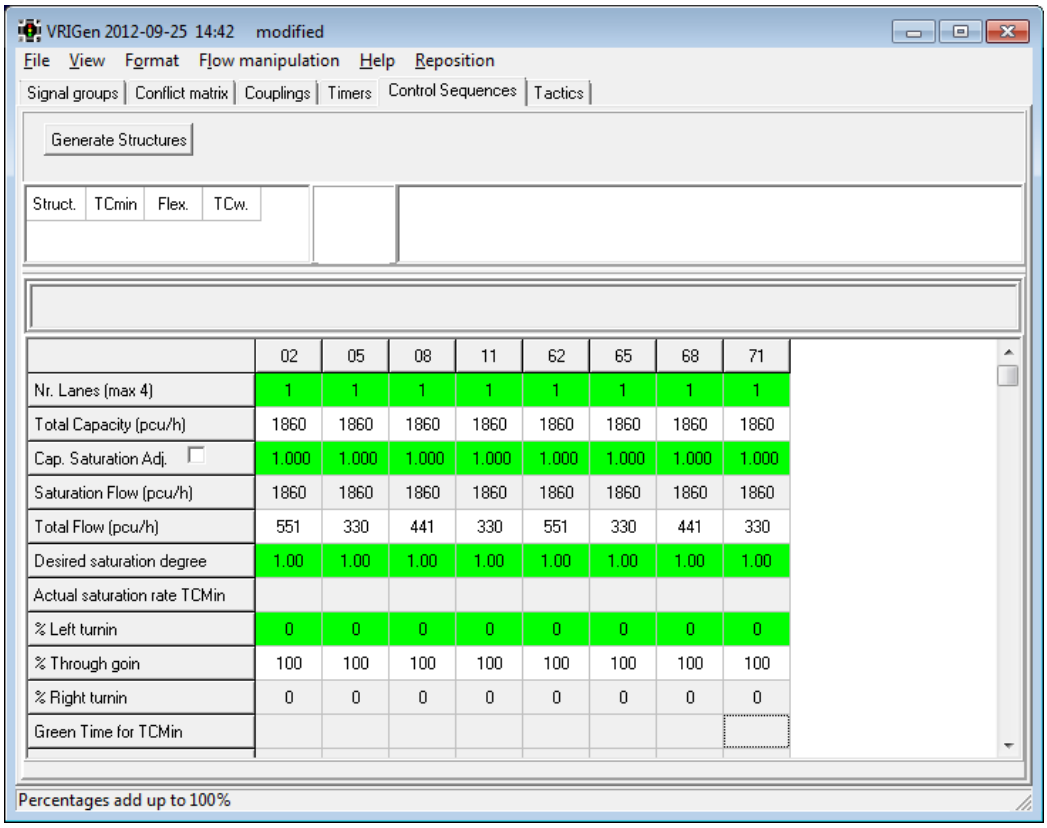


Figure K-4 Timers, default values (except for Yellow use)

[55] *It is not necessary that the main signal and the second interception signal (e.g. 02 and 71) obtain green simultaneously, because vehicles need time to cover the distance between the two stop lines. However, the second interception signal already shows green in the previous phase, so TYveh can be put to zero.*

K.2.5. Control sequences

In the tab Control sequences, the user can specify the characteristics of the signal groups, such as number of lanes, saturation capacity and traffic demand. These topics will be elaborated on in this section.



	02	05	08	11	62	65	68	71
Nr. Lanes (max 4)	1	1	1	1	1	1	1	1
Total Capacity (pcu/h)	1860	1860	1860	1860	1860	1860	1860	1860
Cap. Saturation Adj.	1.000	1.000	1.000	1.000	1.000	1.000	1.000	1.000
Saturation Flow (pcu/h)	1860	1860	1860	1860	1860	1860	1860	1860
Total Flow (pcu/h)	551	330	441	330	551	330	441	330
Desired saturation degree	1.00	1.00	1.00	1.00	1.00	1.00	1.00	1.00
Actual saturation rate TCMin								
% Left turnin	0	0	0	0	0	0	0	0
% Through goin	100	100	100	100	100	100	100	100
% Right turnin	0	0	0	0	0	0	0	0
Green Time for TCMin								

Figure K-5 Control sequences, dependent on demand pattern

Number of lanes

In the tab Control sequences, the number of lanes per signal group needs to be defined. Section 4.2.4 addresses that discussion. Here, the worst case scenario will be used, that is: the number of lanes is 2. That means that every stream on the entrance leg should obtain (2/3) lanes. Unfortunately, the number of lanes can only be specified in VRIGen as an integer, therefore the number of lanes is chosen to be 1 for all streams.

Saturation flow

The saturation flow is chosen based on the field measurements presented in appendix D:

lanes right-turning	1852 pcu/h
lanes straight ahead	1891 pcu/h
lanes left-turning	1843 pcu/h

The average of these values is 1860 pcu/h.

Total flow

The total flow depends on the demand pattern. In VRIGen, the values for the flows determine the green times for *TCmin* (the minimum cycle time) and the extension green times. The absolute values for the green times are not relevant, because the VISSIM simulation will apply TrafCOD to simulate a vehicle-actuated control. In that case, the green phases can be extended as long as needed (within the constraint of the extension green time. As input for this tab, the flow values will be chosen such that the total traffic

demand is 3800 pcu/h [56], with relationships among the flows according to demand pattern 100 (for convenience; in this pattern the left-turning flows are equal to the neighbouring straight-ahead flows).

K.2.6. Tactics

In the tab Tactics, the user can modify the phases of individual streams, but not the structure to be generated. There is no reason to alter the default settings in this tab.

K.2.7. Resulting control program

Figure K-6 shows the resulting control program. Essentially, this is the clockwise four-leg program, originally intended to apply to the rotor roundabout.

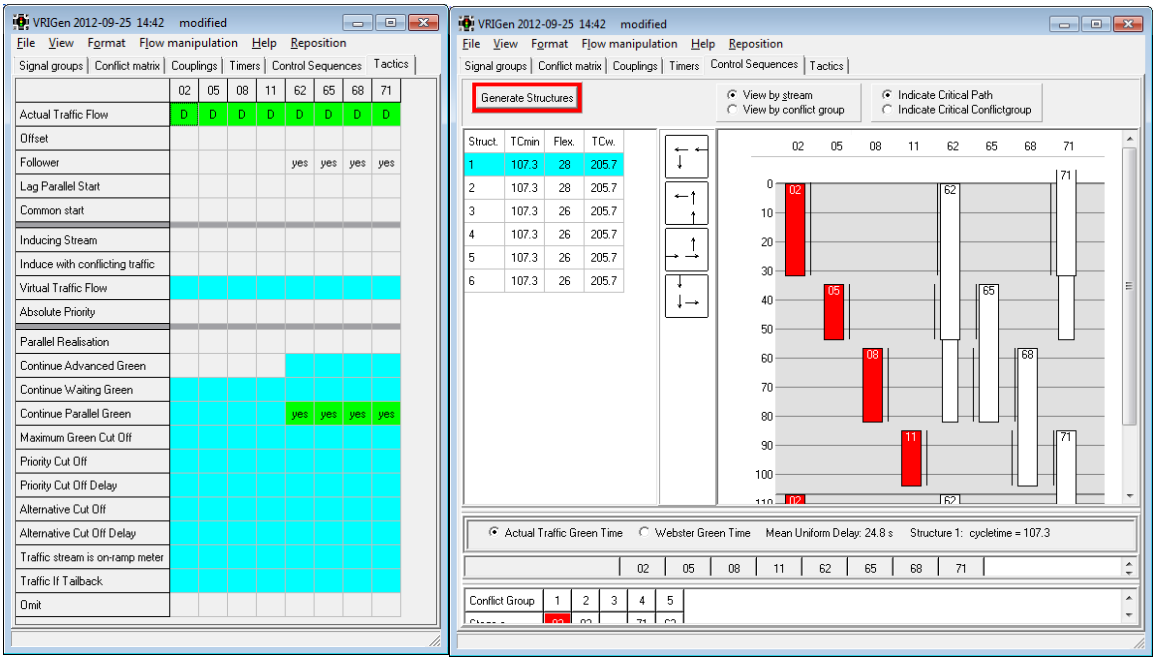


Figure K-6 Tab Tactics (left) and the result of the VRIGen calculation in tab Control Sequences (right)

Examining the phases and their transitions closely yields a disappointing notion: the phase overlaps are equal to zero. A sensitivity analysis with respect to the value for *TYveh* of the first four couplings (set to -3.8 s) yields the conclusion that VRIGen ignores negative values, and acts as if they were equal to zero. Probably, this is a default setting in VRIGen resulting from the Dutch guideline with respect to regular intersections, that start green of an interception signal should not be later than start green of the accessory main signal (Fortuijn, personal communication, April 2013).

This conclusion yields that the phase overlap cannot be incorporated in the VRIGen model by means of ordinary Couplings. Another way of incorporating the phase overlap should be found. The next section shows an entirely different approach, based on the inclusion of spare streams.

K.3. Four-phase leg-by-leg control – with spare streams

The previous section shows that the leg-by-leg traffic control can be modelled by means of VRIGen, but it is not possible to model any phase overlap in the 'common way' (i.e. coupling main signals to the

[56] *This value is chosen randomly. It needs to be large enough to have VRIGen produce green times larger than the minimum green time, but not too large in order to have VRIGen produce a cycle time smaller than the maximum cycle time (120 s).*

interception signals. This gives rise to the presumption that the phase overlap might be modelled by using non-existing streams and leaving out the regular couplings between the main signals and the interception signals. VRIGen accommodates this option by enabling the user to apply spare streams. This project applies a four-phase control, so four spare streams will be applied: 13, 14, 15 and 20.

K.3.1. Spare streams – the strategy

Figure K-7 shows the idea of the spare streams in the phase transition from the eastern leg to the southern leg. Due to the coupling between 13 and 02, 13 obtains red 3.8 s earlier than 02. The conflicts 13/05 and 02/65 cause the green phase of signal 05 to commence 3.8 s earlier than start green 65.

Stream 13 will be attached to the eastern leg (imaginary; the location of the spare stream cannot be communicated to the model). In the conflict matrix, stream 02 will have a conflict with stream 65 and stream 13 will have a conflict with stream 05. In the couplings tab, stream 13 will be coupled to stream 02. They need to obtain green simultaneously, with a time lag *TYveh* in order to obtain a control in which stream 05 obtains green earlier than start green 65. For example, if *TYveh* is equal to 3.8 s, then end green 13 is 3.8 s earlier than end green 02. This means that start green 05 is 3.8 s earlier than start green 65.

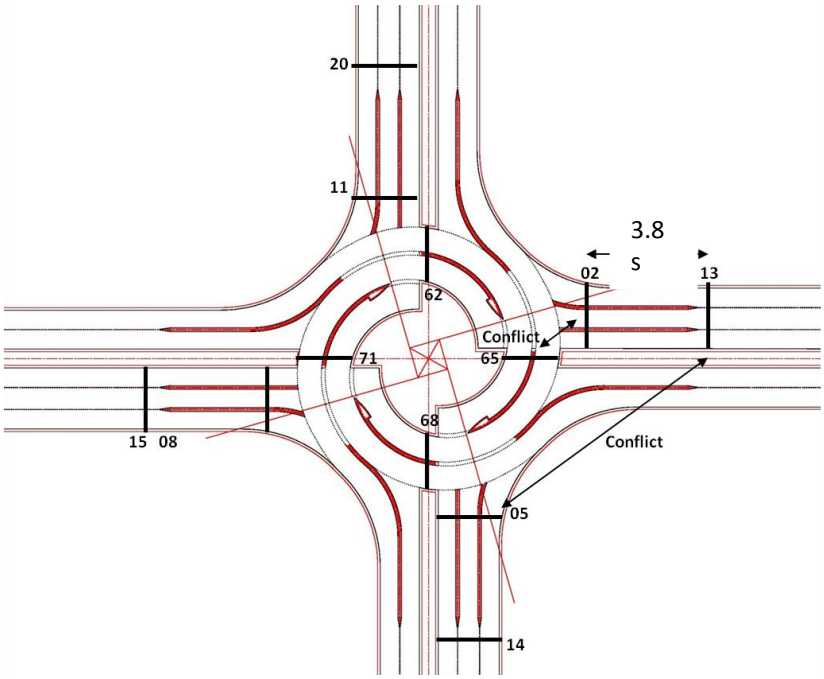


Figure K-7 The non-existing spare streams are coupled to the main streams

The locations cannot be communicated to VRIGen, but the locations are not important. The function in the system of the control is important; this can be communicated to VRIGen by means of conflicts and couplings.

K.3.2. Signal groups

Figure K-8 shows the traffic streams to be used. Again, the main and interception models are included, except for the right- and left-turning streams. All streams on a certain leg are represented by the straight-ahead traffic stream.

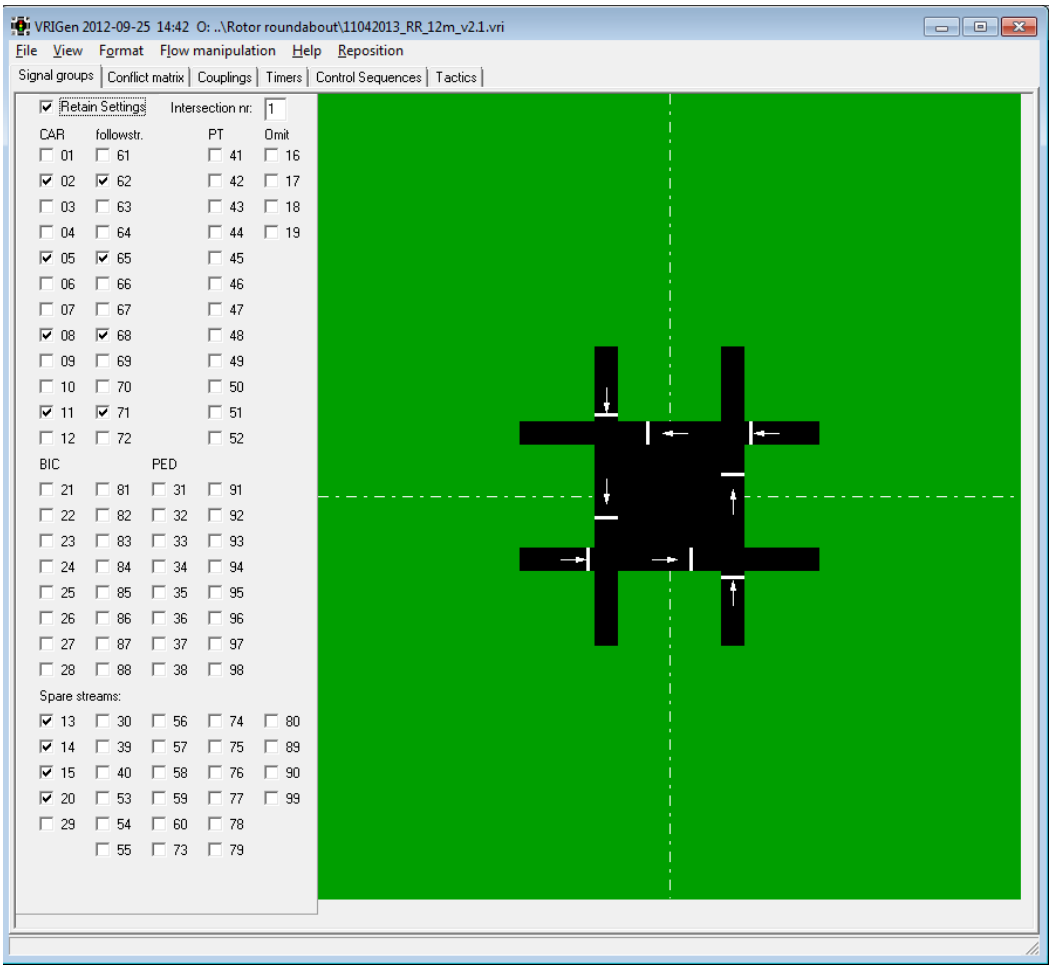


Figure K-8 Codes of used streams and their spatial position

An important issue is how to interpret the spare streams, and how to use them for reaching the goal: to obtain a phase overlap (i.e. the start green of the main stream is earlier than the start green of the interception signal). The following paragraph tries to explain a possible application of the spare streams.

K.3.3. Conflict matrix

Figure K-9 shows the conflict matrix. There are four real conflicts between main signals and interception signals. Two conflicts assure that VRIGen produces leg-by-leg control programs and four conflicts relate the spare streams with the main signals, described in the previous section.

K.3.4. Couplings

In the situation without left-turning traffic streams, the couplings are quite simple, see Figure K-10. The only couplings needed are those which assure that the green phase of the spare stream ends 3.8 s earlier than the green phase of the main stream.

K.3.5. Timers

There is no need to alter the default settings in the tab Timers, except for the Yellow use. These values are set to 2.0 s (default 1.0 s), in accordance with Muller (2011, lecture notes CIE4822 p.66).

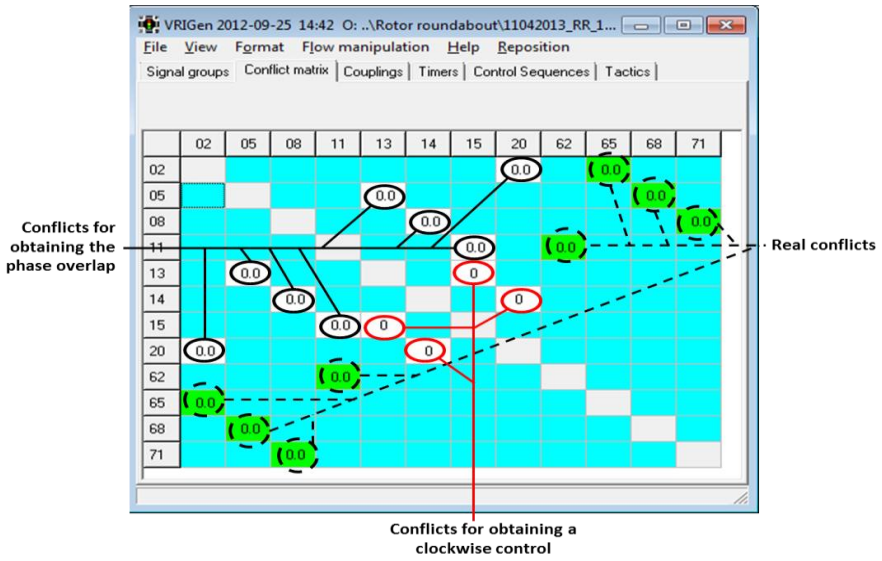


Figure K-9 Conflict matrix

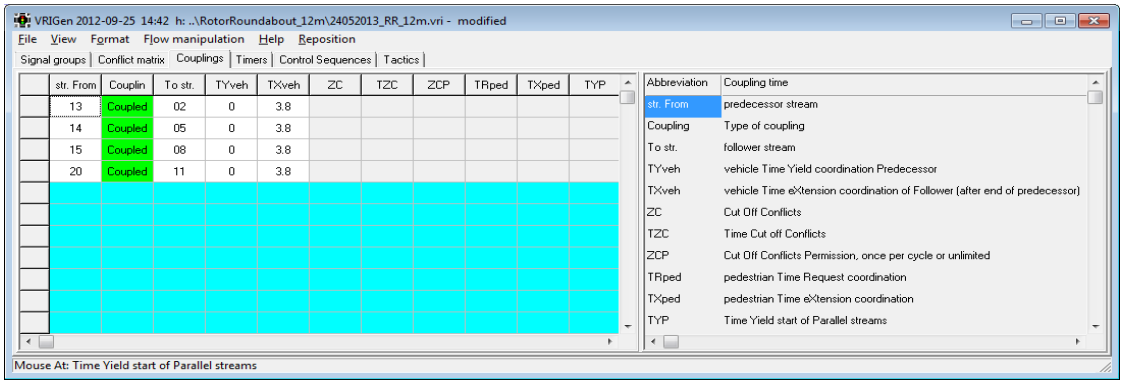


Figure K-10 Couplings of the spare streams with the main streams

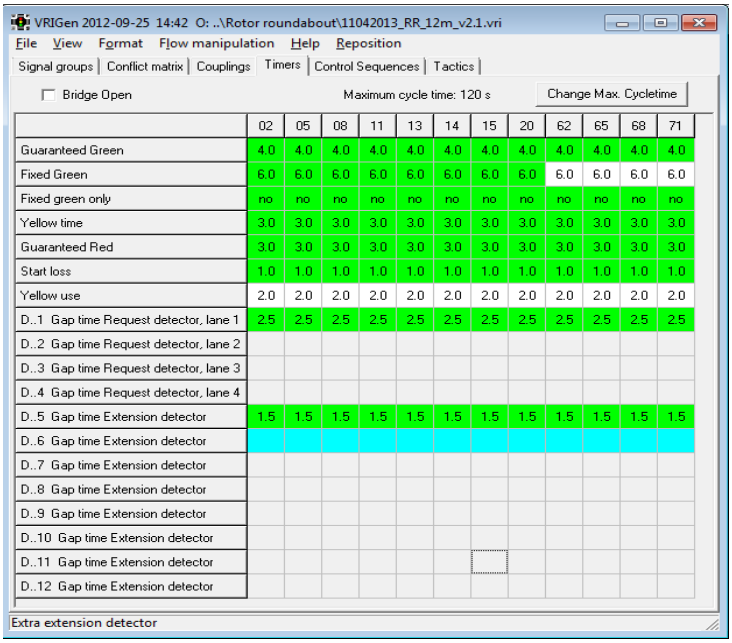


Figure K-11 Timers, default values (exept for Yellow use)

K.3.6. Control sequences

All settings in Control Sequences from the previous section will be used.

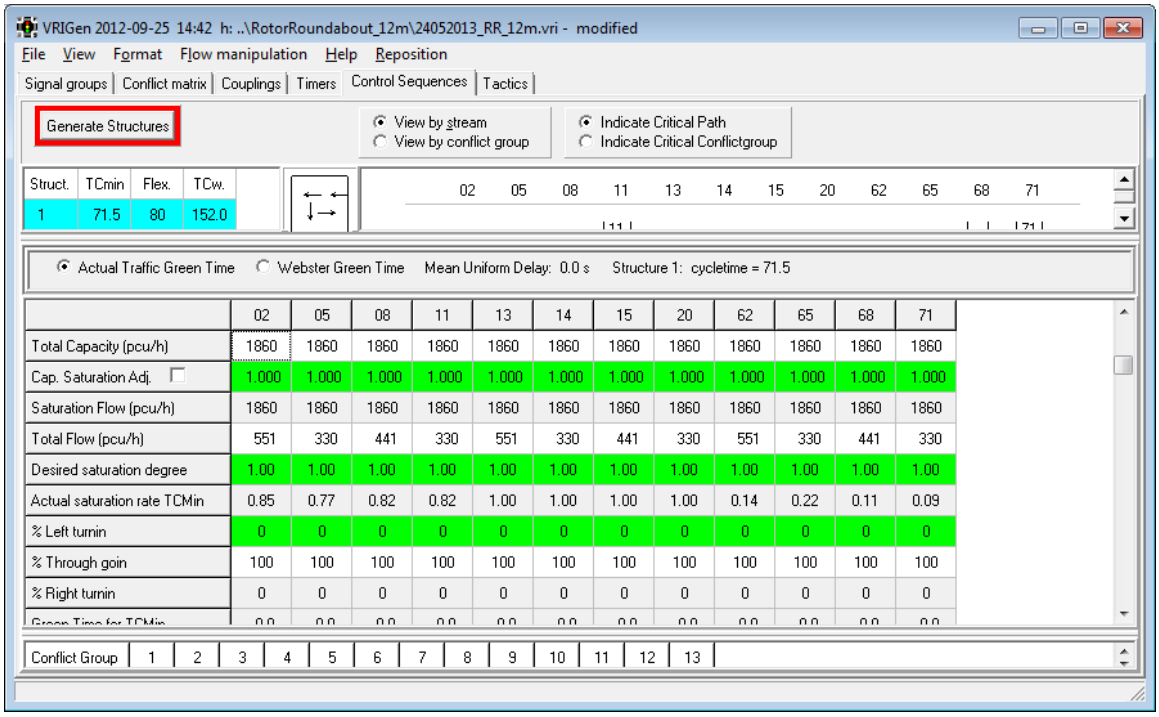


Figure K-12 Control sequences, dependent on demand pattern

K.3.7. Tactics

With respect to the tab Tactics, the default settings are not changed

K.3.8. Resulting control program

Figure K-6 shows the resulting control program. This is the originally intended leg-by-leg control program with phase overlap 3.8 s. Test runs by means of VISSIM show that this structure indeed represents the desired traffic control.

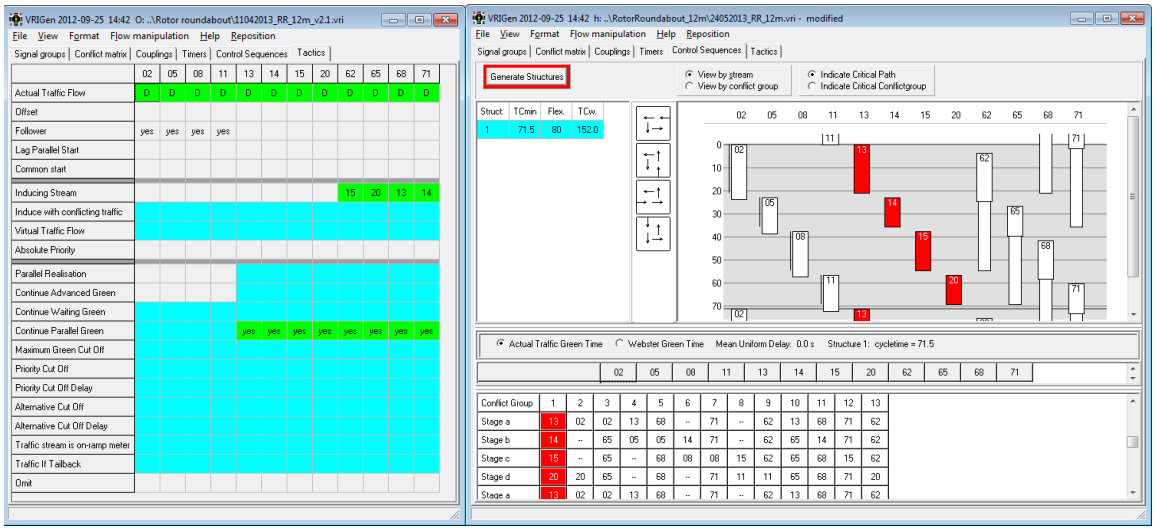


Figure K-13 Tab Tactics (left) and the result of the VRIGen calculation (right)

K.4. Troubleshooting

VISSIM applies TrafCOD to generate a vehicle-actuated traffic control. For this, TrafCOD applies the structure generated by VRIGen and manages (i.e. extends, blocks, omits, etc.) the phases in the structure in a way that suits the actual traffic demand best.

Running TrafCOD with the structure constructed in the previous question (with the spare streams), revealed a major problem: at some moment, the simulation locked in a specific phase and could not transfer to the next phase. Figure K-14 illustrates the problem.

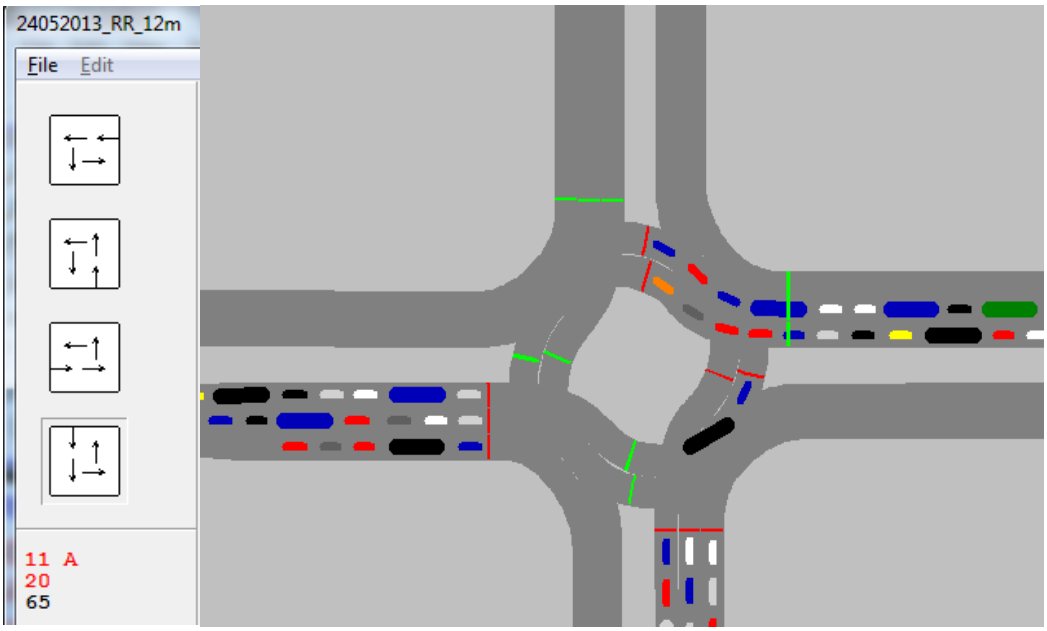


Figure K-14 At some moment, the VISSIM simulation locks in this traffic state

K.4.1. Description of the problem

After having runned for a few simulation hours, the simulation locks in the last phase; that is the phase in which the northern leg (signal group 11) obtains green. The problem occurs in the phase transition from the last phase to the first phase in which the eastern leg obtains green, because signal group 02 also obtains green. The vehicles in 02 face the red interception signal 62. The simulation gets stuck at the moment that signal groups 11 and 02 obtain green at exactly the same moment.

K.4.2. Cause of the problem

The problem is caused by a combination of conflicts and couplings in the structure.

Signal group 20 has a conflict with 02 (see the conflict matrix, Figure K-9). Moreover, signal groups 20 and 11 are coupled (see the couplings, Figure K-10). At the moment the simulation locks, signal groups 11 and 02 both obtain green at exactly the same moment. Signal group 20 [57] will not obtain green as long as 02 has green because of the conflict. Apparently, the conflict with 02 is more important to 20 than the coupling with 11.

[57] *Signal group 20 is an imaginary signal group; in the simulation there are no signal heads added to this signal group. However, the simulation contains detectors added to signal group 20 at the same place as the detectors for signal group 11.*

In the 'locked situation', signal group 11 is in advanced green [58]. It will enter the next green sub phase, as soon as it's coupling with 20 allows it to do so (when 20 obtains green). However, 20 will not obtain green because 02 has green. At that moment, 02 is in parallel green and it will not leave this green sub phase, because 13 has green (02 and 13 are coupled). 13 is in extension green; it will quit this green sub phase as soon as the traffic control transfers to the phase in which 13 obtains green. That will never happen, because the traffic control is stuck in the phase in which the northern leg has green. Therefore, the traffic control will remain in that phase forever (until the end of the simulation).

In other words, 13 obtains extension green because the traffic control has employed the phase in which the northern leg has green. Therefore, 02 obtains green. As long as 02 has green, 20 is blocked. As long as 20 is blocked, 11 will stay in advanced green.

K.4.3. Solution to the problem

The description in the previous section offers several solution directions. The most obvious solutions are to removing one or more couplings and/or conflicts. However, that would harm the structure of the traffic control.

Another solution is to apply a maximum green time, this is possible in the tab Tactics. The lock situation may occur in any phase transition, so the maximum green time should be applied to all signal groups. However, this is a suboptimal solution. On the one hand, it is not an elegant solution, because it does not really solve the problem (the locked situation is still possible, but it will not last). On the other hand, vehicles experience unnecessary delay time as long as the locked situation occurs.

A third (sound) solution direction to prevent 02 from turning green as soon as 11 turns green, is to adjust one of the TrafCOD routines, stated in the stg-file [59]. One of the routines is the blocking criterion, which is assigned to every signal group. For instance, the blocking criterion of 20 is:
B20 = K20+TRG20+G20+L20
The blocking criterion needs to be extended, such that the start green of 20 cannot be blocked if 11 is in advanced green:
B20 = GN11.K20+TRG20+G20+L20
When applying this adjustment to the blocking criteria of all four spare streams, the problem is solved, and the simulation does not end up in the locked situation anymore.

K.5. Three-phase leg-by-leg control – with spare streams

The star roundabout is suitable for a three-phase leg-by-leg control. In this section, the traffic control will be constructed by means of VRIGen, comparable to the construction of the four-phase leg-by-leg control for the rotor roundabout. Again, all tabs in VRIGen will be dealt with in.

K.5.1. Signal groups

The straight-ahead signal groups on the approach legs (02, 05 and 08) are incorporated in the structure. The right- and left-turning traffic streams are represented by the main signal groups. The interception signal groups are 65, 68 and 71, see Figure K-15.

---

[58] *From here on, it is necessary to distinguish between 'phase' as in: one of the four stages in the traffic control, and 'phase' as in: one of the three phase a signal group can employ (green, yellow, red). For an extensive description of these three phases and the five green sub phases, the reader is referred to the lecture notes CIE4822 (Muller, 2011).*

[59] *In the .stg-file, all information on the structure and tactics are laid down, as well as all TrafCOD routines. For an extensive description of the TrafCOD routines, the reader is referred to Muller et al. (2011).*

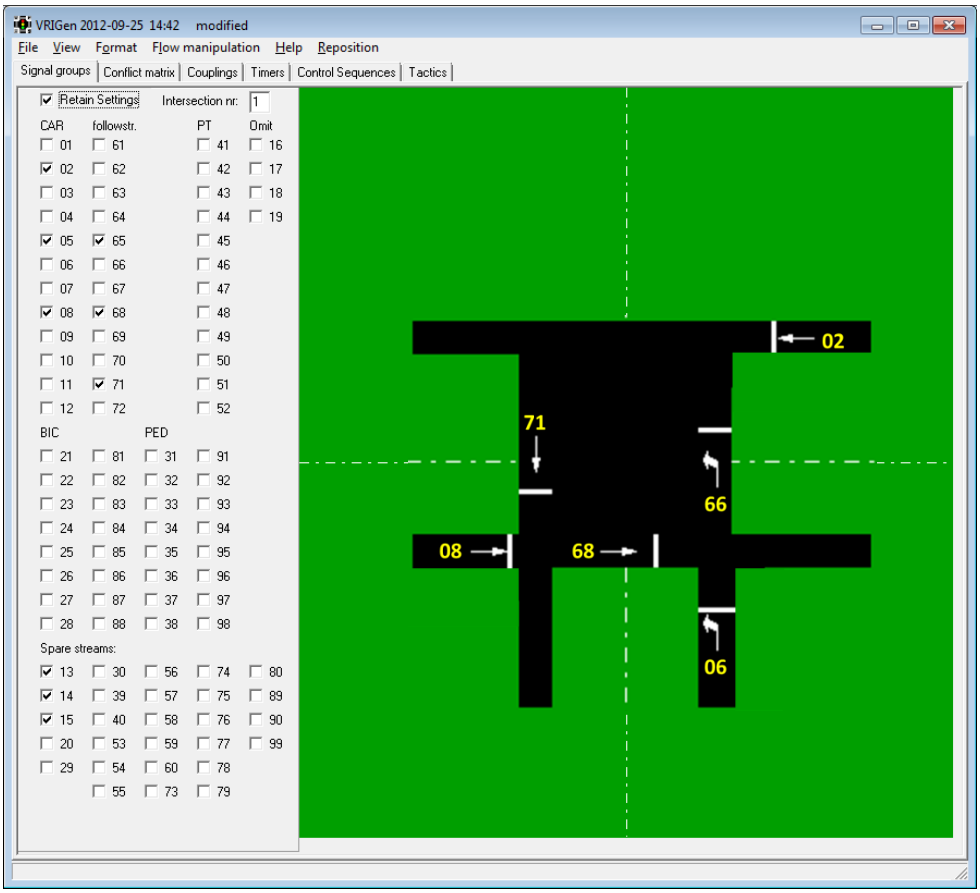


Figure K-15 Traffic streams on the star roundabout

K.5.2. Conflict matrix

Figure K-16 shows the conflict matrix. There are three real conflicts (coloured green). One conflict assures that VRIGen produces leg-by-leg control programs (13/15) and three conflicts relate the spare streams to the main signals (02/15, 05/13 and 08/14).

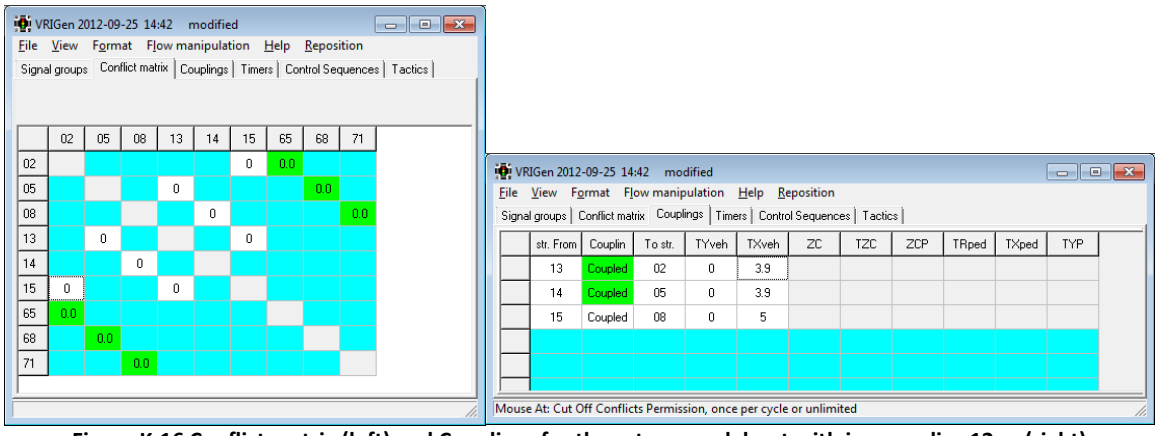


Figure K-16 Conflict matrix (left) and Couplings for the rotor roundabout with inner radius 12 m (right)

K.5.3. Couplings

On the star roundabout, the green phase overlaps are not equal for every phase transition. By means of the simplified acceleration model (see appendix F), it was calculated that the green phase overlap plus yellow time from the western leg to the eastern leg is 5 s. The green phase overlap plus yellow time for the other transitions is 3.9 s. The phase overlap is incorporated in Couplings as in Figure K-16.

K.5.4. Timers

Again, the default settings in the tab Timers are adopted, except for the Yellow use. These values are set to 2.0 s (default 1.0 s), in accordance with Muller (2011, lecture notes CIE4822 p.66).

K.5.5. Control sequences

The settings in Control Sequences for the three-phase control differ from the settings for the four-phase control with respect to the total flow. A total flow of 3800 pcu/h is applied, with demand pattern 100 for three legs.

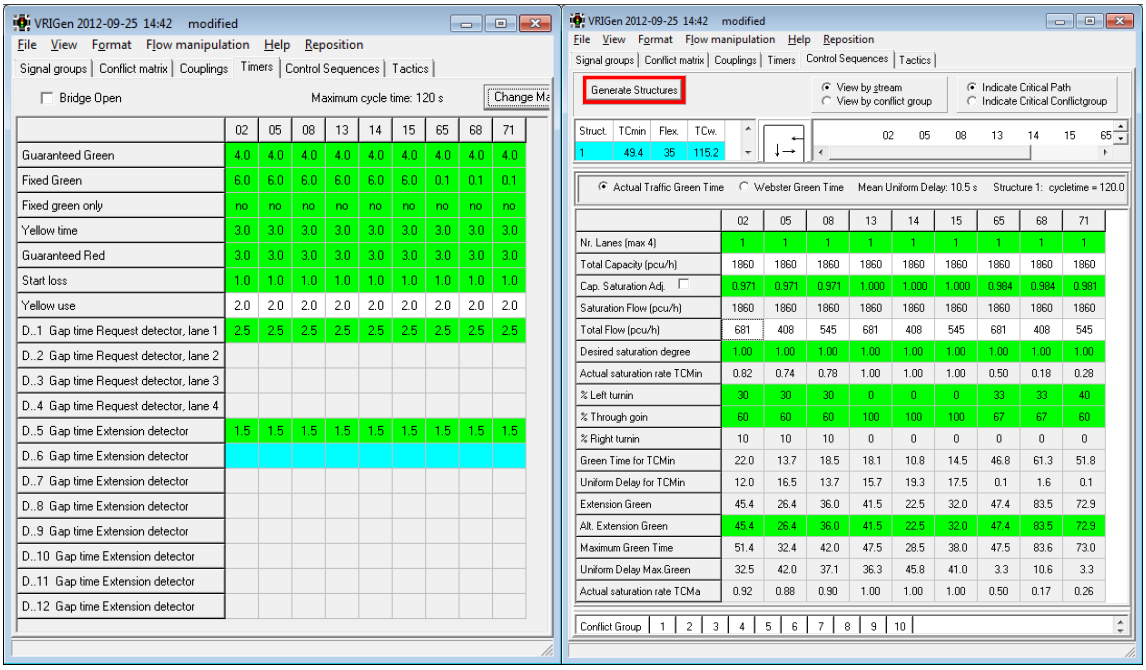


Figure K-17 Tab Timers (left) and Control sequences (right)

K.5.6. Tactics

With respect to the tab Tactics, the default settings are not changed.

K.5.7. Resulting control program

Figure K-18 shows the resulting control program. This is the desired control program, with a phase overlap of 5 s from 08 (western leg) to 02 (eastern leg) and a phase overlap of 3.9 s from 02 to 05 and from 05 to 08.

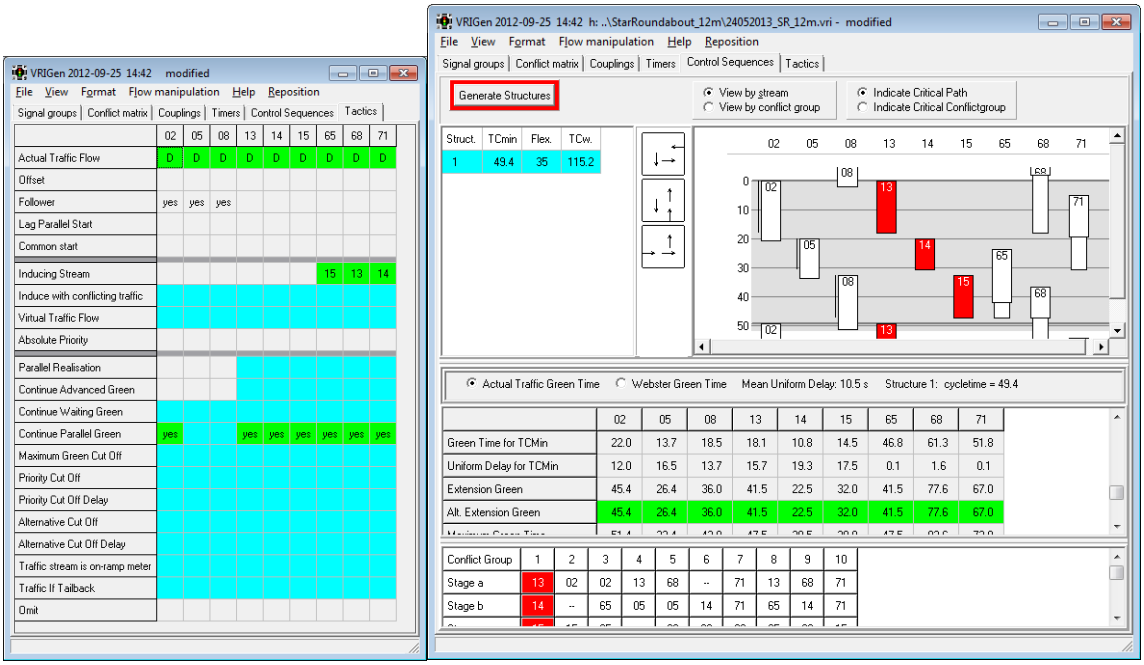


Figure K-18 Tab Tactics (left) and the output of VRIGen: structure of the three-phase leg-by-leg control (right)

K.6. Four-leg two-phase control

This section explains the construction of the two-phase control by means of VRIGen. The two-phase control can be applied to the (partial) turbo circle. The construction of two-phase control is very similar to the VRIGen settings discussed in the first section. Therefore, this section will not address all tabs in VRIGen. Only the tabs that differ from the settings in the first section will be addressed.

K.6.1. Conflict matrix

The conflict matrix for the two-phase control only contains real conflicts: no extra conflicts are necessary to generate a leg-by-leg control, see Figure K-19 (left).

By means of the method of Muller *et al.* (2004), addressed in the appendix E, the clearance times on the (partial) turbo circle can be calculated. The clearance times for all conflicts are calculated to be zero. This holds for the partial turbo circle, the four-leg turbo circle and the three-leg turbo circle, with any value for the inscribed radius.

K.6.2. Couplings

The Couplings tab only incorporates the couplings between every pair of main signal and interception signal, see Figure K-19. The couplings between the main signal and the second interception signal (for the left-turns; 03/71, 06/62, 09/65 and 12/68) are not incorporated, because the left-turning vehicles have to queue up on the circle in front of the second interception signal.

On the (partial) turbo circle, the main signals should turn green later than the interception signals, in order to have the queued left-turning vehicles from the previous phase flowing off. The value for *TYveh* determines the time interval between the start green of the interception signal and the start green of the accessory main signal. *TYveh* depends on the inscribed radius of the turbo circle, and is calculated in the following intermezzo.

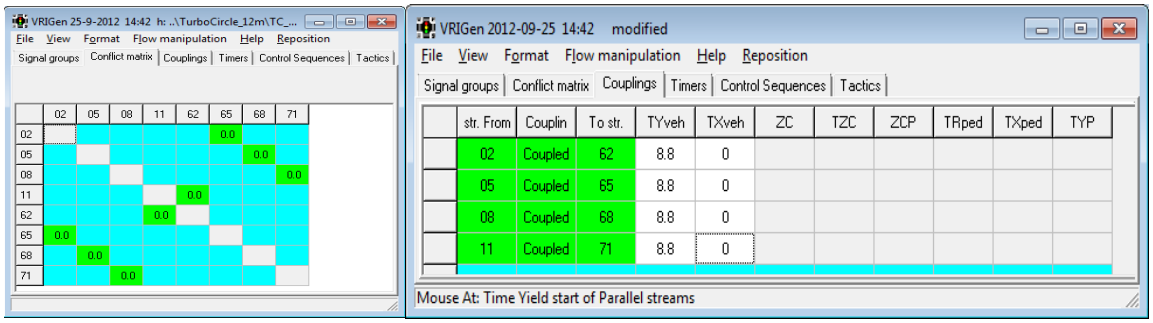


Figure K-19 Conflict matrix (left) and Couplings for the turbo circle with an inscribed radius of 12 m (right)

- Intermezzo: exit time of queued vehicles -

During every phase transition, the queued left-turning vehicles have to clear the conflict area with the entrance leg in the next stage. The queued vehicles need time to do so, therefore the traffic control should accommodate for a time lag between start green of an interception signal and start green of the accessory main signal. In this intermezzo, that time lag will be calculated to be two seconds.

The time lag between start green of the interception signal and start green of the main signal can be calculated by means of the following illustration of the phase transition:

- Imagine the eastern leg has green (in that case, the western leg has green as well);
- The western leg obtains red to enable the green phase for 71 to begin, which is fed by stream 63 (which is in turn fed by stream 03, obtaining red). A queue of vehicles waits in front of the stop line joining stream 71;
- The left-turning vehicles waiting in front of interception signal 71 obtain green after the western leg obtained red and the clearance time $t_{clearance}$ (in this case, zero seconds; see the intermezzo in section K.2) has passed;
- From the moment the first vehicle accelerates from stop line 71, a shockwave starts to move backward in the queue of vehicles;
- After a certain time period $t_{shockwave}$, the wave reaches the back of the tail and the last vehicle starts to accelerate;
- After a certain time period $t_{02,11}$, the last vehicle reaches the conflict area with the northern leg (the time it takes to cover the distance from stop line 02 to the conflict area with 11 $s_{02,11}$);
- The northern leg obtains green after the last vehicle in the left-turning stream has cleared the conflict area. The green phase can start $t_{earlygreen}$ earlier, because the first vehicle needs to cross the distance between the stop line and the conflict area.

The following sections will elaborate on $t_{shockwave}$, $t_{02,11}$ and $t_{earlygreen}$ in order to calculate the time lag between start green of the interception signal 71 and start green of the accessory main signal 11.

Shockwave time $t_{shockwave}$

The time it takes the shockwave to reach the tail of the queue highly depends on the reaction times of the drivers in the queue. This project lacks time and money to perform a study into the speed of the shockwave moving backward; instead, a rule of thumb from traffic flow theory will be applied. This rule of thumb states that a shockwave moves upstream at a speed of ca. 20 km/h (Hoogendoorn, 2011).

In appendix D (Geometrical designs) the maximum queue length on the turbo circle are calculated, see Figure K-20 and Table K-1.

Now, the time it takes the shockwave to reach the tail of the queue can be calculated by means of Equation K-1; Table K-1 shows the results.

$$t_{shockwave} = \frac{A + B}{v_{shockwave}}$$

Equation K-1

where:

$t_{shockwave}$ = the time it takes the shockwave to reach the tail of the queue [s];
A = the queuing length [m];
$v_{shockwave}$ = speed of the shockwave moving upstream [m/s].

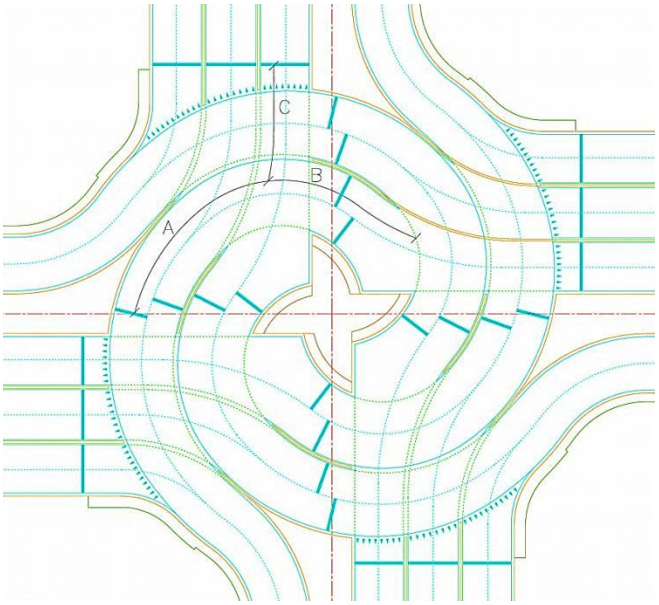


Figure K-20 Indication of the length of circulatory road segments, input to the analytical approach

Table K-1 Values for A and B for the turbo circle

Inner radius	A	B	C	$t_{shockwave}$	$t_{02,11}$	$t_{earlygreen}$	TYveh
12 m	31 m	14 m	15 m	9.9 s	2.3 s	3.4 s	8.8 s
20 m	43 m	36 m	15 m	14.2 s	3.7 s	3.4 s	14.5 s
30 m	55 m	50 m	15 m	18.9 s	4.3 s	3.4 s	19.8 s

Circle clearance time $t_{02,11}$

The circle clearance time $t_{02,11}$ is the time it takes the queued vehicles in stream 03 to clear the conflict area with the leg obtaining green in the next phase: to clear distance B in Figure K-20. Over that distance, vehicles have to accelerate from standing still (in the worst case; i.e. for calculating the maximum value of the time lag between start green 71 and start green 11). Therefore, the acceleration model from appendix F can be applied. The results are shown in Table K-1 in the column $t_{02,11}$.

Early startgreen $t_{earlygreen}$

$t_{earlygreen}$ is defined as the time lag between start green of the main signal and the first departing vehicle entering the conflict area with the queued vehicles. The first departing vehicle accelerates from standing still and crosses distance C in Figure K-20. By means of appendix F, one can calculate the time it takes the vehicle to cross distance C. One second reaction time has to be added to obtain $t_{earlygreen}$.

Time lag *TYveh*

Now, *TYveh* can be calculated by means of Equation K-2; the values are shown in Table K-1.

$$TYveh = t_{shockwave} + t_{02,11} + t_{earlygreen}$$

Equation K-2

- End of intermezzo -

K.6.3. Resulting control program

Figure K-21 shows the resulting control program. This is the two-phase control, applicable to the four-leg (partial) turbo circle.

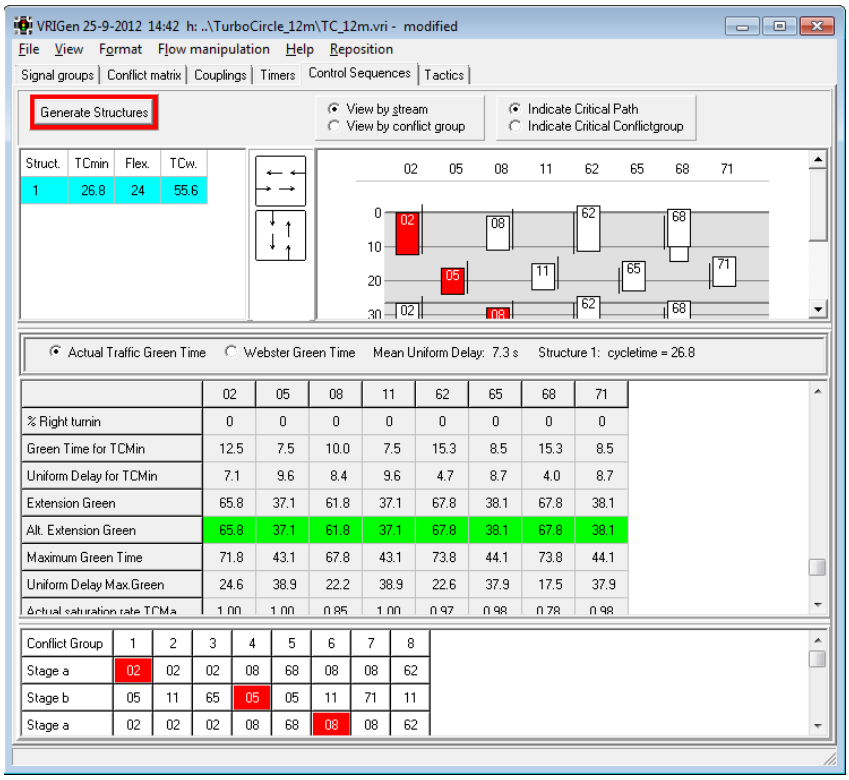


Figure K-21 The result of the VRIGen calculation in tab Control Sequences

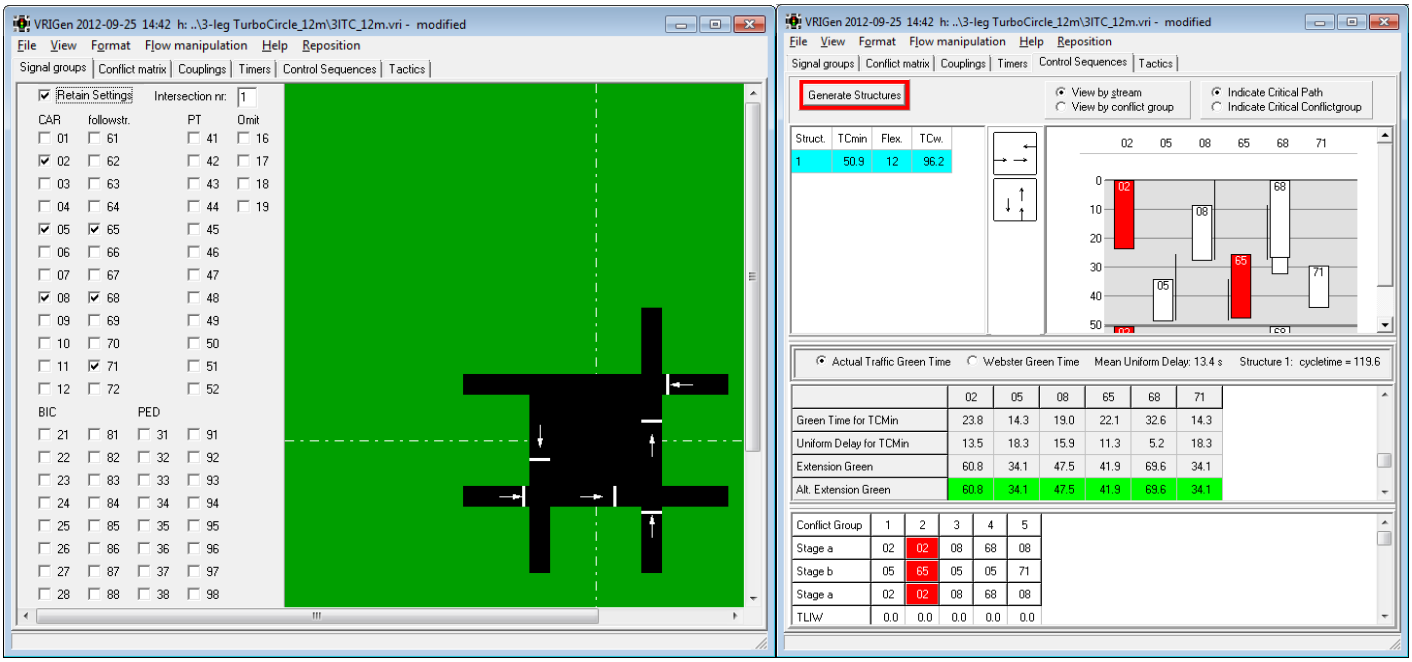


Figure K-22 The Signal groups (left) and the resulting structure for the three-leg turbo circle with an inscribed radius of 12 m (right)

K.7. Three-leg two-phase control

The VRIGen model of the three-leg two-phase control (for the three-leg turbo circle) is in many ways similar to the four-phase control. The most prominent difference is the amount and configuration of traffic streams. These affect the Signals groups (Figure K-22 left), the Conflict matrix (Figure K-23 left), the Couplings (Figure K-23 right) and the output (Figure K-22 right).

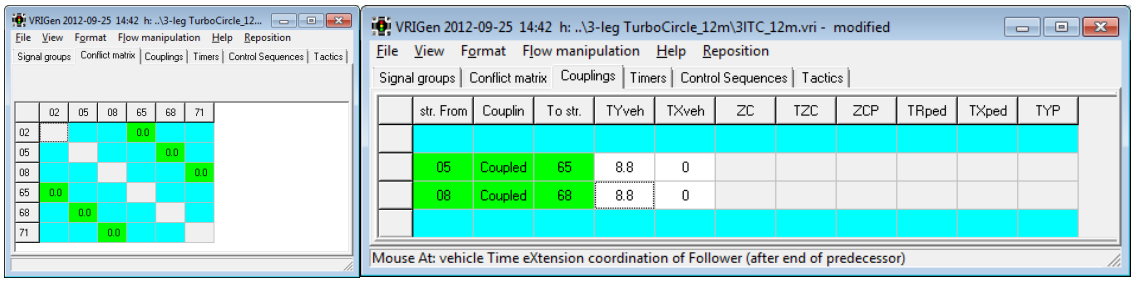


Figure K-23 The Conflict matrix (left) and the Couplings for the three-leg turbo circle with an inscribed radius of 12 m (right)

Appendix L: VISSIM model development

Appendix K described the development of the VRIGen model. The output of VRIGen – the structure of the control program – is input to the VISSIM model. This appendix addresses the models made by means of VISSIM. The appendix is written such, that the reader with basic knowledge of VISSIM should be able to reproduce the models.

The first section addresses all elements within the network: links, nodes, parking lots, priority rules, reduced speed areas, etc. The second section discusses the Base Data. Here, the elementary behaviour of vehicles in the network can be customized. The default settings in VISSIM show some remarkable aspects, especially with respect to the acceleration behaviour. The third section explains how the traffic demand can be added to the simulation by means of a dynamic assignment. The fourth section reveals the communication among VISSIM, TrafCOD and the control structure generated by VRIGen. The evaluation functionalities are discussed in the fifth section.

L.1. Network

L.1.1. Links and connectors

Before designing the rotor roundabout itself, the designer loads a graphic file into the VISSIM model on which he can 'draw' the network. This ensures that the geometrical dimensions of the roundabout are correctly modelled. The geometrical designs described in appendix D, are used in the VISSIM simulations. Figure L-1 shows a drawing of the rotor roundabout, with the centre lines of the links and connectors forming the structure of the roundabout.

The circulatory roadways are modelled by means of connectors, connecting the short links at each of the decision points (the small blue lines at the points where connectors join and diverge; there are twelve of them). There are various other ways to model the road sections. For instance, the road pavement on the roundabout can be modelled by means of links instead of connectors. This choice has been made randomly; it does not influence the output of the model.

The entrance legs accommodate each direction on a separate link (Link 1, 2 and 3). These road sections – where no lane changes are possible – are 50 m long. Figure L-2 shows that upstream, the separate links are connected to one link consisting of three lanes (Link 102). The three-lane link is 1000 m long and the characteristics of the connector are such that drivers try to change lanes 1000 m upstream of the connector. This value is so large, because vehicles may block a 50-m link if they choose the correct lane too late. Of course, these remarks also count for the other three legs.

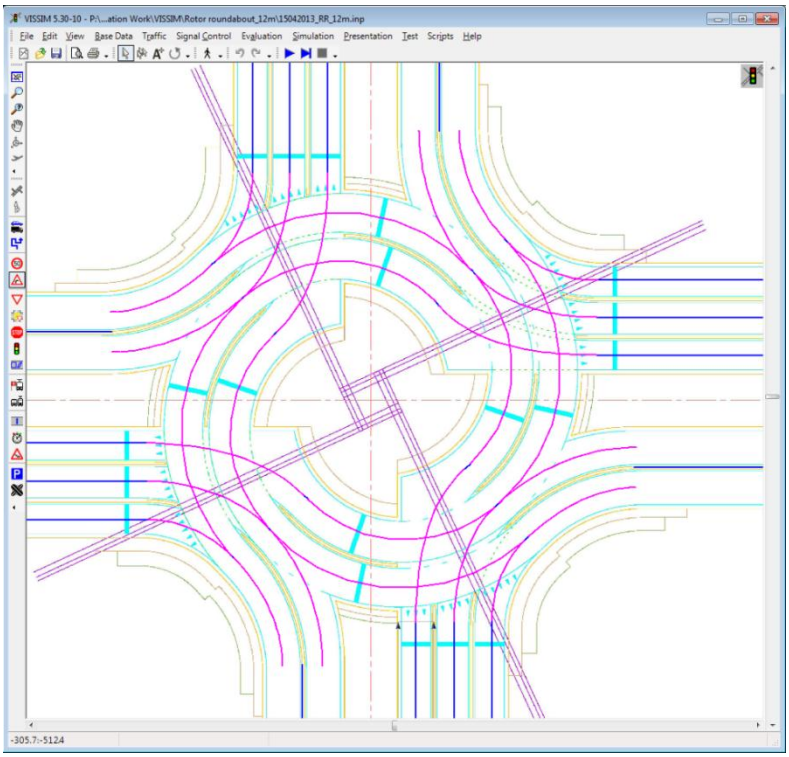


Figure L-1 Links and connectors of the rotor roundabout

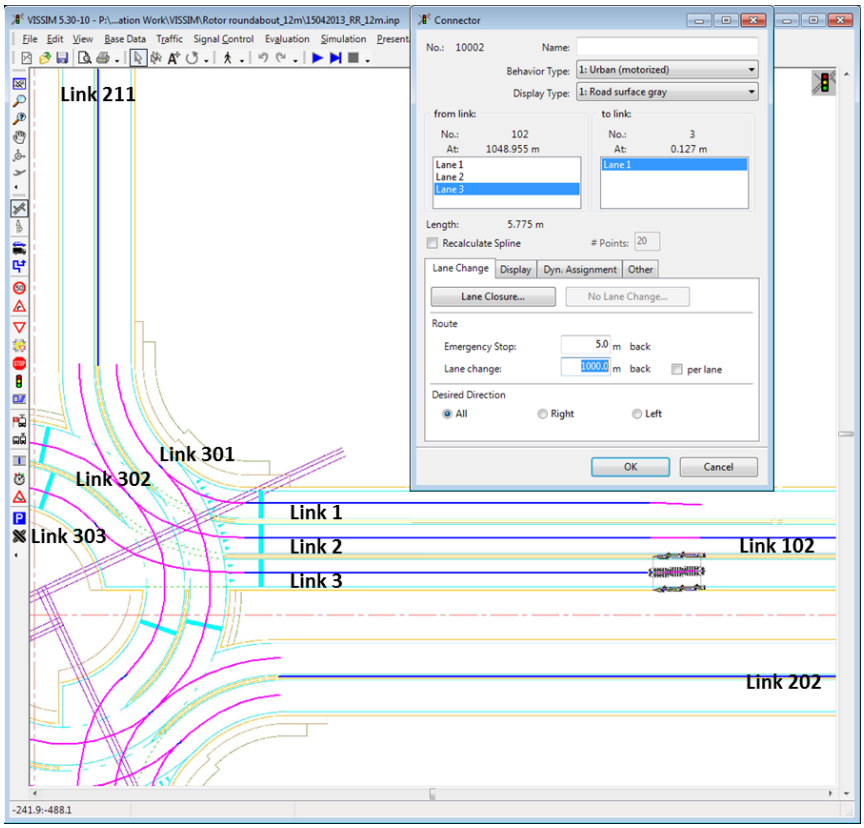


Figure L-2 Drivers try to change lanes 1000 m upstream of the connector

L.1.2. Nodes and parking lots

The nodes are numbered logically, depicted by Figure L-3. Four nodes (Nodes 2, 5, 8 and 11) also appear in the traffic demand matrix. Node 1 (the intersection itself) ensures that the model recognizes the correct route for each pair of origin and destination (OD-pair). The parking lots modelled such, that all traffic leave the parking lot with a desired speed of circa 50 km/h.

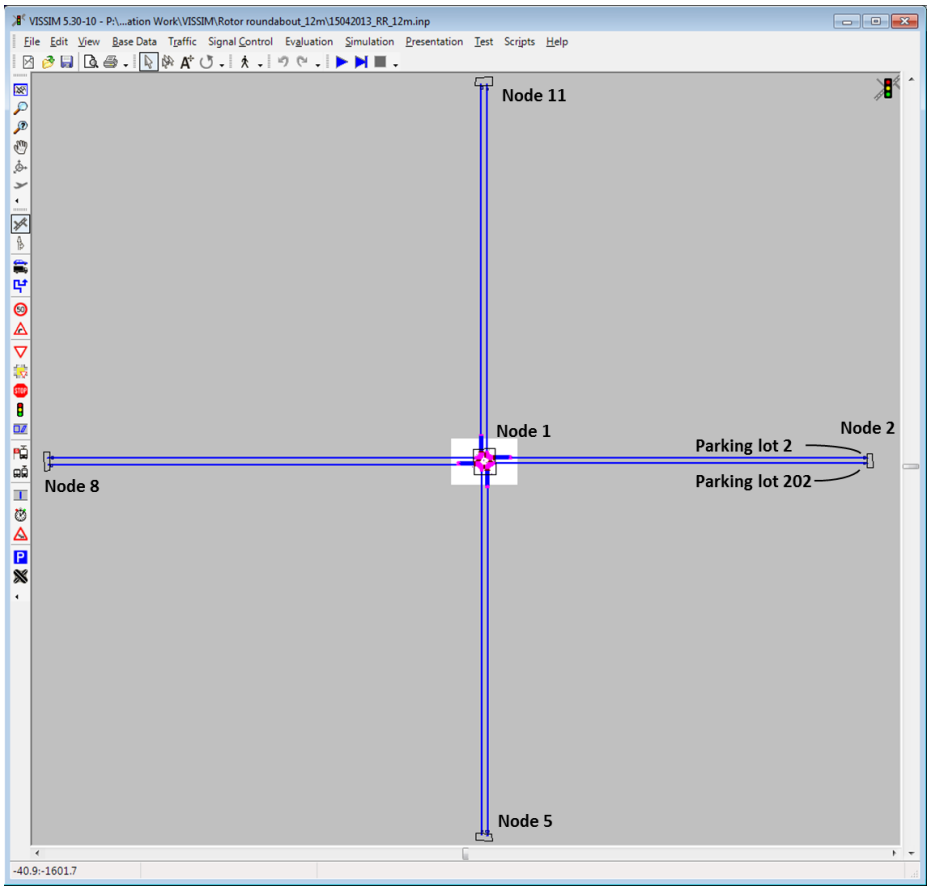


Figure L-3 Numbering of the zones and parking lots

Within Node 1, some edges have to be closed in order to ensure the desired lane change behaviour. Section 3.2.3 explains the reason for this. The geometry of the rotor roundabout allows the right approach lane to serve only right-turning traffic. The middle lane serves right-turning and straight-ahead traffic and the left lane serves straight-ahead and left-turning traffic. If no edges in Node 1 are closed, the model adopts a highly inefficient lane choice behaviour, because VISSIM distributes vehicles randomly over the lanes, as long as the chosen lane is on a route from origin to destination of course. For instance, it might occur that all right-turning vehicles use the middle lane, leaving the right lane unused and unnecessarily overloading the middle lane. This is one of the drawbacks of VISSIM: approaching vehicles do not consider the actual queue length on each of the approach lanes, while in reality drivers do.

L.1.3. Signal heads and detectors

Figure L-4 shows that the number of the signal heads and detectors coincides with the standard coding of traffic streams (see Figure L-44). The VRIGen model does not invoke the right-turning and left-turning traffic streams as separate traffic streams; see appendix K. Therefore, the detector numbering does not strictly coincide with the standard coding; every couple of three detectors on the same leg have the same code. For instance: on all three approach lanes on the eastern leg, the request detectors have coding

1021 and the extension detectors have coding 1022 [60]. The VRIGen model invokes spare streams 13, 14, 15 and 20 on the eastern, southern, western and northern legs respectively. Therefore, the request detectors 1131 and the request detectors 1021 have the same location; similarly, the extension detectors 1132 and the extension detectors 1022 have the same location. This also counts for the other approach legs.

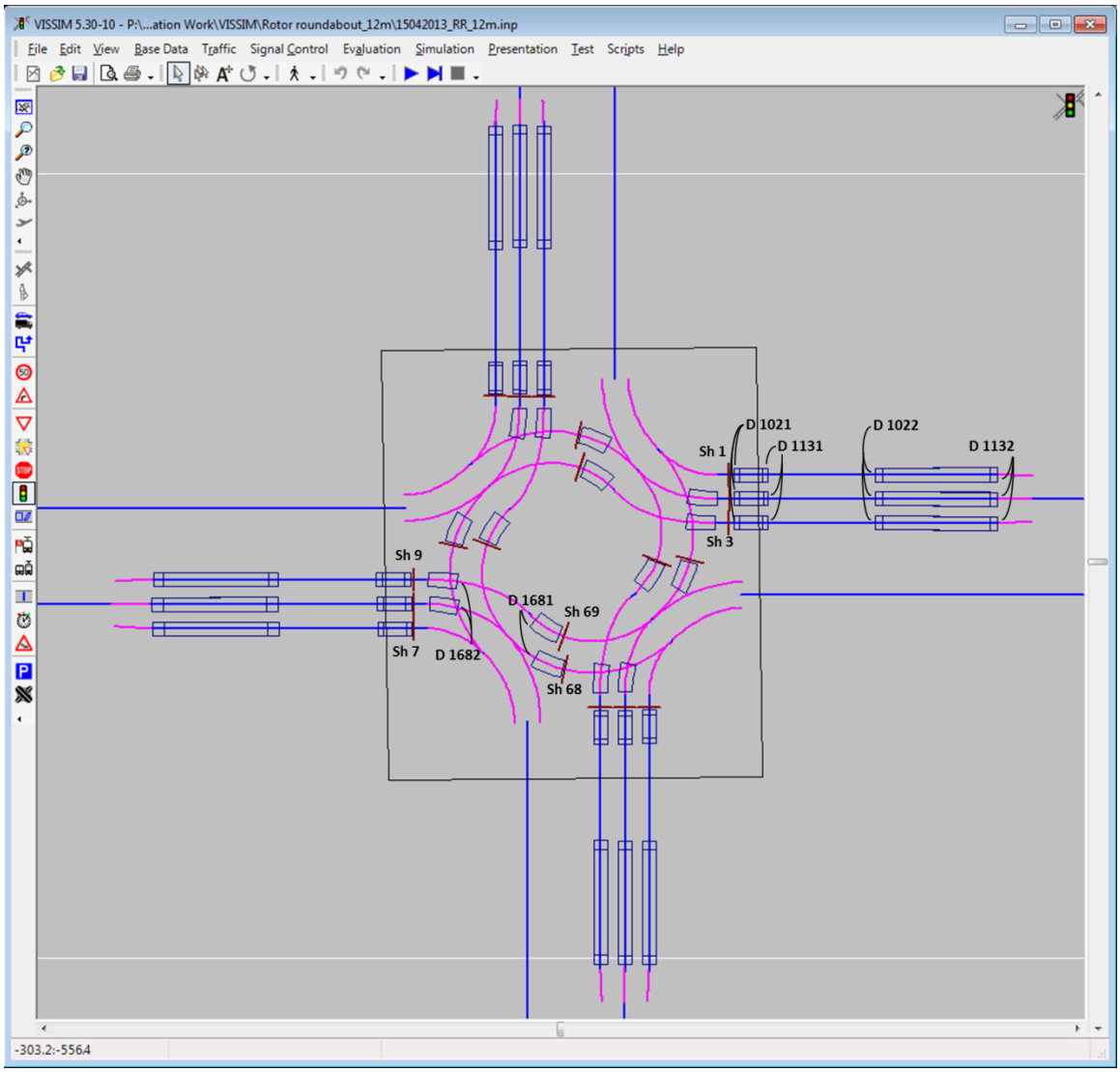


Figure L-4 The numbering of the signal heads (Sh) and detectors (D)

[60] *The middle two characters represent the stream. The coding of the detectors is standardized, in order to secure the correct communication between VISSIM and TrafCOD. The first character (1) represents the number of the intersection; the second and third characters (02) represent the traffic stream; the fourth character (1 and 2) represents the detector number.*

L.1.4. Reduced speed areas

Determined by the settings of the parking lots, all vehicles arrive at the intersection with a desired speed of circa 50 km/h. However, the vehicles do not cross the intersection at that desired speed. The reduced speed areas indicate the road stretches on which the desired speed is lower. The desired speed in the curves of the intersection depends on the radius of the curve according to the following relationship (CROW, 1998, p.40):

$$v_{desired} = 7.4 * \sqrt{R_{curve}}$$

Equation L-1

where:
$v_{desired}$ = desired speed [km/h];
R_{curve} = radius of the driving curve [m].

This formula yields the following tables.

Table L-1 Driving curve radii and desired speed values for the rotor roundabout

		R_{curve}	$v_{desired}$
Rotor roundabout $R_{inner} = 12\ m$	Right approach lane	12.00 m	25 km/h
	Middle approach lane	17.60 m	30 km/h
	Left approach lane	22.50 m	35 km/h
	Right circulatory lane	17.60 m	30 km/h
	Left circulatory lane	12.00 m	25 km/h
	Right exit lane	15.00 m	30 km/h
	Left exit lane	20.20 m	35 km/h
Rotor roundabout $R_{inner} = 20\ m$	Right approach lane	12.00 m	25 km/h
	Middle approach lane	17.60 m	30 km/h
	Left approach lane	22.50 m	35 km/h
	Right circulatory lane	24.70 m	35 km/h
	Left circulatory lane	20.00 m	30 km/h
	Right exit lane	15.00 m	30 km/h
	Left exit lane	20.20 m	35 km/h

Table L-2 Driving curve radii and desired speed values for the star roundabout

		R_{curve}	$v_{desired}$
Star roundabout $R_{inner} = 12\ m$	Right approach lane	12.00 m	25 km/h
	Middle approach lane	17.60 m	30 km/h
	Left approach lane	22.50 m	35 km/h
	Right circulatory lane	22.50 m	35 km/h
	Middle circulatory lane	17.60 m	30 km/h
	Left circulatory lane	12.00 m	25 km/h
	Right exit lane	15.00 m	30 km/h
	Left exit lane	20.20 m	35 km/h
Star roundabout $R_{inner} = 20\ m$	Right approach lane	12.00 m	25 km/h
	Middle approach lane	17.60 m	30 km/h
	Left approach lane	22.50 m	35 km/h
	Right circulatory lane	29.12 m	40 km/h
	Middle circulatory lane	24.70 m	35 km/h
	Left circulatory lane	20.00 m	30 km/h
	Right exit lane	15.00 m	30 km/h
	Left exit lane	20.20 m	35 km/h

Table L-3 Driving curve radii and desired speed values for the partial turbo circle

		R_{curve}	$v_{desired}$
Partial turbo circle $R_{inner} = 12\ m$	Right approach lane	12.00 m	25 km/h
	Middle approach lane	17.60 m	30 km/h
	Left approach lane	22.50 m	35 km/h
	Right circulatory lane	22.50 m	35 km/h
	Middle circulatory lane	17.60 m	30 km/h
	Left circulatory lane	12.00 m	25 km/h
	Right exit lane	15.00 m	30 km/h
	Left exit lane	20.20 m	35 km/h
Partial turbo circle $R_{inner} = 20\ m$	Right approach lane	12.00 m	25 km/h
	Middle approach lane	17.60 m	30 km/h
	Left approach lane	22.50 m	35 km/h
	Right circulatory lane	29.00 m	40 km/h
	Middle circulatory lane	24.70 m	35 km/h
	Left circulatory lane	20.00 m	30 km/h
	Right exit lane	15.00 m	30 km/h
	Left exit lane	20.20 m	35 km/h

Table L-4 Driving curve radii and desired speed values for the turbo circle

		R_{curve}	$v_{desired}$
Turbo circle $R_{inner} = 12\ m$	Right approach roadway right	12.00 m	25 km/h
	Right approach roadway left	18.30 m	30 km/h
	Middle approach roadway right	23.90 m	35 km/h
	Middle approach roadway left	28.60 m	40 km/h
	Left approach roadway right	33.30 m	45 km/h
	Left approach roadway left	37.50 m	45 km/h
	Right circulatory roadway right	36.80 m	45 km/h
	Right circulatory roadway left	32.60 m	45 km/h
	Middle circulatory roadway right	27.80 m	40 km/h
	Middle circulatory roadway left	23.00 m	35 km/h
	Left circulatory roadway right	17.30 m	30 km/h
	Left circulatory roadway left	12.00 m	25 km/h
	Exit roadway right	15.00 m	30 km/h
	Exit roadway left	20.80 m	35 km/h
Turbo circle $R_{inner} = 20\ m$	Right approach roadway right	12.00 m	25 km/h
	Right approach roadway left	18.30 m	30 km/h
	Middle approach roadway right	23.90 m	35 km/h
	Middle approach roadway left	28.60 m	40 km/h
	Left approach roadway right	33.30 m	45 km/h
	Left approach roadway left	37.50 m	45 km/h
	Right circulatory roadway right	42.80 m	50 km/h
	Right circulatory roadway left	38.80 m	45 km/h
	Middle circulatory roadway right	34.40 m	45 km/h
	Middle circulatory roadway left	30.10 m	40 km/h
	Left circulatory roadway right	25.10 m	35 km/h
	Left circulatory roadway left	20.00 m	35 km/h
	Exit roadway right	15.00 m	30 km/h
	Exit roadway left	20.80 m	35 km/h

Turbo circle $R_{inner} = 30\ m$	Right approach roadway right	12.00 m	25 km/h
	Right approach roadway left	18.30 m	30 km/h
	Middle approach roadway right	23.90 m	35 km/h
	Middle approach roadway left	28.60 m	40 km/h
	Left approach roadway right	33.30 m	45 km/h
	Left approach roadway left	37.50 m	45 km/h
	Right circulatory roadway right	50.60 m	50 km/h
	Right circulatory roadway left	46.90 m	50 km/h
	Middle circulatory roadway right	42.80 m	50 km/h
	Middle circulatory roadway left	38.80 m	45 km/h
	Left circulatory roadway right	34.40 m	45 km/h
	Left circulatory roadway left	30.00 m	40 km/h
	Exit roadway right	15.00 m	30 km/h
	Exit roadway left	20.80 m	35 km/h

Table L-5 Driving curve radii and desired speed values for the three-leg turbo circle

		R_{curve}	$v_{desired}$
Three-leg turbo circle $R_{inner} = 12\ m$	Right approach roadway right	12.00 m	25 km/h
	Left approach roadway right	12.00 m	25 km/h
	Left approach roadway left	17.60 m	30 km/h
	Right circulatory roadway right	27.80 m	40 km/h
	Right circulatory roadway left	23.00 m	35 km/h
	Left circulatory roadway right	17.30 m	30 km/h
	Left circulatory roadway left	12.00 m	25 km/h
	Exit roadway right	15.00 m	30 km/h
	Exit roadway left	20.80 m	35 km/h
Three-leg turbo circle $R_{inner} = 20\ m$	Right approach roadway right	12.00 m	25 km/h
	Left approach roadway right	12.00 m	25 km/h
	Left approach roadway left	17.60 m	30 km/h
	Right circulatory roadway right	34.40 m	45 km/h
	Right circulatory roadway left	30.10 m	40 km/h
	Left circulatory roadway right	25.10 m	35 km/h
	Left circulatory roadway left	20.00 m	35 km/h
	Exit roadway right	15.00 m	30 km/h
	Exit roadway left	20.80 m	35 km/h
Three-leg turbo circle $R_{inner} = 30\ m$	Right approach roadway right	12.00 m	25 km/h
	Left approach roadway right	12.00 m	25 km/h
	Left approach roadway left	17.60 m	30 km/h
	Right circulatory roadway right	42.80 m	50 km/h
	Right circulatory roadway left	38.80 m	45 km/h
	Left circulatory roadway right	34.40 m	45 km/h
	Left circulatory roadway left	30.00 m	40 km/h
	Exit roadway right	15.00 m	30 km/h
	Exit roadway left	20.80 m	35 km/h

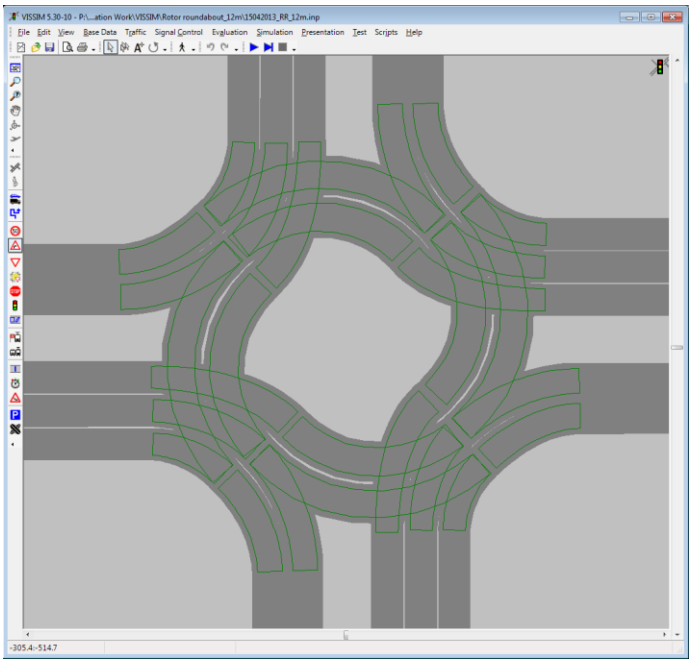


Figure L-5 Locations of the reduced speed areas

L.1.5. Priority rules

On the (partial) turbo circle, a two-phase traffic control can be applied. As a consequence, left-turning vehicles have to queue up on the circle, waiting for the second interception signal showing red. In that case, the simulation might show a traffic situation illustrated by Figure L-6.

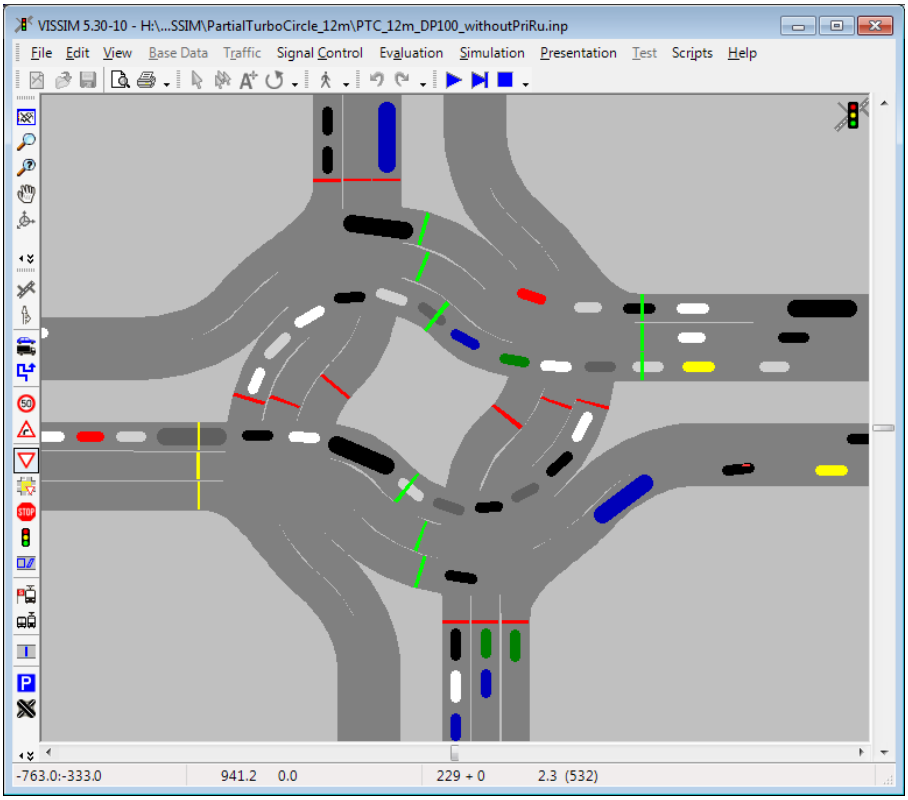


Figure L-6 Left-turning vehicles queuing up and blocking the passage for each other

This situation is highly undesirable, because the left-turning traffic streams block each other. This is called a gridlock: the traffic situation on the circle is such, that the left-turning vehicles cannot escape from the circle anymore.

The solution to this problem is to apply Priority Rules. A Priority Rule in VISSIM prohibits a vehicle to cross a predefined section, if on a predefined road segment the time headway, the distance headway, or the speed is lower than a predefined threshold.

Figure L-7 illustrates the solution. This Priority Rule forces an approaching vehicle to stop in front of the red line (at the edge of the outer circulatory roadway; 4 m beyond the Signal Head) if on the road segment between the green lines (with length 11 m) the speed is smaller than 20.2 km/h. This combination for values of headway and speed is found to be optimal, based on visual assessment of simulations.

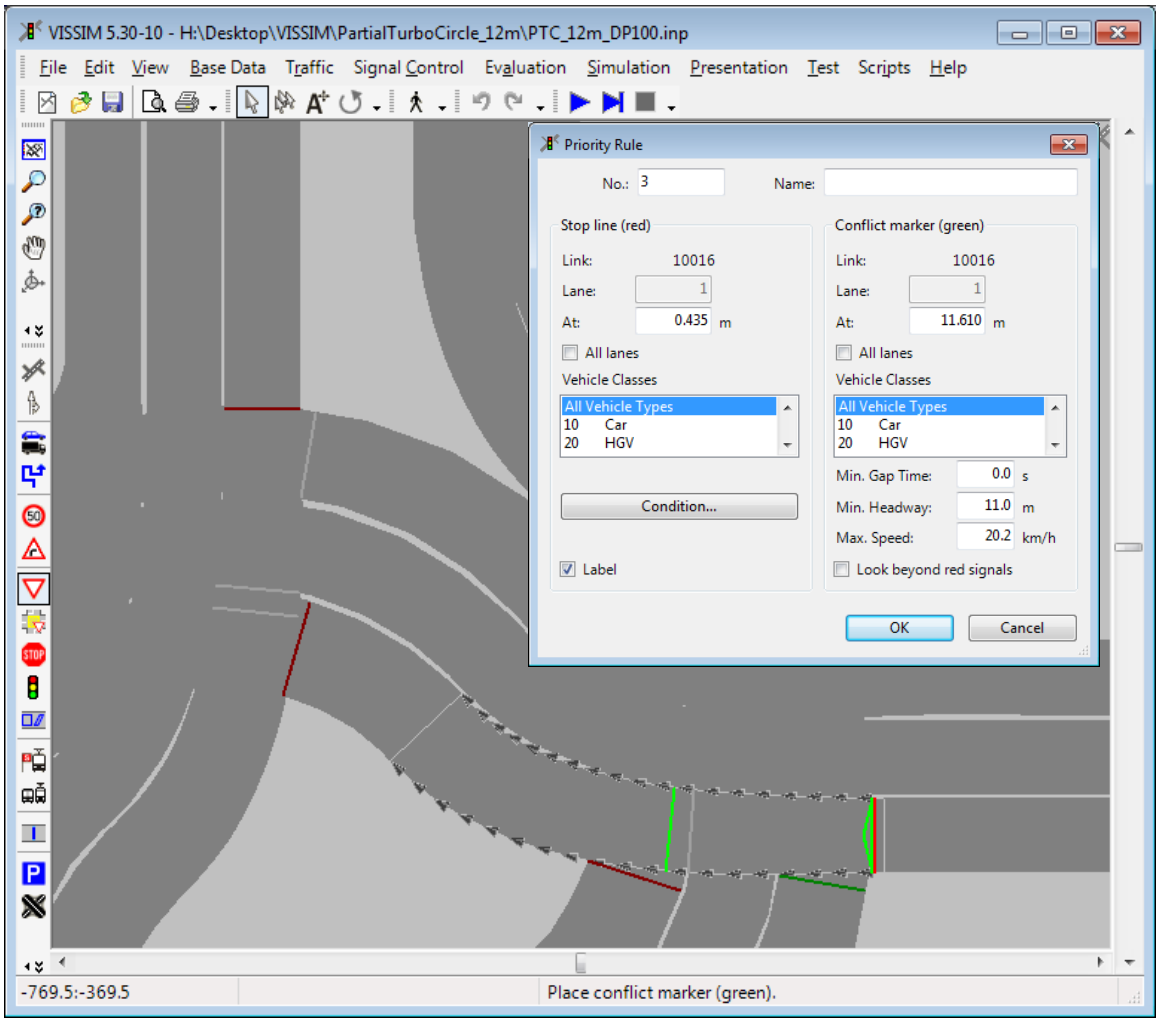


Figure L-7 This priority rule prevents the left-turning streams from causing a gridlock

L.2. Base data

In the pull-down menu Base Data (see Figure L-8) the most important input variables with respect to the microscopic driving behaviour can be defined in the form of functions and distributions. Because the possibilities for validating these functions and distributions on signalized turbo roundabouts are very limited (in fact, absent), the recommended values need to be chosen very carefully. The recommendations should be subject to future research. In this section, the default settings in VISSIM [61] will be discussed and compared with settings used by the Dutch private consultancy companies Oranjewoud (subtracted from a project near the municipality of Barendrecht, The Netherlands), Grontmij (subtracted from a project near the municipality of Leeuwarden, The Netherlands) and Goudappel Coffeng (subtracted from a project near the municipality of 't Harde, The Netherlands), and the German consultancy company Pöyry (subtracted from a project on the Dutch highway A15). Based on this comparison, a set of functions and distributions will be recommended and applied in this project.

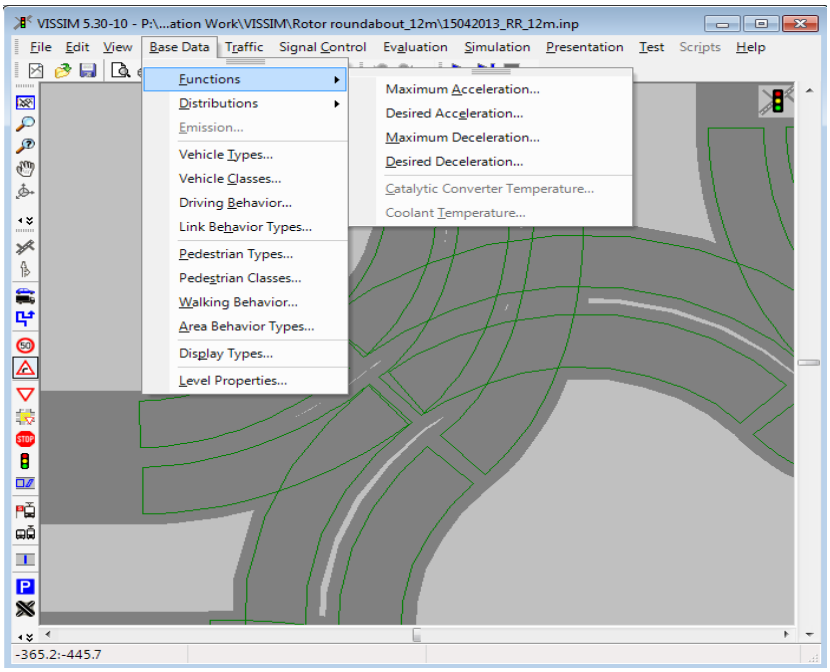


Figure L-8 The pull-down menu Base Data

L.2.1. Vehicle Types

In this menu, the characteristics of the vehicles in the simulated network can be defined. Figure L-9 shows the default Vehicle Types.

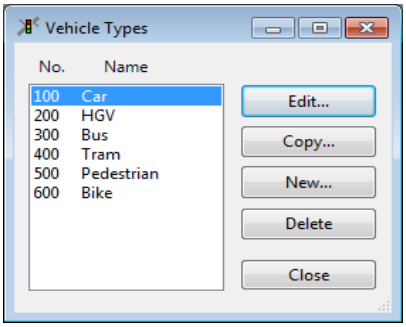


Figure L-9 The menu Vehicle Types

[61] *The default settings in VISSIM are equal in the versions 5.1, 5.2, 5.3 and 5.4. They are all released in 2011.*

In the VISSIM models in this project, public transport, bicycle and pedestrian streams are absent. The only relevant vehicle types are Car and HGV (trucks and lorries). Figure L-10 shows the menu in which characteristics of the vehicle can be changed.

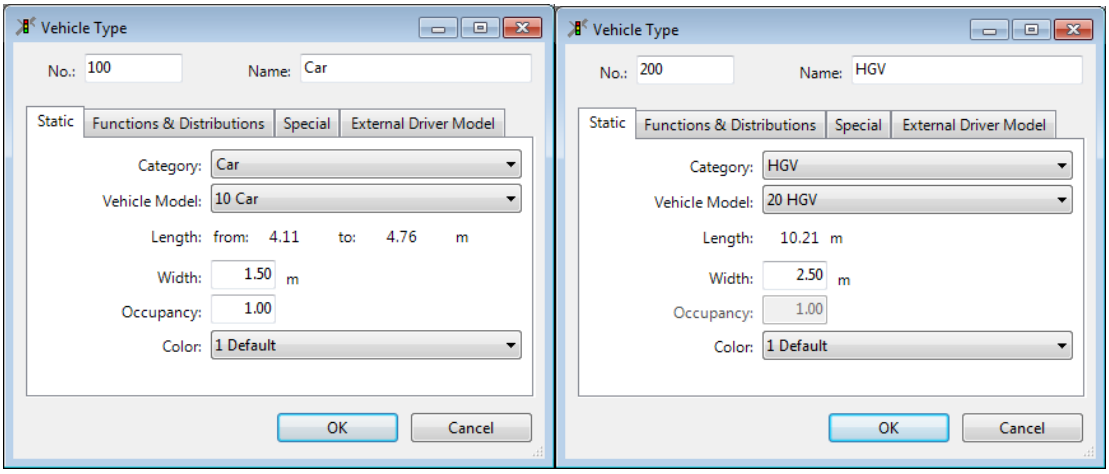


Figure L-10 Vehicle type characteristics for Car and HGV, default settings in VISSIM

In the tab Static, the size of the vehicles can be added. In order to verify these dimensions, one needs a database with information on the fleet on Dutch roads. Unfortunately, such a database is not available; the values can only be judged on their credibility by intuitive sense. The variables shown in Figure L-10 do not show any remarkable values. Furthermore, the default settings are also used in the projects of Oranjewoud, Grontmij, Goudappel Coffeng and Pöyry; the default settings have been applied by various consultancy companies; professional traffic engineers trust these values to be reliable. Therefore, the default values will be used in this project.
In the tab Functions & Distributions, the acceleration, deceleration, power and weight variables can be defined (see next sections). The tabs Special and External Driver Model comprise variables which are not relevant to this project.

L.2.2. Vehicle Classes

In this menu, the Vehicle Classes can be defined. A vehicle class is a selection of the Vehicle Types, which together form a class. These classes can be assigned characteristics in a static assignment. Figure L-11 shows the menu.

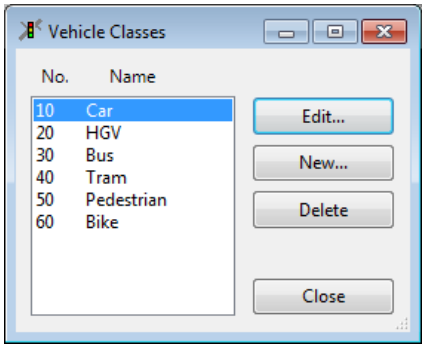


Figure L-11 The menu Vehicle Types

This project applies a dynamic assignment; therefore this functionality is not relevant.

L.2.3. Functions, Maximum Acceleration

In the menu Functions, all parameters that can be expressed as a function of speed can be modified. There are four of these parameters, the first one is Maximum Acceleration.

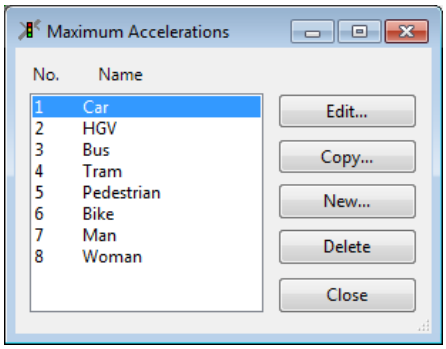


Figure L-12 The menu Maximum Accelerations

As noted in the previous sections, the only relevant modes for this project are Car and HGV. The following figure shows the default distributions in VISSIM.

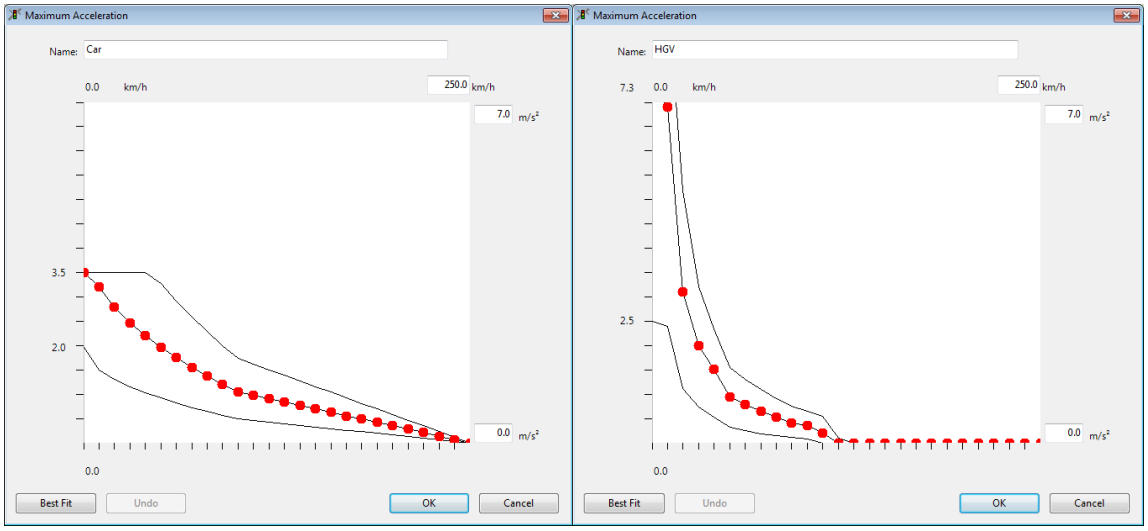


Figure L-13 Maximum Accelerations for Car and HGV, default settings in VISSIM

The default settings for the Maximum Acceleration are also used in the projects of Grontmij and Pöyry. Please take note of the high acceleration values of the mode HGV at low speeds. Those values are even higher than the acceleration values of the mode Car until a speed of circa 20 km/h.

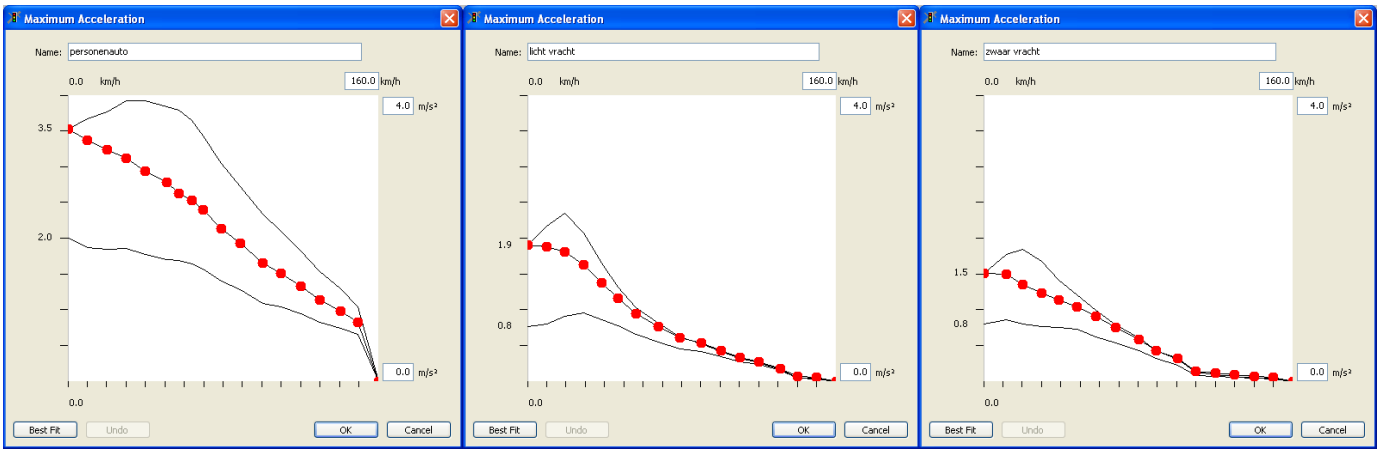


Figure L-14 Maximum Accelerations for Car and trucks, settings in the Oranjewoud project

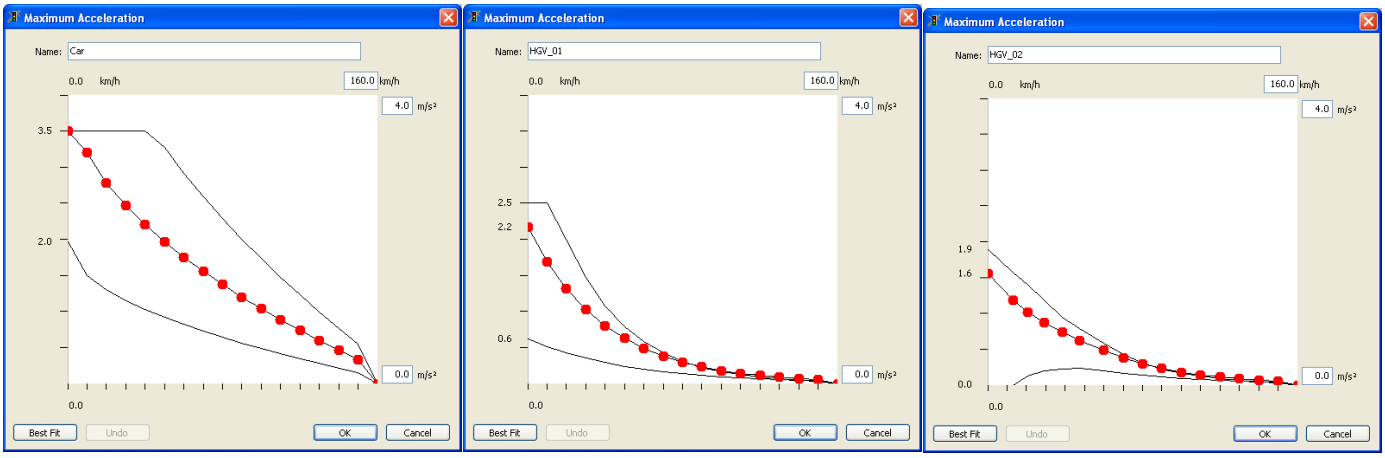


Figure L-15 Maximum Accelerations for Car and trucks, settings in the Goudappel Coffeng project

In the function applied by Goudappel Coffeng for the mode HGV_02, the lower boundary for the maximum acceleration starts at zero. Consequently, trucks that are not able to accelerate from standing still appear in the model, which is highly unlikely.

The Maximum Acceleration functions only become relevant in models with slopes [62] (source: VISSIM 5.30 User Manual, 2011). Regarding the absence of slopes in the models in this project, these functions are irrelevant.

Recommended Maximum Acceleration

The functions for the Maximum Acceleration are not relevant in this project, because there are no slopes in the alignment. Therefore, the default settings will be applied.

[62] *The links can have different values for Begin Height an End Height, to be set in Link Data -> Display.*

L.2.4. Functions, Desired Acceleration

The second parameter that can be expressed as a function of speed is Desired Acceleration.

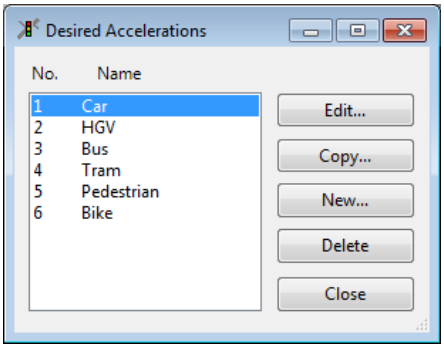


Figure L-16 The menu Desired Accelerations

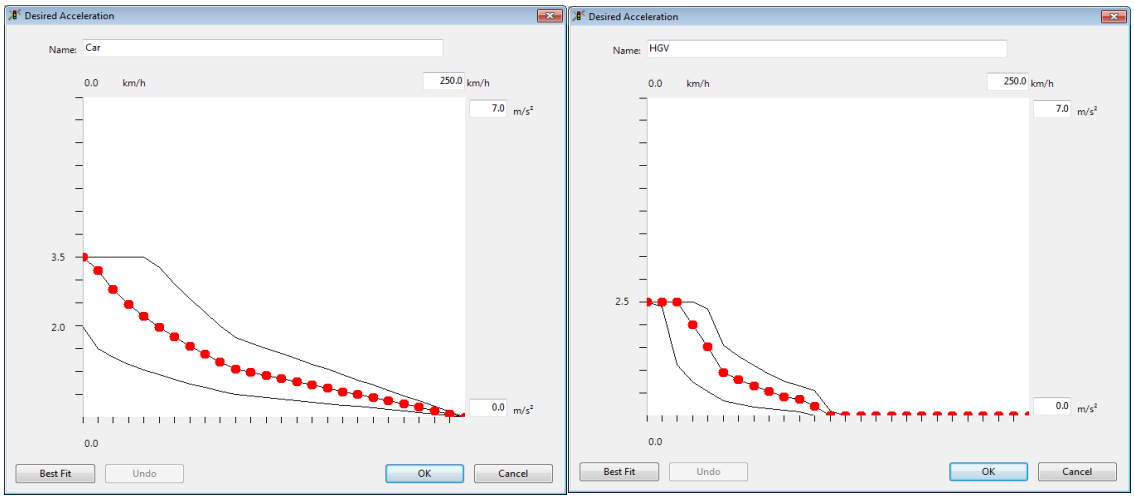


Figure L-17 Desired Accelerations for Car and trucks, default settings in VISSIM

The default settings for the Desired Acceleration are also used in the projects of Grontmij and Pöyry. The acceleration rates of the mode Car are quite high for low values. Field measurements by Grontmij (2001) show that the first vehicle in a queue waiting for a traffic signal accelerates at a rate of 2.5 m/s^2 and the following vehicles accelerate at a rate of 1.0 through 1.5 m/s^2.

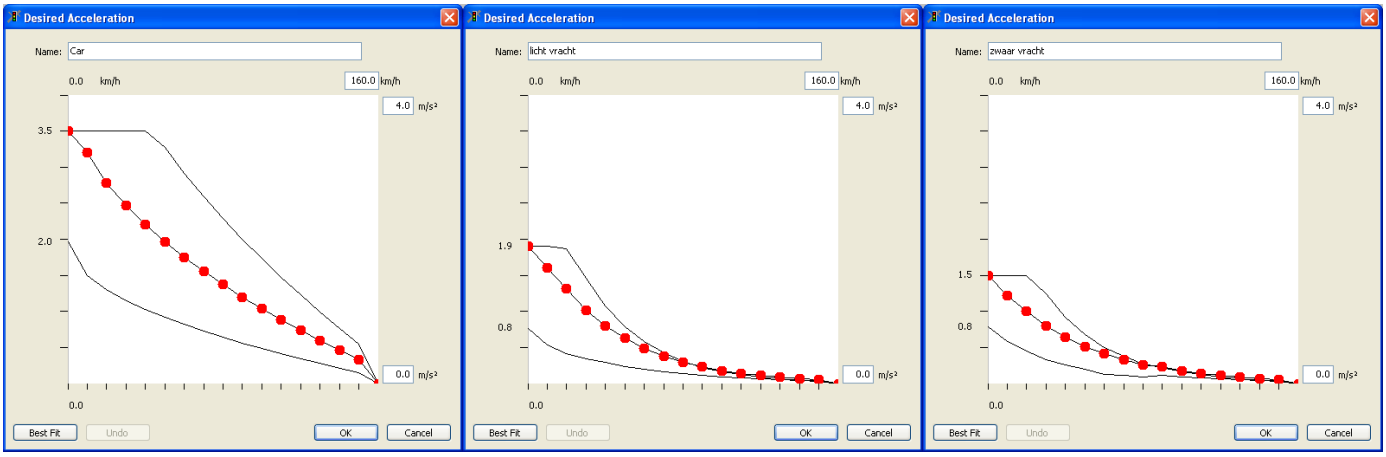


Figure L-18 Desired Accelerations for Car and trucks, settings in the Oranjewoud project

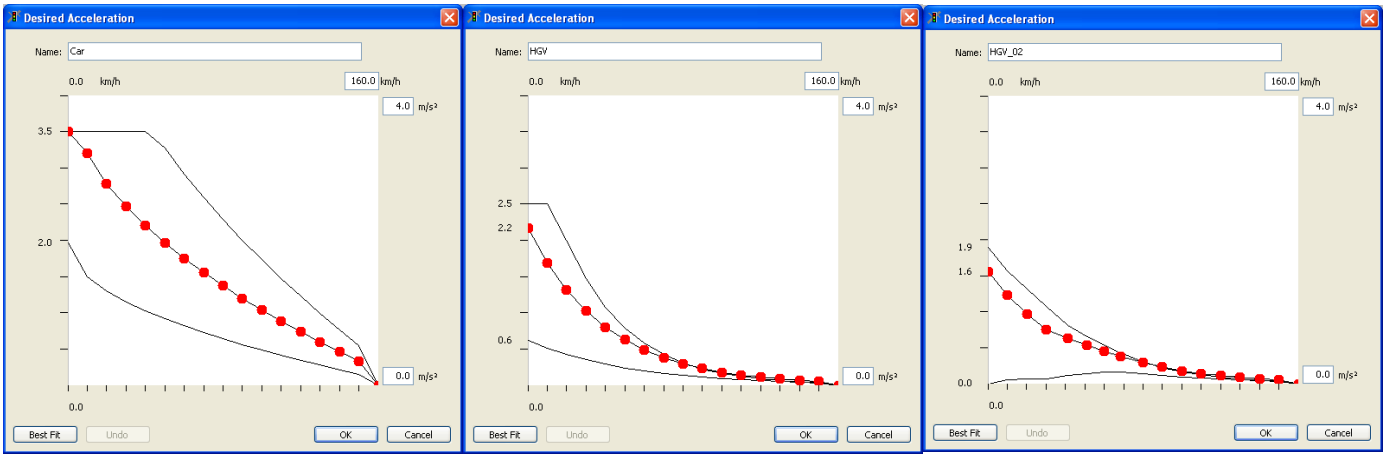


Figure L-19 Desired Accelerations for Car and trucks, settings in the Goudappel Coffeng project

The functions applied by Oranjewoud and Goudappel Coffeng differ slightly from the default settings. These functions are disputable. Most person cars with five or six manual gears obtain the highest acceleration power in the third gear. In that light, the highest acceleration values might be expected in the range of 40 to 60 km/h. In the functions shown above, the highest acceleration values are expected at standstill.

Recommended Desired Acceleration

Regarding the argument in the previous section, a possible acceleration function could have the following values (based on the common sense of the author):

Table L-6 Recommended parameter values for Desired Accelerations

		Speed (km/h)					
Name		0	20	50	70	120	160
Car	Maximum Acceleration (m/s^2)	2,0	3,0	3,5	2,3	1,0	0,0
HGV	Maximum Acceleration (m/s^2)	2,0	2,3	2,5	2,0	0,5	0,0

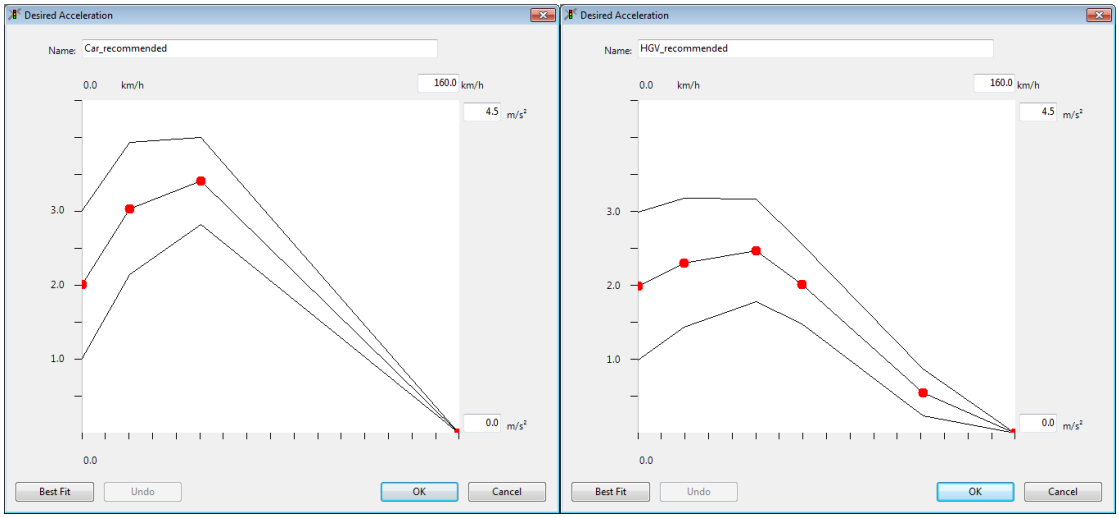


Figure L-20 Desired Accelerations for Car and HGV, recommended settings

L.2.5. Functions, Maximum Deceleration

The third parameter that can be expressed as a function of speed is Maximum Deceleration.

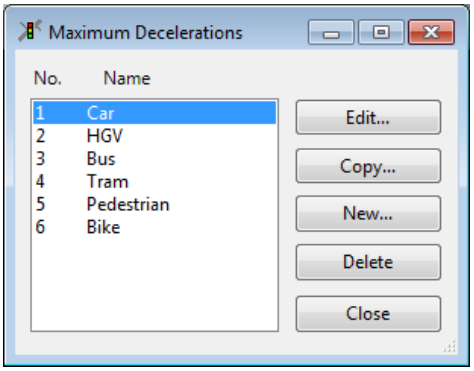


Figure L-21 The menu Maximum Decelerations

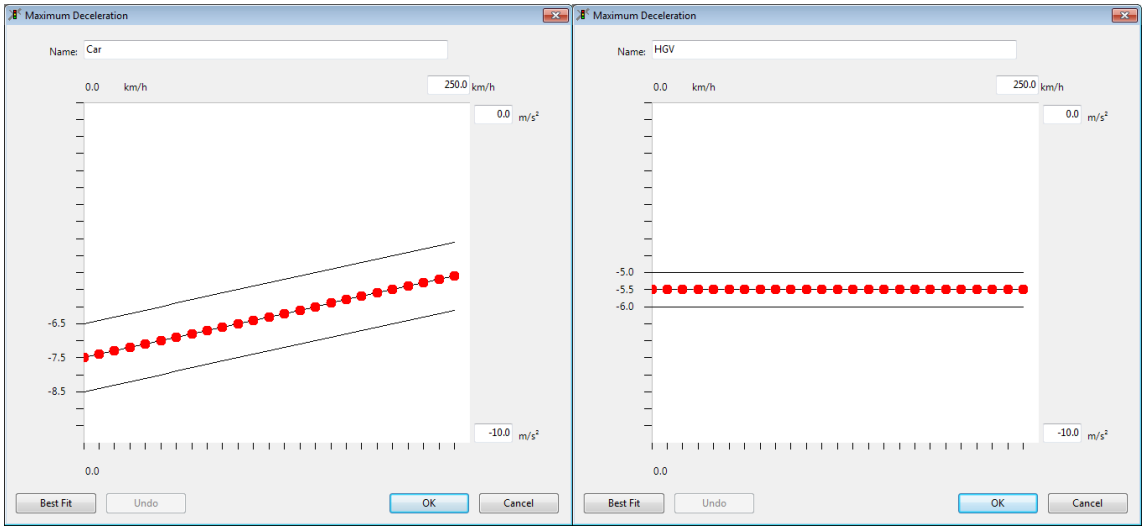


Figure L-22 Maximum Decelerations for Car and HGV, default settings in VISSIM

The default settings for the Desired Acceleration are also used in the projects of Grontmij and Pöyry.

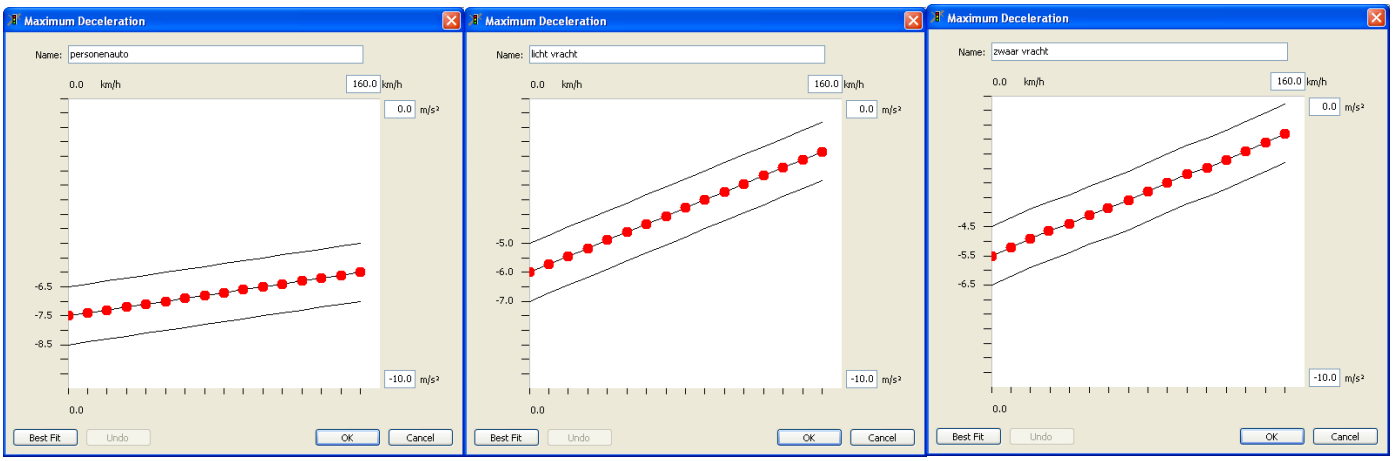


Figure L-23 Maximum Decelerations for Car and trucks, settings in the Oranjewoud project

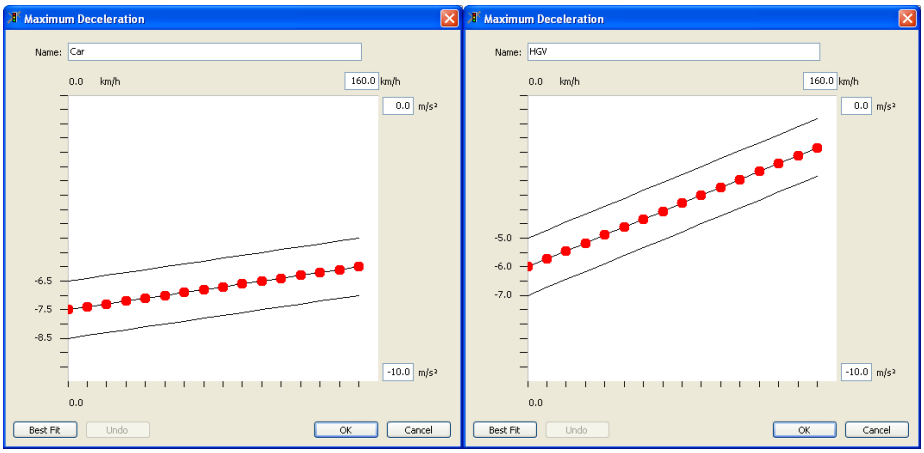


Figure L-24 Maximum Decelerations for Car and trucks, settings in the Goudappel Coffeng project

The Maximum Deceleration function for the mode Car are equal for all projects; therefore the function is expected to be reliable. However, a deceleration rate of -7.5 m/s^2 for low speeds is very high. This value equals a deceleration rate of 27 (km/h)/s; a vehicle driving at 27 km/h would come to a standstill in 1 s.

The Maximum Deceleration depends on various determinants, such as the power of the braking system, the weight of the vehicle, the slope of the road, and the friction coefficient of the tyre with the road pavement. The friction coefficient depends on the roughness [63] of the road pavement, the roughness of the tyre, the weather conditions, the speed of the vehicle and characteristics of the vehicle while skidding [64] (source: Hansen *et al.*, 2007). The friction coefficient as a function of the speed can be expressed by the graph in Figure L-25 (the upper graph represents humid weather conditions, the lower graphs represent wetter weather conditions). Consequently, the Maximum Deceleration decreases as the speed increases.

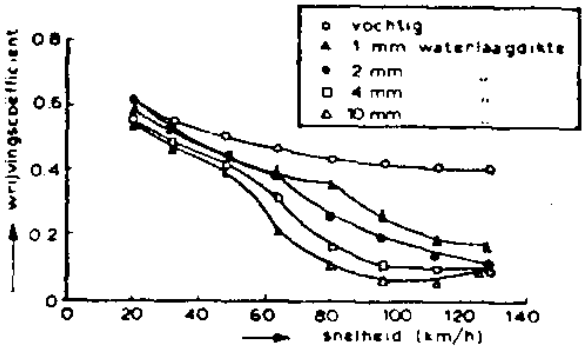


Figure L-25 The friction coefficient (vertical) as a function of the speed (horizontal) for various humidity conditions

Recommended Maximum Deceleration

Although the parameter values of the default settings are high, these values will be applied to this project for two reasons. Firstly, the default settings have been applied by various consultancy companies; professional traffic engineers trust these values to be reliable. Secondly, the functions meet the restriction that the absolute value of the Maximum Deceleration decreases with increasing speed.

[63] *In Dutch: stroefheid*
[64] *In Dutch: wielslip en drifthoek*

L.2.6. Functions, Desired Deceleration

The fourth parameter that can be expressed as a function of speed is Desired Deceleration.

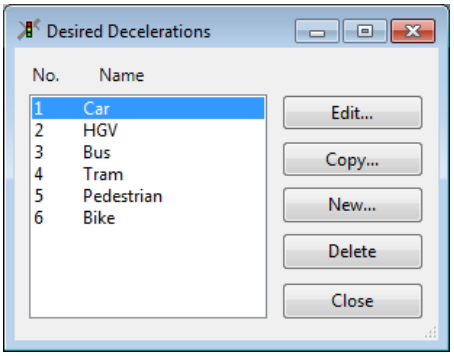


Figure L-26 The menu Desired Decelerations

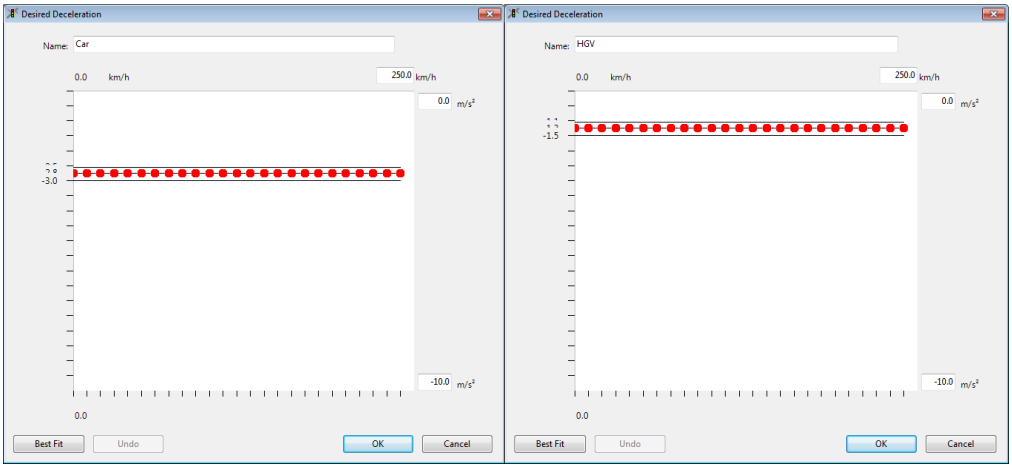


Figure L-27 Desired Decelerations for Car and HGV, default settings in VISSIM

The default settings for the Desired Acceleration are also used in the projects of Grontmij, Pöyry and Goudappel Coffeng.

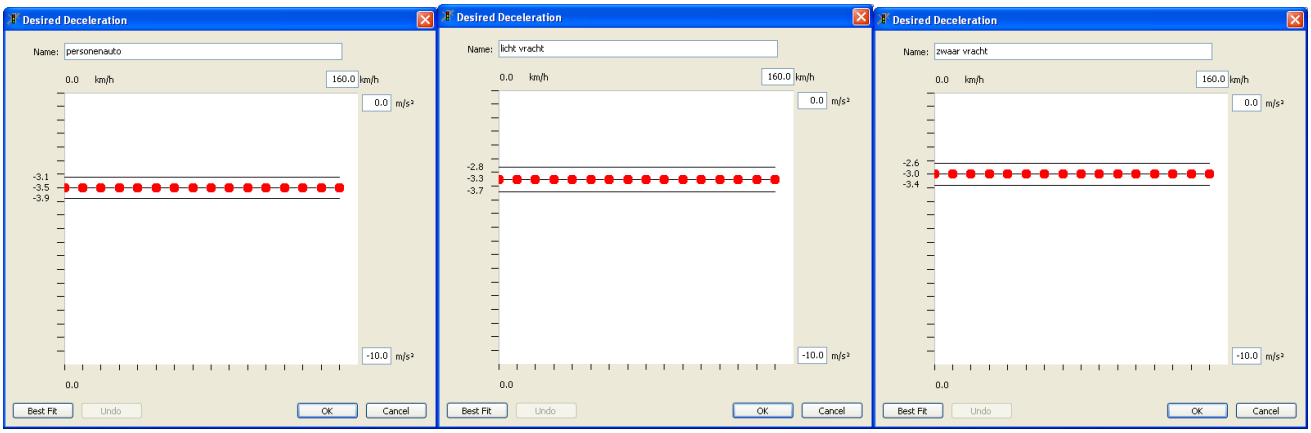


Figure L-28 Desired Accelerations for Car and trucks, settings in the Oranjewoud project

With respect to the HGV mode: the Oranjewoud project applies higher deceleration rates; almost equal to the deceleration rates of the Car mode. This is not plausible, because trucks generally have a lower absolute deceleration rate than person cars. If a truck brakes too hard, the cargo could be damaged.

All functions form a straight flat line, which is disputable regarding the following behavioural description. When a driver approaches a red traffic signal, he will start to decelerate at a rate depending on various factors, such as the driver's aggressiveness. During the first few seconds, the deceleration needs to be introduced, in order to avoid a large jerk (kinetic quantity; the mathematical time derivative of the deceleration); an indicator for discomfort. The maximum comfortable value for the jerk is estimated to be 0.8 m/s^3 (source: Hansen *et al.*, 2007), which means that a deceleration of 2.0 m/s^2 needs to be introduced over a period of 2.5 s. Over a certain period, the driver will decelerate at the maximum comfortable deceleration, and then release the braking pedal gradually in order to come to a standstill fluently.

Recommended Desired Deceleration

Regarding the behavioural description in the previous section, the recommended function could obtain the following form (again, this function is based on *expert judgment*; the common sense of the author):

Table L-7 Recommended parameter values for Desired Decelerations

		Speed (km/h)					
Name		0	20	50	70	120	160
Car	Desired Deceleration (m/s^2)	-0,5	-0,8	-2,5			-2,5
HGV	Desired Deceleration (m/s^2)	-0,5	-0,8	-2,3			-2,3

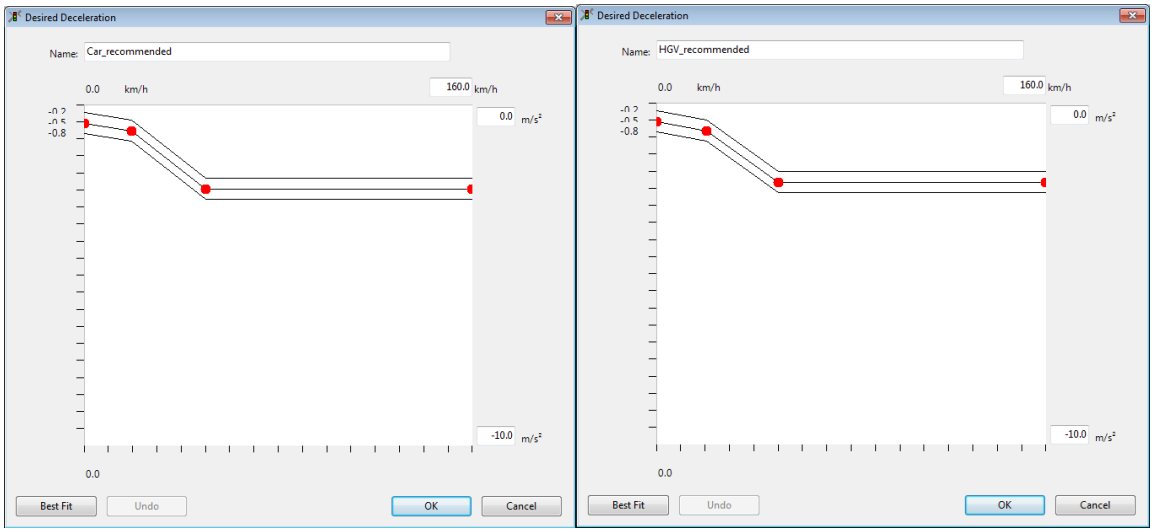


Figure L-29 Desired Accelerations for Car and HGV, recommended settings

L.2.7. Distributions, Desired Speed

In the menu Distributions, there are three parameters influencing the behaviour of drivers in the model, and therefore the model output. The first parameter affecting the model output that can be expressed as a distribution is Desired Speed. The Desired Speed distributions relevant for this project are: 25, 30, 35, 40, 45 and 50 km/h. These distributions will be applied in the Reduced Speed Areas on the roundabout itself and on the Parking Lots at the entrance of the model.

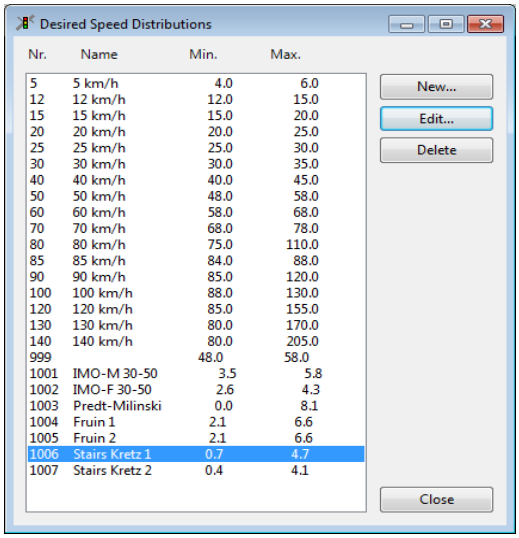


Figure L-30 The menu Desired Speed

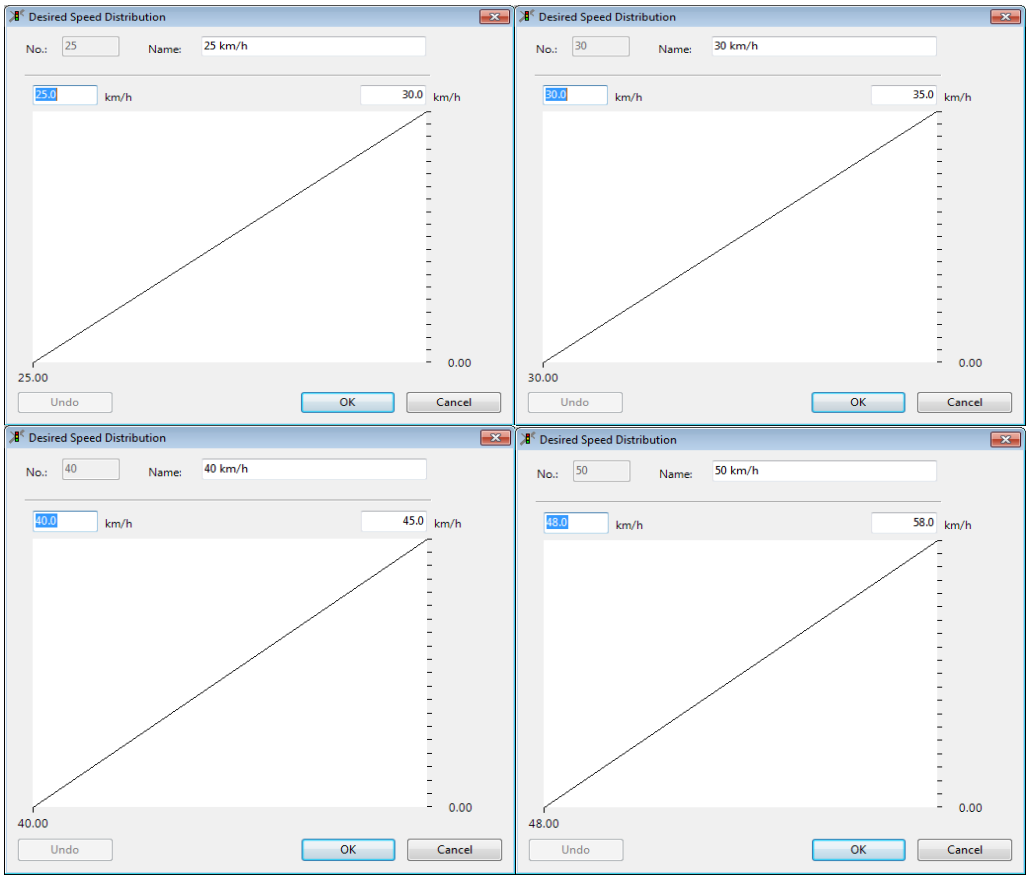


Figure L-31 Desired Speed for 25, 30, 40 and 50 km/h, default settings in VISSIM

The default settings of VISSIM do not accommodate for distributions for the speeds 35 and 45 km/h, these have to be constructed manually. Obviously, VISSIM only applies straight lines as distributions by default. With these distributions, all vehicles drive too fast, except for the 50 km/h-distribution, in which 80% of all vehicles drive faster than 50 km/h. The straight lines indicate that the variation in speeds in high, this is plausible for low speeds. The influence of the distribution form on the variation can be illustrated by means of Figure L-32. On the right, it shows an S-curve, indicating a distribution with low variation (mathematically: a low standard deviation). Most drivers choose a Desired Speed value close to the middle value of the distribution. The left graph shows a converse S-curve, indicating high variation.

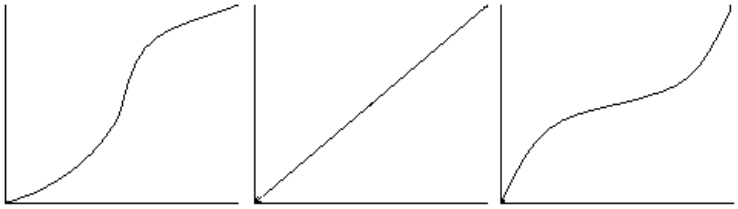


Figure L-32 Various distribution functions

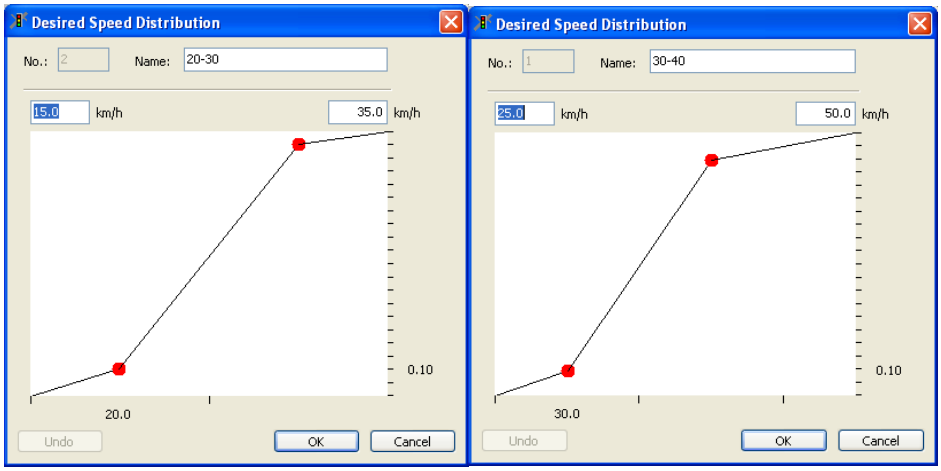


Figure L-33 Desired Speed distributions for 20-30 km/h and 30-40 km/h, settings in the Goudappel Coffeng project

In the distributions applied by Pöyry, all drivers comply very strict to the speed limit; 80% of all drivers choose a speed which differs merely 2 km/h from the speed limit. This high level of accuracy is reasonably not realistic.

Recommended Desired Speed

The following Desired Speed distributions are again based on *expert judgment*.

Table L-8 Recommended parameter values for Desired Speed distributions

25				**30**				**35**			
15 <	*Speed*	< 20	10%	20 <	*Speed*	< 25	10%	25 <	*Speed*	< 30	10%
20 <	*Speed*	< 30	75%	25 <	*Speed*	< 35	75%	30 <	*Speed*	< 40	75%
30 <	*Speed*	< 35	15%	35 <	*Speed*	< 40	15%	40 <	*Speed*	< 45	15%

40				**45**				**50**			
30 <	*Speed*	< 35	10%	35 <	*Speed*	< 40	10%	40 <	*Speed*	< 45	10%
35 <	*Speed*	< 45	75%	40 <	*Speed*	< 50	75%	45 <	*Speed*	< 55	75%
45 <	*Speed*	< 50	10%	50 <	*Speed*	< 55	10%	55 <	*Speed*	< 60	10%
50 <	*Speed*	< 55	5%	55 <	*Speed*	< 60	5%	60 <	*Speed*	< 65	5%

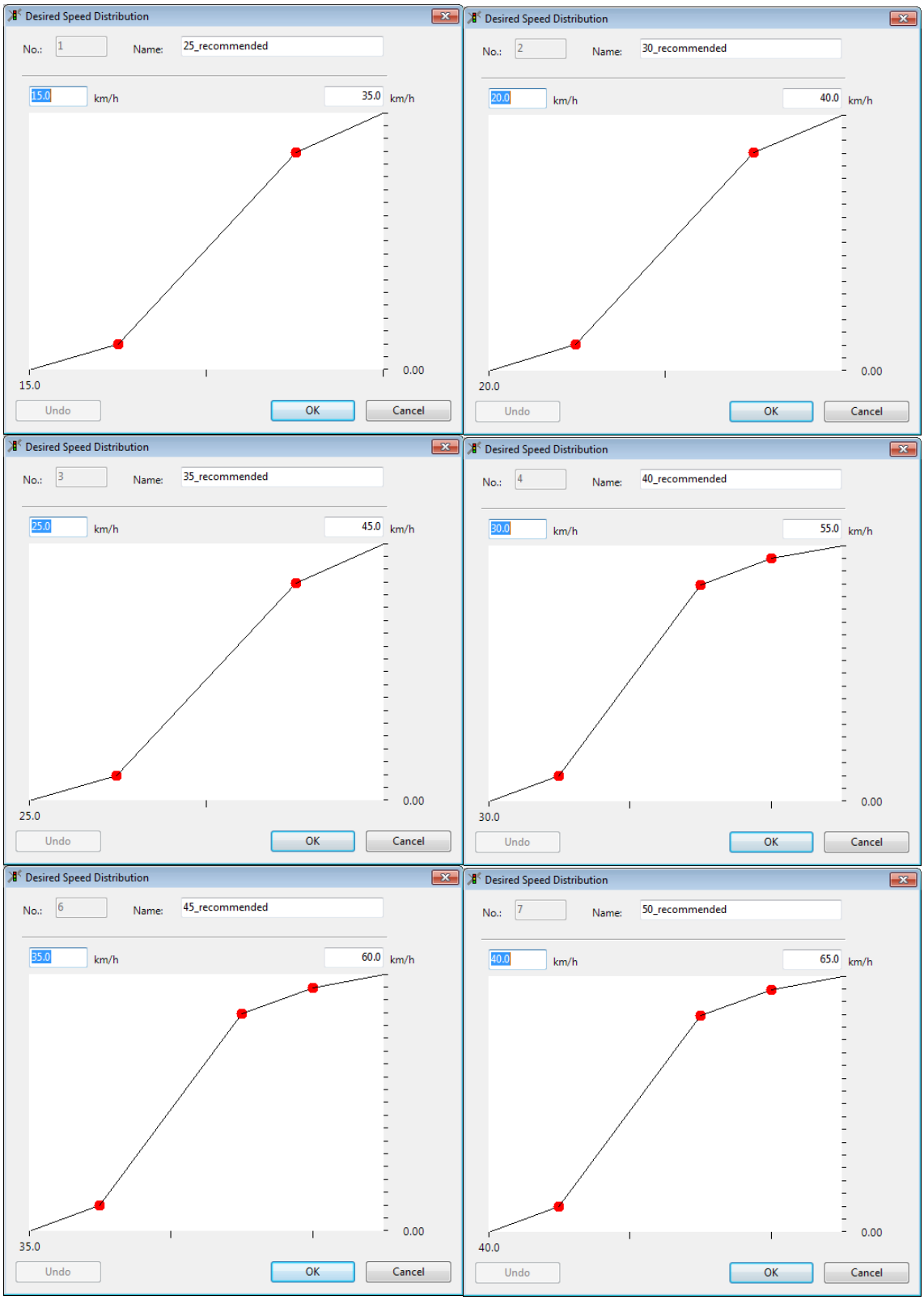


Figure L-34 Desired Speed distributions, recommended settings

L.2.8. Distributions, Power and Weight

The second and third parameters affecting the model output that can be expressed as a distribution are Power and Weight. VISSIM uses these distributions in order to determine a power-to-weight ratio for each vehicle individually; this ratio determines the acceleration of the vehicle (source: VISSIM 5.30 User Manual, 2011).

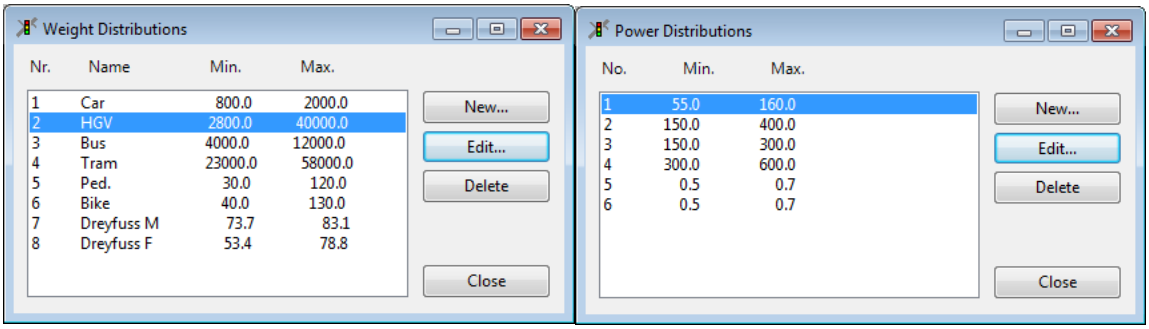


Figure L-35 The menus Weight and Power

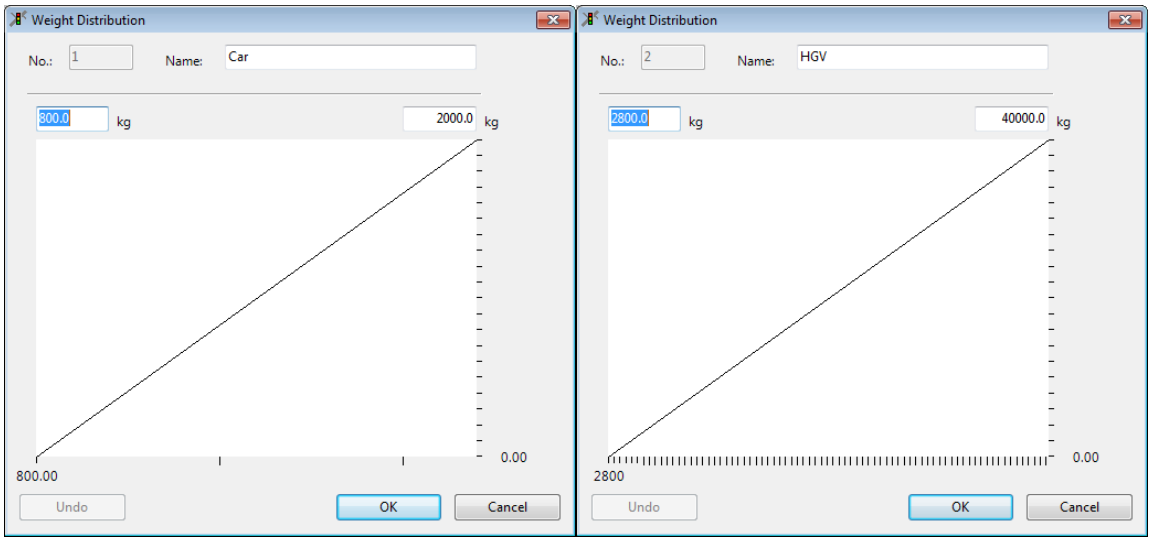


Figure L-36 Weight distributions for modes Car and HGV, default settings in VISSIM

The default settings for the Power and Weight are also used in the projects of Oranjewoud, Grontmij, Pöyry and Goudappel Coffeng.

Recommended Distributions, Power and Weight

The Power and Weight distributions are hard to estimate by means of logical reasoning. They can be estimated by using data on characteristics of the fleet on the Dutch roads, however, such a database is not available. The default values in VISSIM will be adopted in this project.

L.2.9. Driving Behaviour

In this menu, the driving behaviour variables can be defined for every road type separately. In this project, the first road type – Urban (motorized) – will be used only. With regard to the reference projects of Oranjewoud, Grontmij, Goudappel Coffeng and Pöyry, they use the default settings.

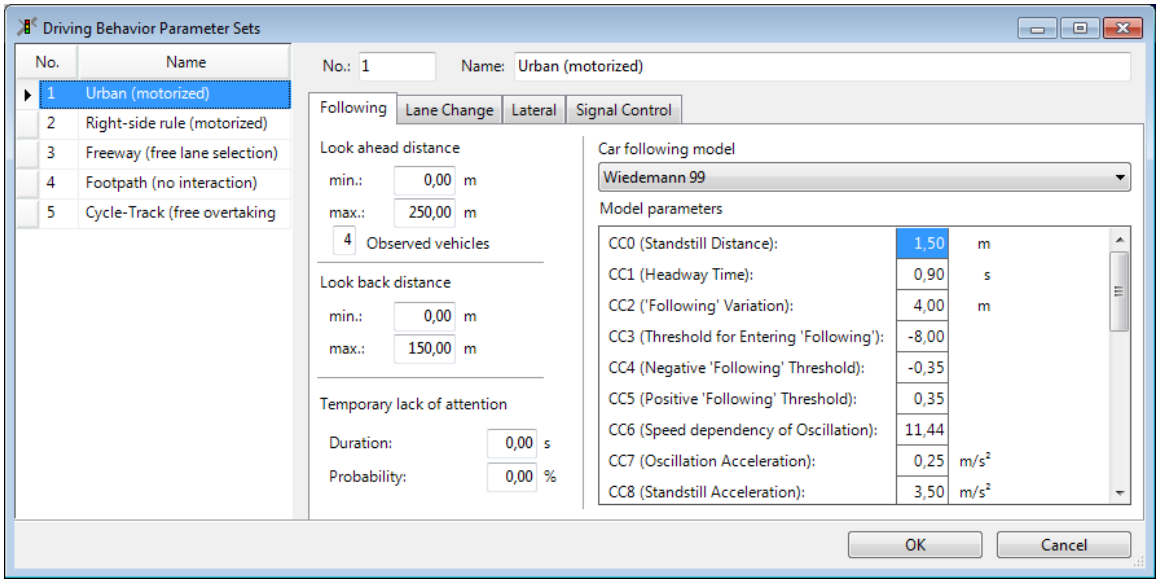


Figure L-37 Default setting for Driving Behaviour, tab Following

Figure L-37 shows the tab Following. Here, the Look ahead distance and the Look back distance can be specified. According to the VISSIM manual, the minimum values are relevant when vehicles can form a queue on a single lane in multiple rows. This variable is relevant to cycle paths, not included in this project. The default value for the maximum look ahead distance is 250 m plus 4 vehicles. The maximum values are relevant in situations with multiple intersections on a shorter travel distance, which is not the case in this project.

The Temporary lack of attention option enables to invoke the possibility of modelling drivers with temporarily increased reaction times. These values are expected to influence the capacity of the intersection, but it is hard to estimate reliable values for this parameter. Therefore, lack of attention will not be modelled.

The VISSIM manual recommends the Wiedemann 99 model for urban roads. This recommendation will be obeyed in this project. The default settings will be applied:

- *CC0*: the desired distance between two vehicles standing still (1.50 m);
- *CC1*: the desired time headway. The safe distance headway is *CC0 + speed*CC1* (0.90 s);
- *CC2*: a driver decides to accelerate when his distance headway is larger than the safe distance headway plus *CC2* (4 m);
- *CC3*: this variable determines the boundary between unconstrained driving and following behaviour (8 m);
- *CC4* en *CC5*: these variables determine the influence of the distance headway on the reaction time: small values invoke small headways and strong responses to perturbations (-0.35 and 0.35 resp.);
- *CC6*: this variable determines the oscillation in stationary traffic flows: a small value leads to little oscillation (11.44);
- *CC7*: acceleration during oscillation (0.25 m/s^2);
- *CC8*: acceleration during oscillation from standing still (3.50 m/s^2);
- *CC9*: acceleration during oscillation at 80 km/h (1.50 m/s^2).

These variables can be changed in VISSIM 5.30, applied in this project. VISSIM 5.40 offers two more variables:

- *Smooth closeup behaviour*: this variable determines the behaviour when multiple vehicles approach a static object;
- *Standstill distance for static objects*.

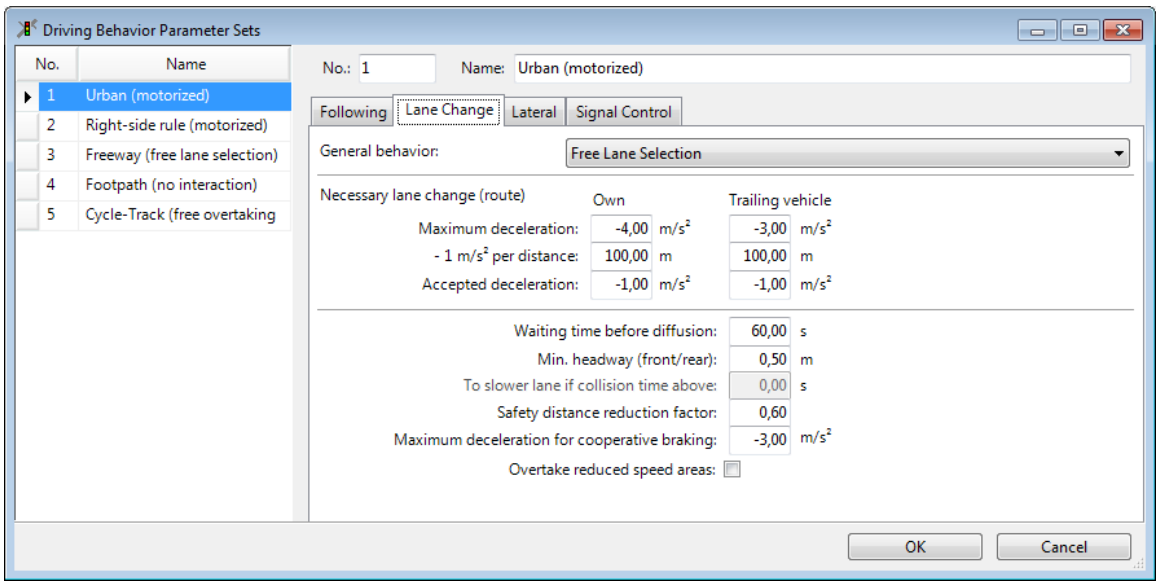


Figure L-38 Default setting for Driving Behaviour, tab Lane Change

Figure L-38 shows the tab Lane Change. VISSIM offers two options with respect to the General behaviour: the Right-side rule and Free Lane Selection. This variable is not relevant to this project, because vehicles approaching the intersection choose a lane according to their destination as soon as they enter the network from the parking lots (see section L.1.1).

A necessary lane change is a lane change needed in order to follow a route. These variables determine the aggressiveness with which these lane change are being carried out. The VISSIM manual explains and defends the default values; they will be used in this project.

When a vehicle is not able to perform the lane change, it comes to standstill at the start of the connector. The Waiting time before diffusion expresses how long the vehicle waits at the connector. If the lane change has not been carried out after 60 s, the vehicle will be taken out of the network. This is highly unrealistic, but it is invoked in VISSIM in order to prevent a gridlock caused by necessary lane changes. In reality, the gridlock will be prevented by breaking traffic rules, which is impossible in VISSIM. The Min. headway (front/rear) determines the minimum gap on a target lane in order to carry out a lane change. The safety distance reduction factor determines the minimum required distance headway just after a lane change has been carried out. The maximum deceleration for cooperative braking expresses a threshold from which a cooperative lane change is required to carry out a lane change. The final variable is a dichotom variable: if Overtake reduced speed areas is selected, drivers performing a lane change will respect the reduced speed area on the target lane. If the variable is not selected, drivers will not perform any lane change in a reduced speed area.

VISSIM 5.40 provides an extra option: Cooperative lane change. With this variable, the model accommodates for courtesy lane changes: a vehicle may change lanes in order to create space for another vehicle performing a necessary lane change.

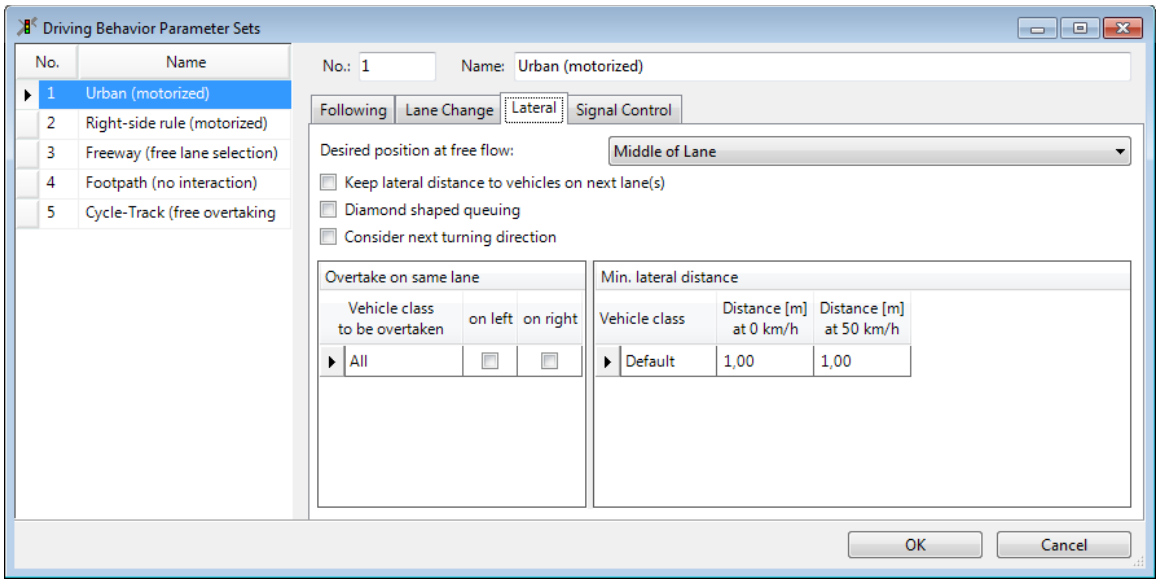


Figure L-39 Default setting for Driving Behaviour, tab Lateral

Figure L-39 shows the tab Lateral driving behaviour. These variables offer the possibility to model vehicles overtaking on a single lane. This project does not model (motor) cyclists, so the values should be chosen such that overtaking on a single lane is not possible. This is the case for the default settings.

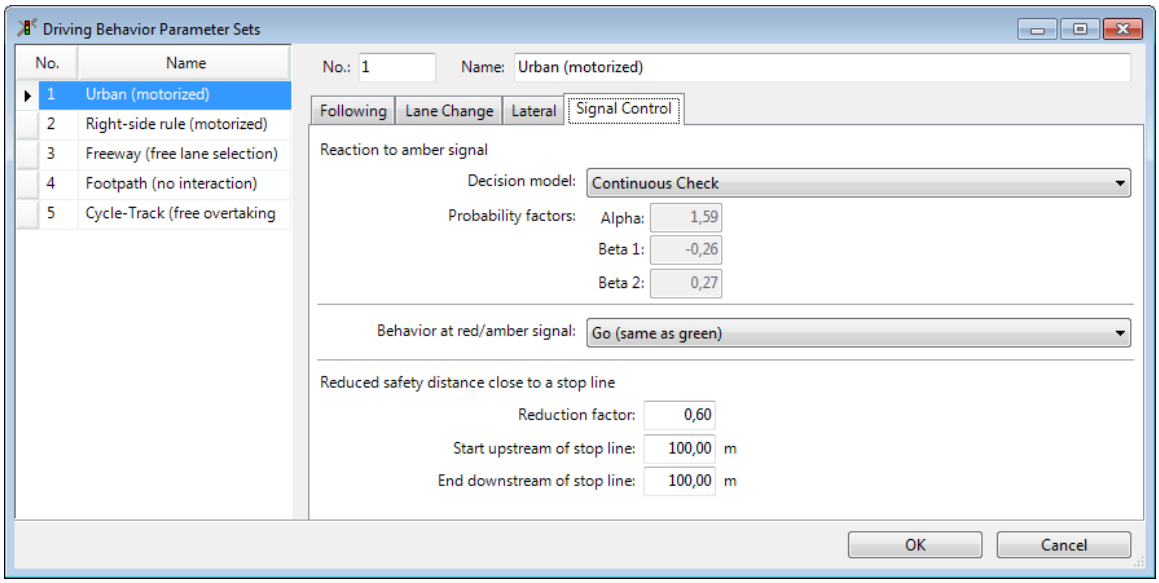


Figure L-40 Default setting for Driving Behaviour, tab Signal Control

Figure L-40 shows the tab Signal Control. Here, the behaviour of drivers approaching a traffic signal can be altered. There are two Decision models available: Continuous Check (in which a vehicle stops for a yellow light if the necessary deceleration does not exceed the maximum deceleration) and One Decision (in which the chance of a vehicle stopping for a yellow light is being calculated by means of logistic regression. For the latter Decision model, empirical data are required in order to estimate the logistic regression function. These data are not available in this project.

The Reduced safety distance close to a stop line affects the behaviour in front of a traffic signal. The reduction factor is being applied over a distance of 200 m (from 100 m in front of the stop line to 100 m beyond the stop line).

L.2.10. Link Behaviour Types

In this menu, the driving behaviour explained in the previous section can be applied to the road types in the model. In this project, only the road type Urban will be used.

L.3. Traffic demand

VISSIM offers two ways to generate traffic on the network: static and dynamic assignment. This project applies a dynamic assignment, because the capacity of the intersections will be measured by increasing the traffic demand over time. Both ways offer this possibility, but the static assignment is highly labour intensive. The dynamic assignment is most efficient and insightful.

Dynamic assignment requires OD-matrices defining how many vehicles are travelling from node to node. These OD-matrices are registered in .fma-files, which can be read by VISSIM. Every OD-matrix is assigned a Vehicle Composition, defining which Vehicle Types are generated by the OD-matrix.

L.3.1. Vehicle composition

The default vehicle composition in VISSIM consists of 98% person cars and 2% trucks and lorries (see Figure L-41 left). In common Dutch design practice, models of urban intersections are evaluated using a truck share of 20%. Therefore, a new vehicle composition will be defined (see Figure L-41 right).

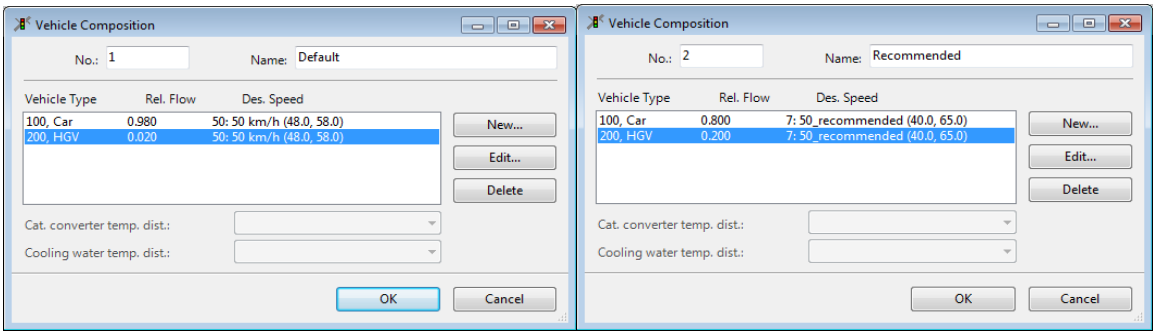


Figure L-41 Default Vehicle Composition (left) and Vehicle Composition used in this project (right)

L.3.2. .fma-files

In the dynamic assignment, VISSIM applies .fma-files to generate traffic on the network. Figure L-42 shows an example of an .fma-file. In order to enable VISSIM to read the file, it starts with a code. Secondly, the period over which the specific traffic demand in the file is defined (in this case 15 minutes). Thirdly, the traffic demand in the file will be multiplied by a factor (in this project equal to one for all files). Fourthly, the number of zones in the networks needs to be specified. Fifthly, the zone numbers are indicated and finally the traffic demand is presented in the form of an OD-matrix.

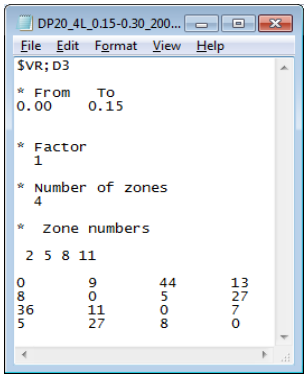


Figure L-42 Example of a Vehicle Composition used in this project: demand pattern 20, total demand 200 pcu/h

In this project, the intersections will be evaluated by means of a set of these .fma-files. The file shown in Figure L-42 shows an OD-matrix which complies to demand pattern 20 (see appendix B) with a total traffic demand of 200 pcu/h. This demand will be applied over 15 minutes. Every 15 minutes, the traffic demand will be raised by 200 pcu/h. As a result, the traffic flow on the intersection will become more saturated as time proceeds. The capacity of the intersection will be determined by evaluating the saturation rate in time.

L.4. Signal control

VISSIM applies TrafCOD to simulate the signal control in the model. Figure L-43 shows the required settings in the menu Signal Control. In the first tab (Signal Groups), the traffic streams used in the VRIGen model need to be represented. All of these traffic streams should be assigned detectors and signal heads in the network (see section 0). In the second tab (Controller TRE) the files required for generating the semi-actuated control should be located. By Program File, VISSIM learns to apply TrafCOD; therefore the TrafCOD.exe-file needs to be located. By STG File, the structure generated by VRIGen should be located. The .VXB-file is an empty file. The function of the file is not relevant to this project.

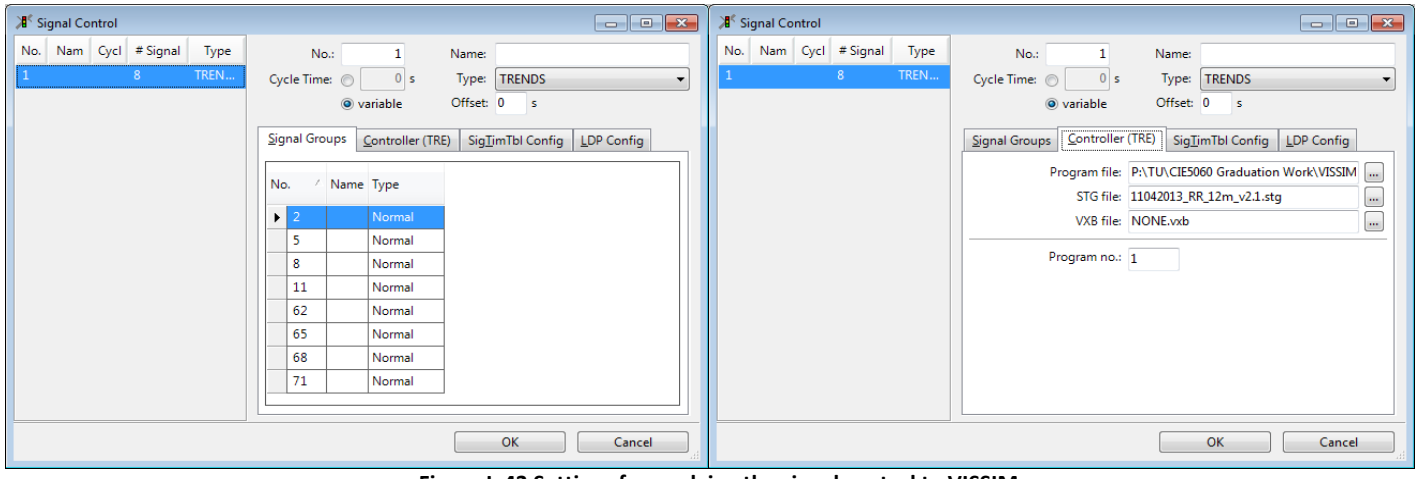


Figure L-43 Settings for applying the signal control to VISSIM

L.4.1. Connection between TrafCOD and VISSIM

The traffic control generated by means of VRIGen (described in appendix H) must be communicated to VISSIM. Therefore, VISSIM applies TrafCOD, which generates a semi-actuated control. That means that the traffic control is based on the structure generated by VRIGen, but each phase in the control will be extended according to the arrival pattern. VISSIM communicates the actual arrival pattern to TrafCOD by means of the detectors in the network.

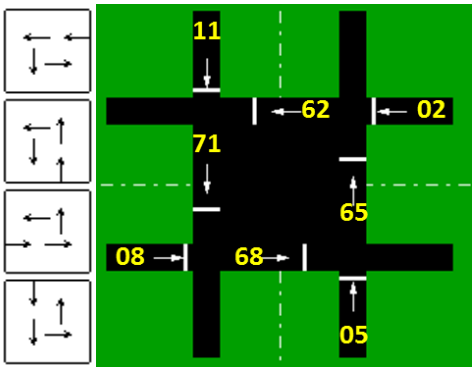


Figure L-44 Structure of the four-phase clockwise control program

When the structure is generated and saved, VRIGen generates amongst others a .tfc-file and a .stg-file. By means of the .tfc-file, VRIGen communicates the structure to TrafCOD. This way, the static structure is turned into a semi-actuated structure, because a phase can be extended if the traffic demand requires so. By means of the .stg-file, the structure can be communicated to VISSIM. VISSIM applies TrafCOD to generate the semi-actuated traffic control by communicating the information from the detectors in the network to TrafCOD. TrafCOD returns the durations of the green times. Therefore, TrafCOD and VISSIM have to communicate well with each other, the coding of the detectors (see section 0) secures this.

L.5. Evaluation

The evaluation of the intersection performance will be based on two assessment criteria (see chapter 3: Evaluation methods):

- Travel time;
- Queue length.

Both criteria can be measured in the VISSIM model, this section explains how.

L.5.1. Travel time

VISSIM accommodates the function Travel Time Sections. After selecting this functionality, the model developer must locate a start section and an end section; the travel time between these section will be registered for each individual vehicle.

The travel times will be measured for all directions separately. The start sections are located just beyond the entrance parking lot. The end sections are located 2000 m downstream of the start section. Figure L-45 shows the example of direction 01. The start section is near parking lot 2 (the small red line) and the end section is located on northbound link (the small green line).

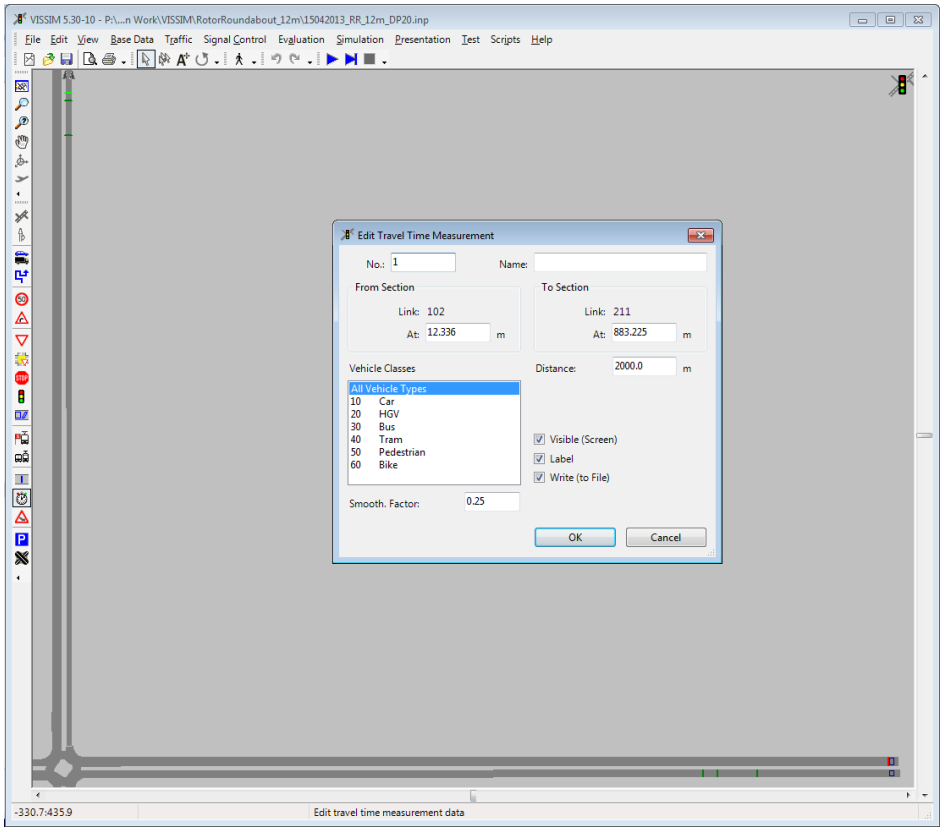


Figure L-45 Settings of the travel time measurement for direction 01

L.5.2. Queue length

The second assessment criterion is queue length. Figure L-46 illustrates how VISSIM registers queue length. Every direction is assigned a Queue Counter. The counter is located just beyond the signal head. The figure illustrates the definition of the queue: a vehicle is assumed to be in the queue if its speed has dropped below 5 km/h (the Begin v). The End v defines the upper threshold: the vehicle is assumed to be out of the queue if it accelerates again to a speed larger than that value. In this project, shockwaves may occur in which vehicles accelerate to 50 km/h after having stood still. In order to assure that these vehicles are also counted to the queue, the value for End v is set to 100 km/h. Max. Headway expresses the maximum gap between two vehicles in the queue. The maximum length of the queue is equal to the length of the approach leg.

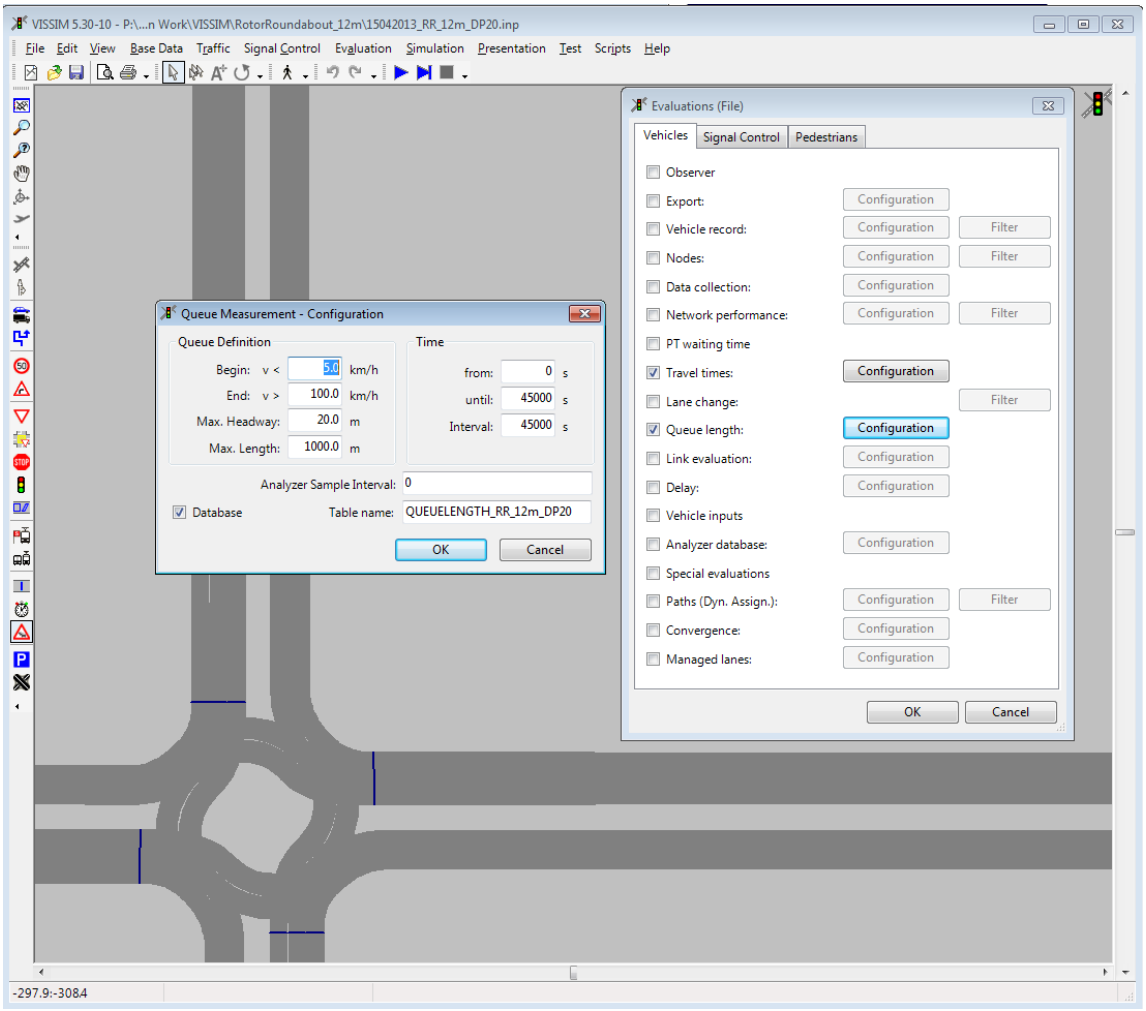


Figure L-46 Settings of the queue measurement

Appendix M: LED illumination

This appendix addresses the subject of LED illumination on the signalized turbo roundabout and turbo circle. LED illumination consists of LED modules within the asphalt pavement. Their aim is to guide the road user while crossing the intersection. The first section will explain why LED illumination is recommendatory on signalized turbo roundabouts. Secondly, the technological state of affairs will be explained at the time of writing (June 2013); to what extent is LED-technology sufficiently developed and ready for implementation? Thirdly, the lay-out of the LED modules on the signalized turbo roundabout will be explained. Finally, this appendix pays attention to the relationship of LED illumination with various other functionalities of and equipment on the turbo roundabout.

M.1. Why LED illumination?

Figure M-3, Figure M-4 and Figure M-5 illustrate the lane configuration of entrance legs to the signalized turbo roundabout, the partial turbo circle and the turbo circle respectively. Clearly, the road user's lane choice is quite complicated since there are three lanes or more next to each other, and while entering the intersection, the lane markings are absent over the width of the circulatory roadways. The chance of an erroneous lane choice, such as the lane choice illustrated by Figure M-9, is quite large, especially for the (partial) turbo roundabout.

In order to help road users choosing the correct lane, and to prevent collisions resulting from erroneous lane choices, the path to be crossed has to be clearly indicated to the road user. The LED pavement markings aim to improve the clarity of the intersection; they assist and guide the road user while crossing the intersection. The LED pavement markings are dynamic: depending on which stream obtains green, the LED modules illuminate.

In order to assess the range of applicability of the LED modules on signalized turbo roundabouts and (partial) turbo circles, a cost-benefit analysis can be carried out. Here, the monetary costs of installing the LED modules should be weighed against the societal costs of (fatal) injuries resulting from a lack of guidance on the intersection. The guideline OEI (Eijgenraam, 2000) presents tools to perform such a cost-benefit analysis. In this project, this is regarded a subject for further investigation.

M.2. Pavement LEDs: state of affairs

Fortuijn (2013, p.133) mentioned that pavement LEDs are a very useful equipment to the turbo circle, but that the LED technology was not sufficiently advanced yet. The LEDs are said to be insufficiently robust: they 'wander' around in the asphalt pavement, caused by lateral tensions of tyres.

However, Figure M-1 and Figure M-2 show examples of LED pavement markings, which are currently merchandised on the Dutch market for LED-technology. This raises the presumption that LED-technology is already sufficiently advanced for implementation.

On the other hand, a European directive is currently under development, stating requirements with respect to the robustness of road pavement LEDs. At the time of writing, no guidelines with respect to the robustness of asphalt LEDs have been composed, so Figure M-1 and Figure M-2 indicate field examples which are not subject to guidelines. The robustness of these examples are therefore not secured (although Inter Traffic Systems claims the opposite, of course).



Figure M-1 LED pavement markings on the M25, United Kingdom (subtracted from the website of the Dutch company Inter Traffic Systems: http://www.intertrafficsystems.nl/)



Figure M-2 Dynamic lane marking on a Dutch highway (subtracted from the website of the Dutch company Inter Traffic Systems: http://www.intertrafficsystems.nl/)

M.3. Lay-out of the LED markings

Figure M-3 shows the configuration of the LED illumination in the asphalt pavement of a rotor roundabout; Figure M-4 and Figure M-5 shows the LED illumination on the (partial) turbo circle. When the circulatory roadways obtain green, the vehicles are being guided by the painted lane markings (continuous and broken) and the LED modules. The LEDs indicating the course for vehicles on the entrance legs are turned off. When the entrance leg obtains green, the LEDs indicating the course for vehicles on the circulatory roadway will be turned off and the LEDs for the entrance leg will be turned on. In that case, the driver on the entrance leg still sees the painted pavement markings on the circulatory roadways, but he will be guided by the LED modules.

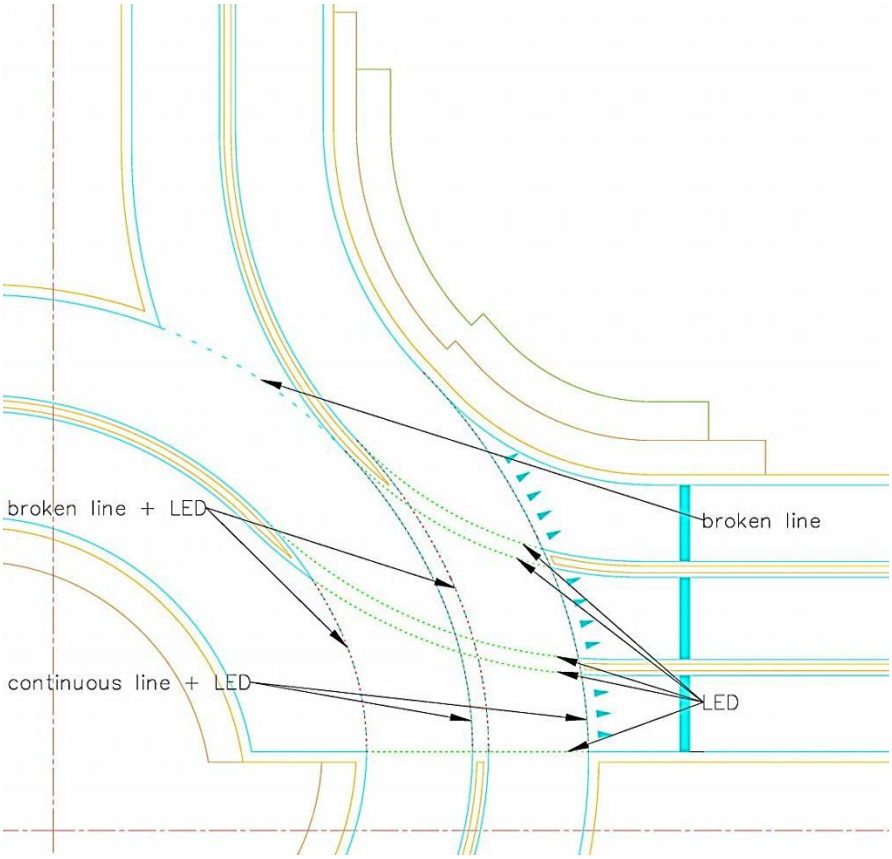


Figure M-3 Rotor roundabout with pavement marking and LED illumination

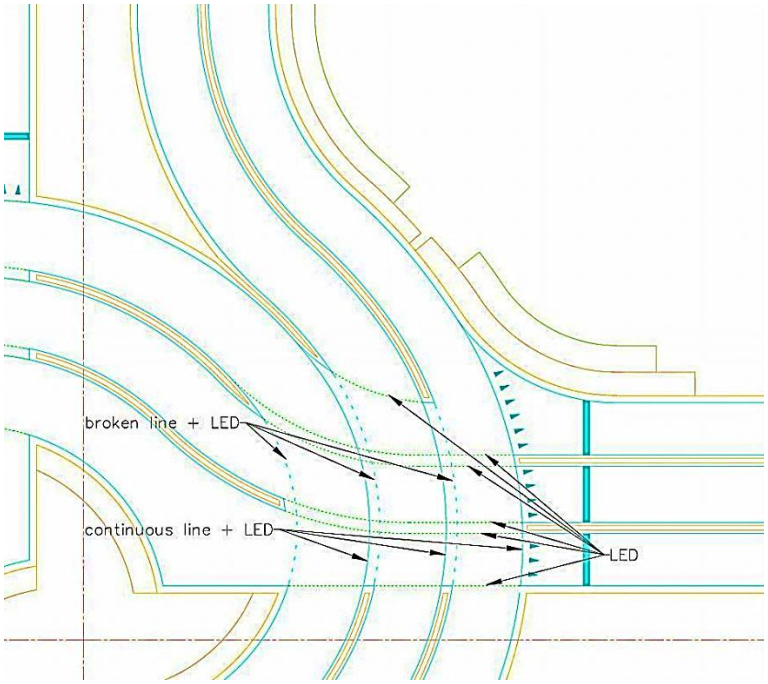


Figure M-4 The partial turbo circle with pavement marking and LED illumination

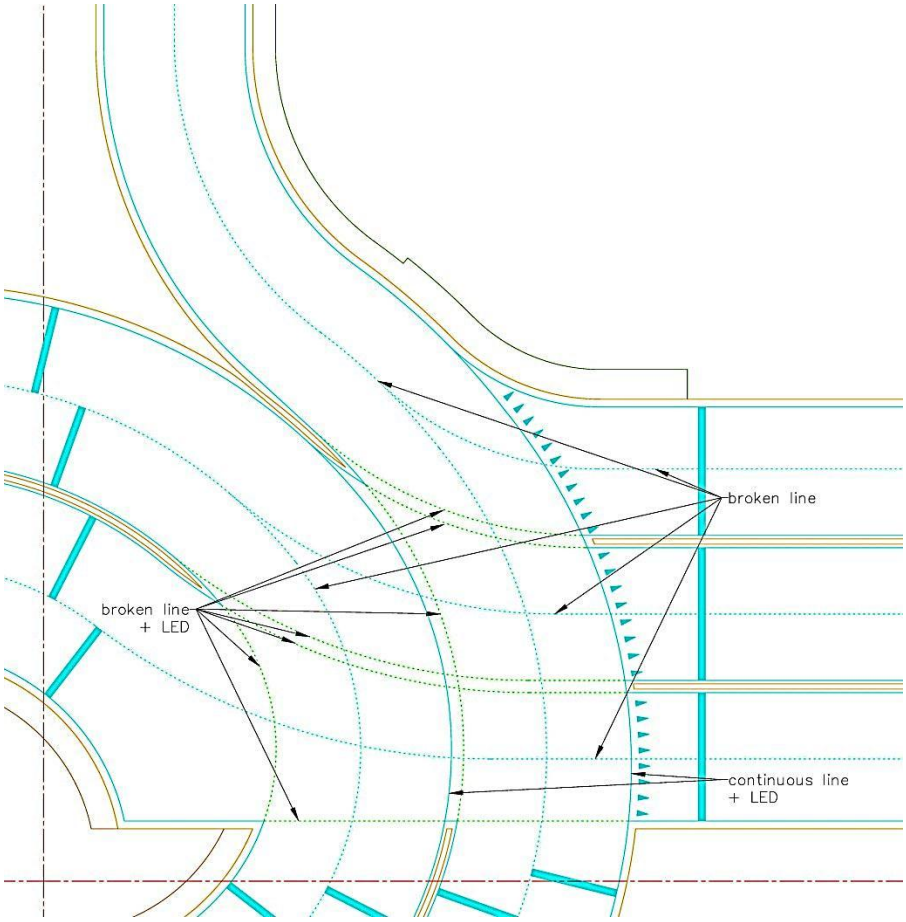


Figure M-5 Turbo circle with pavement marking and LED illumination

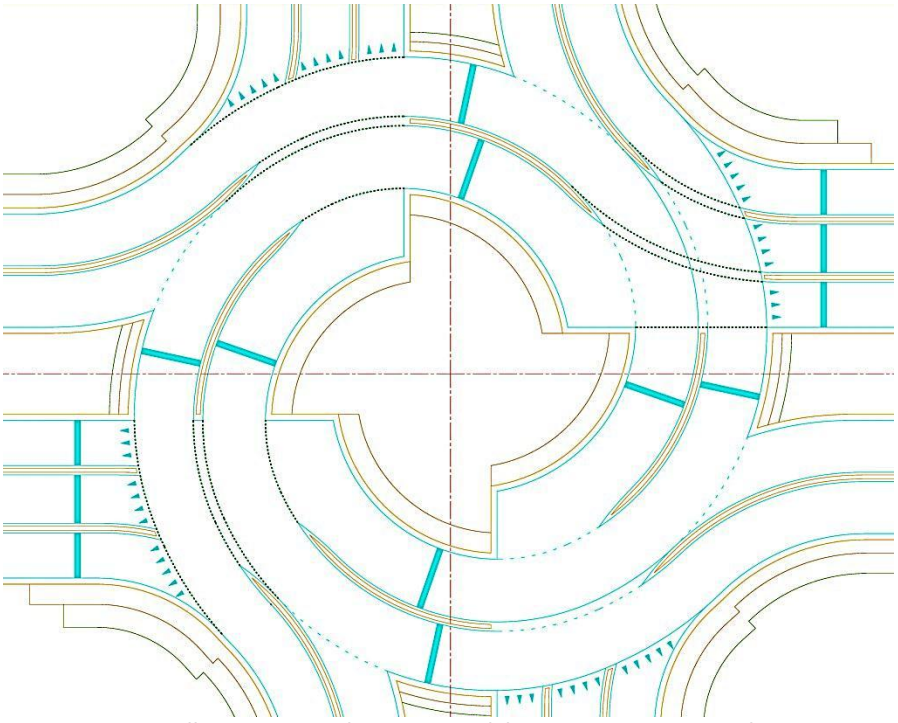


Figure M-6 LED illumination on the rotor roundabout in case stream 02 obtains green

The continuous lanes are marked by means of continuous and broken lines. The reason for this has a legal nature. A vehicle driving on a road with a single or double continuous line is not allowed to change lanes. If the single line is broken, he is allowed to change lanes; if the double line consists of a continuous and a broken line, the vehicle is allowed to change lanes if the broken line is on the vehicle's side of the road. This guideline applies to the roundabout as well: vehicles on the entrance legs should encounter a broken line first, and then a continuous line.

Another discussion topic is psychological in nature: if a traffic stream is not in the green phase, should the LED modules produce a red light (like the traffic light) or should they produce no light at all (turned off)? This question should be answered in order to enhance clarity and predictability of the road environment, and thereby enhancing traffic safety. In this project, this will be regarded as a subject for further research.

M.4. LEDs and functionalities of the turbo roundabout

This section will address the relationship between LED modules and various functionalities of the turbo roundabout and (partial) turbo circle.

M.4.1. Start of the inner circulatory roadway

In the classical design of the turbo roundabout, 'droplets' are designed at the start of every circulatory roadway, opposite of the connection with the entrance leg (Fortuijn, 2013, p.59). These droplets aim to prevent road users from cutting off the right-bending curve, thereby conflicting with other vehicles.

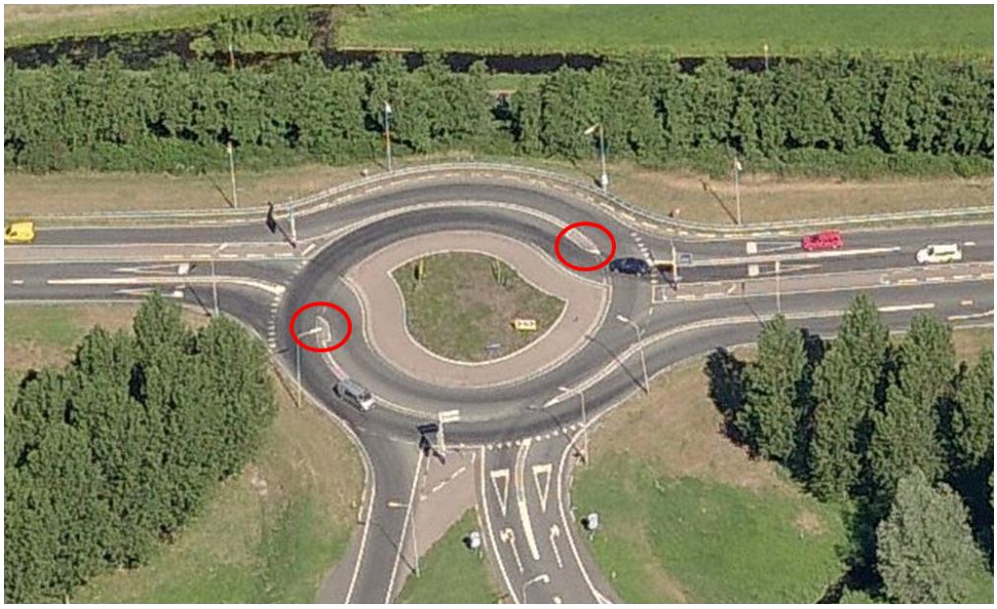


Figure M-7 Droplets indicate the start of the inner circulatory roadway (picture shows the ir. L.G.H. Fortuijnrotonde near the Dutch municipality of Reeuwijk)

With the application of LEDs in the asphalt pavement, these droplets are strictly not necessary. The LEDs indicate to the road user on the left approach lane where the inner circulatory roadway starts and what driving course should be followed. However, the LEDs do not create any discomfort if the driver decides to cut off the curve, as the raised mountable droplets do. Therefore, it is recommended to install the LEDs in addition to the droplets.

M.4.2. Roadway dividers vs. LEDs

In its classical design, the turbo circle is equipped with wide roadway dividers, illustrated in red by Figure M-8 (Fortuijn, 2013, p.132). These roadway dividers aim to conduct the drivers while crossing the turbo circle, so as to prevent them from making an erroneous manoeuvre, illustrated by Figure M-9.

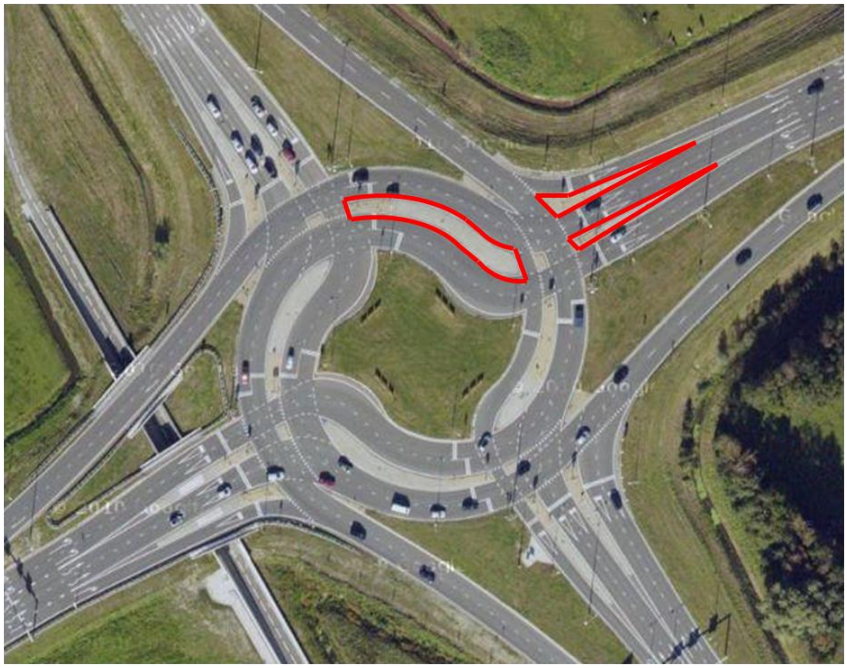


Figure M-8 Wide roadway dividers on the Doenkadeplein

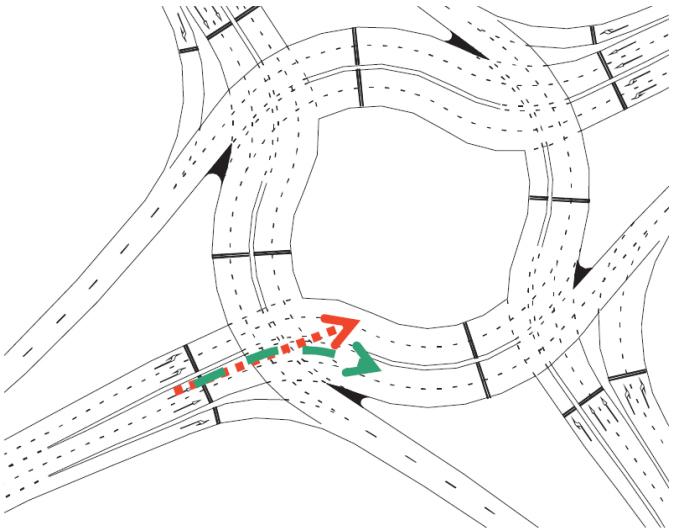


Figure M-9 The roadway dividers aim to prevent an erroneous manoeuvre, illustrated by the red arrow (subtracted from Fortuijn, 2013, p.131)

The wide roadway dividers have the following advantages:

- They decrease the probability of erroneous manoeuvres to occur (Figure M-9);
- They offer drivers lateral space to mend dangerous actions of other drivers;
- They offer space for installing traffic signals on the entrance legs.

The wide roadway dividers also coincide with some disadvantages:

- They increase the space requirement of the intersection;
- They deteriorate the clarity and comprehensibility of the entire intersection, especially to person car drivers. Truck drivers appear to have the best overview (Van der Horst *et al.*, 2008);
- They induce the necessity to install extra traffic signs, and lane and arrow markings (Fortuijn, 2000).

Pavement LEDs may substitute the function of the wide roadway dividers; they conduct the road user while crossing the turbo circle by showing him the driving course to follow. The painted lane markings also accomplish this function, but they are permanently visible. The LEDs can be turned off for the legs that obtain red, thereby improve the clarity of the division of the road space to the road user. Roadway dividers are elevated; the function of creating discomfort cannot be substituted by pavement LEDs. These considerations lead to the following hypotheses:

- The road user's perception is such, that the LEDs help the road user carrying out the driving task.
- The LEDs improve the conductivity of the intersection at least to the same extent the roadway dividers improve the conductivity of the intersection.

M.4.3. Roundabout shields

Figure M-10 shows an example of roundabout shields on the Doenkadeplein. The picture shows that the roundabout shield consists of 3 signs. Roundabout shields aim to warn the road user of a discontinuity in his driving course, by depriving the road user from his view on the horizon. This results in an earlier start of the deceleration phase (farther away from the intersection) and lower speeds on the intersection (improving traffic safety).



Figure M-10 Roundabout shields on the Doenkadeplein, picture taken from the western leg

Pavement LEDs can complement the roundabout shields, because they warn the driver of a discontinuity in his driving course; that is a curve [65]. This is especially useful for the (partial) turbo circle, because the edge of the central island does not intersect with the imaginary extension of the right edge of the approach leg. As a consequence, on (partial) turbo circles with an inscribed radius less than 20 m, the roundabout shields cannot deprive the drivers on the right approach lane from their view on the horizon (see Figure M-11). The central island is not large enough to place the roundabout shields such that they

[65] *Of course, pavement LEDs cannot deprive the road user from his view on the horizon, but they indicate a bend, by which the driver is warned.*

cut the imaginary line connecting the right approach lane with the right exit lane on the opposite leg. The LEDs may substitute the roundabout shields, but it is recommended to install the roundabout shields in addition to the LED illumination, because the roundabout shields offer relief with respect to the driving task. In particular, roundabout shields yield a reduction of workload by reducing the amount of visible information from the environment (Theeuwes, 2012).

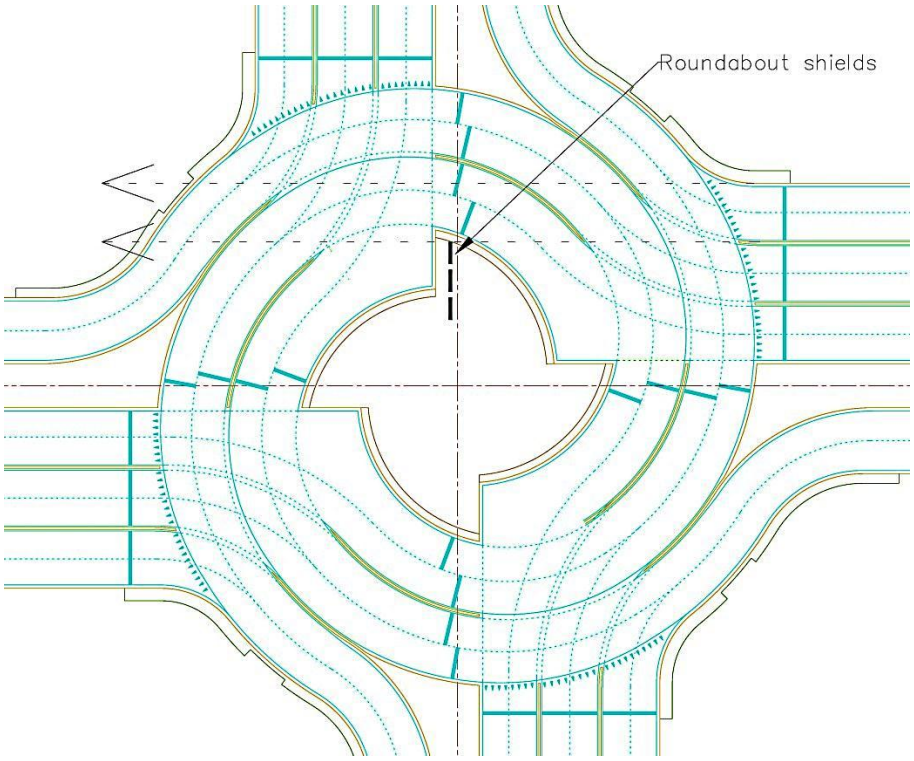


Figure M-11 On turbo circles with an inscribed radius smaller than 20 m, the roundabout shields do not deprive drivers on the right lane from their view on the horizon

M.4.4. Design of the route signs

The design of the route signs introducing the turbo intersection is a point of concern, because it provides the road user with information. This section motivates why the design of route signs deserves special attention.

The driving task can be divided in certain distinct levels. For example, Allen *et al.* (1971) distinguishes among the navigation, guidance and control level. Similarly, Michon (1985) made distinction among the strategic, manoeuvring and control level. The strategic level comprises decisions on planning a trip from origin to destination at the highest level, such as destination choice, mode choice and route choice. The decision maker processes information at this level with time intervals ranging from a few minutes to hours. At the manoeuvring level, tasks on the interaction with the road environment and other road users take place, such as the decision to overtake. Information at this level is processed a time scale ranging from seconds to a few minutes. At the control level, the driver takes decisions on the lateral and longitudinal position of the vehicle; these decisions are performed on a time scale ranging from few seconds to almost continuously decision making.

Making distinction among these levels is important because it provides insight in the way drivers process information (from all senses) and makes decisions. Wickens (1984) proposed a model in which the driver has a limited information processing capacity. In his single-channel information processing system, the

driver processes information at one level; two decisions on different levels cannot be taken simultaneously.



Figure M-12 Route signs offer information at both the strategic (navigation) and the manoeuvring (guidance) level

Figure M-12 shows that this theory is relevant for the design of the route signs introducing a turbo intersection. The signs offer information at the strategic level by indicating the names of municipalities; they offer information at the manoeuvring level as well by means of the curved arrows (Theeuwes *et al.*, 2012, p.92). That means that the single-channel system of the human mind needs to process information at two different levels in a rather short time interval, increasing the work load. A possible consequence is that drivers pay less attention decisions at the control level (for example, drivers may start to swerve because they pay less attention to the lateral position of the vehicle on the lane).

The pavement LEDs may offer a solution to this problem, because they assist the driver at the guidance level. The workload can be reduced by removing the arrows from the route signs, thereby reducing the amount of visual information. Of course, then the question arises whether the driver will be offered enough information for sensing and judging the road environment correctly. This is a subject for further investigation.

M.5. Hypotheses for future research

This appendix formulated presumptions with respect to the influence of LED illumination on microscopic behaviour. This section formulates the presumptions as hypotheses; subjects for future research.

1. A) LED pavement markings relieve the mental workload while crossing the intersection.
1. B) LED pavement markings enhance the clarity and predictability of the road environment.
2. When a stream is not in the green phase, the accessory LED modules should be turned off, rather than showing red.
3. A) LED illumination can substitute the function of the wide roadway dividers on the turbo circle. The function is to conduct the road user while crossing the intersection, and to minimize the amount of erroneous manoeuvres.
3. B) LED illumination can substitute the function of the roundabout shields. The function is to warn approaching drivers of a discontinuity in the driving coarse, already at considerable distance from the intersection.

3. C) LED illumination can substitute the function of the route signs with respect to the manoeuvring level (the arrows on the route signs). The function with respect to the manoeuvring level is to inform approaching drivers about how to cross the intersection.